Catalytic Activation of Small Molecules

Development and Characterisation of Ruthenium Complexes
for Application in Catalysis

Inaugural-Dissertation

zur Erlangung des Doktorgrades

der Mathematisch-Naturwissenschaftlichen Fakultät
der Universität zu Köln

vorgelegt von

Diplom-Chemiker Jong-Hoo Choi

aus

Seoul, Republik Korea

Köln 2016

Berichterstatter (Gutachter)

1. Priv.-Doz. Dr. Martin H. G. Prechtl, Universität zu Köln, Institut für Anorganische Chemie.
2. Prof. Dr. Axel Klein, Universität zu Köln, Institut für Anorganische Chemie.
3. Reader Dr. George Britovsek, Imperial College, London, UK.

Tag der mündlichen Prüfung: 29.10.2015

Acknowledgement

First of all I want to acknowledge Priv.-Doz. Dr. Martin H. G. Prechtl for giving me the opportunity to work and to accomplish my thesis in his group, as well as for the interesting subject and for his supervision.

For the second examination of my thesis, my gratitude goes to Prof. Dr. Axel Klein.

For the third examination of my thesis my gratitude goes to Reader Dr. George Britovsek.

I want to acknowledge the Ministerium für Innovation, Wissenschaft und Forschung des Landes Nordrhein-Westfalen (MIWF-NRW) for financial support within the Energy Research Program for the Scientist Returnee Award for M. H. G. Prechtl (NRW Rückkehrerprogramm).

Dr. Dominic Van-der-Waals, Leo Heim and Hannelore Konnerth are acknowledge for their helpful proofreading of my thesis.

My gratitude goes to Prof. Dr. Dieter Vogt from the University of Edinburgh, School of Chemistry, UK, for giving me the possibility to work as a visiting researcher in his group and for a successful scientific collaboration. Within this collaboration also Dr. Oliver Diebolt from the Université de Limoges, Laboratoire de Chimie des Substances Naturelles, faculté des sciences et techniques, in Limoges, France and Prof. Dr. Piet W. N. M. van Leeuwen, INSA, Laboratoire de Physique et Chimie de Nano-Objets, Toulouse, France are acknowledged. I thank Dr. Dennis Pingen for the successful scientific collaboration, helpful discussions and also for the fun time in Edinburgh, Cologne and Weimar.

Furthermore, I thank every student-intern I supervised for their experimental support. For nuclear magnetic resonance analysis, especially for the T_1-relaxation measurements, I would like to thank Dr. Nils Schlörer and his NMR-Team. Also, my gratitude goes to all the technical employees of the Institute of Inorganic Chemistry for all the discreet but essential work in the background. I want to thank Prof. Dr. Hans-Günther Schmalz and his co-worker Andreas Adler for GC measurements. For LIFDI-MS mea-

surements, I acknowledge Prof. Dr. Thomas Braun and his co-workers Josefine Berger and Dr. Mike Ahrens from the Humboldt University in Berlin. For helpful discussions with the single crystal XRD analysis I would like to thank Dr. Corinna Hegemann, Alexander Krest, Tim Heidemann and Dr. Jörg Neudörfl.

To my friends and colleges from the Institute of Inorganic Chemistry, thank you for all your support and fun over the last few years.

I thank every former and current member of the Prechtl group, especially Dr. Michael Keßler, Dr. Sebastian Sahler, Dr. Dominic Van-der-Waals, Leo Heim, Hannelore Konnerth, Christian Gedig, Andreas Weilhard and Silas Robke for helpful discussions, their patience and for the fun 3-4 years inside and outside the lab.

Last but not least I want to thank my family for supporting me in every possible way. I thank Anne for all her support and patience during my PhD studies.

Yours sincerely

Jong-Hoo Choi

Do or do not. There is no try.

(Master Yoda - Star Wars, The Empire Strikes Back, 1980)

Abstract

In this work, the synthesis, characterisation and catalytic application of ruthenium pincer complexes is presented. In this context, new synthetic strategies are discussed to obtain novel ruthenium pincer dihydrogen complexes. Furthermore, the reactivity of the complexes towards small molecules (e.g. alcohols, boranes, ammonia, amines, nitriles and hydrogen) was observed, delivering fundamental insights into catalytic applications. With the reactivity testing, new borylated B-H σ-complexes were synthesised and characterised. Moreover, decarbonylation of alcohols were observed with these complexes, leading to a new strategy to functionalise ruthenium pincer complexes with CO ligands. In addition to standard analytic methods such as NMR and IR spectroscopy, for the first time LIFDI-MS analysis (liquid injection field desorption/ionisation-mass spectrometry) of the synthesised ruthenium pincer hydride complexes was carried out. This method is a mild approach to analyse reactive compounds such as ruthenium pincer complexes in mass spectrometry. The obtained ruthenium dihydrogen pincer complexes and the CO functionalised ruthenium pincer complexes were tested for their catalytic activity. In dehydrogenation reactions, one of the first homogeneously catalysed transformation of primary alcohols to carboxylic acid salts was achieved in aqueous medium without toxic, oxidative and/or aggressive additives required under mild reaction conditions (120 °C). Furthermore, effective hydrogenation of nitriles was successfully demonstrated, whereby the selectivity of the reaction equilibria can be controlled to obtain either secondary imines or primary amines with up to full conversion and high selectivity under low H_2 pressure at 4 bar, low catalyst loading (0.5-1 mol%) and mild reaction temperatures (50-100 °C). Another catalytic application is the direct amination of alcohols with ammonia, which is a straight-forward approach to transform alcohols directly into the corresponding amines without any additional synthetic steps. Based on the results of investigative catalyst screenings, a new complex was synthesised, this is one of the most active catalyst for this reaction.

Kurzzusammenfassung

Diese Arbeit befasst sich mit der Synthese, der Charakterisierung und der katalytischen Anwendung von Ruthenium-Pincerkomplexen. In diesem Zusammenhang werden neue synthetische Ansätze diskutiert, die zu neuartigen Ruthenium-Pincer-Wasserstoffkomplexen führen. Die Reaktivitäten dieser Komplexe wurden an kleinen Molekülen (z.B. Alkohole, Borane, Ammoniak, Amine, Nitrile und Wasserstoff) getestet, die in der katalytischen Anwendung fundamentale Einblicke zeigten. Durch diese Testreaktionen wurden neuartige, borylierte B-H σ-Komplexe synthetisiert und charakterisiert. Weiterhin wurden mit diesen Komplexen Decarbonylierungsreaktionen von Alkoholen beobachtet. Dadurch wurden neue Synthesewege ermöglicht, um CO-funktionalisierte Ruthenium-Pincerkomplexe zu erhalten. Neben den herkömmlichen Analytikmethoden wie die NMR- und IR-Spektroskopie, wurde zum ersten Mal die LIFDI-Massenspektrometrie (liquid injection field desorption/ionisation-mass spectrometry) an den synthetisierten Ruthenium-Pincer-Wasserstoffkomplexen angewendet. Diese Methode zeigt eine Möglichkeit, besonders reaktive Substanzen wie Ruthenium-Pincerkomplexe, massenspektrometrisch zu untersuchen. Weiterhin wurden die erhaltenen Ruthenium-Pincer-Wasserstoffkomplexe und die CO-funktionalisierten Ruthenium-Pincerkomplexe auf ihre katalytische Aktivität erprobt. Als eine der ersten Reaktionen ihrer Art, wurde, unter milden Reaktionsbedingungen im wässrigen Medium, die homogen-katalysierte Transformierung von primären Alkoholen zu Carbonsäuren erreicht, ohne die Zusätze von toxischen, oxidativen und/oder aggressiven Additiven. Des weiteren wurden erfolgreich Nitrile mit hohen Umsätzen und hoher Selektivität zu sekundären Iminen oder primären Aminen hydriert, wobei die Reaktionsgleichgewichte zu Gunsten der Selektivität gesteuert wurden. Diese Reaktionen wurden unter sehr niedrigen H_2-Druck von 4 bar, niedrigen Katalysatorbeladungen (0.5-1 mol%) und milden Reaktionstemperaturen (50-100 °C) durchgeführt. Eine weitere Anwendung in der Katalyse ist die Direktaminierung von Alkoholen durch Ammoniak; ein direkter Ansatz, um die entsprechenden Amine ohne weitere Zwischenschritte zu erhalten. Basierend auf dem durchgeführte Katalyse-Screening wurde ein neuer Komplex synthetisiert, der zu den aktivsten Katalysatoren für diese Reaktion gehört.

Contents

Abbreviations

δ	chemical shift (NMR)
η^{n}	coordination mode
ν	valence oscillation (IR)
$\tilde{\nu}$	wave number (IR)
J	coupling constant (NMR)
^{i}Pr	*iso*-propyl
^{t}Bu	*tert*-butyl
APT	attached proton test
ATR	attenuated total reflection
BPin	pinacolborane
br	broad
Cat.	catalyst
COD	1,5-cyclooctadiene
Cy	cyclohexyl
Cyp	cyclopentyl
d	distance
d	doublet in NMR
dd	doublet of doublet (NMR)
DEPTQ	distortion less enhancement by polarization transfer including the detection of quaternary nuclei
DFT	density functional theory
dt	doublet of triplet (NMR)
eq.	equivalent
Et	ethyl
FID	field ionisation/desorption
FT	Fourier-transformation
GC	gas chromatography
H/D	hydrogen/deuterium
Hal	halogene
IR	infra red spectroscopy
L	ligand
LIFDI	liquid injection field desorption/ionisation
m	medium (IR), multiplet (NMR)
m/z	mass to charge ratio
Me	methyl
MHz	mega hertz
MS	mass spectrometry
MW	microwave radiation
NMR	nuclear magnetic resonance spectroscopy
Ph	phenyl
PNN	phosphor nitrogen nitrogen - pincer ligand
PNP	phosphor nitrogen phosphor - pincer ligand
POP	phosphor oxygen phosphor - pincer ligand
ppm	parts per million
Py	pyridine
R-OH	primary alcohol
R.T.	room temperature(or r.t.)
r_t	retention time
s	strong (IR), singlet (NMR)
T	temperature
t	time [h, min], triplet (NMR)
T_1	spin lattice relaxation time
THF	tetrahydrofurane
TMS	tetramethylsilane
TON	turnover number
w	weak (IR)

Part I.

Introduction

1. Theoretical Background

1.1. Catalysis - An Introduction

A catalyst (greek *katálysis*; to annul, to untie) is defined as a substance which increases the rate of a chemical reaction by reducing the activation energy without being changed chemically (Figure 1.1).[1] From one of the first "catalysis" in ancient times to produce wine or vinegar, to the revolutionary processes of *Haber-Bosch* and *Ostwald* to produce ammonia or nitric acid through to the present day applications, the use of catalysts to manufacture chemical products has become indispensable. More than 90% of our produced chemical compounds, such as pharmaceuticals, basic materials and chemicals, processed food, etc. are obtained by the effects of catalysts, mainly as heterogeneous catalytic processes (multiphase catalysis).[1,2]

Despite the benefits of using catalysts in manufacturing, the demand for an industrial culture of sustainability is increasing. Many chemical processes including catalytic reactions are still predominantly conducted the "old-fashioned way", often times by involving at some point of the production, stochiometrical reaction pathways, application of aggressive and toxic reactants, generation of unwanted by-products or the use of harsh reaction conditions. Herein, one of the major goals in catalysis research is to develop more efficient and sustainable catalytic systems, to move closer to the ideal twelve principles of "Green Chemistry"; 1. prevention, 2. atom economy, 3. less hazadous chemical syntheses, 4. designing safer chemicals, 5. safer solvents and auxiliaries, 6. design for energy efficiency, 7. use of renew-

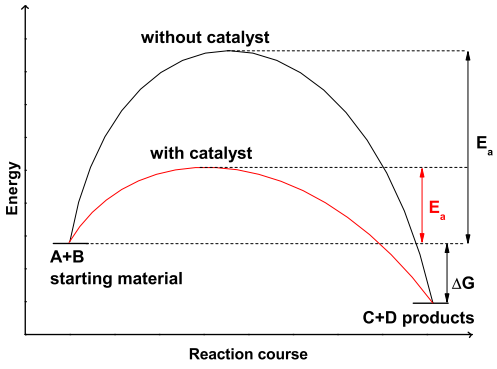

Figure 1.1. – Energy profile of a catalytic reaction.[3]

able feedstocks, 8. reduce derivatives, 9. catalysis, 10. design for degradation, 11. real-time analysis for pollution prevention and 12. inherently safer chemistry for accident prevention.[3,4] This responsibility can be faced by either optimising the established heterogeneous catalysts(multi-site catalysis) or by developing applicable homogeneous catalysts (single-site catalysis) as a different approach. While the greatest challenge in homogeneous catalysis remains in the separation of the catalysts from the products, the advantages are clearly based on the efficiency, controllable selectivity and the use of mild reaction conditions.[3] From this point of view, organometallic complexes have gained further attention during the decades. Many well-known homogeneous catalytic processes involving organo-metallic complexes based on transition metals have already set fundamental milestones in modern chemistry. Certain reaction pathways suddenly became possible, mild, simpler and controllable, such as the selective hydrogenation of olefines developed by *Wilkinson*,[5] the *Ziegler/Natta* polymerisation of olefines which can be performed under very mild reaction conditions,[6] or the C-C coupling reactions by *Stille*,[7] *Heck*[8] and *Suzuki*.[9] By specific catalyst design, asymmetric hydrogenation to obtain chiral molecules became possible by the works of *Knowles*,[10] *Noyori*[11] and *Sharpless*.[12] Furthermore, the rearrangement of different alkenes known as olefine metathesis revolutionised the chemistry by *Chauvin*, *Grubbs*[13] and *Schrock*.[3,14]

In this context, this thesis focusses on an organometallic compound class the so called "pincer complexes" and their fundamental applications in homogeneous catalysis. Pincer complexes have been very efficient in various catalytic reactions, such as CO_2 hydrogenation, C-H activation, general dehydrogenation/hydrogenation reactions under very mild reaction conditions with high atom efficiency and less unwanted waste-products.[15–23] In this work, new synthetic strategies to obtain ruthenium pincer complexes will be discussed along their characterisation, reactivity and catalytic activity.

1.2. Pincer Complexes

The first pincer complexes reported by *Shawn* and *Moulton* in the 1970's opened various new opportunities in coordination chemistry as well as in homogeneous catalysis.[16,17,24,25] A typical pincer ligand is a tridentate chelating agent which coordinates to a transition metal (**M**) with the two donor atoms (**E**) and with the sigma-binding atom (**X**) (Figure 1.2). The electronic and steric properties are defined by the constellation of the pincer complex. Donor atoms (**E**), commonly an amine or phosphine, can increase or decrease the electronic density of the system, while fine tuning is modulated at positions **Y** and **Z** with electronic withdrawing or donating atom groups.[16,20] Ligands (**L**) such as CO or alkyl phosphines can contribute to the total electronic density of the complex.[18,19,26] Alkyl or aryl groups (**R**) can effectively shield the metal centre and provide stability to the complex. The ligands are termed after the constellation of the atoms, a pyridine backbone containing phosphorus donor atoms (**E**) is referred a "PNP" ligand. The rigid cyclometalated coplanar arrangement of a pincer complex shows different reactivity depending on the ligand design, but should provide high thermal stability and high selectivity in a reaction.[16,17,27]

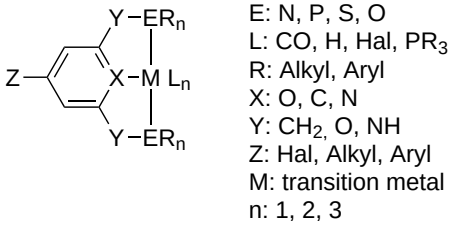

Figure 1.2. – General structure of a pincer metal complex.[18,20]

1.3. Brief Overview of well-known Ruthenium Pincer Complexes

The last two decades, ruthenium pincer complexes have been in the focus in catalysis research.[23] One of the well-known ruthenium pincer complexes was developed by the *Milstein* group, also referred as the *Milstein* catalyst **1** (Scheme 1.1). Catalyst **1** is active towards dehydrogenation/hydrogenation reactions.[19,22,23] Primary alcohols can be dehydrogenated into the corresponding esters, also the reversible hydrogenation reaction of esters back into alcohols is possible.

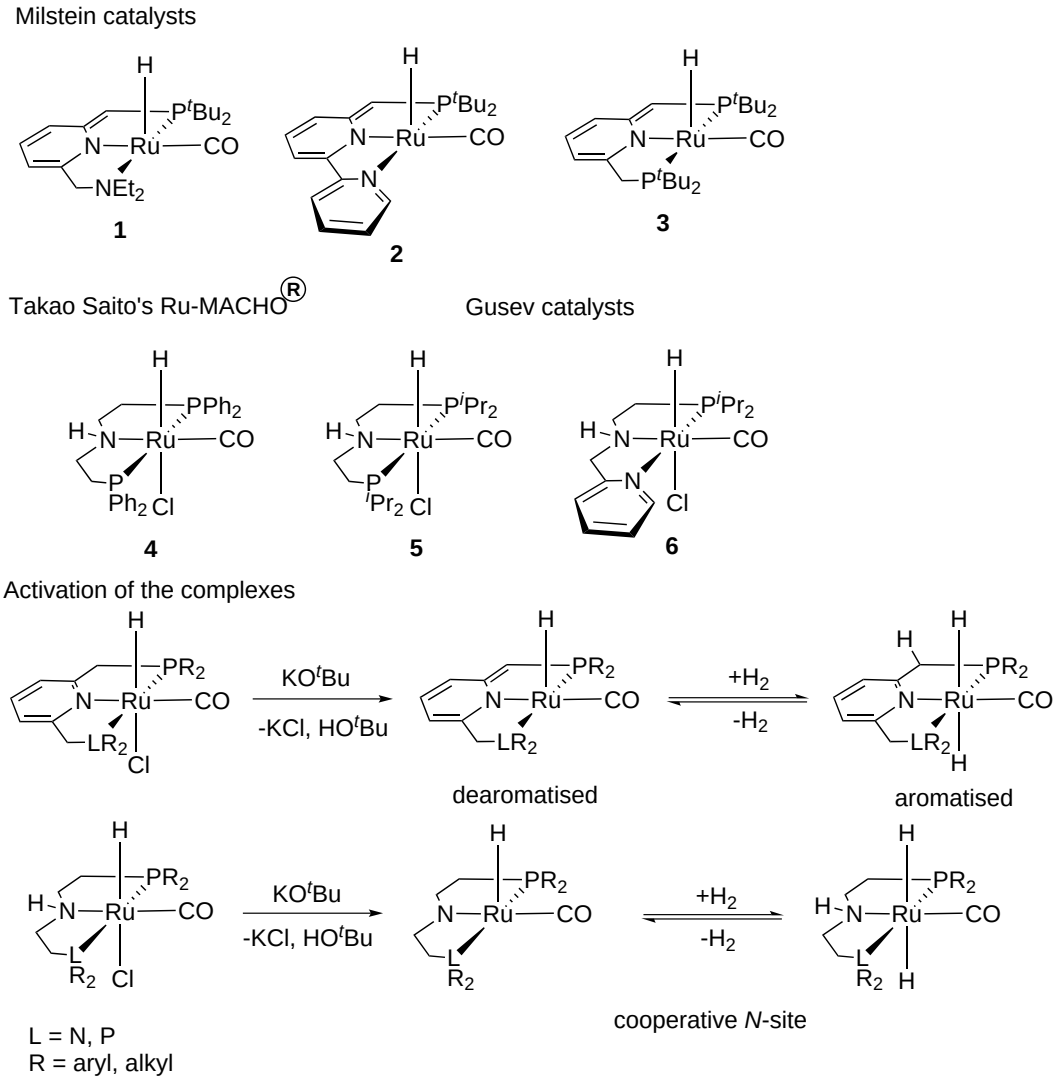

Scheme 1.1 – Overview of well-known ruthenium pincer complexes **1**-**6** and their general activation by base.[19,22,23,28–30]

Since these early reports, various other ruthenium pincer complexes were designed, all known for their excellent catalytic abilities **2**-**6**. Besides the pyridine based complexes, similar pincer complexes based on secondary amine ligands were reported as well, such as the Ru-MACHO® **4** from the *Saito* group or the complexes **5**-**6** developed by *Gusev et al.*[28–30] Typically, the complexes require activation by base, such as KO^{t}Bu, if the catalysts are not readily available as activated species (Scheme 1.1). With the activation, cooperative ligand-metal interaction should occur, which is crucial to accept, transfer or to forfeit an equivalent of H_2. Additionally the opening of the coordination-site for the reactants as basic elementary steps in catalytic dehydrogena-

tion and hydrogenation reactions occurs. The general activation-step is initialised by the base, whereby the chloride and a proton is abstracted, causing dearomatisation in the pyridine backbone in the *Milstein* system, while an amide-type N-Ru bond is formed in the aliphatic ligand system. Besides the ruthenium based pincer complexes, analogue iron and osmium pincer complexes have been reported, which are all excellent hydrogenation catalysts.[29–34] Especially iron, as a non-noble metal, is a low-cost alternative to ruthenium, osmium or iridium.

1.4. Acceptorless Dehydrogenative Coupling Reactions with Pincer Complexes

One of the earliest acceptorless dehydrognative coupling (ADC) reactions were reported in the 80s by the *Shvo* group, with turnover numbers (TON) up to 450 by applying a chair like ruthenium catalyst.[35–37] In general, these reactions proceed very mildly and efficiently, advantageously with only H_2 and appropriately H_2O as by-products (Scheme 1.2).[38] In ADC reactions of alcohols, the first dehydrogenation step to obtain aldehydes as key-intermediates is rate-determining.

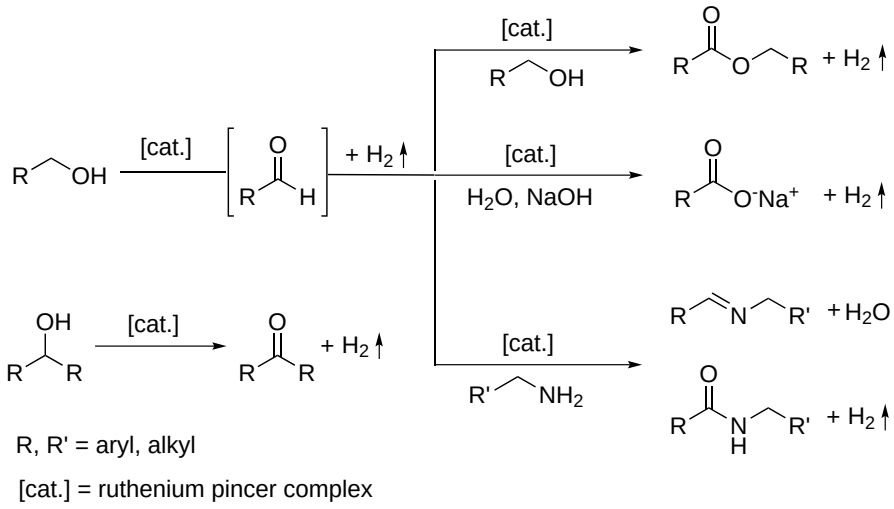

Scheme 1.2 – Overview of acceptorless catalytic dehydrogenation reactions with ruthenium pincer complexes.[23]

The aldehyde can then react with another equivalent of alcohol, amine or water. Around two decades later, a new revival of ADC reactions began with the development of new ruthenium pincer complexes such as **1**,[19] opening up direct pathways to ba-

sic organic chemicals. Esters,[19,38] ketones,[29,30,39] amides,[40] imines,[41] or carboxylic acids[42] are directly accessible without the necessities of carboxylic acid derivates or additives.

Acceptorless Dehydrogenative Coupling of Alcohols into Esters, Imines and Amides with Complex 1 or 3

In Scheme 1.3 an exemplary ADC of alcohols catalysed with the *Milstein* complex systems is proposed, which are so far the most efficient catalytic dehydrogenation systems for primary alcohols.

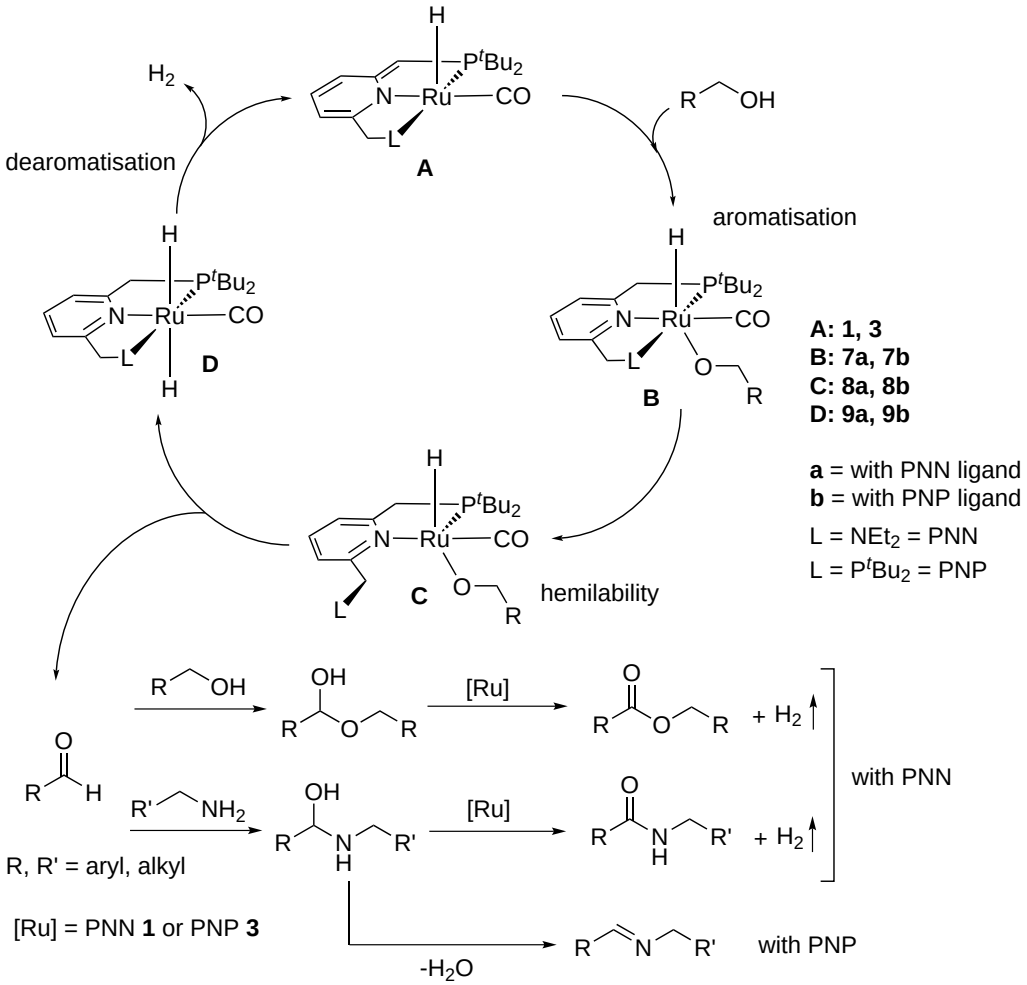

Scheme 1.3 – General catalytic cycle of the acceptorless dehydrogenative coupling of primary alcohols with ruthenium pincer complexes **1** and **3**.[23]

In the first step, an equivalent of alcohol coordinates to the activated complex **A** (**1**

or **3**) which aromatises into the alkoxy intermediate **B** (**7a** or **7b**). In case of the PNN complex **C** (**8a**), the hemilability of the amine-pincer arm provides a more favourable cis coordination of the substrate to undergo a β-H elimination for the aldehyde transformation. The labile dihydride complex **D** (**9a**) releases H_2 to complete the catalytic cycle. The aldehyde intermediate reacts with one equivalent of alcohol to form a hemiacetal; this undergoes a similar second catalytic cycle into the corresponding ester.[23] In the presence of primary amines, the generated aldehyde transforms into the hemiaminal. Similar to the hemiacetal, the hemiaminal is initially dehydrogenated by **1** and the amide is formed.[40] Replacing the PNN system into a PNP system (**3, 7b-9b**), less hemilability is provided due to the strong Ru-P bonding. In consequence, the conversion of alcohols into esters is reduced significantly. As for the hemiaminal, the elimination of H_2O occurs and the secondary imine is formed.[41] The *Milstein* catalysts operates effectively under mild conditions (100-160 °C) with TONs around 900 or higher.[23,41,43]

Dehydrogenative Catalytic Transformation of Primary Alcohols into Carboxylic Acid Salts

The primary source to obtain carboxylic acids are primary alcohols, which can be oxidised. Usually strong and toxic oxidants such as potassium permanganate or chromium trioxide are required to transform the alcohol *via* an aldehyde into the corresponding carboxylic acid.[44–46] Other alternatives for obtaining carboxylic acids are from its derivates by harsh hydrolysis reactions.[47] Overall, in laboratory or in industrial pathways, multiple steps are required to form the desired carboxylic acids. In these processes, the aldehyde is always the key-intermediate to carboxylic acid, which needs to be obtained first.[48] A very desirable pathway is a non-toxic, mild and direct route to carboxylic acids from primary alcohols. One of the first successful examples of homogeneously catalysed transformation of alcohols directly into carboxylic acid salts are reported by *Grützmacher et al.* applying a rhodium catalyst in aqueous medium with ketones as a hydrogen acceptor with high yields and mild conditions.[49] An alternative reaction was performed with dimethylsulfoxide as an oxygen acceptor.[50] A few years later, a similar approach was reported by the *Milstein* group, which includes only water as the only additive in alcohol oxidation (Figure 1.4). With complex **2** in a basic aqueous medium, the alcohol was dehydrogenated and transformed into a carboxylic acid salt by sodium hydroxide over a geminal diol like intermediate, probably stabilised

by the metal centre and the basic aqueous medium.[42] Based on DFT calculations, it is strongly assumed that, in both systems, the aldehyde as the key molecule is generated *in situ* and stabilised as a complex species.[42,49]

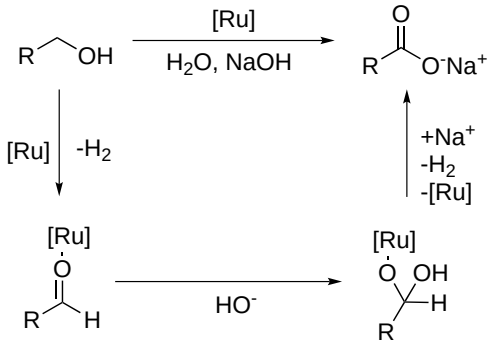

Scheme 1.4 – Transformation of primary alcohol to carboxylic acid.[42]

1.5. Catalytic Hydrogenation Reactions

Hydrogenation of Esters, Ketones and Amides

In general, if a catalyst is capable for ADC reactions, a reversible hydrogenation reactions is possible. In case for the hemilabile PNN *Milstein* catalysts **1**-**2**, hydrogenation of a large scope of esters, amides and ketones into alcohols and amines occurs under mild and efficient conditions at 5-10 bar H_2 and 1 mol% catalyst loadings (Figure 1.5, pathways **A**-**B**).[22,51] While the hydrogenation of esters or ketones are straightforward, reducing amides to primary alcohols is challenging (pathway **B1**) due to the possible of pathway **B2**, starting from the hemiaminal intermediate. On the one hand, with the generation of the primary amine, the obtained aldehyde can be reduced into the desired primary alcohol (**B1**), but on the other hand, the elimination of H_2O is possible and the secondary imine is generated, which can be further hydrogenated into the secondary amine (**B2**). Besides the *Milstein* system, only a small scope of complexes are reported, suitable for selective amide hydrogenation, such as the ruthenium triphos complexes, first reported by *Crabtree* in 2003 and optimised by the groups of *Cole-Hamilton* and *Klankermeyer/Leitner*. The utilisation of ruthenium triphos systems have been a major breakthrough in hydrogenation reactions. With the [Ru(Triphos)(TMM)] (Triphos = 1,1,1-tris(diphenylphosphinomethyl)ethane, TMM = trimethylene methane) complex **10** was reported for the successful hydrogenation of amides and esters.[52,53] Fur-

thermore, *Klankermeyer* and *Leitner* reported an elegant method to reduce CO_2 to methanol with ethanol additives and for the catalytic reduction of carboxylic acids into alcohols.[53,54]

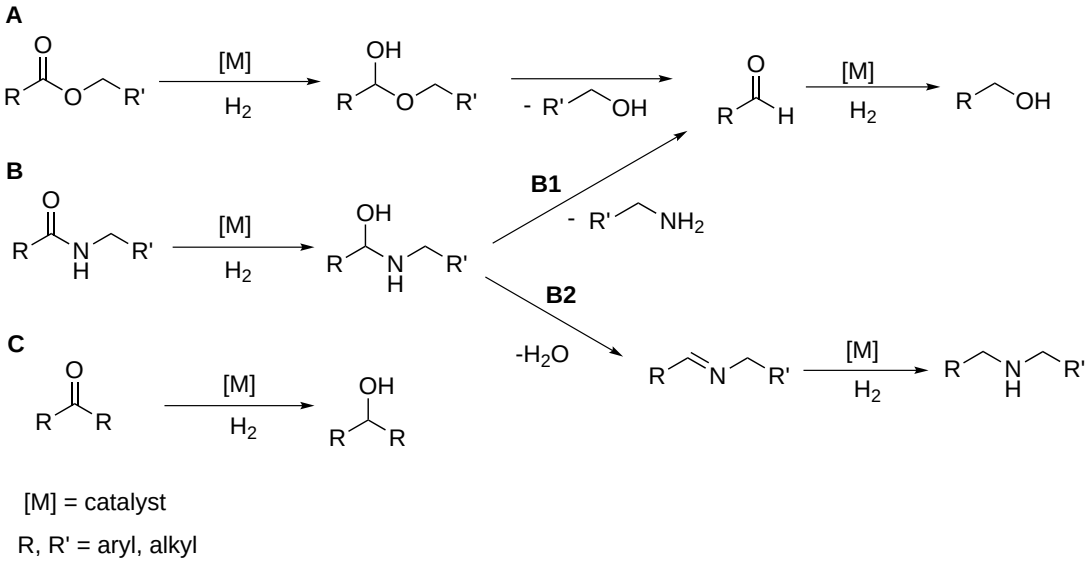

Scheme 1.5 – Basic hydrogenation reactions of esters, amides and ketones.[52]

Other excellent hydrogenation catalysts to reduce esters are the modificated *Noyori*-type complexes such as **11** or **12**.[55] Moreover, the *Bergens* group reported the hydrogenation of secondary and tertiary amides with **11**.[56] Ruthenium pincer complexes **4-6** (Scheme 1.1) with aliphatic ligand backbones are highly active for hydrogenation reactions at higher H_2 pressures around 40-50 bar, with low catalysts loadings as low as 0.025-0.2 mol%. Besides **4** and **6** their analogue osmium catalysts, *Gusev et al.* have reported effective ruthenium SNS complexes **13-14**, as highly active catalysts in hydrogenation reactions of esters (Figure 1.3). TONs up to 10,000 was reached with **14b** within 2 h with methyl hexanoate, while neat ethyl acetate was reduced with a TON of close to 60,000.[52,57] With high efficiency, ketones, imines and olefines were also successfully hydrogenated. Changing the metal to osmium (**15** and **16b)**, resulted in high activity in hydrogenation reactions.[57] Notable is the chemoselectivity of the dimeric complex **16b**, capable to hydrogenate unsaturated fatty acid esters into its corresponding alcohols, which is not possible with **16a**.[30]

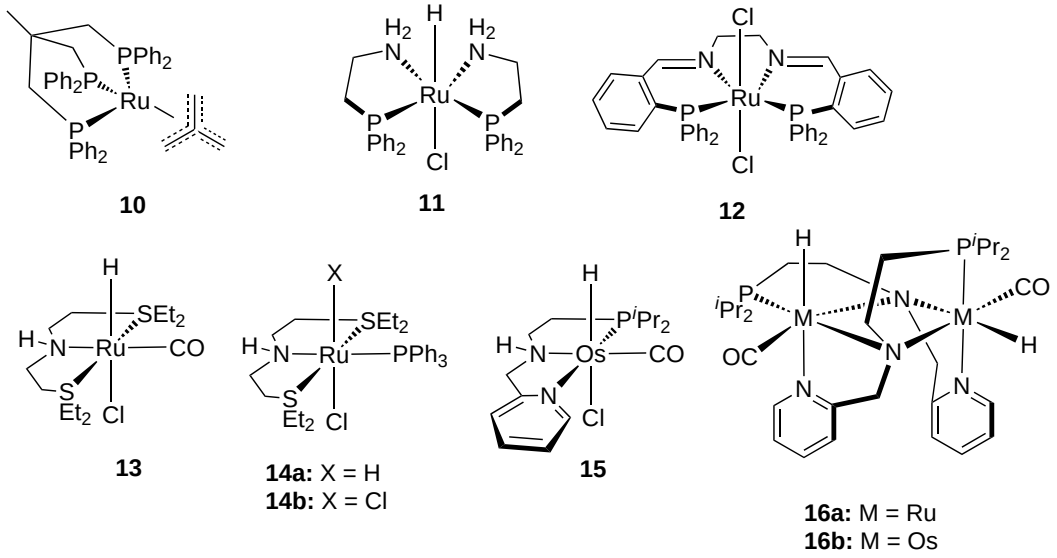

Figure 1.3. – Well-known hydrogenation catalysts **10-16**.[30,52,53,55–57]

Hydrogenation of Nitriles

The catalytic hydrogenation of nitriles is desirable due to its straightforward, atom-economic approach to obtain primary amines.[58–60] Nitriles are found in both natural and synthetic compounds which makes it an attractive amine source for essential industrial and pharmaceutical purposes.[61,62] To maintain control of the catalytic equilibria in hydrogenation of nitriles to obtain primary amines is challenging due to the high reactivity of the primary imine which is generated first (Scheme 1.6).[34,52,63]

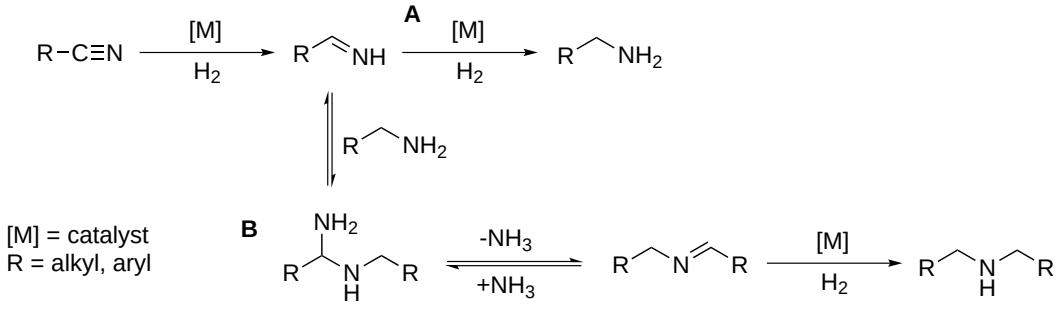

Scheme 1.6 – Possible equilibria in catalytic hydrogenation of nitriles.[63]

In pathway **A**, the primary imine is hydrogenated and the primary amine is formed. In pathway **B**, the primary imine reacts with another equivalent of already formed primary amine to form the aminal. Initially, the secondary imine is formed through

entropically favourable loss of NH_3 which can be further hydrogenated into the secondary amine. The selectivity can be particularly influenced by the temperature, the reaction time, the solvent and the amount of *in situ* generated ammonia.[64–67] While the reaction rate usually increases with the temperature; in the reduction of nitriles the selectivity might increase or decrease. One of the first hydrogenation reactions of nitriles was conducted with a rhodium-catalyst in the late 1970s by *Otsuka* and co-workers under mild conditions (1 bar H_2, 20 °C) selective towards the formation of primary amines.[65] Besides the Rh-catalyst from *Otsuka et al.*, most catalysts for the reduction of nitriles are based on ruthenium hydrides. *Sabo-Etienne et al.* presented a fast and selective hydrogenation reaction of benzonitrile to benzylamine with the ruthenium catalyst **17** at ambient temperature and 3 bar H_2 (Figure 1.4). However, this catalyst is only limited to benzonitrile.[63] Other ruthenium based complexes have been very efficient catalysts, but with the disadvantage of using high H_2 pressure (30-50 bar), high temperatures (>100 °C) and often require a base as an additive.[68–71] Exemplary, non-classical hydride complex **18** (Figure 1.4) is a very selective catalyst towards the reduction of a large scope of nitriles into primary amines. Yields and selectivity can be increased by adding catalytic amounts of water, but with the disadvantages of high pressure (75 bar) and temperature (135 °C).[70] Most recently, the *Beller* group reported the first catalysed hydrogenation of nitriles based on an iron pincer complex **19** (Figure 1.4). Despite need in high pressures within short reaction times (1-3 h), primary amines were obtained. Notable is not only the base-free conditions with iron, but the selective hydrogenation di-nitriles into di-amines, such as the reduction of adiponitrile into the industrial important hexamethylendiamine.[34]

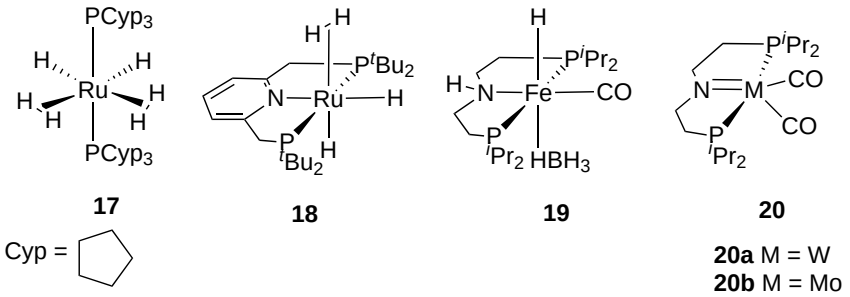

Figure 1.4. – Hydrogenation catalysts for effective reduction of nitriles.[34,52]

Other non-noble metal catalysts for such reactions are based on tungsten, molybdenum or nickel. Although requiring harsh reaction conditions, pincer complexes (**20a-b**) of W and Mo were reported by the *Berke* group for the selective hydrogenation of ni-

triles into secondary imines (Figure 1.4).[72] Applying the *Milstein* complex **2** (Scheme 1.1), secondary imines were obtained under mild conditions. Within this catalytic system, adding different primary amines to the nitriles led to cross-coupled secondary imines.[67]

1.6. Direct Amination of Alcohols with Ruthenium Catalysts

Amination of alcohols is a direct way to obtain amines with only H_2O as the by-product. Alternatively, the reduction of nitriles is a way for obtaining amines as discussed in section 1.5. The syntheses of amines are not straightforward and involve multiple steps, usually with toxic and super-stochiometrical reaction pathways.[73,74] Industrially, one elegant approach to obtain amines is by the amination of olefines, which was first patented in 1945[75] and further developed by the *BASF* group.[76] Moreover, *Beller* and co-workers developed a multi-step catalysis to synthesise linear amines, generating the aldehyde-species with CO/H_2 gas, which then reacts with additional amines.[77] Based on this concept of amine alkylation, C-OH groups were skilfully modified selectively into secondary or tertiary amines using an *in situ* metal ligand systems such as $[Ru_3(CO)_{12}]$ **21** with bulky phosphorus ligands.[78,79] In similarity with the direct hydrogenation of nitriles to obtain primary amines, it is desirable to obtain amines directly by amination of alcohols with NH_3 in one step. Industrial heterogeneous catalysis to transform alcohols into amines are proven to cover the demands for large scale of lower amines, such as methylamine, ethylamine up to amylamines via direct amination with NH_3, but these reactions are accompanied by harsh reaction conditions.[58] In 2008, the *Milstein* group reported the direct amination reaction of primary alcohols into primary amines with an air stable ruthenium pincer complex **22** (Scheme 1.7). Differently to complexes **1** or **4**, **22** is active via "long-range" metal ligand cooperative property, whereby the acridine backbone is dearomatised through alcohol dehydrogenation.[80] Under mild conditions, and around 7-8 bar NH_3, high conversions and high yields were obtained with catalysts loading as low as 0.1 mol%.[81] Two years later, *Beller* and co-workers as well as the *Vogt* group reported independently the first direct amination of secondary alcohols with NH_3 applying a similar *in situ* metal-ligand system based on ruthenium and bulky phosphorous ligands.[82,83] With an extensive ligand and parameter screening, they reported the CataCXiumPCy® **23** as the most efficient ligand

for such reactions (Scheme 1.7). With catalysts loadings of 1-2 mol% combined with 6 mol% ligand at 140-150 °C, various secondary alcohols were transformed into primary amines with high conversions and good selectivities. Furthermore, *Beller* reported the amination of benzyl alcohol and furfuryl alcohol with this system giving moderate to good yields, proving that amination of primary alcohols is generally possible under the given conditions.

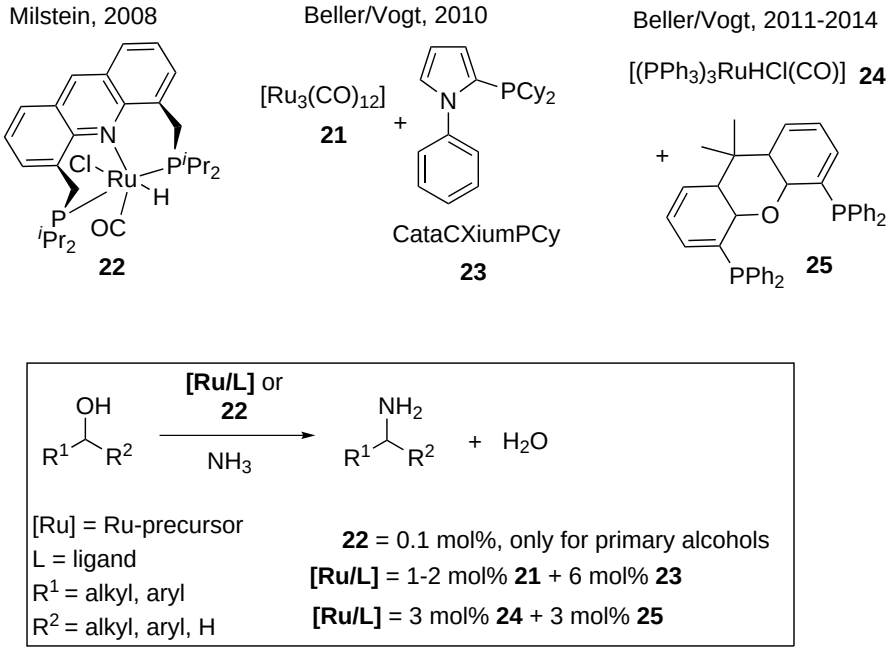

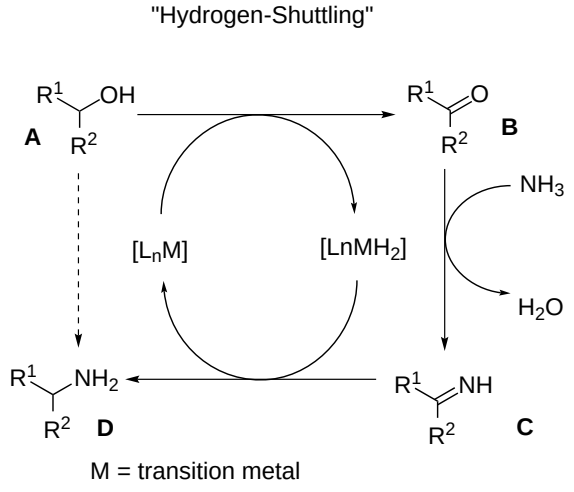

Scheme 1.7 – Catalytic systems for the direct amination of alcohols and the "Hydrogen Borrowing" concept.[84–86]

Applying the ruthenium precursor [$(PPh_3)_3RuHCl(CO)$] **24** together with the Xantphos ligand **25**, an improvement was achieved with regards to conversion and selectivity.[87] Moreover, detailed mechanistic studies were conducted by the *Vogt* group displaying a well-founded insight into the [Ru/Xantphos] catalytic system.[86] The general aspect in direct amination reactions of alcohols is based on the concept of "hydrogen-shuttling" also known as the "borrowing hydrogen methodology" (Scheme 1.7).[84,85,88] In the first step from **A** to **B**, the alcohol undergoes a dehydrogenation step into the ketone/aldehyde intermediate. With the amination reaction and the following water elimination, the primary imine (**C**) is formed. The primary imine (**C**) is hydrogenated with the "borrowed" hydrogen pair by the catalyst ([L_nM] to [L_nMH_2]) into the primary amine (**D**). Regarding the high reactivity of the primary imine, it can not be excluded that the formed primary amine could react with the primary imine to give secondary imines and secondary amines.[86]

1.7. Ruthenium Dihydrogen Complexes - Reactivity towards Functional Groups

Dihydrogen Complexes - Activation of Molecular Dihydrogen

Molecular dihydrogen ligands are typically coordinated in a side-on arrangement to a transition metal centre. This particular type of transition metal hydride is referred to as a dihydrogen (H_2) complex (also known as η^2-H_2-complex or non-classical hydride complex), and was discovered by *Kubas et al.* in the 1980s.[89] Typically, H_2-complexes are surrounded by stabilising bulky ligands such as; PCy_3 or P^iPr_3, pincer ligands or cyclohexyl (Cy) type ligands, often in combination with other donating ligands, such as -H or CO.[90–92] In Figure 1.5, the first discovered non-classical hydride complexes are illustrated.[89,93,94] Up to the present days, countless dihydrogen complexes have been reported and fully characterised, covering various transition metals from vanadium to platinum, with many stable complexes having been isolated.[90] Depending on the metal precursors, the syntheses of H_2-complexes can be achieved by photolysis, hydrogenation of unsaturated precursor, reduction, protonation, or displacement of ligands.[90] For the latter method, the displacement of weaker ligands by hydrogen gas is a simple method to obtain dihydrogen complexes, such as the pincer ligand based non-classical hydride complex **18** (Figure 1.4).[92]

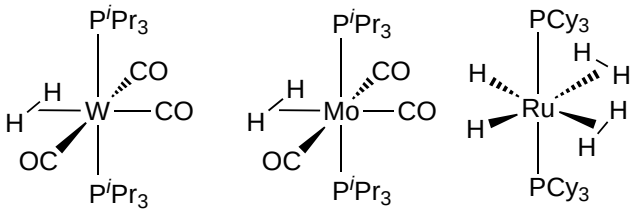

Figure 1.5. – First examples of non-classical hydride complexes.[89,93,94]

The discovery of dihydrogen complexes was fundamental to understand the bonding of molecular hydrogen to transition metals. In theory, the bonding mode of a molecular hydrogen ligand is based on the concept of the lone pair (electron pair) donation by *Lewis* shown in the *Werner* type complex a) (Figure 1.6). For further understanding, the π-complex by *Dewar* b) with π electrons of the olefine binding to the metal is off-fundamental to this concept as a direct comparison to the η^2-H_2-M complex c). The similarity to the *Werner* complex or the *Dewar* complex is perceptible in non-classical hydride complexes, whereby the H_2 ligand shares two electrons with the transition metal as 2-electron, 3-center bond (σ-complex, Figure 1.6).[90,91,95]

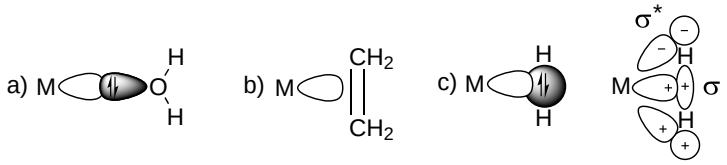

Figure 1.6. – Models of metal-ligand bindings; a) *Werner*-complex, b) *Dewar*-complex, c) σ-complex.[91]

In a M-H_2 complex two main factors are crucial for this configuration. First the donation of the sigma electrons from H_2 into the vacant d orbital of the metal and second, the backdonation of the metal's filled d orbitals to the σ^* orbital. Another criterion is the balance between the σ orbital donation and the influence of the back-donation, which is responsible for the binding and the elongation of the molecular H_2 ligand, which can eventually lead to H-H cleavage forming a di-hydride metal complex. In this context, hydride species are defined by the degree of backdonation which is evidently in the length of the H-H distance (Figure 1.7). Molecular dihydrogen has a H-H distance (d_{HH}) of 0.74 Å, while the (d_{HH}) of a "true" non-classical H_2 complex ranges from 0.8-1.0 Å. In elongated H_2 complexes the d_{HH} is between 1.1-1.36 Å, in a dihydride the distance is 1.6 Å or larger.[91,95]

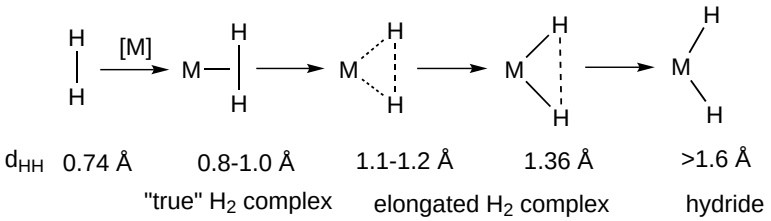

Figure 1.7. – H-H bond distances from crystallography and NMR.[91,95]

Non-classical hydride complexes can be classified with neutron diffraction,[89] but still the most convenient way to characterise H_2 complexes is the calculation of the H-H distances obtained from the data of the temperature dependent T_1 NMR measurement.[96] The defined area of the hydride signals for the T_1 NMR measurement usually appear in the high field between -5 and -25 ppm in the ^{1}H NMR. In this case, resonance time of the inversion-recovery-pulse mechanisms (180°-t-90°) is measured at various temperatures, whereby the T_1 value passes a minimum $T_{1\mathrm{min}}$ at a substance specific temperature θ_{min}. Calculations of the d_{HH} are conducted using the equation 1.1 which regards the rapid H_2 rotation with the correction factor 0.793 and the frequency ν (MHz) of the spectrometer.[95] The T_1 measurement for d_{HH} calculations needs to be interpreted carefully, due to various effects, such as the direct influence of the solvent or the fluxual and rotational behaviour of the hydride ligands.[97,98] Typically, the $T_{1\mathrm{min}}$ value is around $\geqslant$90 ms for classical hydrides and 6-90 ms for nonclassical hydride at the frequency of 200 MHz.[95]

$$d_{HH} = 0.793 \times 5.815\,(T_{1min}\nu^{-1})^{1/6} = 4.611\,(T_{1min}\nu^{-1})^{1/6} \tag{1.1}$$

Furthermore, the direct comparison of H_2-complex with its HD-isotopomer, synthesised with HD gas, can be a reliable indicator to confirm the molecular dihydrogen ligand at the metal centre. In HD-isotopomers, the coupling pattern changes along with the coupling constance $^1J_{HD}$, which is >20 Hz for nonclassical hydrides, 2-3 Hz for classical hydrides and 43 Hz for the free HD gas.[90] Additionally, the IR spectroscopy provides valuable information to the NMR techniques. The vibration band of ν(MH) appears typically between 1700-2300 cm^{-1}, the asymmetric vibrations $\nu_{\mathrm{as}}(MH_2)$ around 1500 cm^{-1} and the symmetric vibrations $\nu_{\mathrm{s}}(MH_2)$ around 800-900 cm^{-1}. The $\nu(H_2)$ appear in the range of 1900-3000 cm^{-1} compared to free H_2 gas at 4300 cm^{-1}.[90,91,95]

LIFDI-MS - A Powerful Tool to Analyse Sensitive Organometallic Hydride Complexes

To complete the list of analytic methods, the LIFDI-MS (liquid injection field desorption/ionisation-mass spectrometry) technique is introduced. Conventionally, ESI-MS (electro spray ionisation mass spectrometry), FAB-MS (fast atom bombardment) and MALDI-MS (matrix assisted laser desorption/ionisation) are used to obtain molecular weight information, often times to analyse polar molecules. In case of molecules with lower polarities or neutral organometallic compounds, FD/I (field desorption/ionisation) is considered as a soft ionisation method, whereby $M^{+\cdot}$ radical cations are formed, delivering often no or little fragmentations under MS conditions.[99–101] With the liquid injection technique developed by *Linden CMS*, highly reactive transition metal complexes can be analysed firmly, which used to be difficult, as the sample reaches the MS directly by injection via a fused capillary under inert condition.[102–104]

Reactivity of Nonclassical Ruthenium Hydride Complexes Towards C-H, B-H and R-OH Bonds

B-H Bond Activation

In terms of B-H activation reactions, non-classical hydrides show high reactivity. **28** reacts rapidly in the presence of simple amine-boranes by forming unique boryl species Bis(σ-B-H)-complexes **29a-c**. In this reaction, the labile molecular dihydrogen ligands are replaced by the amine-borane forming two sigma B-H bonds (Scheme 1.8).[105] Similar σ-B-H-complexes were reported with other metals (e.g. Ti, Ir and Rh).[106,107] These fundamental reactions become interesting in terms of alternative hydrogen storage systems. Amine-boranes (AB) offer a high weight percentage of H_2 which can be unleashed with suitable dehydrogenative catalytic systems, such as the use of noble metals in ionic liquid media[108–110] or with ruthenium hydride complexes.[111,112] Despite the promising advantages of AB in potential organic hydrogen storage, the reversible hydrogenation of the system is limited due to the formed polymeric B-N network.[109,113] Another noteworthy application to activate B-H bonds was reported by the *Leitner* group using non-classical ruthenium hydride complex **18** in the catalytic hydroboration of terminal alkynes with pinacolborane into Z-vinylboronates; which is a potential reagent for the *Suzuki* coupling reaction (Scheme 1.8).[114]

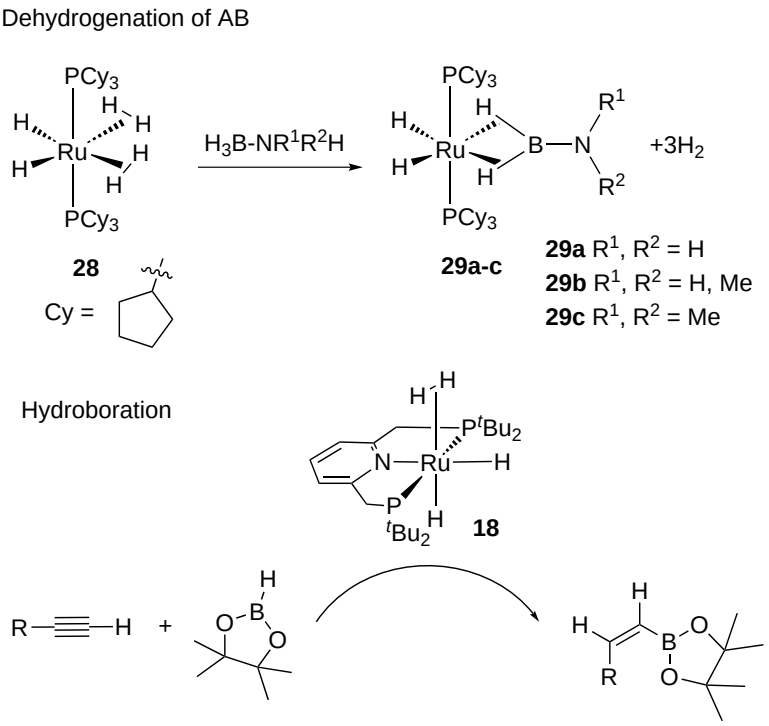

Scheme 1.8 – Reactivity of nonclassical ruthenium hydride complexes **28** in AB dehydrogenation. Hydroboration of alkynes with complex **18**.[105,114]

C-H Bond Activation

For C-H activation, dihydrogen complex **18** is highly active for H/D-exchange reactions. In the presence of deuterated solvents, most impressively with D_2O, aromatic compounds were effectively deuterated under mild reaction conditions (Scheme 1.9).[21,115] Furthermore, with complex **28** the *Murai* reaction was demonstrated very efficiently at room temperature, which was originally reported with a ruthenium complex $[RuH_2(CO)(PPh_3)_3]$ at 130 °C.[116,117]

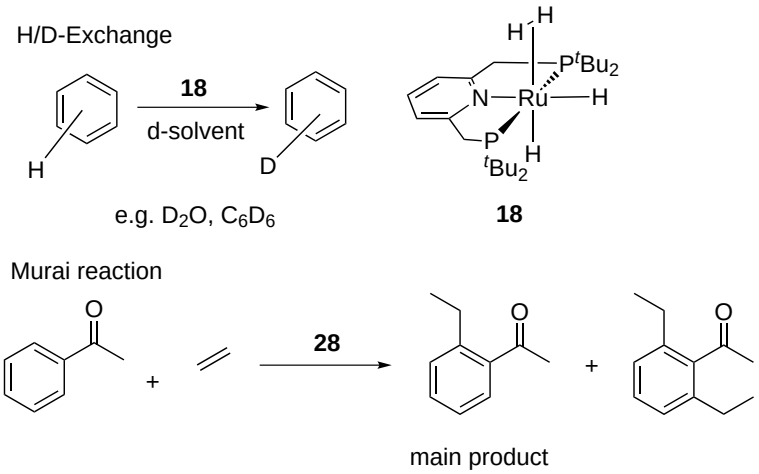

Scheme 1.9 – Reactivity of nonclassical ruthenium hydride complexes **18** in H/D-exchange reactions. *Murai* reaction with **28**.[21,115–117]

C-OH Activation

A small scope of transition metal hydrides (e.g. Ni, Co, Rh, Ru, Ir) have been reported to decarbonylate C-OH bonds and generate CO-ligands with aldehydes, primary alcohols or ketones.[118–122] Primary alcohols as starting point, dehydrogenation occurs first forming the aldehyde. By oxidative addition of the aldehyde to the metal centre, a hydride insertion occurs. Subsequently, the coordinated carbonyl adduct undergoes a decarbonylation forming the CO functionalised complex and releases the corresponding carbohydride (Scheme 1.10).[118] In particular nonclassical ruthenium hydride complexes can be functionalised without any hindrances with a CO ligand, due to the labile H_2 ligand, which opens a vacant site on the metal centre for the coordination of the alcohol.[122,123]

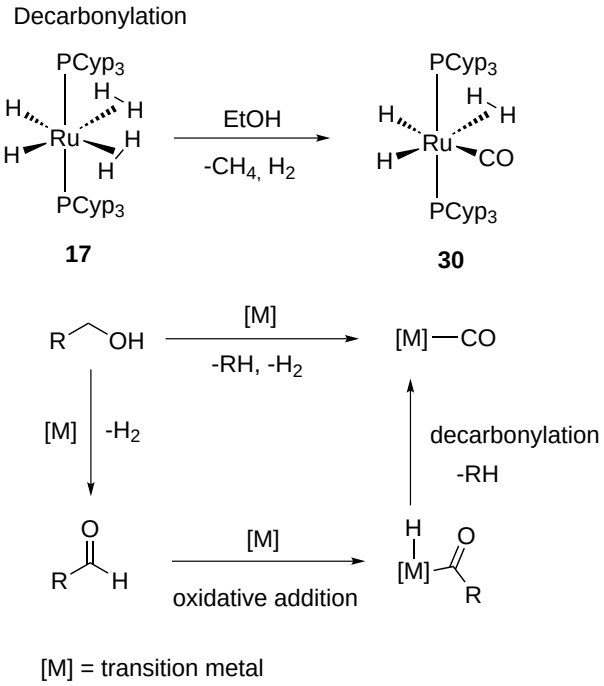

Scheme 1.10 – Decarbonylation reaction of ethanol by **17**[122] and the schematic decarbonylation of a primary alcohol.[118]

Bibliography

[1] F. Schüth, *Chem. unserer Zeit* **2006**, *40*, 92–103.

[2] J. M. Thomas, W. J. Thomas, *Principles and Practice of Heterogeneous Catalysis*, *Vol. 1*, Wiley-VCH, Weinheim, **1996**.

[3] A. Behr, P. Neubert, *Applied Homogeneous Catalysis*, Wiley-VCH, Weinheim, **2012**.

[4] P. T. Anastas, J. Warner, *Green Chemistry: Theory and Practice*, Oxford University Press, New York, **1998**.

[5] J. A. Osborn, F. H. Jardine, J. F. Young, G. Wilkinson, *J. Chem. Soc. A* **1966**, 1711–1732.

[6] K. Ziegler, E. Holzkamp, H. Breil, H. Martin, *Angew. Chem.* **1955**, *67*, 541–547.

[7] D. Milstein, J. K. Stille, *J. Am. Chem. Soc.* **1978**, *100*, 3636–3638.

[8] R. F. Heck, J. P. Nolley, *J. Org. Chem.* **1972**, *37*, 2320–2322.

[9] N. Miyaura, A. Suzuki, *J. Chem. Soc. Chem. Commun.* **1979**, 866–867.

[10] W. S. Knowles, *Angew. Chem.-Int. Edit.* **2002**, *41*, 1998–2007.

[11] R. Noyori, T. Ohkuma, M. Kitamura, H. Takaya, N. Sayo, H. Kumobayashi, S. Akutagawa, *J. Am. Chem. Soc.* **1987**, *109*, 5856–5858.

[12] T. Katsuki, K. B. Sharpless, *J. Am. Chem. Soc.* **1980**, *102*, 5974–5976.

[13] P. Schwab, R. H. Grubbs, J. W. Ziller, *J. Am. Chem. Soc.* **1996**, *118*, 100–110.

[14] R. R. Schrock, *Acc. Chem. Res.* **1990**, *23*, 158–165.

[15] R. Tanaka, M. Yamashita, K. Nozaki, *J. Am. Chem. Soc.* **2009**, *131*, 14168–14169.

[16] D. Morales-Morales, *J. Mex. Chem. Soc.* **2004**, *48*, 338–346.

[17] M. Albrecht, G. van Koten, *Angew. Chem.-Int. Edit.* **2001**, *40*, 3750–3781.

[18] M. Rietveld, D. Grove, G. van Koten, *J. Am. Chem. Soc.* **1997**, *119*, 11317–11318.

[19] J. Zhang, G. Leitus, Y. Ben-David, D. Milstein, *J. Am. Chem. Soc.* **2005**, *127*, 12429–12429.

[20] J. Choi, A. H. R. MacArthur, M. Brookhart, A. S. Goldman, *Chem. Rev.* **2011**, *111*, 1761–1779.

[21] M. H. G. Prechtl, M. Hölscher, Y. Ben-David, N. Theyssen, R. Loschen, D. Milstein, D. Milstein, *Angew. Chem.-Int. Edit.* **2007**, *46*, 2269–2272.

[22] J. Zhang, G. Leitus, Y. Ben-David, D. Milstein, *Angew. Chem.-Int. Edit.* **2006**, *45*, 1113–1115.

[23] D. Milstein, *Top. Catal.* **2010**, *53*, 915–923.

[24] C. Crocker, R. J. Errington, R. Markham, C. J. Moulton, K. J. Odell, B. L. Shaw, *J. Am. Chem. Soc.* **1980**, *102*, 4373–4379.

[25] C. J. Moulton, B. L. Shaw, *J. Chem. Soc. Dalton Trans.* **1976**, 1020–1024.

[26] P. Dani, T. Karlen, R. A. Gossage, S. Gladiali, G. van Koten, *Angew. Chem.-Int. Edit.* **2000**, *39*, 743–745.

[27] P. A. Chase, G. van Koten in *The Chemistry of Pincer Compounds*, (Eds.: C. M. Jensen, D. Morales-Morales), Elsevier Science B.V., Amsterdam, **2007**, pp. 181 –233.

[28] W. Kuriyama, T. Matsumoto, O. Ogata, Y. Ino, K. Aoki, S. Tanaka, K. Ishida, T. Kobayashi, N. Sayo, T. Saito, *Org. Process Res. Dev.* **2012**, *16*, 166–171.

[29] M. Bertoli, A. Choualeb, A. J. Lough, B. Moore, D. Spasyuk, D. G. Gusev, *Organometallics* **2011**, *30*, 3479–3482.

[30] D. Spasyuk, S. Smith, D. G. Gusev, *Angew. Chem.-Int. Edit.* **2012**, *51*, 2772–2775.

[31] M. Bertoli, A. Choualeb, D. G. Gusev, A. J. Lough, Q. Major, B. Moore, *Dalton Trans.* **2011**, *40*, 8941–8949.

[32] R. Langer, M. A. Iron, L. Konstantinovski, Y. Diskin-Posner, G. Leitus, Y. Ben-David, D. Milstein, *Chem.-Eur. J.* **2012**, *18*, 7196–7209.

[33] R. Langer, G. Leitus, Y. Ben-David, D. Milstein, *Angew. Chem.-Int. Edit.* **2011**, *50*, 2120–2124.

[34] C. Bornschein, S. Werkmeister, B. Wendt, H. Jiao, E. Alberico, W. Baumann, H. Junge, K. Junge, M. Beller, *Nat Commun* **2014**, *5*, Article number: 4111.

[35] Y. Blum, Y. Shvo, *J. Org. Chem.* **1985**, *282*, C7 –C10.

[36] Y. Blum, Y. Shvo, *J. Org. Chem.* **1984**, *263*, 93 –107.

[37] Y. Shvo, D. Czarkie, Y. Rahamim, D. F. Chodosh, *J. Am. Chem. Soc.* **1986**, *108*, 7400–7402.

[38] A. Friedrich, S. Schneider, *ChemCatChem* **2009**, *1*, 72–73.

[39] M. Nielsen, A. Kammer, D. Cozzula, H. Junge, S. Gladiali, M. Beller, *Angew. Chem.-Int. Edit.* **2011**, *50*, 9593–9597.

[40] C. Gunanathan, Y. Ben-David, D. Milstein, *Science* **2007**, *317*, 790–792.

[41] B. Gnanaprakasam, J. Zhang, D. Milstein, *Angew. Chem.-Int. Edit.* **2010**, *49*, 1468–1471.

[42] E. Balaraman, E. Khaskin, G. Leitus, D. Milstein, *Nat. Chem.* **2013**, *5*, 122–125.

[43] C. Gunanathan, D. Milstein, *Science* **2013**, *341*, 10.1126/science.1229712.

[44] M. Zhao, J. Li, Z. Song, R. Desmond, D. M. Tschaen, E. J. Grabowski, P. J. Reider, *Tetrahedron Lett.* **1998**, *39*, 5323 –5326.

[45] B. C. Holland, N. W. Gilman, *Synth. Commun.* **1974**, *4*, 203–210.

[46] R. J. Gritter, T. J. Wallace, *J. Org. Chem.* **1959**, *24*, 1051–1056.

[47] V. Y. Kukushkin, A. J. Pombeiro, *Inorg. Chim. Acta.* **2005**, *358*, 1 –21.

[48] G. Tojo, M. Fernandez, *Oxidation of Primary Alcohols to Carboxylic Acids: A Guide to Current Common Practice*, Springer, Luxemburg, Berlin, **2007**.

[49] T. Zweifel, J.-V. Naubron, H. Grützmacher, *Angew. Chem.-Int. Edit.* **2009**, *121*, 567–571.

[50] S. Annen, T. Zweifel, F. Ricatto, H. Grützmacher, *ChemCatChem* **2010**, *2*, 1286–1295.

[51] E. Balaraman, B. Gnanaprakasam, L. J. W. Shimon, D. Milstein, *J. Am. Chem. Soc.* **2010**, *132*, 16756–16758.

[52] S. Werkmeister, K. Junge, M. Beller, *Org. Process Res. Dev.* **2014**, *18*, 289–302.

[53] T. vom Stein, M. Meuresch, D. Limper, M. Schmitz, M. Hölscher, J. Coetzee, D. J. Cole-Hamilton, J. Klankermayer, W. Leitner, *J. Am. Chem. Soc.* **2014**, *136*, 13217–13225.

[54] S. Wesselbaum, T. von Stein, J. Klankermayer, W. Leitner, *Angew. Chem.-Int. Edit.* **2012**, *51*, 7499–7502.

[55] L. Saudan, C. Saudan, C. Debieux, P. Wyss, *Angew. Chem.-Int. Edit.* **2007**, *46*, 7473–7476.

[56] S. Takebayashi, S. H. Bergens, *Organometallics* **2009**, *28*, 2349–2351.

[57] D. Spasyuk, S. Smith, D. G. Gusev, *Angew. Chem.-Int. Edit.* **2013**, *52*, 2538–2542.

[58] K. Hayes, *Appl. Catal. A* **2001**, *221*, 187 –195.

[59] K. Weissermel, H. J. Arpe, *Industrial Organic Chemistry*, Wiley-VCH, Weinheim, **2008**.

[60] M. Santos, *Int. J. Food Microbiol.* **1996**, *29*, 213 –231.

[61] F. F. Fleming, L. Yao, P. C. Ravikumar, L. Funk, B. C. Shook, *J. Med. Chem.* **2010**, *53*, 7902–7917.

[62] F. F. Fleming, *Nat. Prod. Rep.* **1999**, *16*, 597–606.

[63] R. Reguillo, M. Grellier, N. Vautravers, L. Vendier, S. Sabo-Etienne, *J. Am. Chem. Soc.* **2010**, *132*, 7854–7855.

[64] A. M. Joshi, K. S. MacFarlane, B. R. James, P. Frediani in *Progress in Catalysis Proceedings of the 12th Canadian Symposium on Catalysis*, (Eds.: K. J. Smith, E. C. Sanford), Studies in Surface Science and Catalysis, Elsevier, Amsterdam, **1992**, pp. 143 –146.

[65] T. Yoshida, T. Okano, S. Otsuka, *J. Chem. Soc. Chem. Commun.* **1979**, 870–871.

[66] C. de Bellefon, P. Fouilloux, *Catal. Rev. Sci. Eng.* **1994**, *36*, 459–506.

[67] D. Srimani, M. Feller, Y. Ben-David, D. Milstein, *Chem. Commun.* **2012**, *48*, 11853–11855.

[68] S. Takemoto, H. Kawamura, Y. Yamada, T. Okada, A. Ono, E. Yoshikawa, Y. Mizobe, M. Hidai, *Organometallics* **2002**, *21*, 3897–3904.

[69] D. Addis, S. Enthaler, K. Junge, B. Wendt, M. Beller, *Tetrahedron Lett.* **2009**, *50*, 3654 –3656.

[70] C. Gunanathan, M. Hölscher, W. Leitner, *Eur. J. Inorg. Chem.* **2011**, *2011*, 3381–3386.

[71] C. Bianchini, V. Dal Santo, A. Meli, W. Oberhauser, R. Psaro, F. Vizza, *Organometallics* **2000**, *19*, 2433–2444.

[72] S. Chakraborty, H. Berke, *ACS Catal.* **2014**, *4*, 2191–2194.

[73] B. Miriyala, S. Bhattacharyya, J. S. Williamson, *Tetrahedron* **2004**, *60*, 1463 –1471.

[74] G. Bartoli, G. Di Antonio, R. Giovannini, S. Giuli, S. Lanari, M. Paoletti, E. Marcantoni, *J. Org. Chem.* **2008**, *73*, 1919–1924.

[75] Patent, *US Patent to BASF AG* **1945**, US Patent No 2,381,470.

[76] Patent, *US Patent to BASF AG* **1998**, US Patent No 5,773,660.

[77] A. Seayad, M. Ahmed, H. Klein, R. Jackstell, T. Gross, M. Beller, *Science* **2002**, *297*, 1676–1678.

[78] S. Bähn, S. Imm, K. Mevius, L. Neubert, A. Tillack, J. M. Williams, M. Beller, *Chem. Eur. J.* **2010**, *16*, 3590–3593.

[79] S. Bähn, A. Tillack, S. Imm, K. Mevius, D. Michalik, D. Hollmann, L. Neubert, M. Beller, *ChemSusChem* **2009**, *2*, 551–557.

[80] C. Gunanathan, B. Gnanaprakasam, M. A. Iron, L. J. W. Shimon, D. Milstein, *J. Am. Chem. Soc.* **2010**, *132*, 14763–14765.

[81] C. Gunanathan, D. Milstein, *Angew. Chem.-Int. Edit.* **2008**, *120*, 8789–8792.

[82] D. Pingen, C. Müller, D. Vogt, *Angew. Chem.-Int. Edit.* **2010**, *49*, 8130–8133.

[83] S. Imm, S. Bähn, L. Neubert, H. Neumann, M. Beller, *Angew. Chem.-Int. Edit.* **2010**, *49*, 8126–8129.

[84] M. G. Edwards, J. M. J. Williams, *Angew. Chem.-Int. Edit.* **2002**, *41*, 4740–4743.

[85] M. H. S. A. Hamid, P. A. Slatford, J. M. J. Williams, *Adv. Synth. Catal.* **2007**, *349*, 1555–1575.

[86] D. Pingen, M. Lutz, D. Vogt, *Organometallics* **2014**, *33*, 1623–1629.

[87] S. Imm, S. Bähn, M. Zhang, L. Neubert, H. Neumann, F. Klasovsky, J. Pfeffer, T. Haas, M. Beller, *Angew. Chem.-Int. Edit.* **2011**, *50*, 7599–7603.

[88] T. D. Nixon, M. K. Whittlesey, J. M. J. Williams, *Dalton Trans.* **2009**, 753–762.

[89] G. J. Kubas, R. R. Ryan, B. I. Swanson, P. J. Vergamini, H. J. Wasserman, *J. Am. Chem. Soc.* **1984**, *106*, 451–452.

[90] G. J. Kubas, *Chem. Rev.* **2007**, *107*, 4152–4205.

[91] G. J. Kubas, *J. Organomet. Chem.* **2001**, *635*, 37–68.

[92] M. H. G. Prechtl, Y. Ben-David, D. Giunta, S. Busch, Y. Taniguchi, W. Wisniewski, H. Goerls, R. J. Mynott, N. Theyssen, D. Milstein, W. Leitner, *Chem.-Eur. J.* **2007**, *13*, 1539–1546.

[93] G. J. Kubas, R. R. Ryan, *Polyhedron* **1986**, *5*, 473–485.

[94] B. Chaudret, R. Poilblanc, *Organometallics* **1985**, *4*, 1722–1726.

[95] P. G. Jessop, R. H. Morris, *Coord. Chem. Rev.* **1992**, *121*, 155 –284.

[96] D. G. Hamilton, R. H. Crabtree, *J. Am. Chem. Soc.* **1988**, *110*, 4126–4133.

[97] D. G. Gusev, R. L. Kuhlman, K. B. Renkema, O. Eisenstein, K. G. Caulton, *Inorg. Chem.* **1996**, *35*, 6775–6783.

[98] R. H. Morris, R. J. Wittebort, *Magn. Reson. Chem.* **1997**, *35*, 243–250.

[99] H. Beckey, *Research/Development* **1969**, *20*, 26.

[100] J. H. Gross, *J. Am. Soc. Mass Spectrom.* **2007**, *18*, 2254 –2262.

[101] H. Linden, *Eur. J. Mass Spectrom.* **2004**, *10*, 459–468.

[102] S. I. Kallane, T. Braun, B. Braun, S. Mebs, *Dalton Trans.* **2014**, *43*, 6786–6801.

[103] J. Gross, N. Nieth, H. Linden, U. Blumbach, F. Richter, M. Tauchert, R. Tompers, P. Hofmann, English, *Anal. Bioanal. Chem.* **2006**, *386*, 52–58.

[104] W. Monillas, G. Yap, K. Theopold, *Angew. Chem.-Int. Edit.* **2007**, *46*, 6692–6694.

[105] G. Alcaraz, L. Vendier, E. Clot, S. Sabo-Etienne, *Angew. Chem.-Int. Edit.* **2010**, *49*, 918–920.

[106] G. Alcaraz, A. B. Chaplin, C. J. Stevens, E. Clot, L. Vendier, A. S. Weller, S. Sabo-Etienne, *Organometallics* **2010**, *29*, 5591–5595.

[107] G. Alcaraz, S. Sabo-Etienne, *Angew. Chem.-Int. Edit.* **2010**, *49*, 7170–7179.

[108] S. Sahler, S. Sturm, M. T. Kessler, M. H. G. Prechtl, *Chem. Eur. J.* **2014**, *20*, 8934–8941.

[109] S. Sahler, H. Konnerth, N. Knoblauch, M. H. G. Prechtl, *Int. J. Hydrogen Energ.* **2013**, *38*, 3283 –3290.

[110] S. Sahler, M. H. G. Prechtl, *ChemCatChem* **2011**, *3*, 1257–1259.

[111] M. Kaess, A. Friedrich, M. Drees, S. Schneider, *Angew. Chem.-Int. Edit.* **2009**, *48*, 905–907.

[112] A. N. Marziale, A. Friedrich, I. Klopsch, M. Drees, V. R. Celinski, J. Schmedt auf der Günne, S. Schneider, *J. Am. Chem. Soc.* **2013**, *135*, 13342–13355.

[113] M. Grellier, S. Sabo-Etienne, *Dalton Trans.* **2014**, *43*, 6283–6286.

[114] C. Gunanathan, M. Hölscher, F. Pan, W. Leitner, *J. Am. Chem. Soc.* **2012**, *134*, 14349–14352.

[115] M. H. G. Prechtl, M. Hoelscher, Y. Ben-David, N. Theyssen, D. Milstein, W. Leitner, *Eur. J. Inorg. Chem.* **2008**, 3493–3500.

[116] Y. Guari, A. Castellanos, S. Sabo-Etienne, B. Chaudret, *J. Mol. Catal. A: Chem.* **2004**, *212*, 77 –82.

[117] S. Busch, W. Leitner, *Adv. Synth. Catal.* **2001**, *343*, 192–195.

[118] E. P. K. Olsen, R. Madsen, *Chem.-Eur. J.* **2012**, *18*, 16023–16029.

[119] R. Çelenligil-Çetin, L. A. Watson, C. Guo, B. M. Foxman, O. V. Ozerov, *Organometallics* **2005**, *24*, 186–189.

[120] R. Beck, U. Flörke, H.-F. Klein, *Inorg. Chem.* **2009**, *48*, 1416–1422.

[121] B. N. Chaudret, D. J. Cole-Hamilton, R. S. Nohr, G. Wilkinson, *J. Chem. Soc. Dalton Trans.* **1977**, 1546–1557.

[122] P. D. Bolton, M. Grellier, N. Vautravers, L. Vendier, S. Sabo-Etienne, *Organometallics* **2008**, *27*, 5088–5093.

[123] N. Sieffert, R. Réocreux, P. Lorusso, D. J. Cole-Hamilton, M. Bühl, *Chem. Eur. J.* **2014**, *20*, 4141–4155.

Part II.

Results and Discussions - Cumulative Part

2. Objectives and Outline

Ruthenium pincer complexes are an enrichment in catalysis due to their versatile use as catalysts in hydrogenation and dehydrogenation reactions. Many catalytic reactions have been proven to be very efficient, mild and effective applying these catalysts. To contribute to the list of possibilities in ruthenium pincer complex catalysis, the three major challenges are discussed in this work:

1. The discussion of new synthetic strategies to obtain ruthenium pincer complexes,
2. The reactivity testing of the obtained complexes towards small molecules,
3. And their application in catalysis.

The three aspects are thematically and fundamentally geared to each other and complete the whole picture of this work.

The first challenge is the synthesis of new ruthenium hydride complexes based on aliphatic pincer ligands and their characterisation. Besides the standard IR and NMR spectroscopic methods, for the first time, LIFDI-MS analysis (liquid injection field desorption/ionisation-mass spectrometry) for sensitive ruthenium pincer complexes is applied.

The second challenge is a linkage between synthesis and catalytic evaluation of the complexes. Testing the obtained complexes towards functional groups is fundamental to understand their reactivity. In particular within homogeneous catalysis, the catalyst should be able to undergo basic elementary steps, such as reductive elimination, oxidative addition or β-hydride elimination. With selective testing of the obtained complexes towards their reactivity, possible elementary steps can be investigated. As a consequence applicable catalysts can be revealed or excluded for catalysis and even potential complex intermediates can be isolated.

Once a functional catalytic system is found, the third aim is to optimise the system. For the third challenge, applicable complexes were used in catalysis. First, in the catalytic transformation of primary alcohols into carboxylic acid salts. Secondly, in the

selective hydrogenation of nitriles into secondary imines or primary amines and thirdly in the direct amination of alcohols with ammonia. Besides the catalytic performances, mechanistic investigations are focussed upon within this work.

3. Results and Discussions

The main results are summarised in three publications and one submitted manuscript, each subordinated as single sections. Furthermore, an additional section describes miscellaneous unpublished results is induced. To each section, detailed manuscripts of supporting information, containing further experimental descriptions are provided. This manuscript as cumulative dissertation is in order of the PhD regulations of the Faculty of Mathematics and Natural Sciences of the University of Cologne, Germany. The PhD regulations from is available in the Appendix. The contents of the manuscripts, including text, citations, images, tables and data are normed to DIN A4 size and adapted to the general format of this thesis. The copyrights of the published works are held by Wiley-VCH (Weinheim) and by the Royal Society of Chemistry (London). A reprint permission of each manuscript is available in the Appendix. Following manuscripts are itemised chronologically by the date of publication. The order of the chapters reflects the scientific aim of this work (see Objectives and Outline).

1. Jong-Hoo Choi, Nils E. Schloerer, Josefine Berger and Martin H. G. Prechtl*, Synthesis and Characterisation of Ruthenium Dihydrogen Complexes and Their Reactivity Towards B–H Bonds, *Dalton Transactions*, **2014**, *43*, 290-299 (Full-Paper).[1]

2. Jong-Hoo Choi, Leo E. Heim, Mike Ahrens, Martin H. G. Prechtl*, Selective Conversion of Alcohols in Water to Carboxylic Acids by *In Situ* Generated Ruthenium Trans Dihydrido Carbonyl PNP Complexes, *Dalton Transactions*, **2014**, *43*, 17248-17254 (Full-Paper).

3. Jong-Hoo Choi, Martin H. G. Prechtl*, Tuneable Hydrogenation of Nitriles into Imines or Amines with a Ruthenium Pincer Complex under Mild Conditions, *ChemCatChem*, **2015**, *7*, 1023–1028 (Full-Paper).

[1] In this publication complex system **4/5** was discussed in the diploma thesis by the author Jong-Hoo Choi in 2012. An "Additions and Corrections" manuscript was submitted and published (), see Appendix, Supporting Information.

4. Dennis Pingen, Jong-Hoo Choi, Martin H. G. Prechtl*, Dieter Vogt*, Amide vs. Amine Paradigm in the Direct Amination of Alcohols with Ru-PNP Complexes, *ACS Catalysis*, **2015**, (Full-Paper, manuscript in preparation).

5. Jong-Hoo Choi, Miscellaneous Results Part 1: Acceptorless Dehydrogenative Alcohol Coupling with Primary Amines (unpublished results)
   Miscellaneous Results Part 2: Miscellaneous Results Part 2: Synthesis and Characterisation of a Pyrrole-Based PNP Ruthenium Complex (unpublished results).

3.1. Synthesis and Characterisation of Ruthenium Dihydrogen Complexes and Their Reactivity Towards B–H Bonds

Jong-Hoo Choi[a], Nils E. Schloerer[a], Josefine Berger[b] and Martin H. G. Prechtl[a]*, Synthesis and characterisation of ruthenium dihydrogen complexes and their reactivity towards B–H bonds, *Dalton Transactions*, 2014, **43**, 290-299 (Full-Paper). Received , Accepted .
[a] Department of Chemistry, University of Cologne, Greinstr. 6, 50939 Cologne, Germany. E-mail: martin.prechtl@uni-koeln.de; http://www.catalysislab.de; Fax: +49 221 470 1788; Tel: +49 221 470 1981, [b] Institute of Chemistry, Humboldt University at Berlin, Brook-Taylor-Straße 2, D-12489 Berlin, Germany, Electronic supplementary information (ESI) available.[2] CCDC 952413. For ESI and crystallographic data in CIF or other electronic format see DOI:10.1039/c3dt52037d.

Abstract

In this paper the synthesis and characterisation of ruthenium dihydrogen complexes bearing rigid aliphatic PNP pincer-type ligands are described. As one result hydride complexes were synthesised in good to high yields by a one-pot direct hydrogenation reaction. As another finding the dihydrogen complex, stabilised with a N–Me group in the ligand frame, can be converted with dimethylamine borane into a rare σ-boron complex [$RuH_2(BH_3)$(Me-PNP)] with rapid B–N decoupling. Additionally, we present the first mass spectrometric analysis of the synthesised σ-complexes via liquid injection field desorption/ionisation technique (LIFDI-MS).

[2]Supplementary Information is provided in the Appendix.

Introduction

The development of transition metal complexes is still a field of increasing interest for application in homogeneous catalysis such as hydrogenation,[1] dehydrogenation,[2] C–H bond[3] or B–H bond activation.[4] Amongst the large and various number of transition metal complexes, only a small collection is assigned to hydride complexes as intermediates, much less molecular dihydrogen complexes even though *Kubas et al.* first detected the molecular dihydrogen complexes in the 1980s. This expanded the diversity of complex chemistry.[5–7] Since then, several dihydrogen transition metal complexes have been reported. Molecular dihydrogen ligands are coordinated in a side-on arrangement to the metal centre as σ-complexes. This denotation is due to the interaction between the electron donating σ-orbital of the H_2 bond and the empty d-orbital at the metal centre and by the backdonation of the metal's d-orbitals into the empty σ^*-orbital of the hydrogen molecule. This type of bonding is also considered nonclassical due to its 3-centre–2-electron (3c–2e) bonding character.[8,9] Besides molybdenum and tungsten, various ruthenium based molecular dihydrogen complexes were reported, e.g., *Chaudret et al.* focussed on ruthenium based molecular dihydrogen complexes, stabilised by bulky ligands such as PCy_3 (complex **1**, Fig. 3.1).[10–12] Moreover, the reactivity of molecular dihydrogen complexes towards boryl adducts, such as amine boranes, turned into a field of increasing research due to its potential in the development of hydrogen storage systems. In recent reports, *Sabo-Etienne et al.* showed the reactivity of dihydrogen complex **1** in the presence of amine boranes by rapid hydrogen evolution. As a consequence, the transformation of complex **1** into "true" bis(σ-B-H) complexes **2a**–**c** was reported.[13,14] So far, only a small number of "true" σ-borane complexes have been isolated.[14,15]

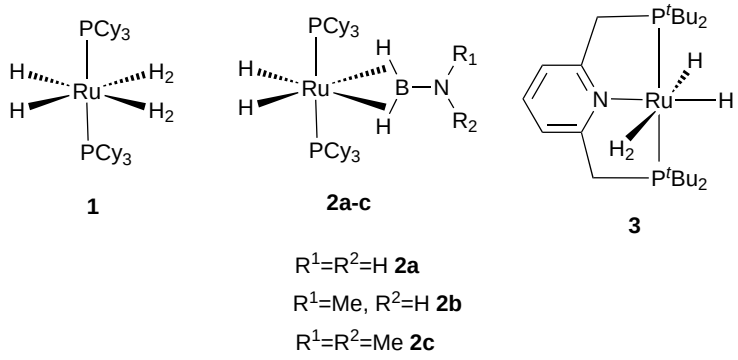

Figure 3.1. – Representative selection of ruthenium dihydrogen complexes and their bis(σ-B–H) aminoborane complexes.

Ruthenium dihydrogen complexes can also be stabilised with pincer ligands, for example complex **3** which was reported by *Leitner*. Complex **3** is capable of H/D exchange, hydrogenation or dehydrogenation and borylation of terminal alkynes.[3,16–18] Besides complex **3**,

Schneider et al. reported ruthenium hydride complexes with an aliphatic, rigid PNP-pincer ligand, which have been applied for homogeneous reduction of molecular dinitrogen to ammonia.[19] In their study, two polyhydride complexes (**4** and **5**) have been assigned as hydride complexes as intermediates (Fig. 3.2). However, the spectroscopic evidence provided by NMR relaxation time measurements was not convincing, since the presented data did not allow the extraction of a clearly defined $T_{1\mathrm{min}}$. The authors found for complex **4** a $T_{1\mathrm{min}}$ of 113 ms at 400 MHz, respectively 41 ms for complex **5**, and calculated H–H distances of 1.57 Å and 1.31 Å. Thus, they could be assumed with certain security as elongated dihydrogen complexes. Elongation of the hydrogen ligand in solution might have been affected by the coordinative character of the deuterated solvent THF. Therefore we used for T_1 measurements of the dihydrogen complexes deuterated toluene as a solvent. Herein we display the defined synthesis and characterisation of complexes **4** and **5** and the modified ruthenium hydride complex **6** bearing an aliphatic PNP ligand with a methylated nitrogen compound, following a typical synthetic protocol of ruthenium dihydrogen complexes.[18] Moreover, we report the reactivity of complex **6** towards B–H bonds. For each complex, we present the first mass spectra of air and moisture sensitive small ruthenium dihydrogen complexes which allowed us a deeper insight into the compositions of our synthesised complexes.

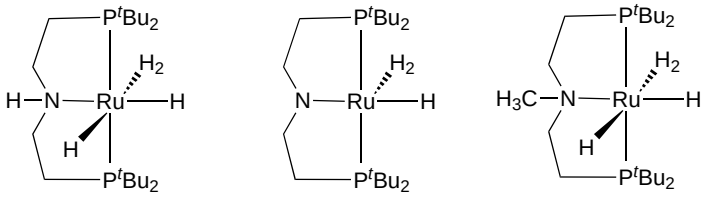

Figure 3.2. – Ruthenium dihydrogen complexes [Ru(H_2)H_2(HPNP)] **4**, [Ru(H_2)H(PNP)] **5** and [Ru(H_2)H_2(Me-PNP)] **6**.

Results and Discussions

Synthesis and Characterisation of Ruthenium Hydride 4 and 5

To synthesise the complexes **4** and **5**, ruthenium precursor **7** and PNP ligand **8** were pressurised with hydrogen gas to obtain a product mixture in 90% yield, consisting of 43% of complex **4** and 57% of complex **5** (Scheme 3.1). Starting with this product mixture, complex **5** was isolated but complex **4** appears to be stable only under a hydrogen atmosphere (see the Experimental section). Therefore, the product mixture was characterised by NMR and IR. The isolated complex **5** was analysed separately by IR and NMR, and the collected data were

compared with the extracted data of the product mixture. The similarity of both hydride species **4** and **5** allows differentiation of the signals in the low field of ^{31}P and in the high field of ^{1}H NMR. Complex **4** shows a singlet at 111.9 ppm in the ^{31}P NMR and a triplet at -8.26 ppm ($^{2}J_{PH}$ = 14.7 Hz) in the ^{1}H NMR spectrum, while the singlet in ^{31}P NMR for **5** appears at 114.3 ppm and its triplet signal in the ^{1}H NMR spectrum at -12.44 ppm ($^{2}J_{PH}$ = 10.6 Hz). For assignment of the ruthenium complexes to elongated and nonclassical hydrides (**4**–**5**), we performed T_1 relaxation time measurements of the complex mixture between 298 K and 193 K at 500 MHz in deuterated toluene. [Ru(H_2)H_2(PNP)] **4** passes through a substance specific minimum ($\theta_{\min}$) at 223 K with a $T_{1\min}$ value of 132 ms at 500 MHz (ESI, Fig. S 5.1). For [Ru(H_2)H(HPNP)] **5**, the $T_{1\min}$ value of 48 ms was matched at 207 K (ESI, Fig. S 5.2). The H-H distance d_{HH} for complex **4** has a calculated value of 1.17 Å and is assigned to the range of an elongated dihydrogen complex (1.1-1.36 Å) defined by *Kubas*.[12] In contrast to complex **4**, the trihydride [Ru(H_2)H(PNP)] **5** is assigned to a nonclassical dihydrogen complex (0.8-1.0 Å),[12] with a calculated H-H bond length of 0.99 Å.

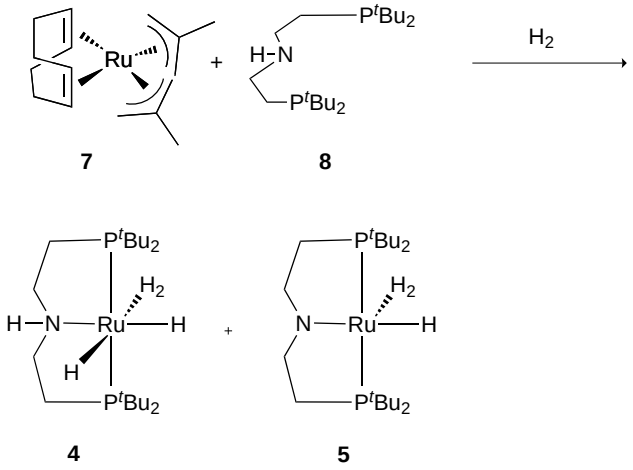

Scheme 3.1 – Synthesis of ruthenium dihydrogen complexes **4** and **5** by one-pot direct hydrogenation.

The IR spectra of both complexes show ν(M-H) bands (ESI, Fig. S 5.5) between 2034 and 2000 cm^{-1} in a typical range of Ru-H bonding.[20,21] For characteristic ν(M-H_2) vibration, complex **4** shows a significant RuH_2 band at 1726 cm^{-1}.[7] Complex **5**, probably due to its pyramidal arrangement and amide-type ligand, seems to have a shorter N-Ru bond length, an elongated Ru-H_2 distance and a shifted Ru-H_2 band at 1975 cm^{-1} as a shoulder of the bigger ν(M-H) band. The isotope pattern of complex **5** in the LIFDI-MS (Fig. 3.3) appears to be different from its simulated isotope pattern (ESI, Fig. S 5.12). This can be explained by the additional overlaps of isotope patterns of co-existent [Ru(H_2)H_2(HPNP)], [RuH_2(PNP)] and [RuH(PNP)] species with the *m/z* isotope pattern of [Ru(H_2)H(PNP)] generated during

the ionisation and analysis process under MS-conditions. Moreover, under MS conditions, we observed the formation of a decomposition product with a mass ∼101 units higher than complex **5** which can be tentatively assigned to a complex coordinating two Ru cores. The same observation has been made with other ruthenium complex under MS conditions. In consequence, summated intensities of ruthenium isotopes of different complexes are observed in the LIFDI-MS, shifting the m/z values of the collective pattern up to Δ2. However, the exact quantitative ratio of the existent ruthenium species could not be defined, but it can be reported that ruthenium hydride subspecies are coexistent in small amounts.

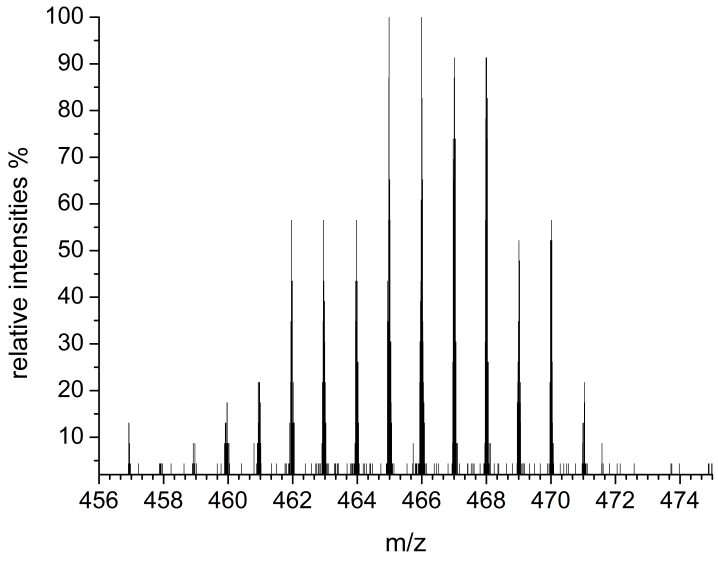

Figure 3.3. – LIFDI-MS analysis of [Ru(H_2)H(PNP)] **5** in toluene. Isotope pattern areas: [RuH(PNP)] 457–466, [RuH_2(PNP)] 458–467 and [Ru(H_2)H(PNP)] 459–468, [Ru(H_2)H_2(HPNP)] 461–470.

Equilibrium of Ruthenium Hydride 4 and 5

We assume that the lability of tetrahydride **4** can be explained by the cooperative properties of the H-PNP pincer backbone. The N-H ligand module can be deprotonated to complex **5**. The nitrogen building block serves as a proton donor and an acceptor similar to the benzylic position in pyridine based PNN or PNP pincer complexes.[1,22,23] Therefore, shifting the equilibrium towards the more stable complex **5** by removing one equivalent of H_2 was facile (Scheme 3.2), while the isolation of pure complex **4** was not possible under an argon atmosphere. Complex **5** in the presence of isopropanol as a hydrogen source in a closed system at 80 °C for 20 h emulates complex **4** until the equilibrium between the tetra- and trihydride complexes is restored. This process was monitored via ^{1}H and ^{31}P NMR in deuterated ben-

zene. Additionally, we achieved the full regeneration of complex **4** by treatment of complex **5** dissolved in deuterated toluene with 2 bar of hydrogen gas; the NMR showed the exclusive presence of tetrahydride **4**, which is stable only under a hydrogen atmosphere.

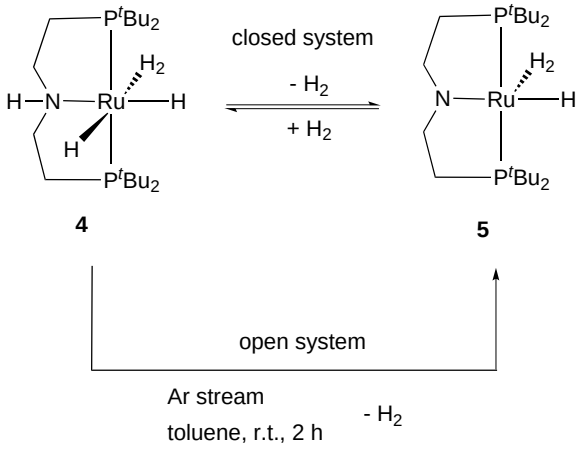

Scheme 3.2 – Equilibrium between ruthenium dihydrogen complexes **4** and **5** in the presence of isopropanol as a hydrogen source in a closed system monitored via ^{1}H and ^{31}P NMR. Complex **5** is isolated through a constant stream of argon.

Synthesis and Characterisation of [Ru(H$_2$)H$_2$(Me-PNP)] 6

Complex **6** was obtained by following the synthetic route of complexes **4** and **5** (Scheme 3.3). Contrary to ligand **8**, ligand **9** contains a methyl group blocking the nitrogen position. Therefore, cooperative properties acting as a proton donor or an acceptor are avoided, thus a conversion of the tetrahydride into a trihydride is not possible due to the absence of a neighbouring proton source. The synthesis of complex **6** provides yields between 64 and 67% as a powderous grey solid.

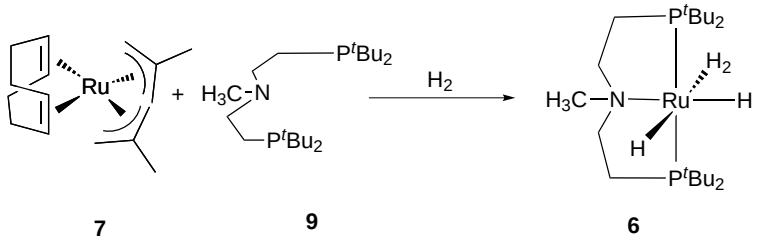

Scheme 3.3 – Synthesis of ruthenium dihydrogen complexes **6** by one-pot direct hydrogenation.

At room temperature, complex **6** shows a singlet signal at 108.7 ppm in the ^{31}P NMR spectrum as well as a characteristic triplet signal at -8.68 ppm ($^{2}J_{PH}$ = 13.8 Hz) in the ^{1}H NMR spectrum, allocating two hydride ligands and one dihydrogen ligand coordinated to ruthenium. The T_1 measurement of complex **6** resulted in a $T_{1\mathrm{min}}$ value of 54 ms at 224 K in deuterated toluene with a spectrometer frequency of 500 MHz. The H-H bond length of 1.01 Å was calculated, which assigns complex **6** to a nonclassical dihydrogen complex (ESI, Fig. S 5.4). The IR spectrum of [Ru(H_2)H_2(Me-PNP)] **6** indicates the dihydrogen ligand vibration ν(M–H) between 1972 and 1923 cm^{-1} (ESI, Fig. 5.6), and the vibration of the hydrides ν(M–H_2) at 1776 cm^{-1}, similar to complex **4** with an analogue octahedral complex arrangement. Compared to the LIFDI-MS isotope pattern of complex **5**, the LIFDI-MS isotope pattern of complex **6** shows a relatively neat isotope pattern of ruthenium species [Ru(H_2)H_2(Me-PNP)] (Fig. 3.4) and is in good agreement with its simulated isotope pattern (ESI, Fig. S 5.17).

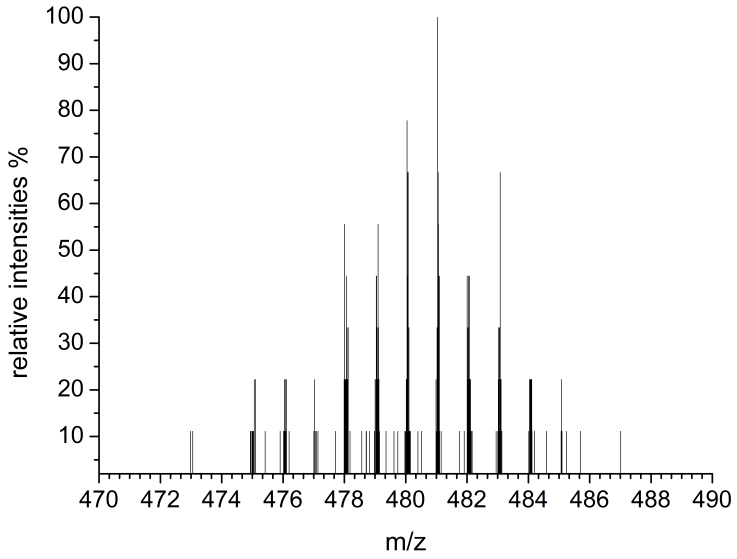

Figure 3.4. – LIFDI-MS analysis of [Ru(H_2)H_2(Me-PNP)] **6** in toluene. Isotope pattern areas: [RuH_2(Me-PNP)] 473–482, [Ru(H_2)H(Me-PNP)] 474–485 and [Ru(H_2)H_2(Me-PNP)] 475–484.

Reactivity of [Ru(H$_2$)H$_2$(Me-PNP)] 6 Towards B–H Bonds

[Ru(H$_2$)H$_2$(Me-PNP)] **6** reacts sensitively to B-H bonds with rapid hydrogen evolution. In this work we particularly identified the reaction with pinacolborane and dimethylamine borane leading to ruthenium boryl complexes **10** and **11**.

Synthesis and Characterisation of [RuH$_2$(HBPin)(Me-PNP)] 10

[RuH$_2$(HBPin)(Me-PNP)] **10** was obtained in toluene with 1.0-1.1 equivalents of pinacolborane under rapid hydrogen evolution as a solid in 88% yield after removing the solvent (Scheme 3.4). The IR spectrum of complex **10** shows the ν(M-H) band at 2024 cm^{-1} and the two bridging hydride bands ν(M-H-B) between 1973 and 1914 cm^{-1} and between 1744 and 1675 cm^{-1} (ESI, Fig. 5.7). In deuterated cyclohexane, the characteristic signals appear in the highfield region of ^{1}H NMR at -5.64, -9.02 and -18.85 ppm as broad singlets assigned to the bridging hydrides and the Ru-H hydride. In contrast to complex **10**, the comparable borylated PNP complex with a pyridine backbone obtained by the ruthenium dihydrogen complex **3** contains only one singlet signal for the bridging hydrides in the ^{1}H NMR spectrum, which is presumably caused by the electronic effect of the ligand and the generally vibrant system of the complex.[17] In fact, only one signal was detected in the ^{31}P NMR spectrum at 92.1 ppm, which excludes the assumption of a second similar complex. LIFDI-MS analysis confirmed structure **10** (m/z 602–610, Fig. 3.5). Furthermore, fragments of [RuH$_2$(Me-PNP)] and [RuH$_3$(Me-PNP)] were detected in the MS. The approaching simulated isotope pattern of [RuH$_3$(Me-PNP)] (red) is in good agreement with the analysed fragment (black) which consists mainly of the [RuH$_3$(Me-PNP)] species.

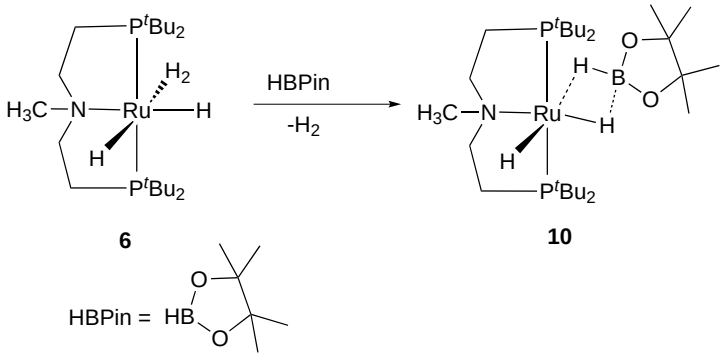

Scheme 3.4 – Reaction of **6** with pinacolborane to complex **10** with evolution of hydrogen gas.

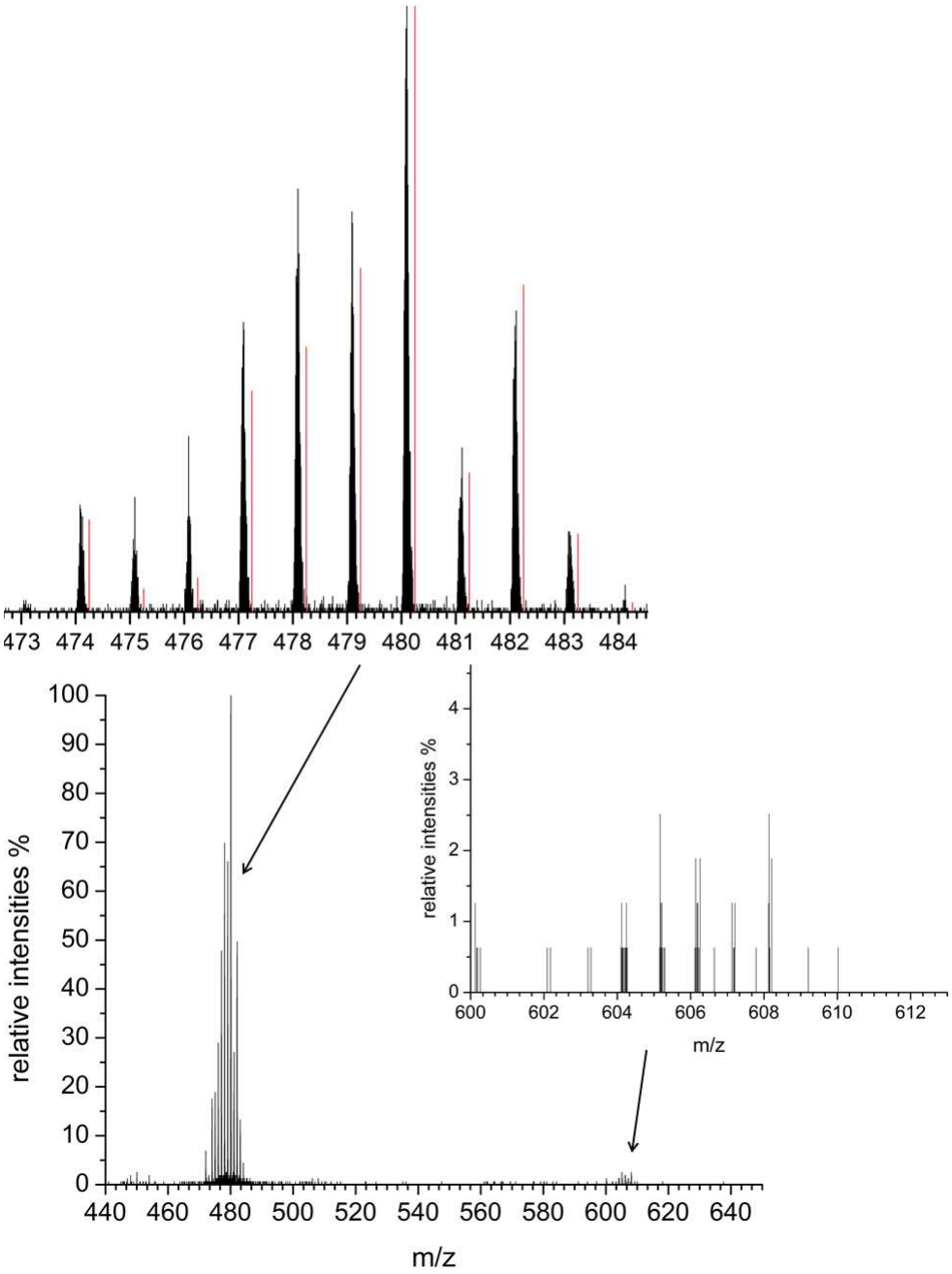

Figure 3.5. – LIFDI-MS analysis of [RuH_2(HBPin)(Me-PNP)] **10** in toluene. Isotope pattern areas: [RuH_2(HBPin)(Me-PNP)] 602–610. [RuH_2(Me-PNP)] 473–482 (black), [Ru(H_2)H(Me-PNP)] 474–484 (black) in comparison to the simulated isotope pattern of fragment [RuH_3(Me-PNP)] 474–484 (red).

Synthesis and Characterisation of (σ-B–H) Complex [$RuH_2(BH_3)$-(Me-PNP)] 11

[$RuH_2(BH_3)$(Me-PNP)] **11** was obtained with different synthetic routes (**a**–**b**, Scheme 3.5). The reaction of dihydrogen complex **6** with 2-3 equivalents of the THF borane complex (1 M in THF) in a mixture of toluene and pentane resulted in rapid hydrogen evolution. Although high yields (89%) and high conversions (>95%) were obtained THF traces were still visible in the ^{1}H NMR. More interestingly, the synthetic route b adding 3-5 equivalents of dimethylamine borane led to the decoupling of the N-B bond with the formation of the (σ-B-H)-ruthenium complex **11** and loss of the dimethylamine in 91% yields. This reactivity stays in contrast to previous reports by *Sabo-Etienne* where the dihydrogen complex [$Ru(PCy_3)_2(H_2)(H_2)_2$] **1** reacts with amine boranes under dehydrogenation to bis-σ-borane complexes **2a**–**c** (Scheme 3.5). In their observation, two dihydrogen σ-ligands were substituted by the borane with formations of σ-B-H bonds and simultaneously the B–N adducts were connected. This observation might be related to slightly different electronic properties of the ruthenium core in [$Ru(PCy_3)_2(H_2)(H_2)_2$] **1** compared to [$Ru(H_2)H_2$(Me-PNP)] **6**, which could be explained by the different ligand types (monodentate ligands vs. pincer ligand). The ^{31}P NMR spectrum of complex **11** shows a singlet signal at 84.9 ppm. At room temperature, the characteristic signals in the ^{1}H NMR appear at 5.42 ppm as a broad singlet signal, attributed to the terminal hydrogen atoms of boron. The broad singlet signals at -5.69 and -19.76 ppm are assigned to the bridging hydrides. The remaining hydride signal appears at -17.85 ppm as a triplet of doublets. At lower temperatures, the broad signals were sharpened and the triplet of doublets at -17.85 ppm was adjusted into a clear triplet (Fig. 3.6). Also integral assignments of the hydrogen atoms in the ^{1}H NMR spectrum were more accurate at temperatures below 278 K.

Reaction of dihydrogen complex **6** with borane compounds:

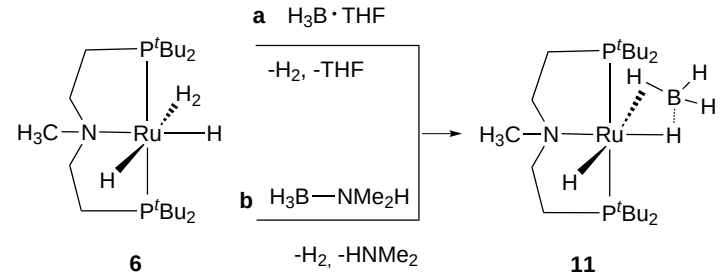

Reaction of dihydrogen complex **1** with amine borane:

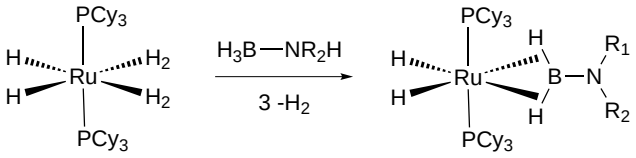

R^1=R^2=H **2a**

R^1=Me, R^2=H **2b**

R^1=R^2=Me **2c**

Scheme 3.5 – Reaction of **6** to complex **1** with evolution of hydrogen gas. Synthetic route a with THF borane complex, synthetic route b with dimethylamine borane in comparison to complex **1** with amine boranes leading to complex **2a**–**c**.[13]

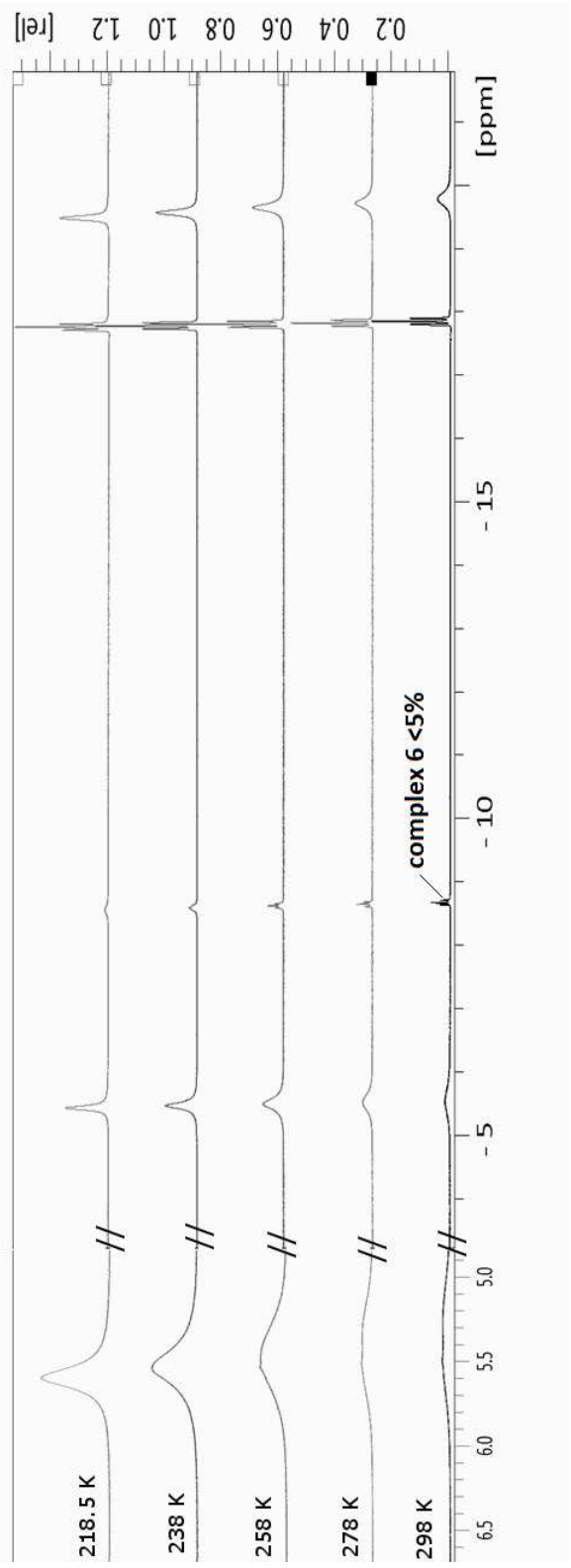

Figure 3.6. – ^{1}H NMR signals (Ru–H, BH_3) of $[RuH_2(BH_3)]$ **11** at various temperatures between 218.5 and 298 K in deuterated toluene (400 MHz).

The IR spectrum of complex **11** obtained with route a contains traces of THF, but is congruent with the complex **11** obtained with route **b** (Fig. 3.7). Two strong bands appear at 2394 and 2330 cm^{-1} in a typical range of terminal B–H region.[4,15,24–26] The ν(M-H) was found at 2020 cm^{-1} and is in accordance with previous reports.[4,20,21,26] The band at 1693 cm^{-1} can be carefully assigned to ν(Ru–H–B).[15] No characteristic N–Me or N–H band of the amine borane adduct was found either in the ^{1}H or ^{13}C NMR spectra or in the IR spectrum in the region of 3000 cm^{-1} or higher. This profoundly indicates that no ruthenium dimethylaminoborane complex has been generated with route b, but a σ-B–H typed BH_3 ruthenium complex instead.

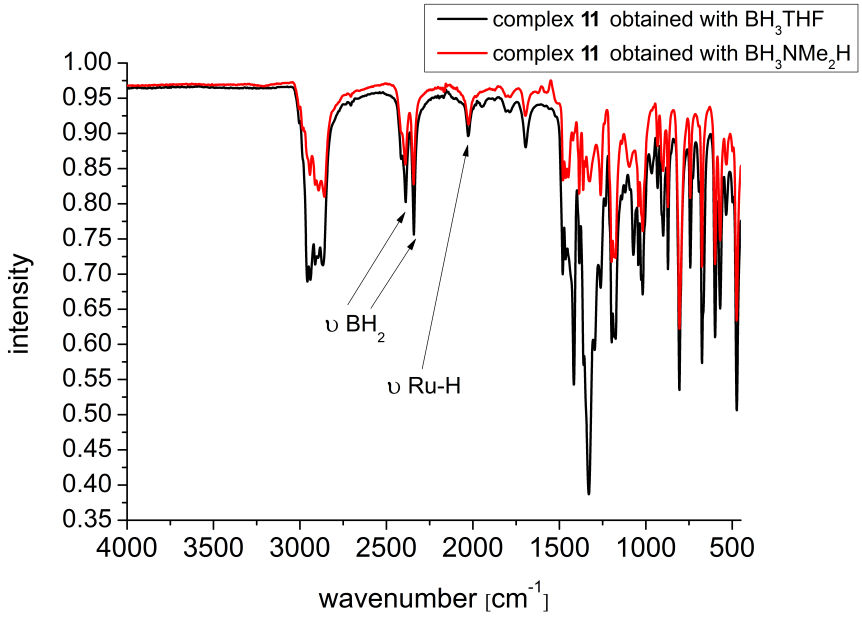

Figure 3.7. – IR spectra of complex **11**. Vibrational bands are identical beside the THF traces independent from the different synthetic routes with BH_3THF (black) or BH_3NMe_2H (red).

The single crystal X-ray analysis of the structure was determined at 293 K (Fig. 3.8, Table 3.1). Further refinement parameters and collected data are listed in the ESI. The hydrogen atoms (H1-H5) were approached by electron densities around the ruthenium and boron atoms. Thus we located the most likely electron density for H1 which contains a short distanced Ru1-H1 bond length of slightly under <1.4 Å. Despite the imprecise short bond length of Ru1-H1, the location of H1 confirms only the *trans* arrangement of the hydride. Furthermore the Ru-B distance is 2.19(2) Å and thus in the range of previously reported agostic ruthenium boron complexes.[13,14] The bridging hydrogen atom (H2), which replaced the position of the molecular hydrogen ligand of complex **6**, is located 1.69(2) Å next to the ruthenium atom and 1.31(6) Å to the boron atom with an angle (degree) of 92.76 for Ru1-H2-B1 on the *trans* axial position to the terminal hydride (H1). This arrangement is in agreement with a typical

"true" (σ-B-H)-bonding to ruthenium reported by *Sabo-Etienne et al.*[13,14] Moreover, H1 can be attributed as a hydride, although the short Ru1-H5 distance of 1.48(8) Å is rarely known in the literature, but throughout transition metal–hydride distances of Ni-H, Fe-H, Pt-H or Ru-H around 1.5 Å or <1.5 Å have been already reported by others.[27–31] More interestingly the B1-H5 distance remains too stretched with 1.84(2) Å for a fixed B-H bonding mode. This fact encouraged us to assume the coordinated boron as a σ-BH_3 adduct instead of the originally considered η^2-type BH_4^- adduct with expected symmetric arrangement for both hydrides H2 and H5 with distances of 1.67-1.85 Å to ruthenium and 1.25-1.3 Å to boron, such as the PNP ruthenium η^2-BH_4^- complex spotted by *Milstein*.[24] In our case, the rare type of σ-boron complex **11** is most comparable with the [$IrH_2(BH_3)$-(POCOP)] complex presented by *Goldberg* and *Heinekey*.[15] Despite the different transition metal, they reported a similar arrangement of the boron and hydrides to the iridium centre. The [$IrH_2(BH_3)$(POCOP)] complex also contains a bridging hydride in a σ-B-H fashion with a distance to ruthenium of around 1.90 Å and to boron of around 1.45 Å. The opposite Ru-H-B bonding distance of 1.74 Å (Ru-H and H-B) is too stretched to be considered as a BH_4^- rather than a BH_3 adduct. All together, the similarity of [$IrH_2(BH_3)$(POCOP)] to complex **11** clearly argues against the assumption of a η^2-BH_4^- adduct, but emphasises the existence of a σ-borane complex. Moreover the solid state structure of **11** confirms the bond cleavage of the dimethylamine borane. The reactivity of complex **6** towards THF borane complex or dimethylamine borane, in routes **a** and **b**, remains still uncleared, but regarding the borane compounds as Lewis-pairs, it is plausible that THF or dimethylamine is replaced by a stronger Lewis base system (Fig. 3.9). In this case, the methyl group of the PNP backbone of complex **6** could electronically influence the ruthenium metal centre by inducing Lewis-base character into the system. This consideration would explain the possibility of a Lewis-pair exchange during the synthesis of complex **11**. Furthermore, the basic character of complex **11** could tend to draw the more "protic" hydride H5 closer to the ruthenium centre, which would explain the short distance of Ru1–H5 of 1.48(8) Å. LIFDI-MS analysis of [$RuH_2(BH_3)$(Me-PNP)] **11** confirms additionally the assumed structure (Fig. 3.10) and is in agreement with the simulated isotope pattern (ESI, Fig. S 5.23).

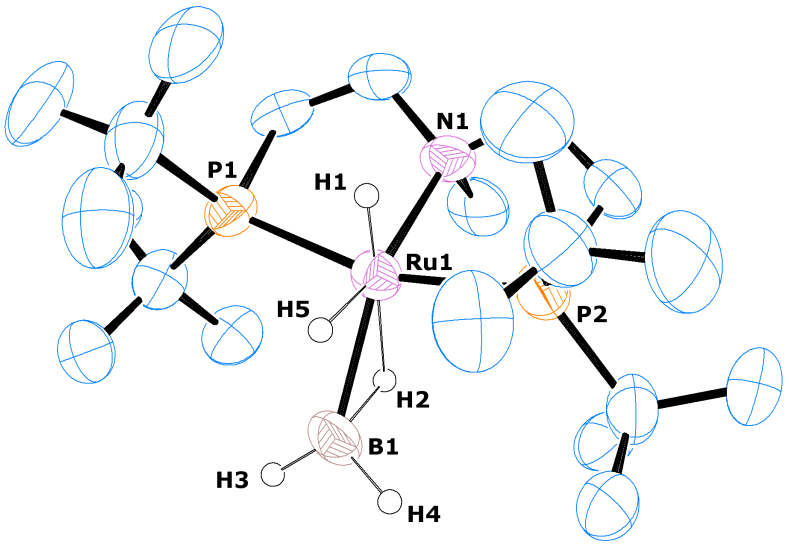

Figure 3.8. – ORTEP diagram of the single crystal structure of complex **11**. Ellipsoids are illustrated at 50% possibility. All hydrogen atoms are faded out except for H1–H5 for clarity.

Table 3.1. – Selected bond distances[a] and angles[b] of complex **11**.

Ru1-P1	2.32(7)	P1-Ru1-P2	163.06
Ru1-P2	2.33(3)	Ru1-H2-B1	92.76
Ru1-N1	2.18(9)	H1-Ru1-H2	170.78
Ru1-H1	1.36(6)	H1-Ru1-P1	63.28
Ru1-H5	1.48(8)	H1-Ru1-P2	65.96
Ru1-H2	1.69(2)	N1-Ru1-B1	143.08
Ru1-B1	2.19(2)	H3-B1-H4	108.16
B1-H2	1.31(6)		
B1-H5	1.84(2)		
B1-H3	1.04(6)		
B1-H4	1.15(7)		

[a] Distances are given in Å.
[b] Angles are reported in degrees.

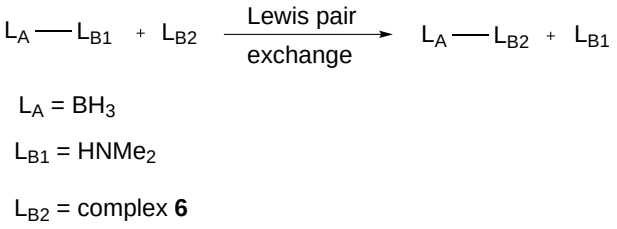

Figure 3.9. – Simplified Lewis pair exchange, THF or $HNMe_2$ is replaced by a stronger Lewis base (complex **6**).

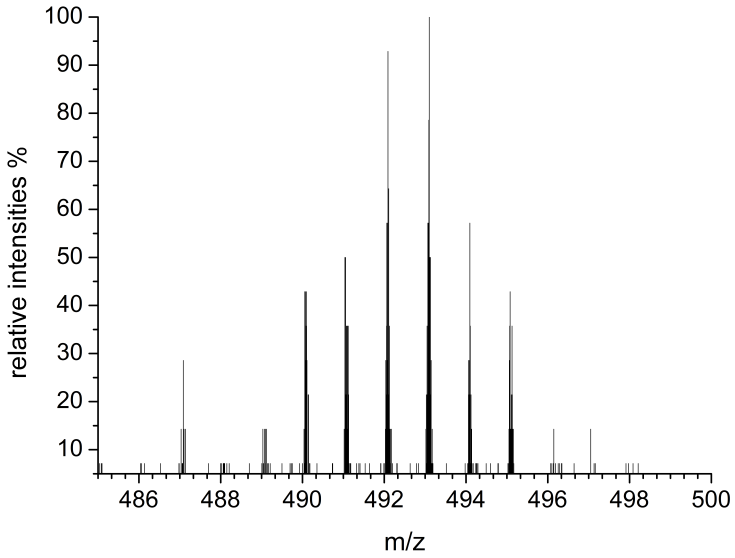

Figure 3.10. – LIFDI-MS analysis of $[RuH_2(BH_3)(Me\text{-}PNP)]$ **11** in toluene. Isotope pattern area: $[RuH_2(BH_3)(Me\text{-}PNP)]$ 487–498.

Conclusion

In summary, we demonstrated an efficient and simple synthesis of ruthenium dihydrogen complexes **4**–**6**, stabilised with a rigid aliphatic PNP backbone. These complexes have been characterised via T_1 spin lattice measurement as molecular dihydrogen complexes (**5** and **6**) and as an elongated dihydrogen complex **4**. The methylated pincer ligand of complex **6** shows the major influence on its electron density and proved to be highly active towards B-H groups, emphasising the formation of complex **10** and the B-N decoupling of the dimethylamine borane to a rare σ-borane complex **11**. All structures have been confirmed by LIFDI-MS analysis, which allowed us a good insight into the complexes.

Experimental Section

General Information

Reactions were generally prepared under an argon atmosphere using *Schlenk* techniques, flame-dried glassware and a *Labmaster 200* glove-box from *Mbraun*. High-pressure hydrogen reactions were performed in a *Büchi Tinyclave* (50 mL) glass autoclave. All solvents and reagents were purchased from *Acros*, *Merck*, *Sigma-Aldrich*, *Fluka*, *Strem* or were acquired from the institute stock. Commercial anhydrous solvents and argon gas packed reagents were used as received and stored in the glove-box under an argon atmosphere. Non-anhydrous solvents were dried and distilled (under vacuum or argon) prior to use, applying standard procedures. The water content of solvents, alcohols and amines has been quantified by *Karl-Fischer* titration.

Analytic Methods

^{1}H, ^{13}C, ^{11}B, ^{31}P NMR spectra were recorded using a *Bruker Avance II 300* spectrometer and a *Bruker Avance II+ 600* spectrometer using deuterated benzene, toluene, cyclohexane, THF and deuterium oxide as solvents at room temperature. ^{1}H NMR spectra measurements at various temperatures were recorded using a *Bruker Avance 400* spectrometer. ^{1}H shifts are reported in ppm (δ_{H}) downfield from TMS and were determined by reference to the residual solvent peaks (C_6D_6: 7.16 ppm, C_7D_8: 7.09 ppm, C_6D_{12}: 1.38 ppm, THF-d_8: 3.58 ppm, D_2O: 4.75 ppm). Chemical shifts are reported as singlet (s), doublet (d), triplet (t), quartet (q) and multiplet (m). Coupling constants J were reported in [Hz]. ^{13}C NMR spectra were recorded using the APT or DEPTQ sequence. ^{13}C shifts are reported in ppm (δ_{C}) relative to the solvent resonance (C_6D_6: 128.0 ppm, C_7D_8: 137.8 ppm, C_6D_{12}: 26.4 ppm, THF-d_8: 25.4 ppm). ^{31}P NMR chemical shifts are reported in ppm (δ_{P}) downfield from H_3PO_4 and referenced to an external 85% solution of H_3PO_4 in D_2O. For measurements of air sensitive chemical compounds and for spin lattice relaxation time (T_1) experiments, *Young-Teflon* Capped NMR tubes from *Wilmad* were used. T_1 measurements were carried out at 500 MHz using a *Bruker DRX 500*. Infrared spectra (IR) were measured at room temperature under argon (Glovebox) using a *Bruker Alpha* spectrometer equipped with a Diamond-ATR IR unit. Data are reported as follows: absorption $\tilde{\nu}$[cm^{-1}], weak (w), medium (m), strong (s). LIFDI-MS (Liquid Injection Field Desorption/Ionization-Mass Spectrometry) was performed using a *Waters micromass Q-ToF-2*$^{\mathrm{TM}}$ mass spectrometer equipped with a *LIFDI 700 ion source (Linden CMS)*.

Synthesis of [Ru(H_2)H_2(PNP)] 4 and [Ru(H_2)H(PNP)] 5

In an argon flushed *Büchi* glass autoclave, 320 mg (1.0 mmol, 1.0 eq.) [Ru(COD)(2-methyl-allyl)$_2$] **7** were added to 400 mg (1.1 mmol, 1.1 eq.) of PNP ligand **8** in 5 mL pentane. After the autoclave was filled with H_2 gas to 5 bar at room temperature, the content was stirred for 48 h at 55 °C. With the increase in temperature to 55 °C, a H_2 pressure of 7 bar was reached. After the reaction mixture was cooled to room temperature, the autoclave was depressurised and flushed twice with argon. After separating the orange mother liquor with a cannula from the yellow solid (mixture **4** and **5**), the product mixture was washed twice with pentane. The pentane was removed via cannula and the product mixture was dried under argon and stored at -34 °C. Yield: 397.0 mg (product mixture), 0.85 mmol, 85%.[3]

Spectral data of complex 4. ^{1}H NMR (500 MHz, toluene-d$_8$): δ_H [ppm] = 4.55 (weak s, 1H, N-H (H/D-exchange)), 2.91-2.86 (m, 2H, NCH_2), 2.54-2.44 (m, 2H, NCH_2), 2.14-2.12 (m, 2H, PCH_2), 1.67-1.63 (m, 2H, PCH_2), 1.41 (t, 18H, $^{3}J_{PH}$ = 6.1 Hz, $PC(CH_3)_3$), 1.36 (t, 18H, $^{3}J_{PH}$ = 6.0 Hz, $PC(CH_3)_3$), -8.26 (t, 4H, $^{2}J_{PH}$ = 14.7 Hz, Ru-H). ^{13}C NMR (75 MHz, benzene-d$_6$): δ_C [ppm] = 55.7 (-CH_2-), 34.7-32.1 ($PC(CH_3)_3$), 30.8-30.5 ($PC(CH_3)_3$), 27.4 (-CH_2-). ^{31}P NMR (121 MHz, toluene-d$_8$): δ_P [ppm] = 111.9 (s). T_1 (500 MHz, toluene-d$_8$) = 298 K (312 ms), 258 K (184 ms), 238 K (148 ms), 228 K (135 ms), 221 K (132 ms), 208 K (141 ms), 198 K (169 ms), 193 K (191 ms); ($T_{1\min}$ = 132 ms, 223 K).

Spectral data of complex 5. ^{1}H NMR (500 MHz, toluene-d$_8$): δ_H [ppm] = 3.46-3.44 (m, 4H, NCH_2), 1.91–1.85 (m, 4H, PCH_2), 1.30 (t, 36H, $^{3}J_{PH}$ = 12.1 Hz, $PC(CH_3)_3$), -12.44 (t, $^{2}J_{PH}$ = 10.6 Hz). ^{13}C NMR (75 MHz, benzene-d$_6$): δ_C [ppm] = 65.6 (-CH_2-), 34.7 ($PC(CH_3)_3$), 29.6 ($PC(CH_3)_3$), 26.1 (-CH_2-). ^{31}P NMR (121 MHz, toluene-d$_8$): δ_P [ppm] = 114.3 (s). T_1 (500 MHz, toluene-d$_8$) = 298 K (138 ms), 258 K (97 ms), 238 K (69 ms), 228 K (59 ms), 221 K (52 ms), 208 K (48 ms), 198 K (50 ms), 193 K (53 ms); ($T_{1\min}$ = 48 ms, 207 K).

IR (**4** and **5**): $\tilde{\nu}$[cm^{-1}] = 3291 (w), 2852-2947 (m), 2034-1995 (m), 1726 (m), 1470 (m), 1383 (m), 1359 (m), 1202 (w), 1174 (m), 1053 (w), 1016 (m), 923 (m), 798 (s), 764 (w), 672 (m), 644 (w), 600 (m), 565 (m), 471 (s), 432 (m).

Isolation of Dihydrogen Complex 5

In an argon flushed *Schlenk* flask, 25 mg (1.0 eq., 0.054 mmol) of the mixture of complexes **4** and **5** were dissolved in 2 mL toluene. The content was stirred for 1 h at room temperature under a slow stream of argon. The brown-red coloured liquid was removed in vacuo until a green solid **5** remained. The product was stored under an argon atmosphere at -34 °C. Yield: 18.0 mg, 0.04 mmol, 75%.

[3] For limited spectral and crystallographic data see ESI.

LIFDI-MS: *m/z* 468.0 (M^+, 91.3), 470.1 (91.3), 466.0 (100), 465.0 (100), 464.0 (56.5), 462.9 (56.5), 462.0 (56.5), 461.0 (21.7), 460.9 (8.7), 460.0 (17.4), 459.0 (8.7).

^{1}H NMR (400 MHz, benzene-d_6): δ_H [ppm] = 3.46-3.42 (m, 4H, NCH_2), 1.90-1.85 (m, 4H, PCH_2), 1.22 (t, 36H, $^2J_{PH}$ = 6.0 Hz, $PC(CH_3)_3$), -12.53 (t, $^2J_{PH}$ = 10.7 Hz). ^{13}C NMR (75 MHz, benzene-d_6): δ_C [ppm] = 65.6 (-CH_2-), 34.7-32.1 ($PC(CH_3)_3$), 29.6 ($PC(CH_3)_3$), 26.1 (-CH_2-). ^{31}P NMR (121 MHz, benzene-d_6): δ_P [ppm] = 114.3 (s).

IR: $\tilde{\nu}$[cm^{-1}] = 3291 (w), 2811-2950 (m), 2024 (m), 1471 (m), 1383 (w), 1361 (m), 1323 (m), 1204 (m), 1171 (m), 1151 (m), 1093 (w), 1058 (m), 1018 (m), 964 (w), 930 (w), 801 (m), 733 (m), 692 (m), 580 (m), 521 (m), 471 (s).

Generation of Dihydrogen Complex 4 under H_2 Atmosphere

11 mg (1.0 eq., 0.023 mmol) of complex **5** was dissolved in 0.1 mL deuterated toluene and introduced in an argon flushed NMR pressure tube. The NMR tube was pressurised with 2 bar of hydrogen gas. After 60 h at room temperature, the colour of the content turned from orange into yellow. Full conversion of complex **5** into **4** was detected by NMR.

Spectral data of complex 4. ^{1}H NMR (600 MHz, toluene-d_8): δ_H [ppm] = 4.55 (weak, 1H, (H/D-exchange)), 2.92-2.88 (weak, m, 2H, NCH_2), 2.58-2.43 (m, 2H, NCH_2), 1.94-1.88 (m, 2H, PCH_2), 1.67-1.63 (m, 2H, PCH_2), 1.41 (t, 18H, $^3J_{PH}$ = 5.9 Hz, $PC(CH_3)_3$), 1.30 (t, 18H, $^3J_{PH}$ = 5.9 Hz, $PC(CH_3)_3$), -8.25 (t, 4H, $^2J_{PH}$ = 14.5 Hz, Ru-H). ^{13}C NMR (75 MHz, toluene-d_8): δ_C [ppm] = 55.7 (-CH_2-), $PC(CH_3)_3$), 30.8-30.4 ($PC(CH_3)_3$), 27.4 (-CH_2-). ^{31}P NMR (121 MHz, toluene-d_8): δ_P [ppm] = 111.9 (s); Note to ^{13}C NMR: The quaternary carbons between 34.7 and 32.1 (see synthesis of complexes **4** and **5**) were not detected due to low solubility of complex **5** in 0.1 mL deuterated toluene, pointing out that the NMR pressure tube has an inner measurable volume of 0.1 mL.

Synthesis of Me-PNP Ligand 9

Synthesis of *N*-methyl bis(2-chloroethyl)amine hydrochloride. 17.0 g (0.096 mol) bis(2-chloroethyl)amine hydrochloride and 10.0 g (0.2 mol) formic acid were added to 20 mL of a 37% formaldehyde solution in a 500 mL round bottom flask equipped with a reflux condenser. After the reaction mixture was refluxed for 3 h at 100 °C and cooled to room temperature, the solvent was removed *in vacuo* until a yellow white solid was obtained. For further purification, the solid was dissolved in 100 mL THF. After removing the solvent, the product was obtained as a white solid which was directly used for the synthesis of PNP ligand **9** (18.41 g, 99%).

^{1}H NMR (300 MHz, D_2O): δ_H = 2.96 (s, 3H, NCH_3), 3.63 (bs, 4H, -CH_2CH_2-), 3.93 (t, 4H, $^2J_{HH}$ = 5.8 Hz, -CH_2CH_2-).

Synthesis of Me-PNP 9

In a flame dried and argon flushed 500 mL *Schlenk* flask, 8.75 mL (47.15 mmol, 2.3 eq.) of di-tert-butyl phosphine was dissolved in 60 mL diethyl ether. After cooling to -78 °C, 18 mL of a 2 M in hexane butyl lithium solution was added dropwise to the content under constant stirring. The reaction mixture was allowed to reach room temperature and the *Schlenk* flask was equipped with a reflux condenser and heated for 4 h at 50 °C under an argon atmosphere until a yellow solid of di-*tert*-butyl phosphine lithium was obtained. In a flame dried and argon flushed 250 mL *Schlenk* flask 3.9 g (20.5 mmol, 1.0 eq.) *N*-methyl bis(2-chloroethyl)amine hydrochloride was dissolved in 50 mL diethyl ether and cooled to -78 °C. Under constant stirring, 8.16 mL of a 2 M in hexane butyl lithium solution was added dropwise within 30 min to the content. After allowing the reaction mixture to reach room temperature, the content was stirred for 2 h and transferred slowly via a transfer cannula to the precooled di-*tert*-butyl phosphine lithium in the 500 mL *Schlenk* flask at -78 °C. The unified reaction mixture was allowed to reach room temperature and then refluxed overnight at 60 °C under an argon atmosphere. The reaction mixture was allowed to reach room temperature, the solution was separated in a flame dried and argon flushed *Schlenk* tube from the solid lithium chloride via centrifuge. The ether was removed *in vacuo* and replaced with 50 mL pentane. The content was extracted 3 times with degassed water and dried over magnesium sulphate. After filtration, the solvent was removed in vacuo to obtain a yellow oil (5.3 g, 14.15 mmol, 69% yield, purity 67%). Major impurities stemmed from the excess of di-*tert*-butyl phosphine. Ligand **9** was used without further purification. For analytical data, the product was dissolved in a solution of pentane and triethylamine (1 : 1). After stirring the content for 30 min, the solvent mixture was removed in vacuo to obtain a clearer oil with a purity of 80% or higher.

^{1}H NMR (300 MHz, benzene-d$_6$): δ_H = 2.91-2.84 (m, 4H, -CH_2CH_2-), 2.40 (s, 3H, CH_3), 1.81-1.74 (m, 4H, -CH_2CH_2-), 1.23 (18H, s, PC$(CH_3)_3$), 1.20 (18H, s, PC$(CH_3)_3$). ^{13}C NMR (75 MHz, benzene-d$_6$): δ_C = 58.9-58.4 (-CH_2-), 41.8 (NCH_3), 31.2-30.6 (PC$(CH_3)_3$), 29.7-29.5 (P$C(CH_3)_3$), 20.0-19.7 (-CH_2-), ^{31}P NMR (121 MHz, benzene-d$_6$): δ_P = 24.7 (s).

Synthesis of [Ru(H_2)H_2(Me-PNP)] 6

In an argon flushed *Büchi* glass autoclave, 240 mg (0.75 mmol, 1.0 eq.) of [Ru(COD)(2-methyl-allyl)$_2$] **7** were added to 413 mg (regarding the purity grade of 67%, 1.1 mmol, 1.45 eq.) of ligand **9** in 5 mL pentane. After the autoclave was filled with H_2 gas to 5.5 bar at room temperature, the content was stirred for 48 h at 60 °C. With the increase in temperature to 60 °C, a H_2 pressure of 6.5 bar was reached. After the reaction mixture was cooled to room temperature, the autoclave was depressurised, flushed twice with argon and stored under an argon atmosphere at -34 °C for 12 h. The dark red mother liquor was separated with a

cannula from the grey solid and the product was washed twice with precooled pentane. The pentane was removed via a cannula and the product was dried under argon and stored at -34 °C. Yield: 242 mg, 0.50 mmol, 67%.

LIFDI-MS: *m/z* 484.1 (M^+, 22.2), 483.1 (66.7), 483.0 (33.3), 482.0 (44.4), 481.1 (100), 480.0 (77.8), 479.1 (55.5), 479.0 (44.4), 478.1 (33.3), 478.1 (44.4), 478.0 (55.6), 477.1 (22.2), 477.0 (11.1), 476.1 (22.2), 476.0 (11.1), 475.1 (22.2), 475.0 (11.1).

^{1}H NMR (300 MHz, toluene-d_8): δ_H ppm = 2.5-2.43 (m, 2H, NCH_2), 2.4 (s, 3H, -CH_3), 2.28-2.18 (m, 2H, NCH_2), 1.81-1.74 (m, 2H, PCH_2), 1.64-1.58 (m, 2H, PCH_2), 1.44 (t, 18H, $^3J_{PH}$ = 6.1 Hz, $PC(CH_3)_3$), 1.31 (t, 18H, $^3J_{PH}$ = 6.1 Hz, $PC(CH_3)_3$), -8.68 (t, 4H, $^2J_{PH}$ = 13.8 Hz). ^{13}C NMR (75 MHz, toluene-d_8): δ_C [ppm] = 66.3-66.2 (-CH_2-), 53.3 (-CH_3), 34.1 ($PC(CH_3)_3$), 31.9 ($PC(CH_3)_3$), 30.9-30.7 ($PC(CH_3)_3$), 25.6 (-CH_2-). ^{31}P NMR (121 MHz, toluene-d_8): δ_P [ppm] = 108.7 (s). T_1 (500 MHz, toluene-d_8) = 299 K (198 ms), 278 K (130 ms), 268 K (106 ms), 258 K (86 ms), 248 K (71 ms), 238 K (60 ms), 228 K (53 ms), 218 K (54 ms), 208 K (62 ms), ($T_{1\mathrm{min}}$ = 54 ms, 224 K).

IR: $\tilde{\nu}$[cm^{-1}] = 2985 (w), 2937-2856 (m), 1972-1923 (m), 1776 (m), 1475-1446 (m), 1415 (w), 1383 (m), 1362 (w), 1350 (m), 1317 (w), 1235 (w), 1207 (m), 1172 (m), 1039 (m), 1018 (m), 930 (w), 913 (w), 878 (m), 806 (s), 737 (m), 670 (m), 652 (m), 597 (m), 564 (m), 527 (w).

Synthesis of Complex [RuH_2(HBPin)(Me-PNP)] 10

In an argon flushed *Schlenk* flask equipped with a bubbler, 100 mg (1.0 eq., 0.20 mmol) of complex **6** were dissolved in 6 mL toluene. 33 μL (1.1 eq., 0.22 mmol) of pinacol borane were added to the content and stirred for 2 h at room temperature. The green coloured solvent was removed *in vacuo* until a green solid (**10**) remained. The product was stored under an argon atmosphere at -34 °C. Yield: 111.0 mg, 0.176 mmol, 88%.

LIFDI-MS: *m/z* 610.0 (M^+, 0.6%), 609.0 (0.6), 608.0 (0.6), 607.4 (1.3), 607.3 (1.3), 606.5 (0.6), 606.4 (0.6), 606.3 (1.3), 605.3 (1.9), 604.4 (1.3), 603.1 (0.6), 602.2 (0.6), 601.3 (0.6), 484.8 (1.3), 482.1 (50.0), 481.9 (19.5), 481.1 (27.0), 480.2 (26.5), 480.1 (100), 480.0 (49.7), 479.1 (66.0), 479.0 (22.6), 478.1 (69.8), 478.0 (13.8), 477.1 (46.5), 477.0 (21.4), 476.0 (28.9), 476.0 (6.3), 475.1 (18.9), 475.0 (3.8).

^{1}H NMR (300 MHz, C_6D_{12}): δ_H [ppm] = 2.61-2.54 (m, 2H, NCH_2), 2.59 (s, 3H, CH_3), 2.44-2.38 (m, 4H, NCH_2), 2.10-1.95 (m, 2H, PCH_2), 1.84-1.72 (m, 2H, PCH_2), 1.49 (t, 18H, $^3J_{PH}$ = 5.8 Hz, $PC(CH_3)_3$), 1.41 (t, 18H, $^3J_{PH}$ = 6.1 Hz, $PC(CH_3)_3$), 1.11 (12H, s, Pin), -5.64 (bs, 1H, Ru-H-B), -9.02 (bs, 1H, Ru-H-B), -18.85 (bs, 1H, Ru-H). ^{13}C NMR (75 MHz, C_6D_{12}): δ_C [ppm] = 80.1 (Pin, Cq), 66.2 (-CH_2-), 34.5-34.3 ($P(C(CH_3)_3$), 32.5-32.2 ($PC(CH_3)_3$), 29.2 ($PC(CH_3)_3$), 25.5 (-CH_2-), 23.8 (Pin-CH_3). ^{31}P NMR (121 MHz, C_6D_{12}): δ_P [ppm] = 92.1 (s), ^{11}B NMR (160 MHz, C_6D_{12}): 37.8 (s).

IR: $\tilde{\nu}$[cm^{-1}] = 2959 (m), 2897-2867 (m), 2032 (w), 1964-1924 (w), 1746-1688 (w), 1482 (m), 1461 (m), 1384 (m), 1360 (m), 1310 (w), 1268 (w), 1218 (w), 1178 (m), 1160 (m), 1040 (s), 933 (w), 877 (m), 804 (s), 739 (m), 570 (m).

Synthesis of (σ-B-H)-Complex [$RuH_2(BH_3)$(Me-PNP)] 11

Route a. In an argon flushed *Schlenk* flask equipped with a bubbler, 70 mg (1.0 eq., 0.14 mmol) of complex **6** were dissolved in 5 mL toluene. 0.36 mL (2.6 eq., 0.36 mmol) THF borane complex of a 1 M THF solution were added to the content and stirred for 2 h at room temperature. The solvent was removed *in vacuo* until a yellow solid **11** remained. The product was stored under an argon atmosphere at -34 °C. Yield: 70.0 mg, 0.13 mmol, 92%.

Route b. In an argon flushed *Schlenk* flask equipped with a bubbler, 50 mg (1.0 eq., 0.1 mmol) of complex **6** were dissolved in a mixture of 4 mL toluene and 2 mL pentane. 29 mg (5.0 eq., 0.5 mmol) of H_3BNHMe_2 were added to the content and stirred for 2 h at room temperature. The solvent was removed *in vacuo* until a yellow solid **11** remained. The product was stored under an argon atmosphere at -34 °C. Yield: 44.0 mg, 0.082 mmol, 82%.

Preparation of [$RuH_2(BH_3)$(Me-PNP)] 11 for Single Crystal Analysis

In a headspace vial, 20 mg of complex **11** were dissolved in 3 mL pentane and kept overnight at room temperature under an argon atmosphere. After the solvent was evaporated under the argon atmosphere, the yellow crystals were stored in 3 mL pentane at -34 °C.

Elementary analysis calculated for $C_{21}H_{52}BNP_2Ru$ (493.47): C 51.22, H 10.64, B 2.20, N 2.84, P 12.58, Ru 20.52; found: C 50.88, H 9.71, B 2.20, N 2.50, P 12.58, Ru 20.52. Atom ratio found by CHN: $C_{20.9}H_{47.5}N_{0.9}B_{1.0}P_{2.0}Ru_{1.0}$.

LIFDI-MS: *m/z* 496.2 (M^+, 7.1), 496.1 (14.3), 495.2 (42.9), 495.0 (7.1), 494.5 (7.1), 494.1 (57.1), 493.2 (14.2), 493.1 (100), 493.0 (35.7), 492.1 (92.9), 492.0 (28.6), 491.1 (35.7), 491.0 (50.0), 490.1 (42.9), 490.0 (7.3), 489.2 (14.3), 488.1 (7.1), 487.1 (28.6), 487.0 (14.3).

^{1}H NMR (400 MHz, toluene-d$_8$): δ_H [ppm] = 5.42 (bs, 2H, BH_2), 2.19 (s, 3H, CH_3), 2.10-2.02 (m, 2H, NCH_2), 2.01-1.93 (m, 2H, NCH_2), 1.68-1.61 (m, 2H, PCH_2), 1.52 (bt, 18H, $^3J_{PH}$ = 4.9 Hz, $PC(CH_3)_3$), 1.48-1.45 (m, overlapped, 2H, PCH_2), 1.40 (t, 18H, $^3J_{PH}$ = 6.1 Hz, $PC(CH_3)_3$), -5.69 (bs, 1H, σ-Ru-H-B), -17.85 (td, 1H, $^2J_{PH}$ = 19.22 Hz, $^2J_{BH}$ = 3.52 Hz, Ru-H), -19.76 (bs, 1H, Ru-H-B). ^{13}C NMR (75 MHz, toluene-d$_8$): δ_C [ppm] = 67.0 (-CH_2-), 51.4 (-CH_3), 35.1 (P$C(CH_3)_3$), 33.9 (P$C(CH_3)_3$), 30.2 (PC(CH_3)$_3$), 24.13 (-CH_2-). ^{31}P NMR (121 MHz, toluene-d$_8$): δ_P [ppm] = 84.9 (s). ^{11}B NMR (160 MHz, toluene-d$_8$): 19.2 (s).

IR: $\tilde{\nu}$[cm^{-1}] = 2966-2861 (m), 2394 (m), 2330 (m), 2020 (m), 1815 (w), 1693 (m), 1472 (m), 1441 (m), 1384 (w), 1363 (w), 1326 (w), 1257 (m), 1097 (w), 1039-1033 (m), 927 (w), 907 (w), 870 (m), 805 (m), 740 (m), 672 (m), 600 (m), 573 (m), 529 (w), 478 (m).

Acknowledgements

We acknowledge the Ministerium für Innovation, Wissenschaft und Forschung NRW (MIWF-NRW) for financial support within the Energy Research Program for the Scientist Returnee Award for M. H. G. Prechtl (NRW-Rückkehrerprogramm). For access to LIFDI-MS analysis, we gratefully acknowledge Prof. Dr. T. Braun (Humboldt-University of Berlin, Germany). J-H. Choi wants to thank C. Hegemann, M. Keßler and S. Sahler for helpful discussion.

References

[1] J. Zhang, G. Leitus, Y. Ben-David, D. Milstein, *Angew. Chem.-Int. Edit.* **2006**, *45*, 1113–1115.

[2] C. Gunanathan, Y. Ben-David, D. Milstein, *Science* **2007**, *317*, 790–792.

[3] M. H. G. Prechtl, M. Hölscher, Y. Ben-David, N. Theyssen, R. Loschen, D. Milstein, D. Milstein, *Angew. Chem.-Int. Edit.* **2007**, *46*, 2269–2272.

[4] G. Alcaraz, L. Vendier, E. Clot, S. Sabo-Etienne, *Angew. Chem.-Int. Edit.* **2010**, *49*, 918–920.

[5] G. J. Kubas, R. R. Ryan, *Polyhedron* **1986**, *5*, 473–485.

[6] G. J. Kubas, R. R. Ryan, B. I. Swanson, P. J. Vergamini, H. J. Wasserman, *J. Am. Chem. Soc.* **1984**, *106*, 451–452.

[7] G. J. Kubas, *Chem. Rev.* **2007**, *107*, 4152–4205.

[8] R. H. Crabtree, M. Lavin, *J. Am. Chem. Soc.* **1985**, *23*, 1661–1662.

[9] D. G. Hamilton, R. H. Crabtree, *J. Am. Chem. Soc.* **1988**, *110*, 4126–4133.

[10] B. Chaudret, R. Poilblanc, *Organometallics* **1985**, *4*, 1722–1726.

[11] Y. Guari, A. Castellanos, S. Sabo-Etienne, B. Chaudret, *J. Mol. Catal. A: Chem.* **2004**, *212*, 77 –82.

[12] G. J. Kubas, *J. Organomet. Chem.* **2001**, *635*, 37–68.

[13] G. Alcaraz, S. Sabo-Etienne, *Angew. Chem.-Int. Edit.* **2010**, *49*, 7170–7179.

[14] G. Alcaraz, A. B. Chaplin, C. J. Stevens, E. Clot, L. Vendier, A. S. Weller, S. Sabo-Etienne, *Organometallics* **2010**, *29*, 5591–5595.

[15] T. J. Hebden, M. C. Denney, V. Pons, P. M. B. Piccoli, T. F. Koetzle, A. J. Schultz, W. Kaminsky, K. I. Goldberg, D. M. Heinekey, *J. Am. Chem. Soc.* **2008**, *130*, 10812–10820.

[16] M. Hölscher, M. H. G. Prechtl, W. Leitner, *Chem.-Eur. J.* **2007**, *13*, 6636–6643.

[17] C. Gunanathan, M. Hölscher, F. Pan, W. Leitner, *J. Am. Chem. Soc.* **2012**, *134*, 14349–14352.

[18] M. H. G. Prechtl, Y. Ben-David, D. Giunta, S. Busch, Y. Taniguchi, W. Wisniewski, H. Goerls, R. J. Mynott, N. Theyssen, D. Milstein, W. Leitner, *Chem.-Eur. J.* **2007**, *13*, 1539–1546.

[19] B. Askevold, J. T. Nieto, S. Tussupbayev, M. Diefenbach, E. Herdtweck, M. C. Holthausen, S. Schneider, *Nat. Chem.* **2011**, *3*, 532–537.

[20] P. G. Jessop, R. H. Morris, *Coord. Chem. Rev.* **1992**, *121*, 155 –284.

[21] T. Arliguie, B. Chaudret, R. H. Morris, A. Sella, *Inorg. Chem.* **1988**, *27*, 598–599.

[22] J. Zhang, M. Gandelman, L. J. W. Shimon, H. Rozenberg, D. Milstein, *Organometallics* **2004**, *23*, 4026–4033.

[23] J. Zhang, G. Leitus, Y. Ben-David, D. Milstein, *J. Am. Chem. Soc.* **2005**, *127*, 12429–12429.

[24] J. Zhang, E. Balaraman, G. Leitus, D. Milstein, *Organometallics* **2011**, *30*, 5716–5724.

[25] D. A. Addy, J. I. Bates, M. J. Kelly, I. M. Riddlestone, S. Aldridge, *Organometallics* **2013**, *32*, 1583–1586.

[26] T. Ohkuma, M. Koizumi, K. Muñiz, G. Hilt, C. Kabuto, R. Noyori, *J. Am. Chem. Soc.* **2002**, *124*, 6508–6509.

[27] M. G. Crestani, M. Muñoz-Hernández, A. A. A. Acosta-Ramírez, J. J. García, *J. Am. Chem. Soc.* **2005**, *127*, 18066–18073.

[28] R. Langer, M. A. Iron, L. Konstantinovski, Y. Diskin-Posner, G. Leitus, Y. Ben-David, D. Milstein, *Chem.-Eur. J.* **2012**, *18*, 7196–7209.

[29] B. Pan, S. Pierre, M. W. Bezpalko, J. W. Napoline, B. M. Foxman, C. M. Thomas, *Organometallics* **2013**, *32*, 704–710.

[30] D. Giunta, M. Hölscher, M.scher, C. W. Lehmann, R. Mynott, C. Wirtz, W. Leitner, *Adv. Synth. Catal.* **2003**, *345*, 1139–1145.

[31] V. Rodriguez, I. Atheaux, B. Donnadieu, S. Sabo-Etienne, B. Chaudret, *Organometallics* **2000**, *19*, 2916–2926.

3.2. Selective Conversion of Alcohols in Water to Carboxylic Acids by in situ generated Ruthenium Trans Dihydrido Carbonyl PNP Complexes

Jong-Hoo Choi[a], Leo E. Heim[a], Mike Ahrens[b] and Martin H. G. Prechtl[a]*, Selective Conversion of Alcohols in Water to Carboxylic Acids by *in situ* generated Ruthenium Trans Dihydrido Carbonyl PNP Complexes, *Dalton Transactions*, 2014, **43**, 17248-17254 (Full-Paper). Received , Accepted .
[a] Department of Chemistry, University of Cologne, Greinstr. 6, 50939 Cologne, Germany. E-mail: martin.prechtl@uni-koeln.de; http://www.catalysislab.de; Fax: +49 221 470 1788; Tel: +49 221 470 1981, [b] Institute of Chemistry, Humboldt University at Berlin, Brook-Taylor-Straße 2, D-12489 Berlin, Germany [4] CCDC 1002031. For ESI and crystallographic data in CIF or other electronic format see DOI:10.1039/c4dt01634c.

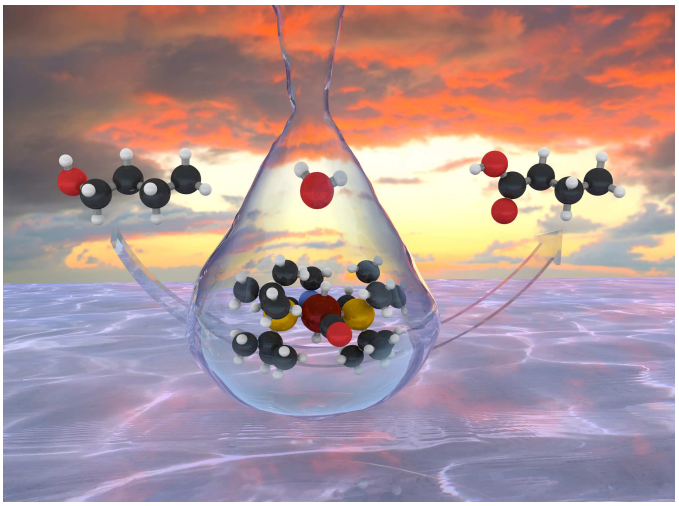

Abstract

In this work, we present a mild method for direct conversion of primary alcohols into carboxylic acids with the use of water as an oxygen source. Applying a ruthenium dihydrogen based dehydrogenation catalyst for this cause, we investigated the effect of water on the catalytic dehydrogenation process of alcohols. Using 1 mol% of the catalyst we report up to high yields. Moreover, we isolated key intermediates which most likely play a role in the catalytic cycle. One of the intermediates was identified as a *trans* dihydrido carbonyl complex which is generated *in situ* in the catalytic process.

[4]Supplementary Information is provided in the Appendix; Cover Art Letter, designed by Leo Heim, 2014, Cologne, Germany.

Introduction

Catalytic oxidation of alcohols is an essential industrial and natural process and leads to important intermediates or products such as aldehydes, ketones or carboxylic acids. Established methods usually require strong and toxic oxidants such as chromium or manganese oxides along with many additives.[1–4] In some cases, the use of stoichiometric oxygen supplying reactants or even the presence of pure pressurized oxygen is required.[5] In terms of synthesis of carboxylic acids, mostly the oxidation of aldehydes as the intermediates or starting materials is needed.[6] The methods of direct oxidation of alcohols to carboxylic acids are still underdeveloped and do not meet today's requirements of a clean and efficient pathway without the need for aggressive and toxic oxidants and avoiding chemical waste products. Despite these disadvantages, only a small number of direct alcohol conversions into carboxylic acids have been reported.[7] For example, Stark *et al.* reported a direct oxidation method of alcohols involving tetran-propylammonium perruthenate (TPAP) in the presence of *N*-methylmorpholine *N*-oxide (NMO) as a key additive to stabilise the aldehyde hydrate intermediate.[8] A different way was obtained by the Grützmacher group; they reported a homogeneous catalytic transformation of alcohols to acids with high yields under very mild conditions applying a rhodium based catalyst with cyclohexanone as a hydrogen acceptor.[9,10] With this similar concept, they also succeeded in converting alcohols into esters or amides. The latest method was reported by the *Milstein* group in 2013 by applying a bipyridine based PNN ruthenium carbonyl hydride catalyst **1** using only water as an oxygen source with no further additives (Fig. 3.11).[11] Usually those pincer type ruthenium complexes bearing cooperative (and hemi-labile) pincer-backbones are known for dehydrogenative coupling of alcohols into esters and their reverse hydrogenation reactions into alcohols, and also for N-alkylation reactions from alcohols and amines.[12–15] In the presence of water, catalyst **1** is highly active for catalytic conversion of different alcohols into their corresponding carboxylic acid salts.

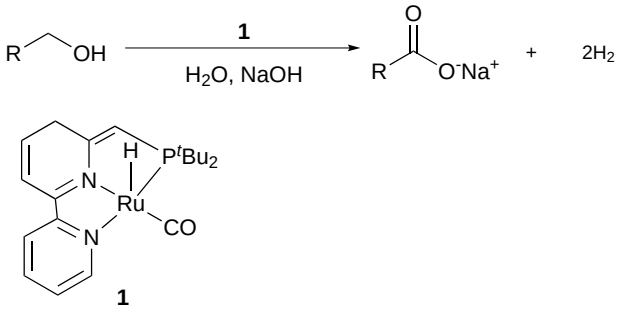

Figure 3.11. – Direct oxidation of alcohols using a bipyridine ruthenium catalyst **1**.[11]

Other studies on alcohol dehydrogenation in aqueous solution at low temperature, in particular methanol[16–18] and methanediol,[19] also showed the possibility of acceptorless dehydrogenation. In these certain cases the dehydrogenation resulted in the formation of carbon dioxide and hydrogen gas. Inspired by the latest achievements, we present a setup using ruthenium PNP pincer complexes [Ru(H_2)H_2(Me-PNP)] **2**[20] and [RuH_2(CO)(Me-PNP)] **3** for catalytic dehydrogenation of primary alcohols in the presence of water, respectively in the absence of any other oxidants (Fig. 3.12). Our reactions were conducted with aq. NaOH solution as the only additive to obtain the carboxylic acid salts in up to high yields. Furthermore, we isolated complex intermediates **3** and **4a**–**b** separately and from the catalytic process (Fig. 3.12). In our system, complex **2** serves as a precursor which converts *in situ* via alcohol decarbonylation reaction into a *trans* dihydrido complex [RuH_2(CO)(Me-PNP)] **3**. Separately, complex **3** was used for catalytic alcohol dehydrogenation reactions in water. Based on achievements in earlier reports,[12,13,21–25] we investigated the decarbonylation behaviour of a similar PNP pincer based ruthenium complex [Ru(H_2)H(PNP)] **5**. Complex **5** can be transformed into a carbonyl complex [RuH(CO)(PNP)] **6** and converted into a*trans* dihydride complex [RuH_2(CO)(H-PNP)] **7** under a hydrogen atmosphere (Fig. 3.12). Those complexes are important intermediates for different transformations reported by others.[26,27]

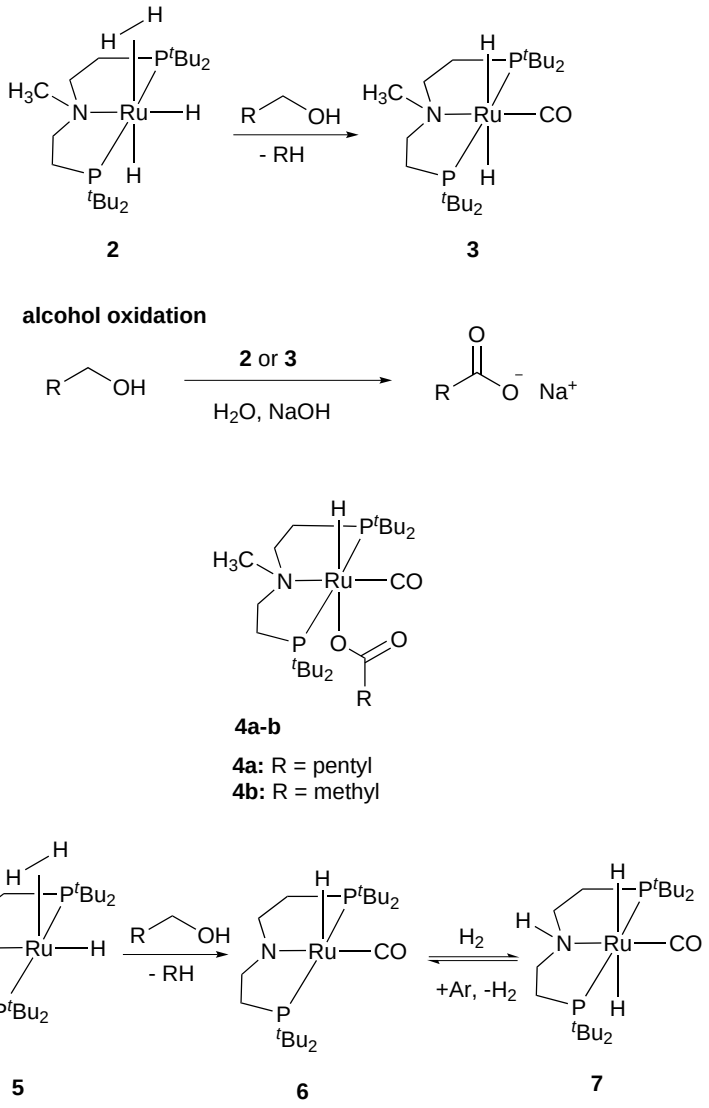

Figure 3.12. – Ruthenium hydride [Ru(H_2)H_2(Me-PNP)] **2** and *trans* dihydrido carbonyl complex [RuH_2(CO)(Me-PNP)] **3** for alcohol oxidation, complex intermediates **4a**–**b**, [Ru(H_2)H(PNP)] **5** and carbonyl complexes [RuH(CO)-(PNP)] **6** and [RuH_2(CO)(H-PNP)] **7**.

Results and Discussion

Catalytic oxidation of Alcohols

For the standard catalytic procedure, a mixture of 2 mL water, 5 mmol of alcohol, 5.5 mmol of NaOH and 1.0 mol% of [Ru(H_2)H_2(Me-PNP)] **2** or [RuH_2(CO)(Me-PNP)] **3** was refluxed under continuous argon flow in an open system for 20 h at 120 °C. The addition of a base (NaOH) is necessary to obtain the carboxylic acid salt and to shift the reaction equilibrium towards the product. After the reaction time, the predominant single aqueous phase was treated with diethyl ether to extract the catalyst. The aqueous layer was then acidified to convert the carboxylic acid salt into its corresponding carboxylic acid which was subsequently extracted with ethyl acetate. Isolated yields of the carboxylic acids are presented in Table 3.2. In this catalytic oxidation of alcohols we tested a series of aliphatic alcohols along with benzyl alcohol. Best results using catalyst **2** were obtained with hexanol and pentanol yielding 88 and 71% (entries 1 and 2), while butanol gave a moderate yield of 63% (entry 3). Catalysing longer aliphatic chained alcohols (entries 4 and 5), the isolated yields dropped down to 33%. This is probably due to a lack of miscibility of these less polar long-chain aliphatic alcohols with water. Benzyl alcohol and cyclohexyl methanol gave yields between 59 and 65% (entries 6 and 7). After the reaction and extracting the complex with diethyl ether, the organic phase contained only traces of unreacted alcohol, but no ester as a by-product. A slight increase of the yields was obtained with complex **3**. The reaction of hexanol to hexanoic acid gave similar yields (entries 1 and 8); for butanol and pentanol (entries 9 and 10) an increase of around 10% was obtained. Isolated yields for octanol and decanol (entries 11 and 12) remained unchanged. The oxidation of benzyl alcohol to benzoic acid improved from 65% yield to 85% (entry 13). In contrast, the conversion of cyclohexyl methanol dropped to 36%. With complexes **5** and **6** the yields for the hexanol oxidation were 53% and 61% (entries 15 and 16).

Table 3.2. – Dehydrogenation of alcohols in the presence of water.

Entry[a]	Cat.	Alcohol	Product	Yield
1	2	Hexanol	Hexanoic acid	88
2	2	Pentanol	Valeric acid	71
3	2	Butanol	Butyric acid	63
4	2	Octanol	Caprylic acid	42
5	2	Decanol	Decanoic acid	33
6	2	Benzyl alcohol	Benzoic acid	65
7	2	Cyclohexyl methanol	Cyclohexyl carboxylic acid	59
8	3	Hexanol	Hexanoic acid	92
9	3	Pentanol	Valeric acid	83
10	3	Butanol	Butyric acid	73
11	3	Octanol	Caprylic acid	45
12	3	Decanol	Decanoic acid	32
13	3	Benzyl alcohol	Benzoic acid	85
14	3	Cyclohexyl methanol	Cyclohexyl carboxylic acid	36
15	5	Hexanol	Hexanoic acid	53
16	6	Hexanol	Hexanoic acid	61

[a] Reaction at 120 °C, 20 h with 1 mol% cat. **2**, **3**, **5** or **6**, 5 mmol alcohol, 5.5 mmol NaOH.

Formation of the Active Species and Characterisation of the Isolated Complex Intermediates

At the beginning of the catalysis, the *trans* dihydrido carbonyl complex [RuH_2(CO)(Me-PNP)] **3** is formed through decarbonylation of the primary alcohol by [Ru(H_2)H_2(Me-PNP)] **2** (Scheme 3.6). Separately in another experiment, complex **3** was obtained by adding 3.5 equivalents of ethyl, pentyl or hexyl alcohols to [Ru(H_2)H_2(Me-PNP)] **2** in a closed system at 80 °C for 48 h, with very good yields, which is stable under an argon atmosphere at room temperature. Furthermore, a series of gas phase mass spectra were recorded to detect the fragmentations of the evolved aliphatic hydrocarbons from the decarbonylation reactions of the corresponding alcohols (ESI Fig. S5.25-5.26). The gas phase MS analysis clearly showed the formation of methane and butane from ethanol, respectively pentanol.

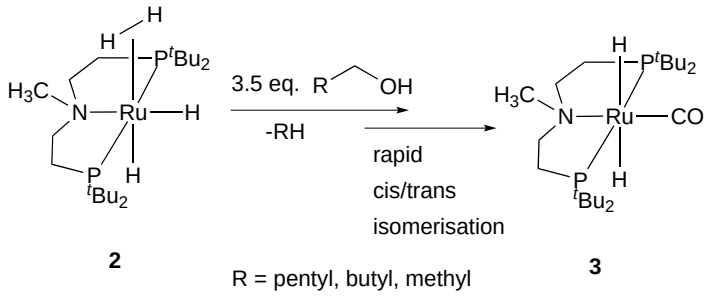

Scheme 3.6 – Decarbonylation of [Ru(H_2)H_2(Me-PNP)] **2** to [RuH_2(CO)(Me-PNP)] **3** via *cis/trans* isomerisation reaction.

Using deuterated ethanol with these hydride catalysts, we observed the formation of CD_3H confirming the interaction of the hydride-site with the substrate. Moreover, we confirmed the molar mass of complex **3** via the LIFDI-MS technique (ESI Fig. S5.27). Mechanistic investigations of decarbonylation reactions with ruthenium complexes were pioneered by *Kubas* and *Caulton*.[25] Following these observations and other indications,[28,29] *Sabo-Etienne et al.* reported the decarbonylation reaction of alcohol by a molecular dihydrogen ruthenium complex, whereby, similar to our system, the dihydrogen ligand is replaced by a CO ligand.[22] Moreover, *Foxman* and *Ozerov* reported the CO functionalisation of a PNP type ruthenium pincer hydride complex obtained through decarbonylation of acetone.[23] Based on previous reports by *Milstein et al.*, we accordingly assume that a *cis*-[RuH_2(CO)(Me-PNP)] complex is generated in the first step, which undergoes then, despite the high *trans* influence of the hydride ligands, a rapid *cis-trans* isomerisation into the thermodynamically more stable and sterically more favourable *trans* isomer **3**.[28,30–33] Furthermore, we observed no isomeric change in the ^{1}H and ^{31}P{^{1}H} NMR after heating complex **3** at 80 °C for 10 h. [RuH_2(CO)(Me-PNP)] **3** shows in the ^{1}H NMR spectrum at 300 MHz a multiplet assigned to two hydrides at -5.40 ppm.

At higher frequencies of 600 MHz, the multiplet resolves into two clean triplet signals at -5.43 ppm ($^2J_{HP}$ = 16.1 Hz) and -5.54 ppm ($^2J_{HP}$ = 19.3 Hz). Two signals for two hydride signals next to each other in the chemical shifts with a $^2J_{HP}$ coupling constant between 16 and 24 Hz is similar to other reported *trans* dihydride PNP pincer complexes with aliphatic backbones by *Gusev* and *Schneider*.[34–37] In the ^{13}C NMR spectrum, the CO signal was found at 210.8 ppm (t, $^2J_{CP}$ = 13.2 Hz), which was further confirmed by decarbonylation reactions of ^{13}C labeled ethanol (ESI, Fig. S5.40). The νCO band was detected at 1871 cm^{-1} while the comparable ^{13}CO band was found with a Δ43 at 1828 cm^{-1}. Vibration of the hydrides was found at 1642 cm^{-1} for complex **3** and 1640 cm^{-1} for the ^{13}C labeled complex (ESI, Fig. S5.34). This is in agreement with the case of a typical *trans* dihydride arrangement. The CO stretching mode is located in the typical range with higher wave numbers followed by the M-H vibrations as one single, sharp band at lower wave numbers.[30,32,38] In contrast, for *cis* bonding modes of metal dihydrides, the hydride *trans* to a pincer backbone would have the highest wave number, followed then by the CO band and then with the lowest wave number the hydride *trans* to the carbonyl ligand.[38] Comparing the decarbonylation reactivity of **2**, similar observations were made from the reaction of the analogue ruthenium complex [Ru(H$_2$)H(PNP)] **5** whose synthesis was reported in earlier studies (Scheme 3.7).[20,26]

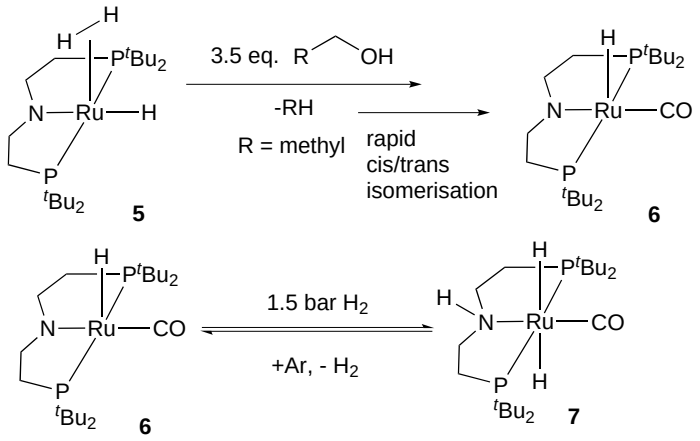

Scheme 3.7 – Decarbonylation of [Ru(H$_2$)H(PNP)] **5** to [RuH(CO)(PNP)] **6** via *cis*/*trans* isomerisation and the hydrogenation of **6** to [RuH$_2$(CO)(HPNP)] **7**.

Decarbonylation reaction of ethanol by complex **5** gave the carbonyl complex [RuH(CO)-(PNP)] **6** in excellent yields. In the ^{1}H NMR spectrum, the hydride ligand gives a triplet signal in the upfield at -20.87 ppm ($^2J_{HP}$ = 16.3 Hz), which indicates the configuration of the hydride ligand *cis* to the pincer ligand.[34] Experiments with ^{13}C labeled ethanol resulted in a triplet signal at 208.8 ppm ($^2J_{CP}$ = 10.5 Hz) for the CO ligand in the ^{13}C$_{\mathrm{APT}}$ NMR spectrum. IR signals were found at 1872 cm^{-1} for the non-labeled νCO vibration along with a weaker

νRu-H band at 2052 cm^{-1} which are characteristic of pincer based carbonyl monohydride compounds.[30] For the ^{13}C labeled complex, the ^{13}CO band was detected at 1830 cm^{-1} and with a νRu-H vibration around 2062 cm^{-1} (Fig. S5.37). Pressurising complex **6** with 1.5 bar H_2 gas showed around 79% conversion of **6** into *trans* dihydride **7**, which exhibits, similar to complex **3**, two triplet signals at -5.86 ppm ($^2J_{HP} = 18.2$ Hz) and -6.13 ppm ($^2J_{HP} = 17.4$ Hz). Isolation of complex **7** was not possible due to the rapid degeneration into **6**.

Catalytic Cycle and the Isolation of Intermediates 4a and b

Similar to the system reported by *Milstein et al.*, we assume that complex **3** dehydrogenates the alcohol into an aldehyde intermediate complex. It is also possible that the aldehyde converts independently with water into an aldehyde hydrate intermediate. However, due to the rapid equilibrium between the aldehyde and the aldehyde hydrate intermediate,[11] it seems more plausible that the reaction with water under basic conditions generates an aldehyde hydrate, stabilised as a geminial diolate complex, which can be dehydrogenated into the carboxylate complex **4a** (Fig. 3.13).[11] From there on, the carboxylate is salted out by sodium cations.

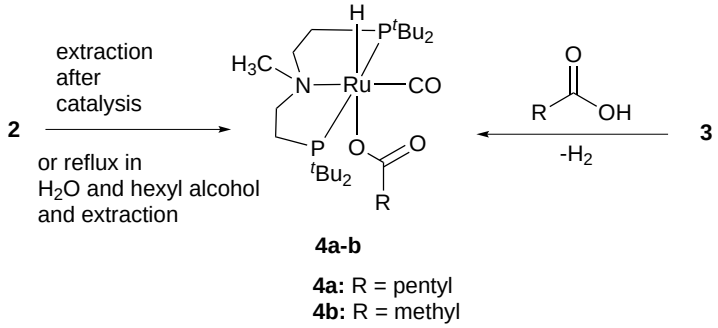

Figure 3.13. – Isolation of complexes **4a** and **4b**. Complex **4a** was obtained by extraction with toluene after the catalytic reaction with **2** or by refluxing **2** with hexyl alcohol in water. Adding acetic or hexanoic acid to complex **3** led directly to **4a** and **4b**.

In the presence of water, no formation of esters was observed since only unreacted alcohol residues were found in the reaction mixture after the appropriate reaction time. This observation confirms yet again that water suppresses the formation of ester.[11] Compared to previous studies[11] it is unclear whether the mechanism involves a metal–ligand cooperativity during the catalytic reaction. We achieved the conversion of alcohols to carboxylic acids using catalysts **2** and **3** bearing a "non-cooperative" Me-PNP-ligand. The experimental data show that a basic position as a proton acceptor/donor is not crucial for this reaction as no H/D exchange has been observed in the ligand backbone. The lack of H/D exchange in the ligand

backbone lets us tentatively exclude cooperative effects of the ligand. It is likely that the acceptorless dehydrogenation and oxygen-transfer from water solely take place at the ruthenium core. The attempt to isolate the complex intermediate species after the reaction time led to the isolation of **4a** which was extracted with toluene. Separate attempts led also to the isolation of **4a** either by refluxing complex **2** in hexyl alcohol and water or by the reaction of **3** with hexanoic acid (Fig. 3.13). For the latter one, **4a** was obtained in very good yields within minutes under hydrogen evolution. The analogue, complex **4b**, was obtained by adding acetic acid to complex **3** (Fig. 3.13). Both complexes almost do not differ in their chemical shifts in the $^{31}P\{^{1}H\}$ NMR showing singlets around 81.4 ppm (complex **4a**) and 81.3 (complex **4b**), while exhibiting triplet signals in the upfield at -17.08 ppm ($^{2}J_{PH}$ = 20.7 Hz, complex **4a**) and at -17.49 ppm ($^{2}J_{PH}$ = 20.4 Hz, complex **4b**). IR spectra show the νCO for both complexes at 1908 cm^{1}, while exhibiting the νCO band at 1593 cm^{1} (ESI, Fig. S5.35-5.36). LIFDI-MS/MS analysis of complex **4a** showed only a fragmentation with the mass value of 506 *m/z*, which can be explained by the loss of the hexanoate under MS conditions, showing only the carbonyl monohydride species (for more details see ESI, Fig. S5.29-5.30). This observation is in full agreement with our recent experiments applying LIFDI-MS analysis to ruthenium pincer hydride complexes.[20] During a soft ionisation process, a mixture of similar fragmentations can be detected with this kind of compound class, which can be explained by the loss of the hydride ligands (-Δ1-2 *m/z*) causing a shift towards lower mass values.[20] In contrast to **4a**, LIFDI-MS/MS analysis of **4b** revealed the molar mass of 565 *m/z*, which is in good agreement with the simulated isotope pattern (in red) illustrated in Fig. 3.14. Compared to the simulated isotope pattern of [RuH(CO)($OOCCH_3$)(Me-PNP)] 565 *m/z* in red, the LIFDI-MS/MS pattern is slightly shifted towards lower mass value, which can be explained by the detection of a fragmentation of the subspecies [Ru(CO)($OOCCH_3$)(Me-PNP)] 564 which is generated during the ionisation process. A single crystal structure of **4b** was obtained from crystals grown as a red prism in a mixture of benzene and heptane at room temperature (Fig. 3.15, selected bond distances and angles are given in Table 3.3). The structure shows a distorted octahedral coordination of the ruthenium core, where both locations of the P-atoms of the P-Ru-P axis are twisted out of plane with a P1-Ru-P2 angle of 157.24°. The same applies for the *trans*-arrangement of the hydride and the carboxylate with an angle of 169.20° (H1-Ru-O2). The X-ray pattern allowed the localisation of the hydride H1 giving a Ru-H distance of 1.57(4) Å. Furthermore, the *trans* arrangement of the CO ligand to the PNP-ligand is confirmed, which was discussed earlier in this work. The N-Ru-CO angle is closer to 180° (176.16°); consequently the H1-Ru-CO angle is near orthogonal (92.20°).

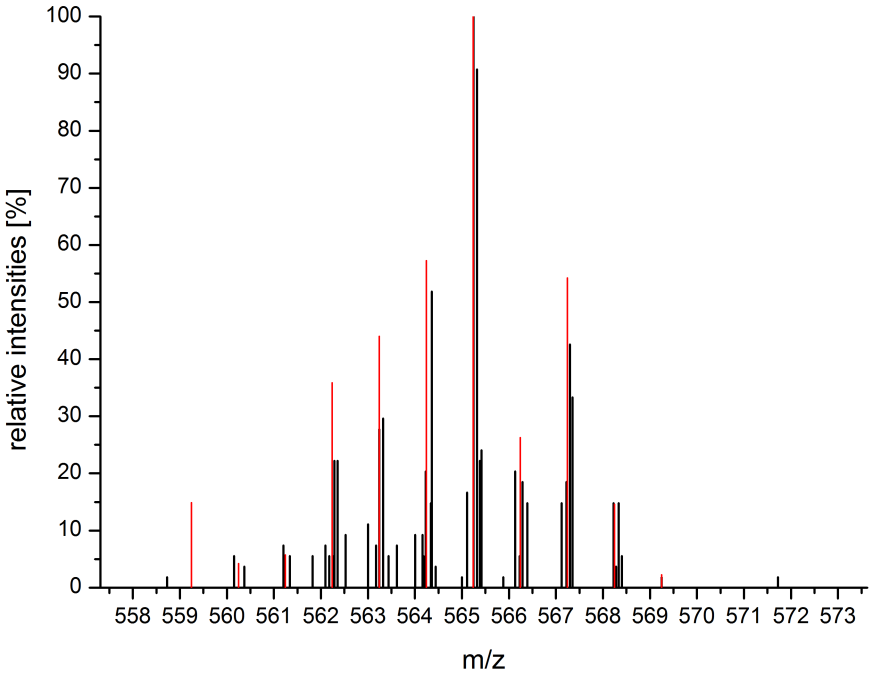

Figure 3.14. – LIFDI-MS/MS analysis of [RuH(CO)($OOCCH_3$)(Me-PNP)] 565 **4b** in toluene. Isotope pattern area 558–570 (black) in comparison with the simulated isotope pattern of [RuH(CO)($OOCCH_3$)(Me-PNP)] 565 (red).

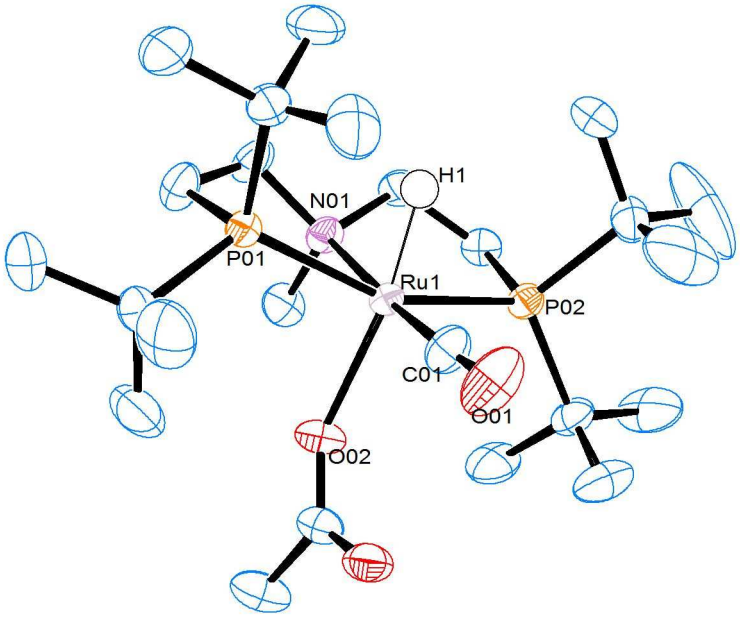

Figure 3.15. – ORTEP diagram of the single crystal structure of complex **4b**. Ellipsoids are illustrated at 50% probability. All hydrogen atoms are not depicted here except for H1 for clarity.

Table 3.3. – Selected bond distances[a] and angles[b] of complex **4b**

Ru1–P1	2.34(9)	P1–Ru1–P2	157.24
Ru1–P2	2.34(6)	N01-Ru1-C01	176.16
Ru1–C01	1.82(0)	H1–Ru1–O02	169.30
Ru1–O02	2.21(9)	H1–Ru1–C01	92.20
Ru1–H1	1.57(4)		
Ru1–N01	2.24(7)		

[a] Distances are given in Å.
[b] Angles are reported in degrees.

Conclusions

In summary, we presented an approach for catalytic dehydrogenation of primary alcohols in water yielding carboxylic acid salts using ruthenium hydride complexes. Moreover, we confirmed that complexes **2** and **5** convert *in situ* into carbonyl *trans* dihydride complexes **3** and **6** by decarbonylation reaction of alcohols. Complex intermediate **4a**, which was isolated

after the catalysis as well as synthesised in different ways, is believed to be one of the complex species taking part in the catalytic cycle.

Experimental Section

Reactions were generally performed under an argon atmosphere using *Schlenk* techniques, flame-dried glassware and a *Labmaster 200* glove-box from *MBraun*. High-pressure hydrogen reactions were performed in a *Büchi Tinyclave* (50 mL) glass autoclave. All solvents and reagents were purchased from *Acros, Merck, Sigma-Aldrich, Fluka*, or *Strem* or were acquired from the institute stock. Commercial anhydrous solvents and argon as-packed reagents were used as received and stored in the glove-box under argon. Non-anhydrous solvents were dried and distilled (under vacuum or argon) prior to use, applying standard procedures.

Analytical Methods

^{1}H, ^{13}C, ^{31}P NMR spectra were recorded at 300 MHz (^{1}H), 75 MHz (^{13}C) and 121 MHz (^{31}P) on a *Bruker Avance II 300* and on a *Bruker Avance II+ 600* spectrometer at 600 MHz (^{1}H), 150 MHz (^{13}C) and 242 MHz (^{31}P) using deuterated benzene and toluene at room temperature. ^{1}H shifts were reported in ppm (δH) downfield from TMS and were determined by reference to the residual solvent peaks (C_6D_6: 7.16 ppm, C_7D_8: 7.09 ppm). Chemical shifts were reported as singlet (s), doublet (d), triplet (t), quartet (q) and multiplet (m). Coupling constants J were reported in Hz. For hydrogenation experiments, *Young-Teflon* capped NMR tubes from *Wilmad* were used. Infrared spectra (IR) were measured at room temperature with a *Bruker Alpha* spectrometer equipped with a Diamond-ATR IR unit. Data are reported as follows: absorption ν[cm^{-1}], weak (w), medium (m), strong (s). Mass-spectrometric investigations of the gas composition in the gas phase were conducted with a *HPR-20* gas analysis system by *Hiden Analytical* and were directly connected to the reaction setup under an argon atmosphere. The *HPR-20 QIC (Hiden Analytical)* has a MS detection limit <0.09 ppm as xenon in air is detectable. Note that the MS has sensitivity down to partial pressures of 10^{-10} torr (note: the spectrometer specific unit is torr not MPa).

General Catalytic Procedure

For the standard catalytic procedure, 0.05 mmol of complex **2** or complex **3** were added to 5.5 mmol NaOH and 5 mmol of alcohol. After the addition of 2 mL degassed water, the content was refluxed at 120 °C for 20 h under constant argon flow in an open system. After the reaction time, the aqueous phase was extracted with diethyl ether to extract the catalyst and alcohol residues. The aqueous layer was then acidified with 20% aq. HCl and treated

five times with 20 mL ethyl acetate. After the organic layers were combined and dried for 1 h over $MgSO_4$, the solution was filtered and the solvent was removed under reduced pressure to obtain the isolated carboxylic acid. Yields are given in Table 1.

Synthesis of [RuH_2(CO)(Me-PNP)] 3

In an argon flushed *Büchi* glass autoclave 100 mg (0.198 mmol) of [Ru(H_2)H_2(Me-PNP)] **2** were dissolved in 6 mL toluene. The synthesis of complex **2** is described in our previous report.[20] After the addition of 3.5 eq. (0.693 mmol) of a primary alcohol (e.g. ethyl, pentyl, hexyl alcohol), the content was heated at 80 °C for 48 h. After the appropriate time, the solvent was removed in vacuo and the residue was washed twice with pentane. The grey powder was stored at -34 °C. Yield: 80%.

LIFDI-MS (argon collided): *m/z* 511.3 (2), 510.3 (19), 509.3 (55), 508.3 (33), 507.3 (100), 506.3 (73), 505.3 (74), 504.3 (65), 503.3 (30), 502.3 (17), 501.3 (22).

^{1}H NMR (600 MHz, benzene-d_6): δH [ppm] = 2.32 (m, 2H, CH_2), 2.11 (s, 3H, NCH_3), 1.93 (m, 2H, NCH_2), 1.61 (m, 2H, PCH_2), 1.55-1.52 (m, 2H, overlapped, PCH_2), 1.50 (dt, 36H, $^3J_{PH}$ = 6.7 Hz, $PC(CH_3)_3$), -5.43 (t, 1H, $^2J_{PH}$ = 16.1 Hz, Ru-H), -5.54 (t, 1H, ^{2}JJ_{PH} = 19.4 Hz, Ru-H).$^{13}C_{APT}$ NMR (75 MHz, benzene-d_6): δC [ppm] = 210.8 ppm (t, $^2J_{CP}$ = 13.2 Hz, *C*O, data extracted from ^{13}CO labeled probe), 65.8 (t, $^2J_{CP}$ = 5.1 Hz, N*C*H_2), 52.9 (N*C*H_3), 36.4 (t, $^1J_{CP}$ = 8.9 Hz, P*C*$(CH_3)_3$), 33.9 (t, $^1J_{CP}$ = 7.4 Hz, P*C*$(CH_3)_3$), 30.3 (t, $^2J_{CP}$ = 3.3 Hz, PC(*CH₃*)$_3$), 30.1 (t, $^2J_{CP}$ = 2.9 Hz, PC(*CH₃*)$_3$), 24.4 (t, $^1J_{CP}$ = 5.3 Hz, P*C*H_2). ^{31}P{^{1}H} NMR (121 MHz, benzene-d_6): δP [ppm] = 106.3 (s).

IR: [cm^1] = 2950-2864 (m), 1871 (s), 1640 (s), 1474 (m), 1458 (m), 1416 (w), 1383 (m), 1381 (m), 1351 (m), 1310 (w), 1208 (w), 1171 (m), 1049 (w), 1025 (m), 930 (w), 915 (w), 881 (m), 801 (m), 739 (m), 679 (m), 644 (w), 613 (m), 566 (m), 529 (w), 508 (w), 478 (m), 432 (m).

Isolation of [RuH(CO)(hexanolate)(Me-PNP)] 4a

In an argon flushed *Schlenk* flask equipped with a bubbler, 50 mg (0.1 mmol) of [RuH_2(CO)-(Me-PNP)] **3** were dissolved in 5 mL toluene. After the addition of 1.5 eq. (0.15 mmol) hexanoic acid, the content was stirred for 30 min under a constant stream of argon. The solvent was removed in vacuo and the product was washed twice with pentane. The grey powder, yielding 85%, was stored at -34 °C.

LIFDI-MS/MS (fragment 506): *m/z* 509.3 (13.1), 508.3 (33.3), 507.3 (16.7), 507.2 (9.5), 506.3 (100), 505.3 (97.6), 504.3 (47.6), 503.3 (16.7), 502.2 (16.7), 501.1 (4.8), 500.2 (9.5).

^{1}H NMR (600 MHz, benzene-d_6): δH [ppm] = 2.51 (t, 2H, $^2J_{CH}$ = 7.6 Hz, OOC*C*H_2-$(CH_2)_3CH_3$), 2.17 (s, 3H, NCH_3), 2.14 (m, 4H, NCH_2), 1.70 (m, 2H, $OOCCH_2$*C*$H_2(CH_2)_2$-

CH_3), 1.55-1.51 (m, 8H, overlapped, 4H PCH_2 and 4H $OOC(CH_2)_2(CH_2)_2CH_3$), 1.38 (t, 18H, $^3J_{PH}$ = 6.5 Hz, $PC(CH_3)_3$), 1.23 (t, 18H, 3^3J_{PH} = 6.1 Hz, $PC(CH_3)_3$), 0.99 (t, 3H, $^2J_{CH}$ = 7.3 Hz, $OOC(CH_2)_4CH_3$), -17.08 (t, 1H, $^2J_{PH}$ = 20.7 Hz, Ru-H). $^{13}C_{DeptQ}$ NMR (150 MHz, benzene-d_6): δC [ppm] = 208.5 ppm (s, *C*O), 175.8 (s, CH_3-*C*OO), 65.8 (s, N*C*H_2), 45.6 (s, N*C*H_3), 40.8 (s, OOC*C*$H_2(CH_2)_3CH_3$), 37.5 (t, $^1J_{PC}$ = 5.1 Hz, P*C*$(CH_3)_3$), 36.8 (t, $^1J_{PC}$ = 10.3 Hz, P*C*$(CH_3)_3$), 33.0 (s, $OOCCH_2CH_2(CH_2)_2CH_3$), 30.6 (s, $PC(CH_3)_3$), 30.5 (s, $PC(CH_3)_3$), 27.2 (s, $OOC(CH_2)_2CH_2CH_2CH_3$), 23.7 (s, OOC-$(CH_2)_3CH_2CH_3$), 23.4 (s, P*C*H_2), 14.2 (s, $OOC(CH_2)_4CH_3$). $^{31}P\{^1H\}$ NMR (121 MHz, benzene-d_6): δ [ppm] = 81.4 (s).

IR: $\tilde{\nu}$[cm^{-1}] = 2959-2868 (m), 2126-2075 (w), 1908 (s), 1595 (s), 1466 (m), 1429 (w), 1389 (m), 1369 (m), 1354 (m), 1175 (m), 1043 (m), 1024 (m), 958 (w), 933 (w), 907 (w), 879 (m), 828 (w), 807 (m), 736 (m), 680 (m), 643 (m), 609 (m), 570 (m), 546 (m), 531 (m).

Isolation of [RuH(CO)($OOCCH_3$)(Me-PNP)] 4b

In an argon flushed *Schlenk* flask equipped with a bubbler, 30 mg (0.06 mmol) of [RuH_2(CO)-(Me-PNP)] **3** were dissolved in 5 mL toluene. After the addition of 1.5 eq. (0.09 mmol) acetic acid, the content was stirred for 30 min under a constant stream of argon. The solvent was removed in vacuo and the product was washed twice with pentane. The grey powder, yielding 81%, was stored at -34 °C.

LIFDI-MS/MS: *m/z* 569.2 (1.9), 568.2 (14.8), 567.3 (42.6), 566.3 (18.5), 565.3 (100), 564.4 (51.9), 563.2 (27.8), 561.2 (7.4), 560.2 (5.6).

^{1}H NMR (600 MHz, benzene-d_6): δH [ppm] = 2.22 (s, 3H, OOC*CH*$_3$), 2.13 (m, 4H, NCH_2), 2.09 (s, 3H, NCH_3), 1.63 (m, 2H, PCH_2), 1.49 (m, 2H, PCH_2), 1.31 (t, 18H, $^3J_{PH}$ = 6.4 Hz, $PC(CH_3)_3$), 1.18 (t, 18H, $^3J_{PH}$ = 6.2 Hz, $PC(CH_3)_3$), -17.49 (t, 1H, $^2J_{PH}$ = 20.4 Hz, Ru-H). $^{13}C_{DeptQ}$ NMR (150 MHz, benzene-d_6): δC [ppm] = 208.8 ppm (s, *C*O), 175.4 (s, CH_3-*C*OO), 65.7 (s, N*C*H_2), 45.2 (s, N*C*H_3), 37.2 (t, $^1J_{CP}$ = 5.3 Hz, P*C*$(CH_3)_3$), 36.7 (t, $^1J_{CP}$ = 10.2 Hz, P*C*$(CH_3)_3$), 30.5 (s, $PC(CH_3)_3$), 30.2 (s, $PC(CH_3)_3$), 23.6 (s, P*C*H_2). $^{31}P\{^1H\}$ NMR (242 MHz, benzene-d_6): δP [ppm] = 81.3 (s).

IR: $\tilde{\nu}$[cm^{-1}] = 2956-2859 (m), 2145-2059 (w), 1906 (s), 1593 (s), 1464 (m), 1389 (m), 1368 (m), 1354 (m), 1259 (s), 1175 (m), 1087 (s), 1021 (s), 934 (w), 907 (w), 878 (m), 800 (s), 735 (m), 680 (m), 609 (m), 569 (m), 546 (w), 529 (w), 478 (m).

Synthesis of [RuH(CO)(PNP)] 6

In an argon flushed *Büchi* glass autoclave 100 mg (0.215 mmol) of [Ru(H_2)H(PNP)] **5** were dissolved in 6 mL toluene. The synthesis of complex **5** is described in our previous report.[20] After the addition of 3.5 eq. (0.753 mmol) of a primary alcohol (e.g. ethyl, pentyl, hexyl

alcohol), the content was heated at 80 °C for 48 h. After the appropriate time, the solvent was removed in vacuo and the residue was washed twice with pentane. The orange powder was stored at -34 °C. Yield: 90%.

LIFDI-MS/MS: *m/z* 495.1 (1.0), 494.3 (15.9), 493.3 (46.1), 492.3 (14.6), 491.3 (100), 490.2 (34.7), 489.2 (39.6), 488.3 (28.9), 487.3 (4.6), 486.2 (2.4), 485.3 (15.5).

^{1}H NMR (300 MHz, benzene-d_6): δH [ppm] = 3.49 (m, 2H, CH_2), 3.14 (m, 2H, CH_2), 1.88 (m, 4H, PCH_2), 1.26 (dt, 36H, $^{2}J_{PH}$ = 14.3 Hz, $PC(CH_3)_3$), -20.87 (t, 1H, $^{2}J_{PH}$ = 16.3 Hz, Ru-H). $^{13}C_{APT}$ NMR (75 MHz, benzene-d_6): δC [ppm] = 208.8 ppm (t, *C*O, $^{2}J_{CP}$ = 10.5 Hz, data extracted from ^{13}CO labeled probe in toluene-d_8), 63.5 (t, $^{2}J_{CP}$ = 7.1 Hz, N*C*H_2), 35.4 (t, $^{1}J_{CP}$ = 7.7 Hz, P*C*$(CH_3)_3$), 33.9 (t, $^{1}J_{CP}$ = 7.4 Hz, P*C*$(CH_3)_3$), 29.7 (t, $^{2}J_{CP}$ = 3.0 Hz, $PC(CH_3)_3$), 28.5 (t, $^{2}J_{CP}$ = 3.2 Hz, $PC(CH_3)_3$), 26.0 (t, $^{1}J_{CP}$ = 6.9 Hz, P*C*H_2). $^{31}P\{^{1}H\}$ NMR (121 MHz, benzene-d_6): δP [ppm] = 110.1 (s).

IR: $\tilde{\nu}$[cm^{-1}] = 2943-2800 (m), 2706 (w), 2628 (w), 2068-2048 (m), 1869 (s), 1469 (m), 1454 (m), 1385 (m), 1358 (m), 1318 (w), 1262 (m), 1206 (m), 1178 (m), 1157 (w), 1106 (w), 1063 (m), 1017 (m), 967 (m), 936 (w), 806 (s), 773 (w), 729 (s), 695 (m), 674 (w), 611 (m), 579 (m), 536 (m), 471 (s).

Hydrogenation of [RuH(CO)(PNP)] 6 to [RuH_2(CO)(HPNP)] 7

In a *Young-Teflon* capped NMR tube, 7 mg (0.014 mmol) [RuH(CO)(PNP)] 6 were dissolved in 0.5 mL deuterated benzene. The content was pressurised with 1.5 bar H_2 gas. After 10 h, 79% conversion was detected via $^{31}P\{^{1}H\}$ NMR. Only hydride signals are clearly visible.

^{1}H NMR (300 MHz, benzene-d_6): δH [ppm] = -5.86 (t, 1H, $^{2}J_{PH}$ = 18.2 Hz, Ru-H), -6.13 (t, 1H, $^{2}J_{PH}$ = 17.4 Hz, Ru-H). $^{31}P\{^{1}H\}$ NMR (121 MHz, benzene-d_6): δP [ppm] = 110.1 (s, 21%, complex **6**), 108.9 (s, 79%, complex **7**).

Acknowledgements

We acknowledge the Ministerium für Innovation, Wissenschaft und Forschung NRW (MIWF-NRW) for financial support within the Energy Research Program for the Scientist Returnee Award for M. H. G. Prechtl (NRW-Rückkehrerprogramm). For access to LIFDI-MS analysis, we gratefully acknowledge Prof. Dr T. Braun (Humboldt-University of Berlin, Germany). J.-H. Choi wants to thank Dr J. Neudörfl, T. Heidemann and A. Krest for helpful discussion. P. Kliesen is acknowledged for technical support for the XRD measurement.

References

[1] M. Zhao, J. Li, Z. Song, R. Desmond, D. M. Tschaen, E. J. Grabowski, P. J. Reider, *Tetrahedron Lett.* **1998**, *39*, 5323 –5326.

[2] B. C. Holland, N. W. Gilman, *Synth. Commun.* **1974**, *4*, 203–210.

[3] R. J. Gritter, T. J. Wallace, *J. Org. Chem.* **1959**, *24*, 1051–1056.

[4] M. Zhao, J. Li, E. Mano, Z. Song, D. M. Tschaen, E. J. J. Grabowski, P. J. Reider, *J. Org. Chem.* **1999**, *64*, 2564–2566.

[5] T. Mallat, A. Baiker, *Chem. Rev.* **2004**, *104*, 3037–3058.

[6] G. Tojo, M. Fernandez, *Oxidation of Primary Alcohols to Carboxylic Acids: A Guide to Current Common Practice*, Springer, Luxemburg, Berlin, **2007**.

[7] G.-J. t. Brink, Arends, I. W. C. E., R. A. Sheldon, *Science* **2000**, *287*, 1636–1639.

[8] A.-K. C. Schmidt, C. B. W. Stark, *Org. Lett.* **2011**, *13*, 4164–4167.

[9] T. Zweifel, J.-V. Naubron, H. Grützmacher, *Angew. Chem.-Int. Edit.* **2009**, *121*, 567–571.

[10] S. Annen, T. Zweifel, F. Ricatto, H. Grützmacher, *ChemCatChem* **2010**, *2*, 1286–1295.

[11] E. Balaraman, E. Khaskin, G. Leitus, D. Milstein, *Nat. Chem.* **2013**, *5*, 122–125.

[12] J. Zhang, M. Gandelman, L. J. W. Shimon, H. Rozenberg, D. Milstein, *Organometallics* **2004**, *23*, 4026–4033.

[13] J. Zhang, G. Leitus, Y. Ben-David, D. Milstein, *J. Am. Chem. Soc.* **2005**, *127*, 12429–12429.

[14] C. Gunanathan, Y. Ben-David, D. Milstein, *Science* **2007**, *317*, 790–792.

[15] J. Zhang, M. Gandelman, L. J. W. Shimon, D. Milstein, *Dalton Trans.* **2007**, 107–113.

[16] R. E. Rodriguez-Lugo, M. Trincado, M. Vogt, F. Tewes, G. Santiso-Quinones, H. Grützmacher, *Nat. Chem.* **2013**, *5*, 342–347.

[17] E. Alberico, P. Sponholz, C. Cordes, M. Nielsen, H.-J. Drexler, W. Baumann, H. Junge, M. Beller, *Angew. Chem.-Int. Edit.* **2013**, *52*, 14162–14166.

[18] M. Nielsen, E. Alberico, W. Baumann, H.-J. Drexler, H. Junge, S. Gladiali, M. Beller, *Nature* **2013**, *495*, 85–89.

[19] L. E. Heim, N. E. Schloerer, J.-H. Choi, M. H. G. Prechtl, *Nat Commun* **2014**, *5*.

[20] J.-H. Choi, N. E. Schloerer, J. Berger, M. H. G. Prechtl, *Dalton Trans.* **2014**, *43*, 290–299.

[21] E. P. K. Olsen, R. Madsen, *Chem.-Eur. J.* **2012**, *18*, 16023–16029.

[22] P. D. Bolton, M. Grellier, N. Vautravers, L. Vendier, S. Sabo-Etienne, *Organometallics* **2008**, *27*, 5088–5093.

[23] R. Çelenligil-Çetin, L. A. Watson, C. Guo, B. M. Foxman, O. V. Ozerov, *Organometallics* **2005**, *24*, 186–189.

[24] Y.-Z. Chen, W. C. Chan, C. P. Lau, H. S. Chu, H. L. Lee, G. Jia, *Organometallics* **1997**, *16*, 1241–1246.

[25] L. S. Van der Sluys, G. J. Kubas, K. G. Caulton, *Organometallics* **1991**, *10*, 1033–1038.

[26] B. Askevold, J. T. Nieto, S. Tussupbayev, M. Diefenbach, E. Herdtweck, M. C. Holthausen, S. Schneider, *Nat. Chem.* **2011**, *3*, 532–537.

[27] Z. Han, L. Rong, J. Wu, L. Zhang, Z. Wang, K. Ding, *Angew. Chem.-Int. Edit.* **2012**, *51*, 13041–13045.

[28] B. N. Chaudret, D. J. Cole-Hamilton, R. S. Nohr, G. Wilkinson, *J. Chem. Soc. Dalton Trans.* **1977**, 1546–1557.

[29] T. M. Douglas, A. S. Weller, *New J. Chem.* **2008**, *32*, 966–969.

[30] B. Rybtchinski, Y. Ben-David, D. Milstein, *Organometallics* **1997**, *16*, 3786–3793.

[31] B. L. Shaw, M. F. Uttley, *J. Chem. Soc. Chem. Commun.* **1974**, 918–919.

[32] H. Salem, L. J. W. Shimon, Y. Diskin-Posner, G. Leitus, Y. Ben-David, D. Milstein, *Organometallics* **2009**, *28*, 4791–4806.

[33] R. S. Paonessa, W. C. Trogler, *J. Am. Chem. Soc.* **1982**, *104*, 1138–1140.

[34] M. Bertoli, A. Choualeb, A. J. Lough, B. Moore, D. Spasyuk, D. G. Gusev, *Organometallics* **2011**, *30*, 3479–3482.

[35] A. Friedrich, M. Drees, J. Schmedt auf der Günne, S. Schneider, *J. Am. Chem. Soc.* **2009**, *131*, 17552–17553.

[36] M. Kaess, A. Friedrich, M. Drees, S. Schneider, *Angew. Chem.-Int. Edit.* **2009**, *48*, 905–907.

[37] A. Friedrich, M. Drees, M. Kaess, E. Herdtweck, S. Schneider, *Inorg. Chem.* **2010**, *49*, 5482–5494.

[38] S. M. Kloek, D. M. Heinekey, K. I. Goldberg, *Organometallics* **2006**, *25*, 3007–3011.

3.3. Tuneable Hydrogenation of Nitriles into Imines or Amines with a Ruthenium Pincer Complex under Mild Conditions

Jong-Hoo Choi and Martin H. G. Prechtl[a]*, Dedicated to Prof. Armando Pombeiro on the occasion of his 65th birthday, Tuneable Hydrogenation of Nitriles into Imines or Amines with a Ruthenium Pincer Complex under Mild Conditions, *ChemCatChem*, 2015, **7**, 1023-1028 (Full-Paper). DOI: 10.1002/cctc.201403047, Received , Published online .[5]

[a] Department of Chemistry, University of Cologne, Greinstr. 6, 50939 Cologne, Germany. E-mail: martin.prechtl@uni-koeln.de; http://www.catalysislab.de; Fax: +49 221 470 1788; Tel: +49 221 470 1981.

Abstract

The selective hydrogenation of aromatic and aliphatic nitriles into amines and imines is described. Using a ruthenium pincer complex, the selectivity towards amines or imines can be controlled by simple parameter changes. The reactions are conducted under very mild conditions between 50-100 °C at 0.4 MPa H_2 pressure without any additives at low catalytic loadings of 0.5-1 mol%, which results in quantitative conversions and high selectivity.

[5] Supplementary Information is provided in the Appendix.

Introduction

Nitrile groups exist in several natural and synthetic organic compounds, which include pharmaceuticals, and can be processed by hydrolysis or hydrogenation reactions.[1–4] Methods for the catalytic hydrogenation of nitriles are interesting because of their straightforward approach to obtain primary amines that are industrially and biologically essential.[5–7] The general challenge in the hydrogenation of nitriles is to control the selectivity of the reaction.[8–11] The catalytic hydrogenation of nitriles is accompanied by many equilibrium reactions, in particular the equilibrium of the primary imine formed and the reaction with the primary amine to its corresponding secondary imine and amine (Scheme 3.8).[12,13] Typically, precious-metal hydrides such as Ru or Rh are applied for the hydrogenation of nitriles, and non-noble metals such as Ni, W, Mo and Fe have been tested.[9,13–20] The first Rh based hydrogenation of nitriles to amines under very mild conditions (0.1 MPa H_2, 20 °C) was reported by *Otsuka* and co-workers in the late 1970s but has fallen into disregard.[16] Under similar conditions, *Sabo-Etienne* and co-workers applied a bis(dihydrogen) ruthenium complex for the selective hydrogenation of benzonitrile to benzyl amine at room temperature and 0.3 MPa H_2.[18] The use of some other Ru complexes was successful for the selective formation of amines from nitriles but mostly harsh conditions (e.g., 3.0-7.5 MPa H_2) and often additives such as base were required.[9,13,14,21] For non-noble metals, *Beller et al.* reported the first Fe-based catalyst for the hydrogenation of various nitriles to amines, notable also for the hydrogenation of adiponitrile into 1,6-hexamethylenediamine.[19] For the formation of secondary imines as major products, only a few non-noble catalysts based on Ni, W and Mo have been reported. These non-noble metal catalysts are good alternatives to precious metals, even so relatively high pressures (W, Mo) or high temperatures (Ni) are required.[20,22]

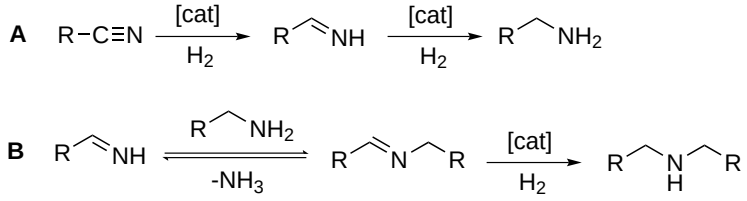

Scheme 3.8 – A) Hydrogenation of nitriles to primary amines and B) the subsequent side-reaction to imines and secondary amines.

Furthermore, the selective catalytic coupling of nitriles with various amines to secondary imines was achieved by *Milstein* and co-workers using a tridentate PNN Ru pincer complex under mild conditions at 70 °C and 0.4 MPa H_2.[23] Until now many groups have maintained the control of the reaction selectively (90–99%) into amines or imines, but to the best of our knowledge, no homogenous catalyst has been reported yet that can be used intentionally to

hydrogenate nitriles selectively into both amines and imines by simple parameter changes. Herein, we present the first Ru pincer complex system in which one catalyst can be used for the synthesis of secondary imines or primary amines (Scheme 3.9). Our optimised reaction conditions are very mild, in particular, low pressure and temperature are used as well as a relatively low catalyst loading, and generally high conversion and high selectivity of the tested range of substrates are reported.

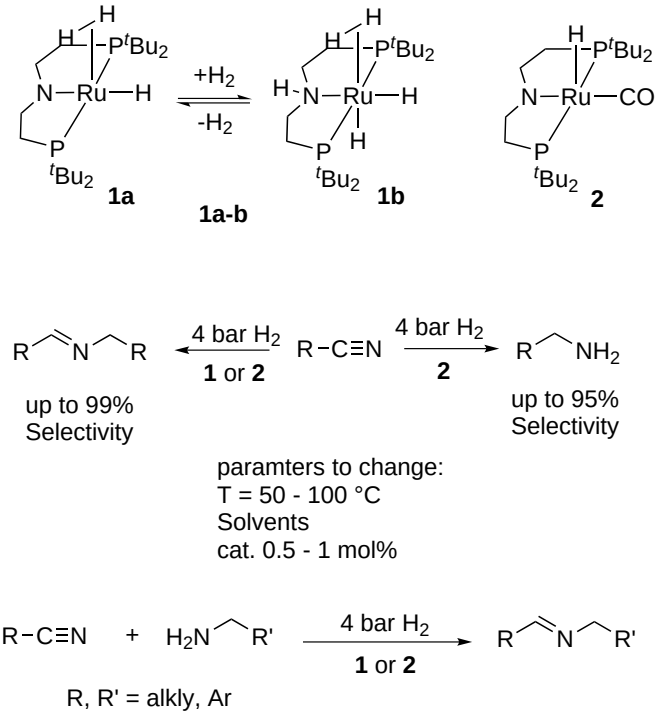

Scheme 3.9 – Hydrogenation of nitriles to amines or imines catalysed by **1** and **2**.

Results and Discussion

Catalyst Screening and Reaction Optimisation: Secondary Imines

In recent reports, we described the formation of ruthenium carbonyl hydrido complexes through the decarbonylation of primary alcohols by ruthenium hydrides (Figure 3.16).[24,25] To test the activity of **1a**-**4** and to optimise the hydrogenation reaction of nitriles, benzonitrile was used as a model substrate. The catalyst screening at 70 °C and 0.4 MPa H_2 for 20 h with a catalyst loading of 1 mol% showed high activity for **1** and **2**. Interestingly, the Me-PNP-based Ru complexes **3** and **4** were basically not active (9% conversion with **3** and 0% with **4**). Complex **1** is predominantly present as trihydride **1a** under Ar and solely present as tetrahydride **1b** under H_2.[24] The nonclassical ruthenium hydride **1** was used for further evaluation, and the results are summarised in Figure 2. Under the given reaction conditions,

74% conversion selectively to the secondary imine *N*-benzylidenebenzylamine was reached with **1** (Figure 3.17, entry 1). As the reaction parameters were varied (Figure 3.17, entries 2-6), a clear temperature and time dependence is observed.

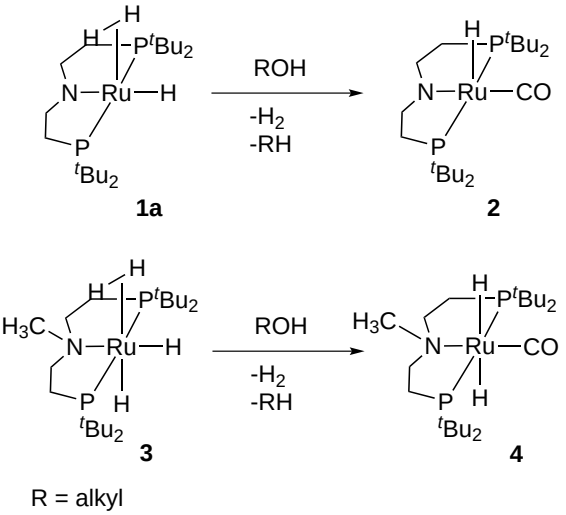

Figure 3.16. – Formation of ruthenium carbonyl hydrido complexes **2** and **4** by the decarbonylation of alcohol by **1a** and **3**.[25]

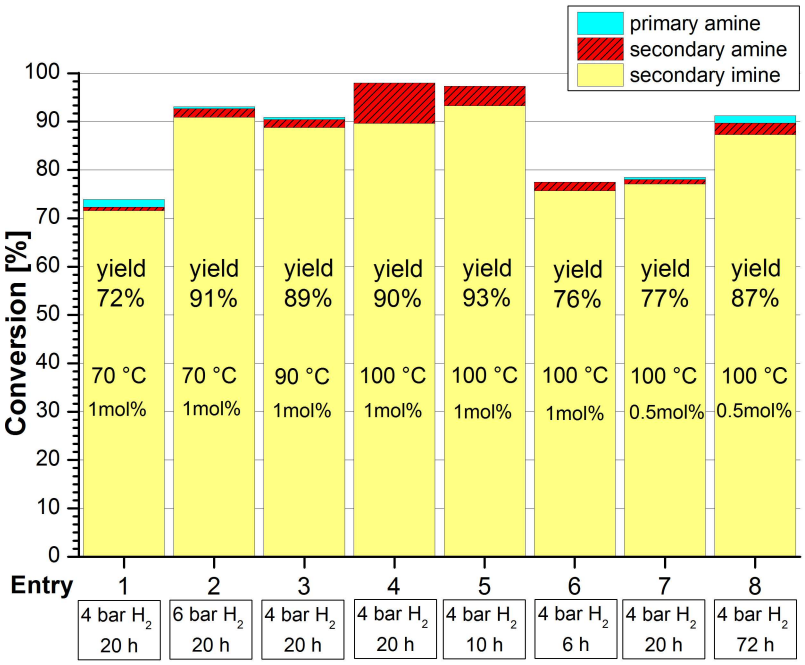

Figure 3.17. – Catalytic hydrogenation of benzonitrile (2 mmol) to secondary imine, secondary amine and primary amine by **1** in 3 mL toluene with a catalyst loading of 0.5-1 mol%. Conversions and yields were determined by GC with flame ionisation detection (FID).

Complex **1** is active to hydrogenate nitriles selectively to secondary imines, which is best at 100 °C and 0.4 MPa H_2 within 10 h at a catalyst loading of 1 mol%. A lower catalyst concentration at 0.5 mol% led to a lower conversion of the benzonitrile (Figure 3.17, entries 7 and 8). Complex **2** shows a generally high activity at 70 °C (Figure 3, entry 1) with almost full conversion, but only 58% of the secondary imine and 39% of the primary amine were obtained. Furthermore, the results show that the selectivity towards secondary imines is temperature dependent. Increasing the temperature lowered the selectivity of the secondary imine (Figure 3.18, entries 2 and 3). The best selectivity of the secondary imine was reached at 50 °C within 20 h with a catalyst loading as low as 0.5 mol% (Figure 3.18, entries 5 and 6). Almost no conversion was reached at room temperature, which indicates that, despite the high activity of 2, a minimum temperature of around 50 °C is required (Figure 3.18, entry 7).

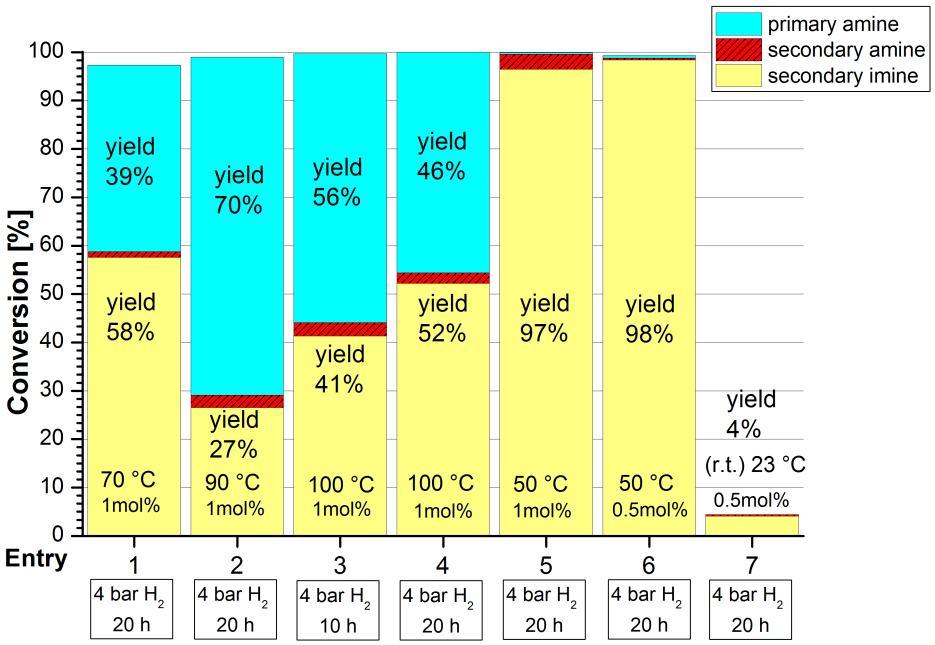

Figure 3.18. – Catalytic hydrogenation of benzonitrile (2 mmol) to secondary imine, secondary amine and primary amine by **2** in 3 mL toluene with a catalyst loading of 0.5-1 mol%. Conversions and yields were determined by GC–FID.

Hydrogenation of Nitriles to Secondary Imines and the Cross-Coupling of Various Amines

We tested different nitrile substrates under the optimised reaction conditions to favour the imine selectivity by **1** and **2**. Furthermore, we added various amines to the nitriles for crosscoupling experiments (Scheme 3.10).

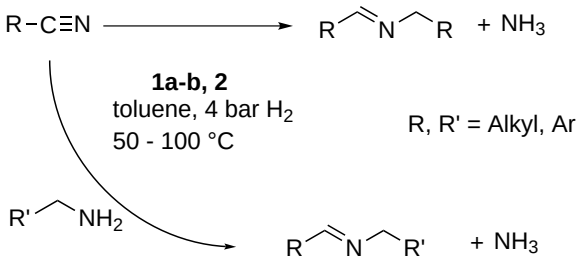

Scheme 3.10 – Hydrogenation of nitriles to secondary imines by **1** and **2** and the cross-coupling of amines.

The results are summarised in Table 3.4. Cross-coupling reactions with benzonitrile and hexylamine or cyclohexylamine gave quantitative conversions with good to excellent selectivity (Table 3.4, entries 1a/b and 2 a/b). For the direct coupling of *p*-bromobenzonitrile with hexylamine, 91% conversion and a yield of 83% of the imine was obtained with **1**, whereas moderate conversion and yield were obtained with **2** in a shorter reaction time (Table 3.4, entry 3 a/b). Without the addition of amine, moderate conversion was obtained with both complexes (Table 3.4, entry 4a/b). For **2**, in addition to the imine (32%), a significant yield (27%) of the secondary amine was obtained. The full conversion of *p*-tolunitrile into imine was obtained with good to excellent yields with both complexes (Table 3.4, entry 5a/b). Unexpectedly, the addition of cyclohexylamine did not lead to good yields with **1** (Table 3.4, entry 6a/b), despite quantitative conversion as with the analogue benzonitrile (Table 3.4, entry 2 a). Moreover, 2 gave only 5% conversion and yield (Table 3.4, entry 2b). If we added the smaller and less bulky isobutylamine (Table 3.4, entry 7 a), higher conversions with **1** were obtained but the selectivity remained low and gave yields of only 25% of the coupled imine product and 51% of the corresponding secondary imine of *p*-tolunitrile. If we used **2** (Table 3.4, entry 7 b), almost full conversion was achieved, but only 9% of the coupled imine and 90% of the primary amine were obtained. With both complexes, the short-chained butyronitrile was coupled with hexylamine to butylidenehexylamine with excellent yields and almost full conversion (96%, Table 3.4, entry 8 a/b). The heptyl cyanide (Table 3.4, entry 9a) gave 97% conversion with **1**, but mostly the octylamine was obtained with 94% yield. Complex **2** converted 54% of the heptyl cyanide to give only 36% imine and 17% octylamine (Table 3.4, entry 9 b). The addition of cyclohexylamine to heptyl cyanide led to almost no conversion with **1** (Table 3.4, entry 10a), whereas a good conversion of 71% was achieved with **2** accompanied by a moderate selectivity (46% yield; Table 3.4, entry 10 b). 4-Propoxybenzonitrile was hydrogenated in the presence of hexylamine to give quantitative conversions with both complexes (Table 3.4, entry 11a/b), and excellent yields of the coupled imine were obtained (**1**, 98%; **2**, 97%).

Table 3.4. – Hydrogenation of nitriles (2 mmol) to secondary imines by **1** (1 mol% at 100 °C) and **2** (0.5 mol% at 50 °C) at 0.4 MPa H_2 in 3 mL toluene.

Entry	Nitrile[a]	Amine[a]	Catalyst	t [h]	Conversion[b] [%]	Imine yield[b, c] [%]
1a	A	B	**1**	20	99	81
1b			**2**	20	99	99
2a	A	C	**1**	24	97	69
2b			**2**	20	99	97
3a	D	B	**1**	72	91	83
3b			**2**	48	76	67
4a	D		**1**	72	73	49
4b			**2**	72	79	32
5a	E		**1**	48	99	85
5b			**2**	48	99	98
6a	E	C	**1**	20	99	31
6b			**2**	20	5	5
7a	E	I	**1**	20	98	25 (+51)[d]
7b			**2**	20	99	9 (+90)
8a	F	B	**1**	20	96	96
8b			**2**	20	99	98
9a	G		**1**	20	97	3 (+94)[e]
9b			**2**	20	54	36 (+17)[e]
10a	G	C	**1**	24	2	1
10b			**2**	24	71	46
11a	H	B	**1**	24	99	98
11b			**2**	24	99	97

[a] Substrates: benzonitrile (A), hexylamine (B), cyclohexylamine (C), *p*-bromobenzonitrile (D), *p*-tolunitrile (E), butyronitrile (F), heptyl cyanide (G), 4-propoxybenzonitrile (H), isobutylamine (I).

[b] Conversions and yields were determined by GC-FID.

[c] Cross-coupled R-R' secondary imines are given as yields, in the case of no additional primary amine, the corresponding secondary imines to nitriles are given as yields. Other products are the corresponding primary amines or secondary amines.

[d] Secondary imine.

[e] Primary amine.

Optimisation and Catalytic Results of the Selective Hydrogenation of Nitriles into Primary Amines

According to the results of the optimisation experiments for the selectivity of secondary imines, **1** is only selective towards secondary imines, whereas the total conversion increases at higher temperatures (Figure 3.17, entries 1-5). Conversely, if **2** is used, the amine ratio increases significantly at a higher temperature of 90 °C up to 70% and decreases to under 50% at 100 °C (Figure 3.18, entries 1-3). Varying the reaction parameters, a higher H_2 pressure (1.0 MPa) did not favour the selectivity towards primary amines (Figure 3.19, entry 1). A longer reaction time of 30 h at 90 °C with a catalyst loading of 1 mol% and 0.4 MPa H_2 in toluene did not improve the product ratio, nor did a higher catalytic loading of 1.5 mol% within 20 h (Figure 3.19, entries 2 and 3). The use of a different solvent such as THF did not favour the amine selectivity, in contrast to 2-propanol, the use of which yielded 88% of the primary amine (Figure 3.19, entries 3 and 4). Generally, the use of 2-propanol as the solvent also led to a secondary acetone imine as a sideproduct. *N*-(Isopropylidene)benzylamine is generated from the side-reaction of the obtained primary amine and acetone formed from 2-propanol after the release of the hydrogen pressure. A decrease of the catalytic loading to 0.5 mol% led to 55% of the primary amine and 27% of the side-product (Figure 3.19, entry 6). At a lower temperature of 50 °C, the reaction was improved significantly and a very good yield of primary amine (89%) was obtained, despite the slightly increased amount of secondary imine (Figure 3.19, entry 7). A decrease of the reaction time to 10 h with the given reaction conditions at 90 °C and a catalyst loading of 0.5 mol% led to the formation of the secondary imine as the dominant species (Figure 3.19, entry 8), which is different to 20 h reaction time (Figure 3.19, entry 6). The solvent effect of 2-propanol that favoured the selectivity of the primary amine was reported recently by *Beller et al.* who used an Fe pincer complex for the hydrogenation of various nitriles.[19] Moreover, their treatment of the reaction medium with HCl after the hydrogenation possibly avoided the formation of the secondary acetone imine by salting out the amine.[19] Under the reaction conditions given in Figure 3.19, entry 5, a variety of nitriles was hydrogenated into primary amines (Table 3.5). If we take into account the side-reaction between the generated primary amine and acetone, all substrates give very good to excellent yields. Different para substitutions on aromatics, such as that in *p*-bromobenzonitrile, *p*-tolunitrile or *p*-proproxybenzonitrile, do not influence the reduction of the nitrile group (Table 3.5, entries 1-3), and even ortho-amine-functionalised 2-aminebenzonitrile was hydrogenated to a diamine (Table 3.5, entry 4). Furthermore, aliphatic heptyl cyanide was hydrogenated without any hindrance with high conversion (Table 3.5, entry 5).

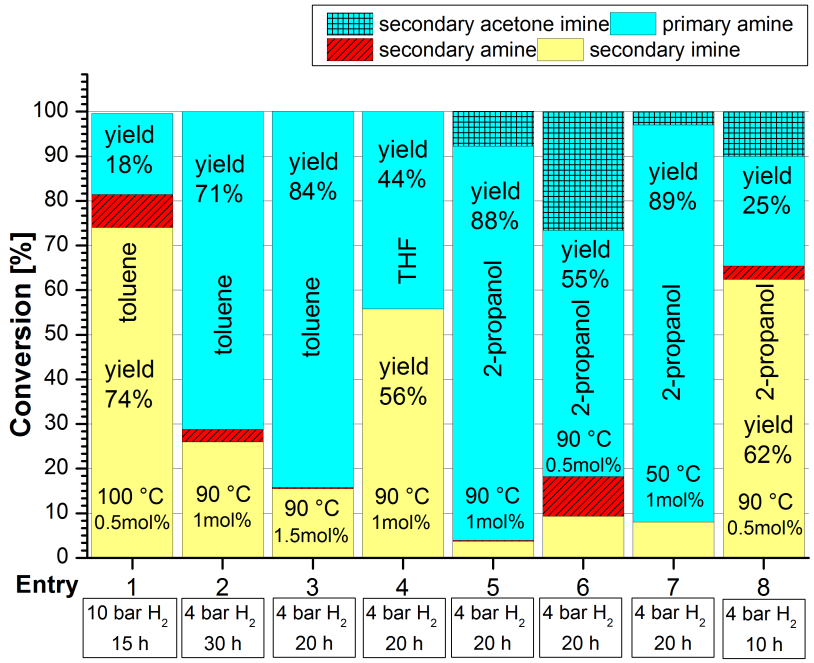

Figure 3.19. – Catalytic hydrogenation of benzonitrile (2 mmol) to primary amine in 3 mL of the given solvent catalysed by **2** (0.5-1 mol%). Conversions and yields were determined by GC-FID. Secondary acetone imine was obtained as a side-product after the catalysis in 2-propanol.

Table 3.5. – Hydrogenation of nitriles (2 mmol) to primary amines by **2** (1 mol% at 90 °C, 0.4 MPa H_2) in 3 mL 2-propanol.

Entry	Nitrile[a]	t [h]	Conversion[b] [%]	Amine yield[b] [%]	Secondary acetone imine yield[b] [%]
1	D	22	99	86	11
2	E	20	99	80	16
3	H	24	99	92	7
4	J	24	81	81	-
5	G	22	93	56	29

[a] Substrates: *p*-bromobenzonitrile (D), *p*-tolunitrile (E), heptyl cyanide (G), 4-propoxybenzonitrile (H), 2-aminebenzonitrile (J).
[b] Conversions and yields were determined by GC-FID.

General Aspects

The inactivity of **3** and **4** is thought to be because of the occupied methyl group at the *N* atom of the PNP pincer backbone, thus the metal-ligand cooperativity to accept a hydrogen pair on the *N* site and Ru is necessary for the hydrogenation of nitriles. Complexes **1** and **2** are highly active in the reduction of nitriles, in which the outer-sphere mechanism takes place.[19] Contrary to aliphatic PNP pincer complexes, in particular the non-classical hydride complex **1**, a similar ruthenium hydride complex with an aromatic PNP pincer backbone was reported to reduce nitriles directly at the metal centre without the involvement of the pincer backbone.[14,26] Under the given conditions, the selectivity towards secondary imines is favoured with **1**, with the exception of the bulky, long-chained heptyl cyanide, which was converted selectively into octyl amine (Table 3.4, entry 9a). Conversely, **2** can be used exclusively for the reduction of nitriles into primary amines by small parameter changes, for which temperature is an important factor.[21,23] Besides the influence of the catalyst loading and reaction time, the use of a more protic, polar solvent, such as 2-propanol, is crucial for the selectivity towards primary amines in such systems, possibly because of its protonating properties.[19] We monitored the selectivity during the reaction and observed that full conversion was reached in the first hour and the secondary imine was initially formed almost quantitatively (Figure 3.20). In reported kinetic studies, it is proposed that the first hydrogenation to primary imine by the catalyst is the ratedetermining step. The following reactions to primary amines or secondary imines are believed to be much faster (Scheme 3.11).[27,28] The formation of the secondary imine is favoured at the beginning of the reaction until saturation takes place (Figure 3.20, t=0.5 h). A retrograde reaction occurs possibly through the concentrated presence of generated ammonia and the solvent influence (Scheme 3.11).[18,28]

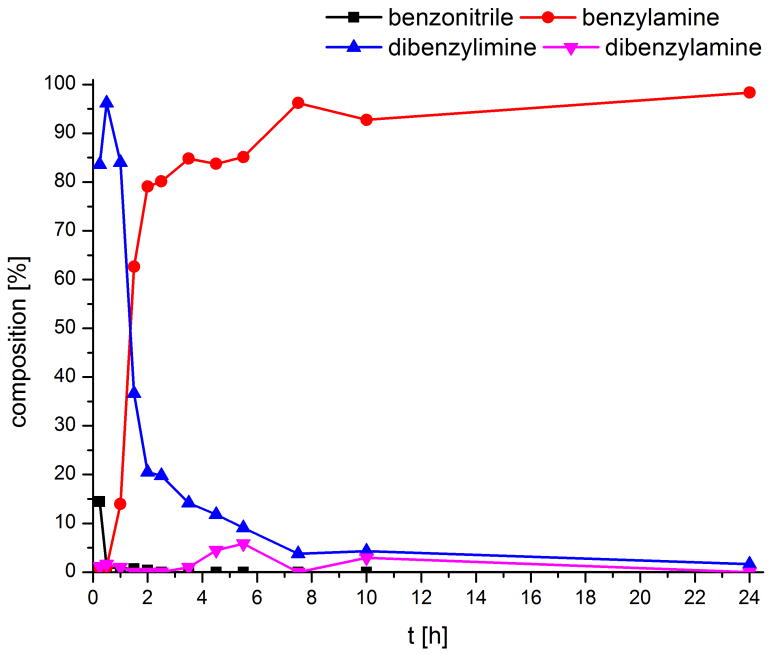

Figure 3.20. – Monitoring the selectivity of the hydrogenation of benzonitrile into benzylamine in 2-propanol at 90 °C by 1 mol% 2, 0.4 MPa (Note: the yield of *N*-(isopropylidene)benzylamine was included in that of benzylamine). Samples were taken at t=0.25, 0.5, 1, 1.5, 2, 2.5, 3, 3.5, 4.5, 5.5, 7.5, 10 and 24 h.

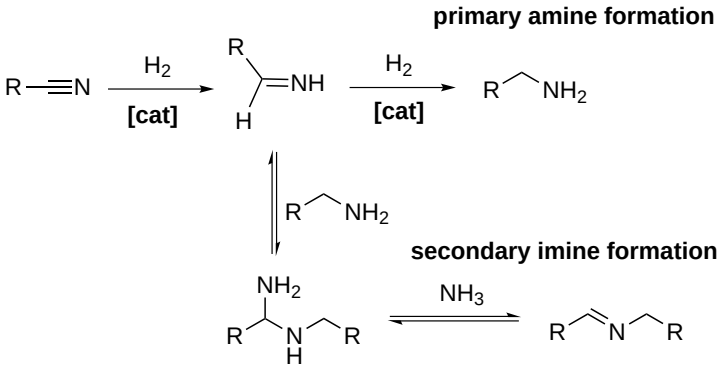

Scheme 3.11 – Possible equilibrium reactions during the catalytic hydrogenation of nitriles.

For complex **2**, we assume the possible mechanism illustrated in Scheme 3.12 with the model substrate benzonitrile. The coordination of the nitrile to the metal centre of **2** gives the coordinated nitrile complex, which is assigned tentatively as **2a**. A non-classical hydride complex is formed if **2a** accepts a hydrogen pair.[14,25] Intermediate **2b** transfers one hydrogen atom from the H_2 to the coordinated nitrile via **2c** to the primary imine, and **2** is generated again. The primary imine undergoes a second catalytic cycle to the primary amine (Scheme 3.12).

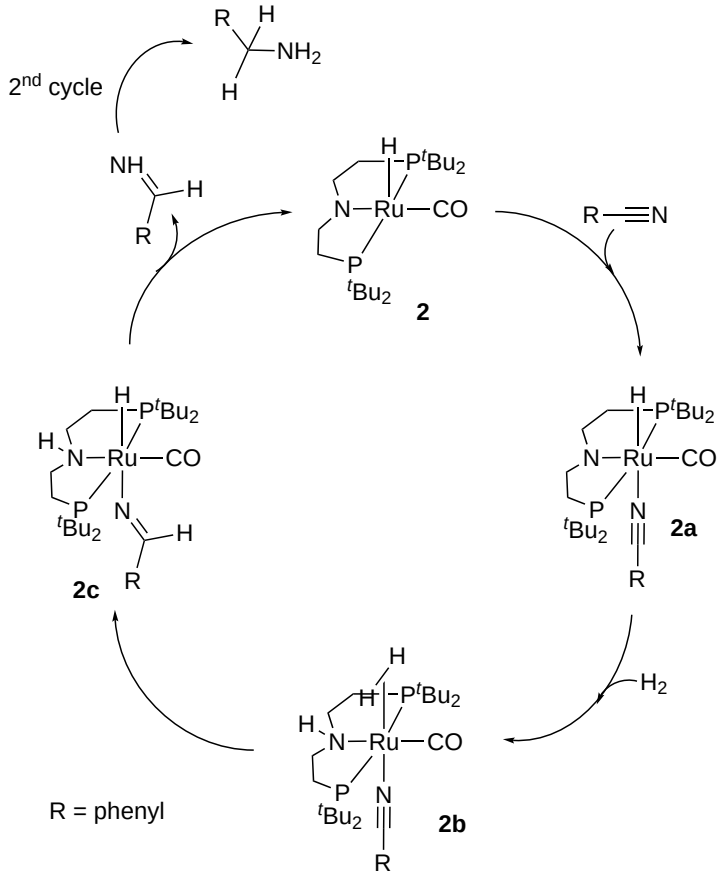

Scheme 3.12 – Possible mechanism for the selective hydrogenation of nitriles by **2** with benzonitrile as a model substrate.

Under the given conditions (50 °C, 0.4 MPa H_2), the formation of the gem-diamine intermediate occurs by the condensation of the primary imine with an equivalent of primary amine. The immediate elimination of ammonia gives the secondary imine. We attempted to isolate the possible stable intermediate **2a** by adding an excess of benzonitrile to **2** following a similar protocol to that reported by *Sabo-Etienne* and co-workers.[18] As **2a** is very soluble in common solvents, it was isolated only as a muddy residue (Supporting Information). However, a clear signal in the ^{31}P NMR spectrum is visible at $\delta = 88.4$ ppm along with a change

in the Ru-H signal from δ = -20.87 (t, $^2J_{PH}$ = 16.3 Hz) to -14.45 ppm (t, $^2J_{PH}$ = 21.4 Hz). Routine ^{31}P NMR spectroscopy of the reaction contents after the catalytic hydrogenation of benzonitrile shows the signal of **2a** at δ = 88.4 ppm (Figures S5.60 and S5.61). Liquid injection field desorption/ionisation mass spectrometry (LIFDI-MS) shows only the fragment of [RuH(CO)(PNP)] at m/z 491 caused by the loss of Ph-CN under MS conditions. In the IR spectrum, the C≡N band of PhC≡N-Ru is not visible, probably because of overlap with the νCO signal at $\tilde{\nu}$ = 1898 cm^{-1}. The νCO and Ru-H stretching bands are shifted towards higher frequencies by approximately 30-40 cm^{-1}. Even though a back-bonding interaction between Ph-CN and the metal centre can decrease the stretching frequency of C≡N slightly, the range remains between $\tilde{\nu}$ = 2300-2100 cm^{-1}, which is contrary to our results.[18,29–33] Moreover, the *in situ* generation of a C=N ligand that exhibits a stretching band at around $\tilde{\nu}$ = 1400-1500 cm^{-1} is not likely as no hydrogen was added or generated in the preparation of **2a**.[30] To further evidence this consideration, a similar observation was made by adding acetonitrile to **2**. Despite partial conversion, key signals in the same area at δ = 88.3 ppm (t, $^2J_{PH}$ = 21.4 Hz) in the ^{31}P NMR spectrum and δ = -14.41 ppm in the ^{1}H NMR spectrum were found (Figures S5.58 and S5.59). Apart from **2a**, no other complex intermediate could be assigned.

Conclusion

We report the hydrogenation of aromatic and aliphatic nitriles by ruthenium pincer complexes **1** and **2** selectively to imines and the cross-coupling with different amines to imines under very mild conditions with generally high conversions and high selectivity. The highlight of our report is the use of **2** not only to reduce various nitriles selectively into imines but also selectively into amines with full conversions and high selectivity by simply changing reaction parameters and still under mild reaction conditions.

Acknowledgements

We acknowledge the Ministerium für Innovation, Wissenschaft und Forschung NRW (MIWF-NRW) for financial support within the Energy Research Program for the Scientist Returnee Award for M.H.G.P. (NRW-Rückkehrerprogramm). M.H.G.P. acknowledges the Ernst-Haage Foundation at the Max-Planck-Institute for Chemical Energy Conversion for the Ernst-Haage Prize awarded for our research achievements. For access to LIFDI-MS analysis, we gratefully acknowledge Prof. Dr. T. Braun, Dr. M. Ahrens and J. Berger (Humboldt-University Berlin, Germany). J.-H.C. thanks M. Springer and M. Fetzer for experimental support.

References

[1] F. F. Fleming, *Nat. Prod. Rep.* **1999**, *16*, 597–606.

[2] F. F. Fleming, L. Yao, P. C. Ravikumar, L. Funk, B. C. Shook, *J. Med. Chem.* **2010**, *53*, 7902–7917.

[3] S. Liu, Y. Yang, X. Zhen, J. Li, H. He, J. Feng, A. Whiting, *Org. Biomol. Chem.* **2012**, *10*, 663–670.

[4] F. J. Weiberth, S. S. Hall, *J. Org. Chem.* **1986**, *51*, 5338–5341.

[5] K. Hayes, *Appl. Catal. A* **2001**, *221*, 187 –195.

[6] K. Weissermel, H. J. Arpe, *Industrial Organic Chemistry*, Wiley-VCH, Weinheim, **2008**.

[7] M. Santos, *Int. J. Food Microbiol.* **1996**, *29*, 213 –231.

[8] S. Gomez, J. Peters, T. Maschmeyer, *Adv. Synth. Catal.* **2002**, *344*, 1037–1057.

[9] S. Takemoto, H. Kawamura, Y. Yamada, T. Okada, A. Ono, E. Yoshikawa, Y. Mizobe, M. Hidai, *Organometallics* **2002**, *21*, 3897–3904.

[10] X. Miao, C. Fischmeister, P. H. Dixneuf, C. Bruneau, J.-L. Dubois, J.-L. Couturier, *Green Chem.* **2012**, *14*, 2179–2183.

[11] L. Hegedűs, T. Máthé, T. Kárpáti, *Appl. Catal. A* **2008**, *349*, 40 –45.

[12] X. Xie, C. L. Liotta, C. A. Eckert, *Ind. Eng. Chem. Res.* **2004**, *43*, 7907–7911.

[13] D. Addis, S. Enthaler, K. Junge, B. Wendt, M. Beller, *Tetrahedron Lett.* **2009**, *50*, 3654 –3656.

[14] C. Gunanathan, M. Hölscher, W. Leitner, *Eur. J. Inorg. Chem.* **2011**, *2011*, 3381–3386.

[15] S. Werkmeister, K. Junge, M. Beller, *Org. Process Res. Dev.* **2014**, *18*, 289–302.

[16] T. Yoshida, T. Okano, S. Otsuka, *J. Chem. Soc. Chem. Commun.* **1979**, 870–871.

[17] R. A. Grey, G. P. Pez, A. Wallo, *J. Am. Chem. Soc.* **1981**, *103*, 7536–7542.

[18] R. Reguillo, M. Grellier, N. Vautravers, L. Vendier, S. Sabo-Etienne, *J. Am. Chem. Soc.* **2010**, *132*, 7854–7855.

[19] C. Bornschein, S. Werkmeister, B. Wendt, H. Jiao, E. Alberico, W. Baumann, H. Junge, K. Junge, M. Beller, *Nat Commun* **2014**, *5*, Article number: 4111.

[20] S. Chakraborty, H. Berke, *ACS Catal.* **2014**, *4*, 2191–2194.

[21] C. Bianchini, V. Dal Santo, A. Meli, W. Oberhauser, R. Psaro, F. Vizza, *Organometallics* **2000**, *19*, 2433–2444.

[22] P. Zerecero-Silva, I. Jimenez-Solar, M. G. Crestani, A. Arévalo, R. Barrios-Francisco, J. J. García, *Appl. Catal. A* **2009**, *363*, 230 –234.

[23] D. Srimani, M. Feller, Y. Ben-David, D. Milstein, *Chem. Commun.* **2012**, *48*, 11853–11855.

[24] J.-H. Choi, N. E. Schloerer, J. Berger, M. H. G. Prechtl, *Dalton Trans.* **2014**, *43*, 290–299.

[25] J.-H. Choi, L. E. Heim, M. Ahrens, M. H. G. Prechtl, *Dalton Trans.* **2014**, *43*, 17248–17254.

[26] M. H. G. Prechtl, Y. Ben-David, D. Giunta, S. Busch, Y. Taniguchi, W. Wisniewski, H. Goerls, R. J. Mynott, N. Theyssen, D. Milstein, W. Leitner, *Chem.-Eur. J.* **2007**, *13*, 1539–1546.

[27] A. M. Joshi, K. S. MacFarlane, B. R. James, P. Frediani in *Progress in Catalysis Proceedings of the 12th Canadian Symposium on Catalysis*, (Eds.: K. J. Smith, E. C. Sanford), Studies in Surface Science and Catalysis, Elsevier, Amsterdam, **1992**, pp. 143 –146.

[28] C. de Bellefon, P. Fouilloux, *Catal. Rev. Sci. Eng.* **1994**, *36*, 459–506.

[29] E. Benedetti, G. Braca, G. Sbrana, F. Salvetti, B. Grassi, *J. Org. Chem.* **1972**, *37*, 361 –373.

[30] C. P. Guengerich, K. Schug, *J. Am. Chem. Soc.* **1977**, *99*, 3298–3302.

[31] J. Chatt, G. Leigh, N. Thankarajan, *J. Org. Chem.* **1970**, *25*, C77 –C79.

[32] A. Misono, Y. Uchida, M. Hidai, T. Kuse, *J. Chem. Soc. D* **1969**, 208a–208a.

[33] P. C. Ford, R. E. Clarke, *Chem. Commun. (London)* **1968**, 1109–1110.

3.4. Amide vs. Amine Paradigm in the Direct Amination of Alcohols with Ru-PNP Complexes

Dennis Pingen[b], Jong-Hoo Choi[c], Martin H. G. Prechtl[c]* and Dieter Vogt[a]*, Amide vs. Amine Paradigm in the Direct Amination of Alcohols with Ru-PNP Complexes, *ACS Catalysis*, 2015, (manuscript in preparation).

[a] Dr. D. Vogt, School of Chemistry, King's Building, Joseph Black Building, The University of Edinburgh, EH9 3JJ, Scotland, UK, E-mail: d.vogt@ed.ac.uk; [b] Dr. D. L. L. Pingen, Chemical Materials Science, Department of Chemistry, University of Konstanz, Universitätsstrasse 10, Konstanz, Germany. E-mail: dennis.pingen@uni-konstanz.de [c] Department of Chemistry, University of Cologne, Greinstr. 6, 50939 Cologne, Germany. E-mail: martin.prechtl@uni-koeln.de.[6]Supporting Information is provided in the appendix.

Abstract

New fundamental insights into the effect of PNP ligands on ruthenium complexes for the direct amination of alcohols using ammonia have been revealed. A small scope of complexes containing PNP ligands, based on secondary amines or tertiary amines, were tested for such reaction. Ruthenium complexes with tertiary amine ligands were found to be active, while complexes with secondary amines, able to form a *N*-Ru amide bonds are not. Based on this results, we report the synthesis of a new ruthenium complex with a tertiary amine PNP ligand, which is highly active for direct amination reaction of alcohols. The amide-amine paradigm in ruthenium PNP systems was previously not considered as a key element for successful amination reactions of alcohols until now.

[6]This is a shortened, rewritten version of the original manuscript and focusses on the experimental results obtained by the author of this thesis Jong-Hoo Choi. The original manuscript contents further results and discussions from the Vogt group,[a] Dr. O. Diebold (Université de Limoges, Laboratoire de Chimie des Substances Naturelles, faculté des sciences et techniques, Limoges, France) and Prof. Dr. P. van Leeuwen (INSA, Laboratoire de Physique et Chimie de Nano-Objets, Toulouse, France).

Introduction

Direct amination of alcohols with ammonia is a straight-forward, attractive approach to obtain primary amines, due to the direct replacement of the alcohol group with an amine group. In homogeneous catalysis, the transformation of primary alcohols into primary amines was first realised by *Milstein et al.* in 2008.[1] Since then, other systems have been reported for analogue reaction with other primary and secondary alcohols.[2–6] In amination reactions, the mechanistic aspects are still unclear, even though the general concept of the methodology of "Borrowing Hydrogen" established by *Williams et al.* is widely accepted.[7,8] In this theory, the catalyst serves both as a hydrogen acceptor and donor (Scheme 3.13). In the dehydrogenation step of the alcohol to the ketone or aldehyde, the catalyst accepts and "stores" an equivalent of hydrogen. The carbonyl intermediate reacts with ammonia to form the imine intermediate. Subsequently, the imine intermediate is hydrogenated to the primary amine with an equivalent of hydrogen "borrowed" by the catalyst in the previous dehydrogenation sequence. In an operative catalytic system, the balance between the catalyst loading and intermediate concentration is important, since the applied catalysts need to be available for their two functional tasks, normally to dehydrogenate and to hydrogenate.[9]

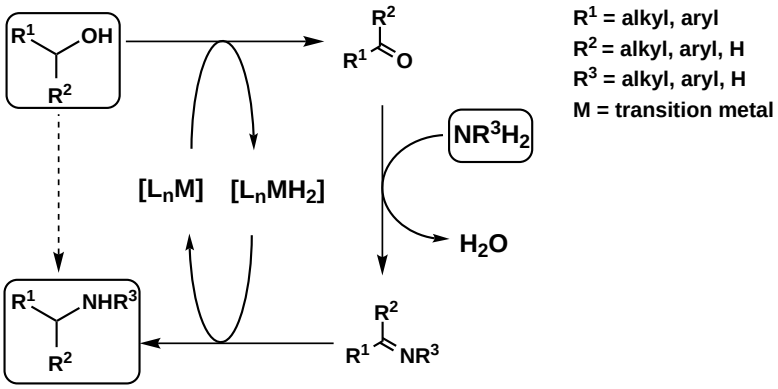

Scheme 3.13 – Concept of "Hydrogen Borrowing" in the direct amination reaction of an alcohol.

The involvement of PNP pincer ligands in ruthenium complexes proved to be highly effective for the amination of alcohols. An example of this is the acridine-based PNP ruthenium complex **1** reported by *Milstein* (Scheme 3.14).[1] *Vogt et al.* employed the same ligand for the amination of primary and secondary bio-alcohols.[2] In later reports, *Milstein* and co-workers postulated that long-range metal-ligand cooperation might be involved in the direct amination reactions of alcohols, whereby the C9 (in the ligand backbone, *para* to the N in the ring) is crucial in this catalytic reaction.[10] The activation can occur in the presence of base or NH_3 to form complexes **1a** or **1b**. However, in recent studies by *Hofmann et al.*, it is claimed that

this long-range cooperation is not necessarily required for the catalytic amination process itself.[11] In fact, more studies are needed to explain the behaviour of PNP pincer ligands in direct amination reactions to make a definitive statement.

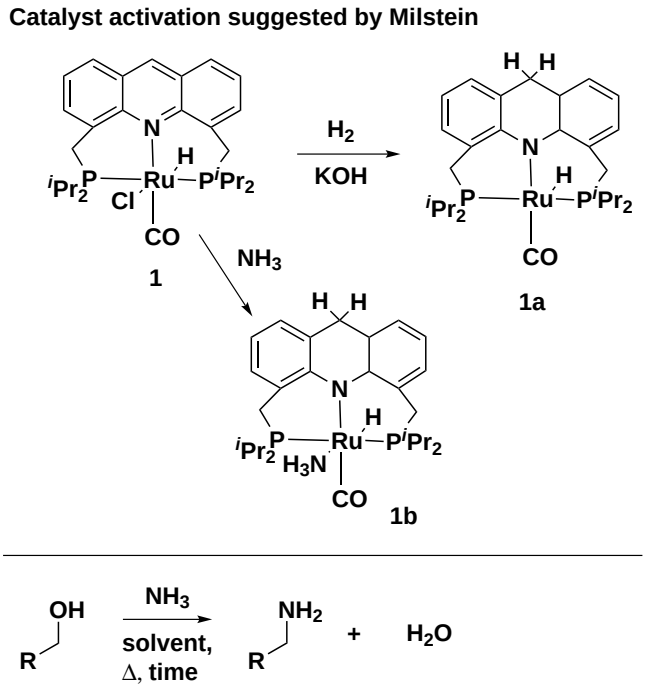

Scheme 3.14 – The activation of the Ru-based complex **1** bearing an acridine PNP ligand by *Milstein* is described. **1** was employed in the direct amination of primary alcohols.[1]

To the current state of the art, we contribute more detailed information of the much discussed mechanical aspects. For this purpose, we tested the ruthenium PNP pincer complexes **2**-**5** based on the aliphatic ligand backbone reported by the *Prechtl* group (Figure 3.21).[12,13] Complexes **2** and **3** are classified as non-classical hydride complexes and can be transformed by decarbonylation reaction of alcohols into the corresponding CO functionalised ruthenium complexes **4** and **5**.[13] Moreover, **2** and **4** contain steady tertiary amine ligand backbones, while **3** and **5** contain secondary amine ligand backbones in hydrogen atmosphere, respectively with the addition of an equivalent H_2 (**2a** and **5a**). *N*-Ru amide-bonds are formed in argon atmosphere, respectively with the loss of a H_2. In non-classical hydride species **2** and **3**, the H_2-ligand are thermally dissociable. A very few reports are known, that ruthenium hydride complexes are light sensitive, whereby the dissociation of the hydride ligands in form of H_2 is observed.[14]

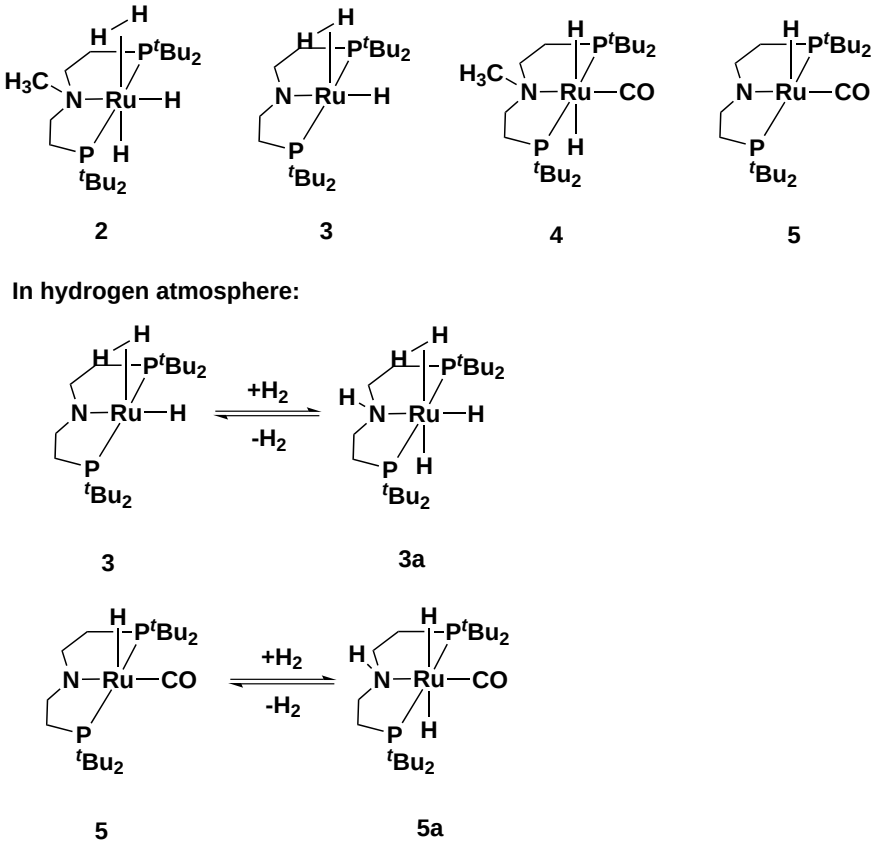

Figure 3.21. – Polyhydride Ru-PNP complexes **2-3** and CO functionalised Ru-PNP complexes **4-5**. **3a** and **5a** are formed in hydrogen atmosphere.

Results and Discussions

Catalytic Results

From the experiences from previous reports for the direct amination of alcohols, the standard reaction conditions were setted at 150 °C with 2.5 mL (l) NH_3 (97.5 mmol) in *t*-amylalcohol. Typical additives for such reactions are substrate intermediates such as cyclohexanone, which can accelerate the reaction course as reported previously.[9] Furthermore, the addition of base (e.g. KO^tBu) can be employed to activate typical complex precursor (L_nRuH_xCl), by abstracting the chloride, or by deprotonating the alcohol substrate. Model substrates, cyclohexanol and benzylalcohol were used giving possible products illustrated in Scheme 3.15.

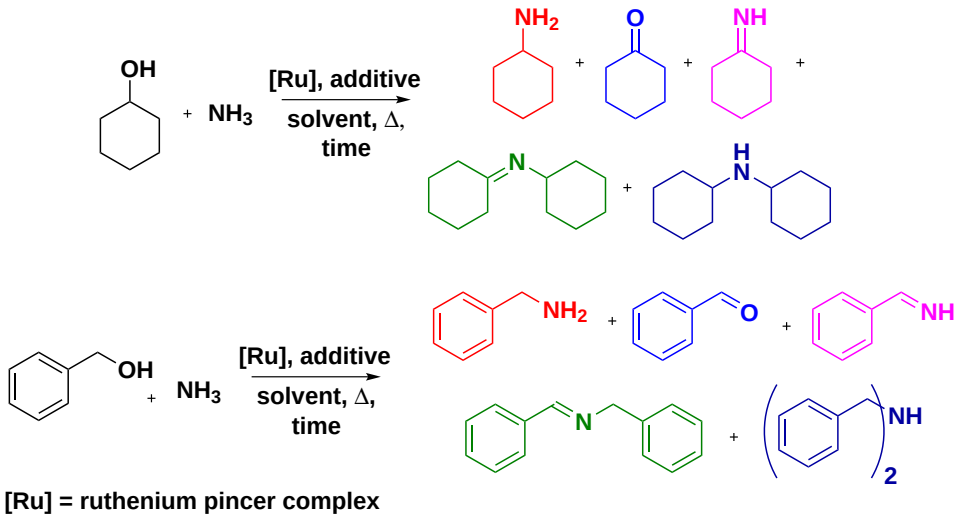

Scheme 3.15 – Cyclohexanol and benzylalcohol as model substrates, listing possible observable products.

From our small scope of complexes, **3** and **5** were found to be inactive for amination of cyclohexanol (see Supporting Information, SI Figure S 5.70-5.71). No significant conversions were detected in the first 22.5 h for either complexes at given conditions (150 °C). The complexes showed no activity when the reactions continued for another 22.5 h, after the addition of 10 mol% cyclohexanone (SI, Figure S 5.74-5.75). Adding 1 mol% of KO^tBu in the third catalytic run (22.5 h) was also not beneficial, as no conversion was detected (SI, Figure S 5.72-5.73). For primary alcohols, benzylalcohol was employed with **3** and **5** under standard reaction conditions resulting in no conversion (in *t*-amylalcohol and toluene). In contrast to **3** and **5**, complexes **2** and **4** were active for direct amination of cyclohexanol under standard conditions (Figure 3.22-3.23). After 52 h, significant conversion was reached with complex **2**, lower conversion was reached with complex **4**. Both complexes indicate that changing the

N-site of the PNP ligand from a secondary to a tertiary amine results in a rapid change in their activity in this reaction. Further intention to increase the reaction rate by the addition of 10 mol% cyclohexanone was investigated in a separate experiment. Contrary to the experiences in direct amination of cyclohexanol with [RuHCl(CO)(Xantphos)(PPh_3)],[9] the addition of cyclohexanone caused the deactivation of the catalysts **2** and **4** (SI, Figure S 5.76-5.77). To ensure our assumption that cyclohexanone is deactivating the catalysts, the reaction was performed again with catalyst **4** without any additives. After 23.5 h, 10 mol% cyclohexanone was added and the reaction mixture was re-charged with 2.5 mL (l) NH_3. Once again, deactivation of the catalyst occurred after the addition of cyclohexanone (SI, Figure S 5.78).

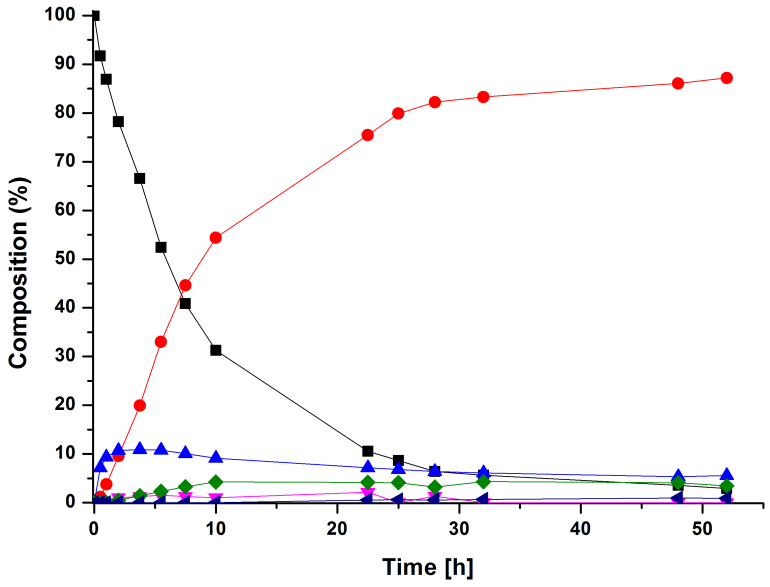

Figure 3.22. – Amination of cyclohexanol with complex **2**. Conditions: 0.04 mmol **2**, 5 mmol cyclohexanol, 15 mL *t*-amylalcohol, 2.5 mL NH_3, 150 °C, 52 h. ■ = cyclohexanol, ● = cyclohexylamine, ▲ = cyclohexanone, ▼ = cyclohexylimine, ♦ = dicyclohexylimine, ◀ = dicyclohexylamine.

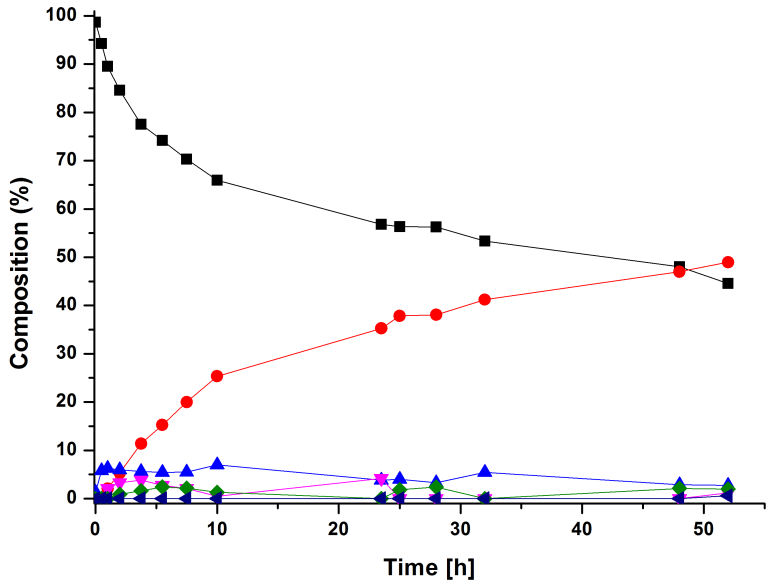

Figure 3.23. – Amination of cyclohexanol with complex **4**. Conditions: 0.04 mmol **4**, 5 mmol cyclohexanol, 15 mL *t*-amylalcohol, 2.5 mL NH_3, 150 °C, 52 h. ■ = cyclohexanol, ● = cyclohexylamine, ▲ = cyclohexanone, ▼ = cyclohexylimine, ♦ = dicyclohexylimine, ◀ = dicyclohexylamine.

Transition metal hydrides, especially ruthenium hydrides are capable of decarbonylating alcohols, aldehydes or ketones.[15–18] Previous investigation displayed that polyhydride **2** and **3** can be CO functionalised by decarbonylation of primary alcohols and the formation of the corresponding aliphates.[13] Furthermore, *Ozerov* and co-workers reported a ruthenium pincer complex capable to decarbonylate acetone to form a carbonyl complex, whereby temporarily the cleaved methyl groups are coordinated to the metal centre.[19] In order to investigate the cause of the deactivation we expected a similar behaviour of **2** in the presence of cyclohexanone, predicting a decarbonlyation reaction followed by a rigid metallacyclic coordination of the generated aliphatic compound (-$(CH_2)_4$-) to the ruthenium core (**6**, Scheme 3.16).

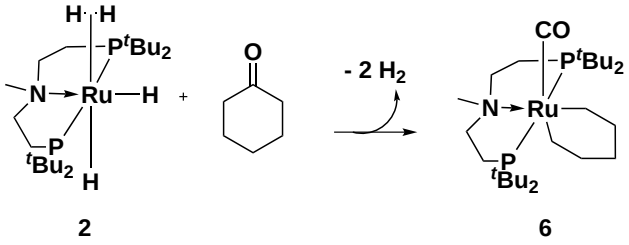

2 **6**

Scheme 3.16 – Reaction of PNP complex **2** with cyclohexanone via decarbonylation.

Among the isolated mixture of subspecies and decomposed complexes from the reaction of **2** with cyclohexanone, detectable amounts of the postulated complex **6** were found in the LIFDI-MS (liquid injection field desorption/ionisation-mass spectrometry) spectrogram. The MS pattern is overall in good agreement to the simulated pattern [Ru(Me-PNP)CO($CH_2CH_2CH_2CH_2CH_2$)] 575 (Figure 3.24, more information is provided in the SI). Furthermore, under MS conditions, significant amounts of the fragment [Ru(Me-PNP)CO] 505 was found, which strongly indicates, in conjunction with the measured IR spectrum (νCO, 1878 cm^{-1}, Figure S 5.84), our considerations that decarbonylation takes places (SI, Figure S 5.82-5.83). In a separate experiment, the deactivation process was monitored via NMR, providing further evidence of the effect of cyclohexanone on complex **2** (SI, Figure S.5.89-5.94). For the deactivation of **4**, similar observations are conceivable.

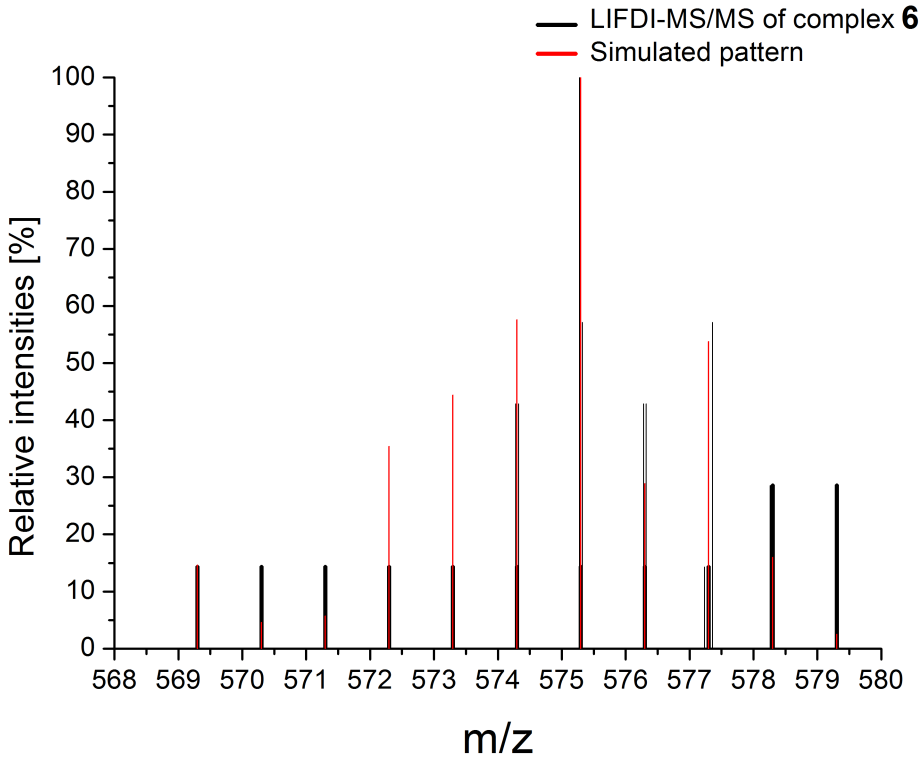

Figure 3.24. – LIFDI MS/MS of complex **6** in comparison with simulated pattern of [Ru(Me-PNP)CO($CH_2CH_2CH_2CH_2CH_2$)] 575, 569-579.

Therefore, we assume that the initial decarbonylation reaction of the cyclohexanone occurs first by complex **2**, followed by a cyclo-metallisation to yield complex **6**, which causes the deactivation of the reaction. On the other hand, in the presence of benzaldehyde, the catalysts **2** and **4** were not deactivated. Further reactions with cyclohexanol catalysed by complexes **2** and **4** with benzylaldehyde as additive showed no deactivation of the reactions

during the active process of the catalysis. With that conclusion, complexes **2** and **4** were tested for the direct amination of benzylalcohol (SI, 5.79-5.80). Complex **2** is active towards benzylalcohol, but conversion remained very low and was selective only towards the dibenzylimine product. After the addition of benzylaldehyde, the catalytic performance increased slightly, but only dibenzylimine was detected. Analogues complex **4** was employed for amination of benzylalcohol, showing no activity. Significantly low increase in activity was detected in the presence of added benzylaldehyde. For further confirmation of our conclusion that PNP complexes able to form an amide bond with the ruthenium metal centre are not active, the commercially available PNP ruthenium carbonyl complex **7** (Ru-MACHO™) was tested for direct amination of cyclohexanol (Figure 3.25). The ligand structure is closely related to **3** and **5**. All three complexes contain a secondary amine bond in the hydrogenated state (**3a** and **5a**, Scheme 3.21, **7a-b**, Figure 3.25). Complex **7** is known for its excellent hydrogenation abilities to reduce esters;[20] as a dehydrogenation catalyst, it was used for the decomposition of methanol into hydrogen and carbon dioxide.[21] As expected, **7** showed no activity under the standard reaction conditions. No activity was shown adding base or cyclohexanone (Figure 3.26).

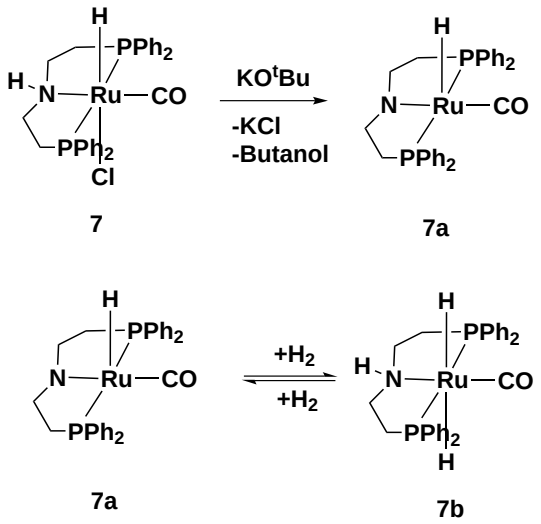

Figure 3.25. – Ru bis(diphenylphosphino)ethylamine carbonyl chloro hydride complex **7**. Amide-Ru bond is formed (**7a**) by the addition of KO^{t}Bu to **7**. **7a** and **7b** can be interconverted by adding or removing an equivalent of H_2.

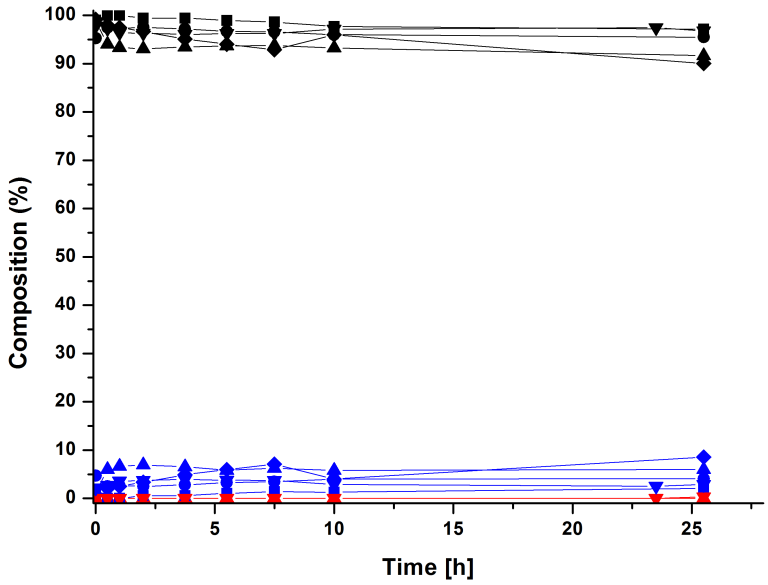

Figure 3.26. – Combined results of the amination of cyclohexanol with complex **7**. Conditions: 0.04 mmol **7**, 5 mmol cyclohexanol, 15 mL *t*-amylalcohol, 2.5 mL NH_3, 150 °C, 52 h. ■ = cyclohexanol, no further additives, ● = 10 mol% benzaldehyde added, ▲ = 1 mol% KO^{t}Bu added, ▼ = 10 mol% KO^{t}Bu added, ♦ = Toluene as solvent ● = cyclohexylamine, ▲ = cyclohexanone, ▼ = cyclohexylimine, ♦ = dicyclohexylimine, ◀ = dicyclohexylamine.

Based on the experiences of testing complexes **2**-**5** and **7**, complex **8** was synthesised, containing the same PNP ligand backbone with the methylated *N*-site as the active species **2** and **4**. For direct comparison to Ru-MACHO™ **7**, **8** was employed for amination reaction of cyclohexanol with high expectations to be active.

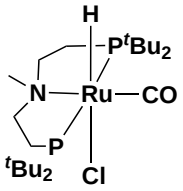

8

Figure 3.27. – Ru bis(diphenylphosphino)ethylamine complex **8**, with a tertiary amine ligand backbone.

In the presence of base, under the standard reaction conditions, high activity of **8** was observed as predicted. Within the first 10 h, high conversion was detected, selective towards cyclohexylamine (Figure 3.28). For the direct amination of primary alcohols, hexanol was tested as the model substrate. Surprisingly, **8** also showed high activity for amination of primary alcohols after the addition of base to the reaction mixture (Figure 3.29). In addition to the experiences with complexes **2**-**5** and **7**, the employment of complex **8** strongly underlines our assumption of the important tertiary amine ligand.

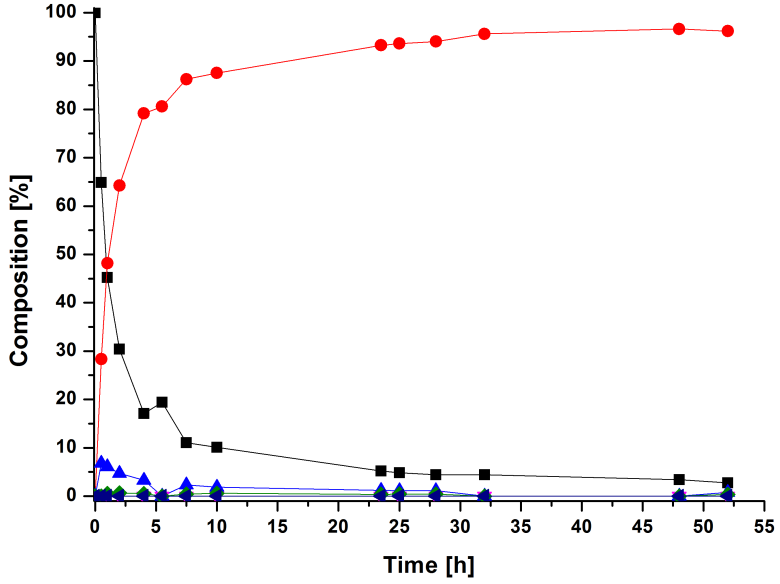

Figure 3.28. – Amination of cyclohexanol employing complex **8** in the presence of K^{t}Bu. Conditions: 0.04 mmol **8**, 5 mmol cyclohexanol, 0.5 mmol K^{t}Bu, 15 mL *t*-amylalcohol, 2.5 mL NH_3, 150 ^{o}C. ■ = cyclohexanol, ● = cyclohexylamine, ▲ = cyclohexanone, ▼ = cyclohexylimine, ♦ = dicyclohexylimine, ◀ = dicyclohexylamine.

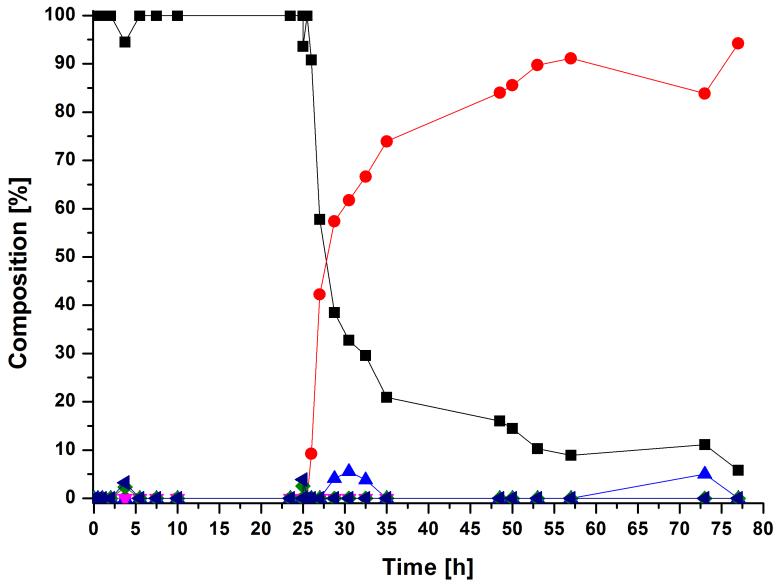

Figure 3.29. – Amination of hexanol employing complex **8**. KO^{t}Bu was added after 25 h. Conditions: 0.04 mmol **8**, 5 mmol cyclohexanol, 0.5 mmol KO^{t}Bu, 15 mL *t*-amylalcohol, 2.5 mL NH_3, 150 °C. ■ = hexanol, ● = hexylamine, ▲ = hexanal, ▼ = hexylimine, ♦ = dihexylimine, ◀ = dihexylamine.

General Aspects

To substantiate the consideration that those ruthenium pincer complexes unable to form a *N*-Ru amide bond are active for the direct amination of alcohols, the comparison to other active complexes is necessary. As a different system, one of the most active complexes for such reactions is the catalyst **9** based on a POP Xantphos ligand (Scheme 3.17).[9] Generally, these systems can be generated *in situ* with ruthenium precursors, such as [RuHCl(CO)(PPh_3)$_3$]. **9** is then initially activated to **9a** by alcohol and NH_3. A beneficial intervention of the catalytic process can be conducted by adding substrate intermediates to the reaction. No anionic bond formation to the metal centre is possible due to the oxygen site of the ligand. Moreover, it is known that other Xantphos type ligands are moderately to highly active for direct amination of cyclohexanol.[6] The most superior catalysts so far for amination reactions, in particular for primary alcohols, are the complexes based on acridine PNP ligands **1** (Scheme 3.14) and **10** (Scheme 3.17). Both systems are activated by alcohol and NH_3 causing a dearomatisation in the ligand backbone.[9–11] Based on DFT calculations, *Hofmann et al.* proposed that the ligand remains dearomatised, whereby their isolated intermediate **9b** contains a steady *N*-Ru amide bond.[11] Contrary, this work considers a different approach that *N*-Ru amide bonds

are not beneficial for such amination reactions. It is also assumable that the actually active species in *Hofmann's* system appears as aromatisised complex, which does not have an amide bond. In any case, more detailed investigations are required to make a final statement.

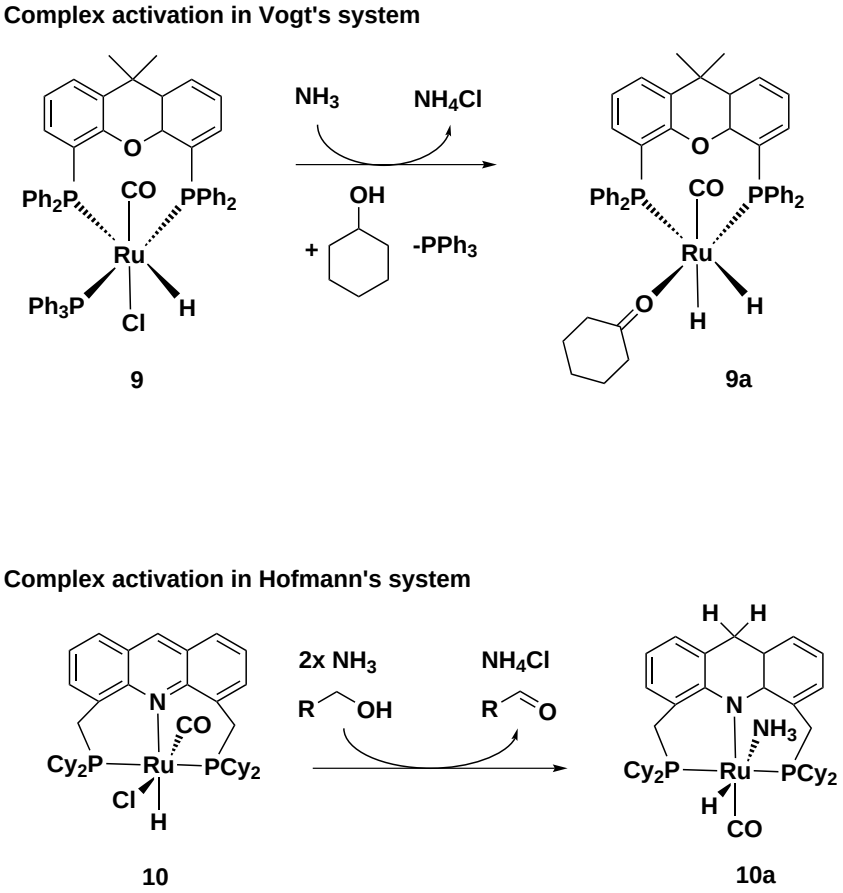

Scheme 3.17 – Xantphos based catalyst **9** and PNP acridine based catalyst **10** can be activated initially by alcohol and NH_3 to **9a** and **10b**.

Conclusion and Summary

In this work, a small scope of aliphatic PNP ruthenium pincer complexes were tested for the direct amination of alcohols. It is clear that complexes **3**, **5** and **7** with PNP ligands containing a secondary amine backbone able to form a *N*-Ru amide bond are generally not active, while complexes **2**, **4** and **8** containing tertiary amine PNP ligands are active. Contrary to previous reports, the acceleration of a reaction does not occur, but deactivation of the catalysts takes place instead, when additional substrate intermediates, such as ketones, are added to the complexes (**2** and **4**). With further investigations, it was shown with separate NMR and LIFDI-MS experiments, that **2** is deactivated by decarbonylation of the

cyclohexanone followed by a subsequent metalcyclisation. With the synthesis of complex **8**, one of the most active catalyst was presented, although activation with base is required. More studies are still required, however to fully estimate the Amide vs. Amine Paradigm in the direct amination of alcohols with Ru-PNP complexes. Similar active and inactive ligand systems can thus be employed for further investigations.

Acknowledgements

We acknowledge the Ministerium für Innovation, Wissenschaft und Forschung NRW (MIWF-NRW) for financial support within the Energy Research Program for the Scientist Returnee Award for M.H.G.P. (NRW-Rückkehrerprogramm). M.H.G.P. acknowledges the Ernst-Haage Foundation at the Max-Planck-Institute for Chemical Energy Conversion for the Ernst-Haage Prize awarded for our research achievements. For access to LIFDI-MS analysis, we gratefully acknowledge Prof. Dr. T. Braun and J. Berger (Humboldt-University Berlin, Germany).

References

[1] C. Gunanathan, D. Milstein, *Angew. Chem.-Int. Edit.* **2008**, *120*, 8789–8792.

[2] D. Pingen, O. Diebolt, D. Vogt, *ChemCatChem* **2013**, *5*, 2905–2912.

[3] D. Pingen, C. Müller, D. Vogt, *Angew. Chem.-Int. Edit.* **2010**, *49*, 8130–8133.

[4] S. Imm, S. Bähn, M. Zhang, L. Neubert, H. Neumann, F. Klasovsky, J. Pfeffer, T. Haas, M. Beller, *Angew. Chem.-Int. Edit.* **2011**, *50*, 7599–7603.

[5] S. Imm, S. Bähn, L. Neubert, H. Neumann, M. Beller, *Angew. Chem.-Int. Edit.* **2010**, *49*, 8126–8129.

[6] D. Pingen, T. Lebl, M. Lutz, G. S. Nichol, P. C. J. Kamer, D. Vogt, *Organometallics* **2014**, *11*, 2798–2805.

[7] M. H. S. A. Hamid, P. A. Slatford, J. M. J. Williams, *Adv. Synth. Catal.* **2007**, *349*, 1555–1575.

[8] M. G. Edwards, J. M. J. Williams, *Angew. Chem.-Int. Edit.* **2002**, *41*, 4740–4743.

[9] D. Pingen, M. Lutz, D. Vogt, *Organometallics* **2014**, *33*, 1623–1629.

[10] C. Gunanathan, B. Gnanaprakasam, M. A. Iron, L. J. W. Shimon, D. Milstein, *J. Am. Chem. Soc.* **2010**, *132*, 14763–14765.

[11] X. Ye, P. N. Plessow, M. K. Brinks, M. Schelwies, T. Schaub, F. Rominger, R. Paciello, M. Limbach, P. Hofmann, *J. Am. Chem. Soc.* **2014**, *136*, 5923–5929.

[12] J.-H. Choi, N. E. Schloerer, J. Berger, M. H. G. Prechtl, *Dalton Trans.* **2014**, *43*, 290–299.

[13] J.-H. Choi, L. E. Heim, M. Ahrens, M. H. G. Prechtl, *Dalton Trans.* **2014**, *43*, 17248–17254.

[14] M. C. Nicasio, R. N. Perutz, P. H. Walton, *Organometallics* **1997**, *16*, 1410–1417.

[15] L. S. Van der Sluys, G. J. Kubas, K. G. Caulton, *Organometallics* **1991**, *10*, 1033–1038.

[16] N. Sieffert, R. Réocreux, P. Lorusso, D. J. Cole-Hamilton, M. Bühl, *Chem. Eur. J.* **2014**, *20*, 4141–4155.

[17] E. P. K. Olsen, R. Madsen, *Chem.-Eur. J.* **2012**, *18*, 16023–16029.

[18] Y.-Z. Chen, W. C. Chan, C. P. Lau, H. S. Chu, H. L. Lee, G. Jia, *Organometallics* **1997**, *16*, 1241–1246.

[19] R. Çelenligil-Çetin, L. A. Watson, C. Guo, B. M. Foxman, O. V. Ozerov, *Organometallics* **2005**, *24*, 186–189.

[20] D. Spasyuk, S. Smith, D. G. Gusev, *Angew. Chem.-Int. Edit.* **2012**, *51*, 2772–2775.

[21] M. Nielsen, E. Alberico, W. Baumann, H.-J. Drexler, H. Junge, S. Gladiali, M. Beller, *Nature* **2013**, *495*, 85–89.

3.5. Miscellaneous Results Part 1: Acceptorless Dehydrogenative Alcohol Coupling Reactions in the Presence of Primary Amines

Introduction

In this section, the ruthenium pincer complex catalysed acceptorless dehydrogenative coupling (ADC) reactions of primary alcohols in the presence of primary amines are discussed. As described in section 1.4, in ADC reactions the primary alcohol is transformed in to the short-lived, highly active aldehyde, which subsequently reacts with an equivalent of primary amine to form the hemiaminal-intermediate (Chapter 1.4). For the *Milstein* complex **1**, the hemilability of the PNN pincer ligand causes the formation of the amide due to the favoured *cis*-coordination of the intermediate. In PNP ligand systems, the hemilabile property of the pincer arm is reduced, due to the strong P-M bond (M = metal). Therefore, the hemiaminal-intermediate favours the elimination of an equivalent of water and the corresponding imine is formed.[1,2] In this work, the non-classical ruthenium complexes **2** and **3** were applied in such reactions as catalysts (Figure 3.30). Despite high conversions, by-products of esters, secondary and tertiary amines were detected besides the favoured imines.

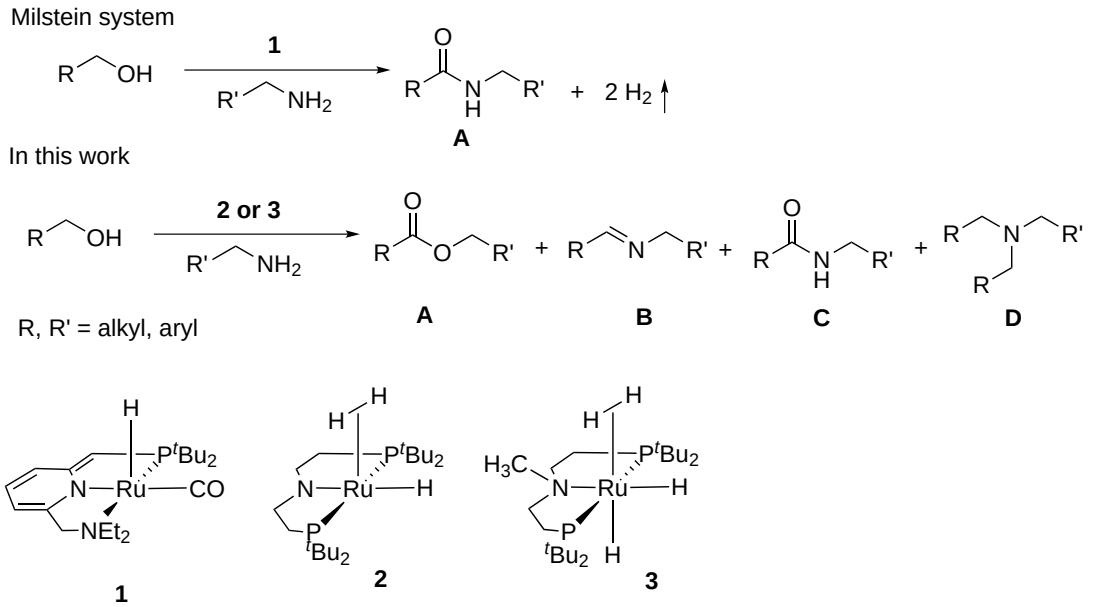

Figure 3.30. – ADC reactions of primary alcohols in the presence of primary amines to esters (**A**), secondary imines (**B**), amides (**C**) and tertiary amines (**D**).

Results and Discussions

In Situ Formation of the Active Species

As reported previously, the non-classical ruthenium hydride complexes **2** and **3** undergo decarbonylation reactions in the presence of primary alcohols and form the carbonylated complex species **4** and **5**. Acceleration of this reaction can be conducted in a microwave reactor, reducing the reaction time from 2 days to 15 min. In aqueous medium, similar behaviour of **2** and **3** was observed, which was discussed in the previous section 3.2. Accordingly, decarbonylation reaction of primary alcohols takes in the presence of primary amine, too. For instant-testing under microwave radiation, a small excess of ethyl alcohol and hexylamine was added to a solution of **2** (Scheme 3.18). $^{31}P\{^{1}H\}$ NMR analysis displayed high conversion of **2**, mostly the active species **4** was present. Under the same reaction conditions, mostly **5** was obtained from complex **3** (Supporting Information, SI, Figure S 5.95-5.98).

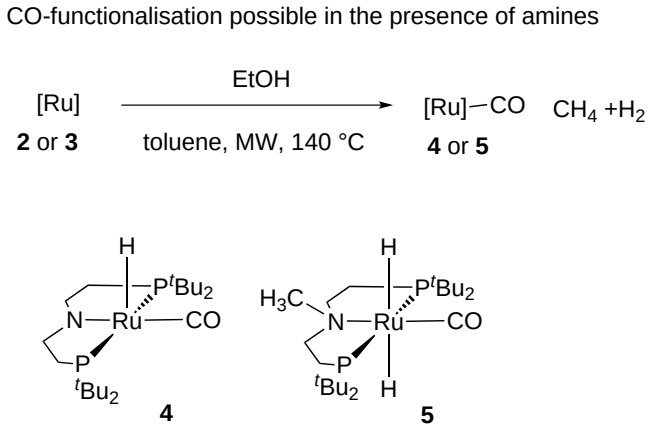

Scheme 3.18 – Decarbonylation of primary alcohols by **2** or **3** in the presence of primary amines to form **4** and **5**.

Catalytic Results

Having proven that the catalytic active species **4** and **5** is generated *in situ* from the hydride species, **2** and **3** were directly applied as precursors for ADC reactions of primary alcohols in the presence of primary amines, using hexanol, benzyl alcohol and benzyl amine as model substrates. For complex **2**, reactions with 1 mol% catalyst loadings in toluene led to low conversions around 40% in the dehydrogenative coupling reactions of hexanol or benzylalcohol in the presence of benzylamine (Table 3.6). Predominantly the secondary imine (**B**) was formed, followed by some parts of ester (**A**) and amide (**C**)

(Entry 1-2,[7] Table 3.6). For hexanol and benzylamine in neat conditions, quantitative conversion was reached at 140 °C, with lower catalyst loading of 0.5 mol%, yielding a product mixture in a ratio of (**A**:**B**:**C**:**D**) 0.6 : 6 : 1.2 : 2.2 (Entry 3, Table 3.6).

Table 3.6. – ADC reactions in the presence of primary amine with complexes **2-3**.

Entry[a]	Alcohol (eq.)	Amine (eq.)	[mol%]	TON	Product ratio[c, d] **A**:**B**:**C**:**D**
1[b]	hexanol (1)	benzylamine (1)	1	39	**1 : 7 : 2 : 0**
2[b]	benzyl alcohol (1)	benzylamine (1)	1	45	**0.7 : 8.6 : 0.7 : 0**
3	hexanol (1)	benzylamine (1)	0.5	215	**0.6 : 6 : 1.2 : 2.2**
4	hexanol (2)	benzylamine (1)	0.5	209	**0.1 : 0.4 : 0.7 : 9.4**
5	hexanol (1)	benzylamine (2)	0.5	215	**0 : 6.5 : 0 : 3.5**
6	hexanol (2)	benzylamine (1)	0.1	1021	**0 : 0.7 : 0 : 9.3**
7	hexanol (1)	benzylamine (2)	0.1	1054	**0 : 2 : 0 : 8**
8	benzyl alcohol (1)	benzylamine (2)	0.5	176	**0 : 10 : 0 : 0**
9	benzyl alcohol (2)	benzylamine (1)	0.5	215	**0 : 10 : 0 : 0**
10	octanol (2)	octylamine (1)	0.5	215	**0 : 4 : 1 : 5**
11[e]	hexanol (2)	benzylamine (1)	0.5	209	**0.1 : 6.2 : 0.3 : 3.4**
12[e]	hexanol (1)	benzylamine (2)	0.5	215	**0 : 5 : 1.1 : 3.9**

[a] Reaction conditions: 8.6 mmol (1 eq.) substrate, neat, 140 °C, 20 h **2**, reflux under Ar-stream.
[b] Reaction conditions: 2 mmol (1 eq.) substrate, 5 mL toluene, 120 °C, 20 h with **2**, reflux under Ar-stream.
[c] Conversion and product ratio were determined via GC/MS(FID).
[d] **A** Ester, **B** Secondary imine, **C** Amide, **D** Tertiary amine.
[e] Reaction conditions: 8.6 mmol (1 eq.) substrate, neat, 140 °C, 20 h with **3**, reflux under Ar-stream.

[7] The results of this reaction in Entry 1-2 were obtained from the diploma thesis from the author of this thesis Jong-Hoo Choi.

Due to the formation of the tertiary amine, an excess of hexanol (2 eq.) was added, relative to the benzyl amine (1 eq.) in Entry 4 favouring the formation of product **D** (9.4). In an excess of benzylamine, the formation of **B** was favoured, but a significant amount of tertiary amine was also formed (Entry 5, **B**:**D**, 6.5 : 3.5). In Entry 6-7 the same ratio of hexanol and benzylamine was added, the catalyst loading was lowered to 0.1 mol% giving a TON of $\geq$ 1000. While the excess of hexanol led mostly to product **D** (Entry 6); the excess of benzylamine was not selective, giving a product ratio (Entry 7, **B**:**D**) of 2.0 : 8.0. Best results were obtained with benzylalcohol and benzylamine (Entry 8-9), with a catalyst loading of 0.5 mol%, selective only towards **B**. Different substrates were tested with octanol (2 eq.) and octyl amine (1 eq.) under the same reaction conditions, giving full conversion, but the selectivity in favour of a product remained poor (Entry 10, **B**:**C**:**D**, 4.0 : 1.0 : 5.0). Testing the methylated complex **3** with hexanol and benzylamine, despite high conversion, reaction mixtures of **A**-**D** were obtained in Entry 11-12.

General Aspects, Outlook and Conclusion

Complexes **2** and **3** are highly active for the amination of alcohols via ADC reactions. Generally, the selectivity remains poor and was not controlled by adding an excess of primary alcohols, with respect to the primary amine. Only the benzylalcohol/benzylamine system was selective towards secondary imine formation (Table 3.6, Entry 8-9). Furthermore, selectively, tertiary amine was produced from an excess of hexanol with regards to benzylamine. From the obtained results in this work, it assumable that other alcohol/amine combination are not selective either, based on the tested model substrates. Besides the system of *Milstein*, *Gusev et al.* reported an osmium catalyst **6** based on aliphatic PNP pincer ligand for the dehydrogenative coupling of amines alkylation with alcohol. By adding base to **6** to abstract the chloride, the highly active catalyst **6a**, respectively **6b** is formed (Scheme 3.19). Different to this work, the reactions were performed in a closed system. With the dehydrogenation of the alcohol, followed by a subsequent amination reaction, an *in situ* hydrogen transfer occurs ("hydrogen borrowing") giving selectively the secondary amine.[3] In this system, high temperatures of 200 °C were required presumable for two factors. First, the catalyst requires a certain energy level to be active and second, product selectivity is influenced by the temperature. Therefore, it is possible that the selectivity can be controlled with the employed complexes **2** and **3**, as well.

Another similar work to compare was reported by *Williams et al.* in 2011 (Scheme 3.19). In their system, $[Ru(p\text{-cymene})Cl_2]_2$ complexes were applied in combination with DPEphos ((oxydi-2,1-phenylene)bis(diphenylphosphine)) as a ligand. Primary alcohols were selectively coupled with various secondary amines under microwave radiation via a "hydrogen borrowing" mechanism.[4] In this context, microwave reactions for alkyl aminations are highly interesting, due to the short reaction time. The formation of tertiary amines, which is then irreversible in the catalytic equilibria, occurs with catalysts **2** and **3**, could be avoided by shortening the reaction time.

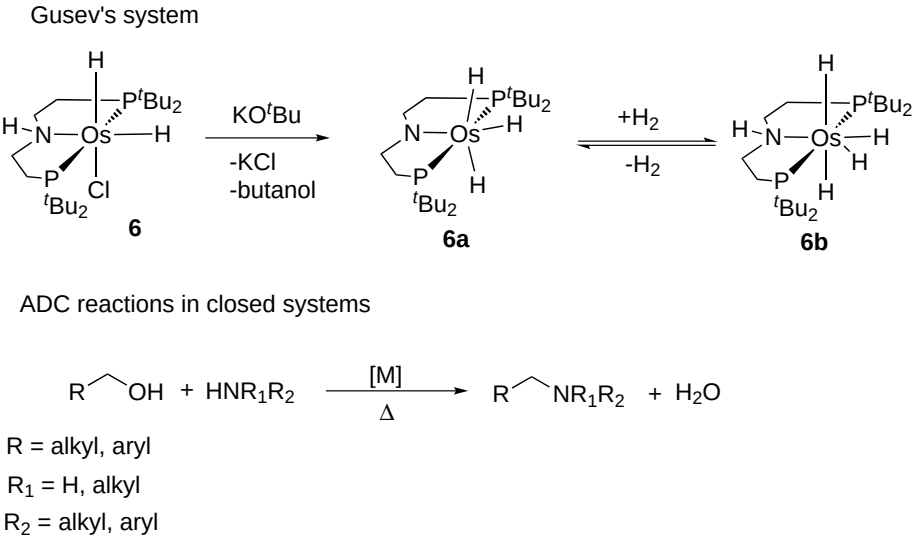

Scheme 3.19 – Osmium PNP hydride complex **6** can be activated by base to **6a**. In a hydrogen atmosphere, **6b** is formed. ADC reactions in the presence of amines in a closed system.

References

[1] C. Gunanathan, Y. Ben-David, D. Milstein, *Science* **2007**, *317*, 790–792.

[2] B. Gnanaprakasam, J. Zhang, D. Milstein, *Angew. Chem.-Int. Edit.* **2010**, *49*, 1468–1471.

[3] M. Bertoli, A. Choualeb, D. G. Gusev, A. J. Lough, Q. Major, B. Moore, *Dalton Trans.* **2011**, *40*, 8941–8949.

[4] A. J. A. Watson, A. C. Maxwell, J. M. J. Williams, *J. Org. Chem.* **2011**, *76*, 2328–2331.

3.6. Miscellaneous Results Part 2: Synthesis and Characterisation of a Pyrrole-Based PNP Ruthenium Complex

Introduction

With great success, various pincer complexes have been reported over the last two decades based on transition metals with aliphatic or aromatic pincer ligands and have been successfully applied in catalysis.[1–6] Beside the extensively studied complexes with pyridine or acridine based ligand backbones, not much is reported for PNP pincer complexes based on pyrroles.[7–10] From approximately a dozen known pyrrole PNP complexes, Scheme 3.20 displays one of the few bearing Ni, Pd or Pt (**1**-**4**).[8,9] Reasonably, little is known about the catalytic properties of pyyrol based complexes. Among the reports, an elegant application was reported by the *Tonzetich* group employing a nickel PNP pyrrole complex **4** for the *Kumada* coupling reactions of aryl chlorides with aryl and alkyl *Grignard* reagents (Scheme 3.20). Impressively, the reactions were performed with low catalyst loading (0.4 mol%) at room temperature giving mostly good to very good yields.[9]

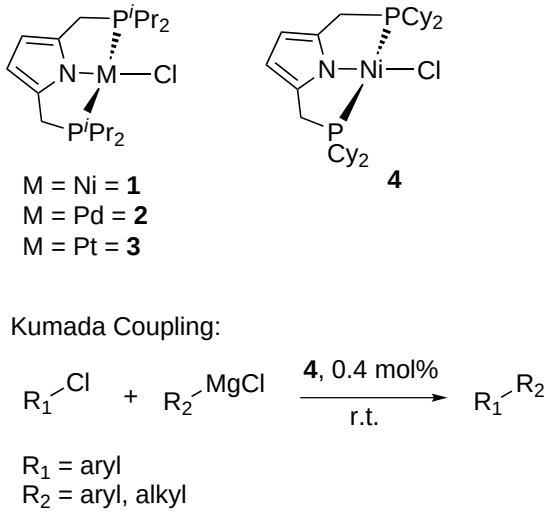

Scheme 3.20 – Pyrrole based PNP complexes **1**-**4**. The *Kumada* coupling with complex **4** is described.[8,9]

Contributing to the small selection of pyrrole based PNP pincer complexes, this work presents the synthesis, characterisation and the first catalytic tests with a new ruthenium carbonyl hydrido complex **5** (Figure 3.6).

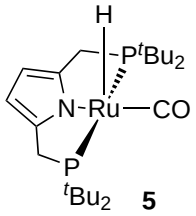

5

Results and Discussions

Synthesis of Complex 5

Synthesis of Ligand 9: Following the protocol of others, the ligand precursor **8** was synthesised via a *Mannich*-type reaction, starting from pyrrole in the presence of 2 equivalents of dimethylamine hydrochloride and aqueous formaldehyde (Scheme 3.21).[11] With the addition of the di-*tert*-butyl-phosphine, substitution, via S_{N2}, occurs and the pyrrole PNP ligand **9** is formed.

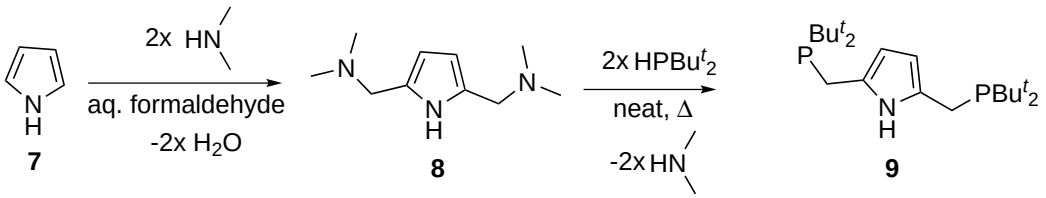

7 **8** **9**

Scheme 3.21 – Synthetic pathway to pyrrole PNP ligand **9**.

Synthesis of Complex 5 First, the hydrogenation reaction of the precursor [Ru-(COD)(2-methylallyl)$_2$] **12** (COD = 1,5-cyclooctadiene) in the presence of ligand **9** were performed, with the intention to form a ruthenium hydride species **11**. Complex **13** was formed, but the isolation as a solid was not achieved, even though, analysis of the $^{31}P\{^1H\}$ and ^1H NMR spectra of the oily residue confirmed the proper formation of **11** (SI, Figure S 5.102-5.103). In the hydride area significant Ru-H exhibits traces of the multiplet signal at -15.39 ppm (C_6D_6 at 300 MHz), while a clean phosphorus signal appears as a singlet of 105.0 ppm (C_6D_6 at 121 MHz). From experiences from previous reports (Section 1.4),[12] ruthenium complexes can be functionalised with a CO ligand via decarbonylation reaction of alcohols. With that in mind, an excess of ethanol

was added to complex **11** and placed under microwave radiation. Crystallised in cold diethylether, **5** was obtained as an orange solid. $^{31}P\{^{1}H\}$ NMR spectrum exhibits a singlet signal at 101.5 ppm (C_6D_6 at 121 MHz) and the ^{1}H NMR spectrum characteristic hydride triplet signal of the Ru-H appears at -25.57 ppm ($^{3}J_{PH}$ = 17.2 Hz in C_6D_6 at 300 MHz). The carbonyl signal was not detected in the ^{13}C NMR spectrum, but the decarbonylation was confirmed in the IR spectrum as a typical strong vibration absorption band at 1889 cm^{-1}. The Ru-H vibration band was detected at 2109 cm^{-1} as a weak signal (SI, Figure S 5.107).

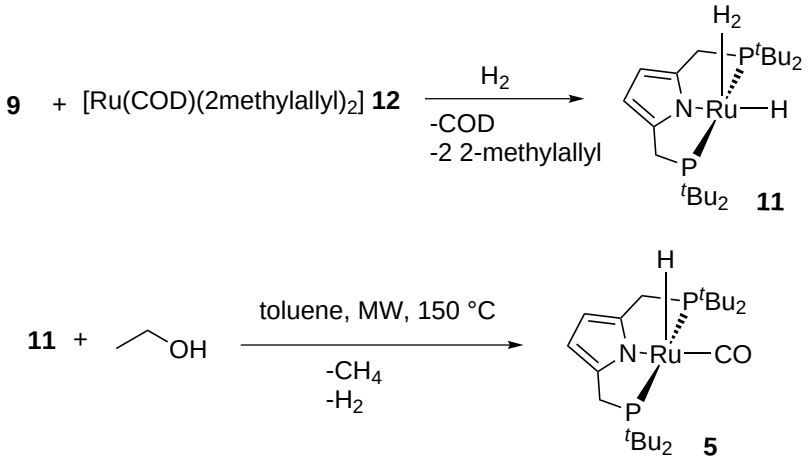

Scheme 3.22 – Synthetic strategies **A**-**B** to obtain ruthenium carbonyl complexes with ligand **9**.

Catalytic Test Reactions with Complex 5

With the successfully obtained complex **5**, the first catalytic tests were performed for acceptorless dehydrogenative coupling (ADC) reactions of hexanol (Scheme 3.23. Expecting that **5** could be active for such reactions, under given conditions at 120 °C, 20 h in toluene under reflux, no conversion to hexyl hexanoate was observed, even after the addition KO^{t}Bu as base. Furthermore, ADC reactions of hexanol in the presence of hexylamine were performed under the same reaction conditions to obtain the corresponding secondary imine, but no conversion was detected. Moreover, the hydrogenation of ethyl acetate to ethanol at 140 °C with 1 mol% of complex **5** was performed under a H_2 pressure of 50 bar. Again, no activity was observed.

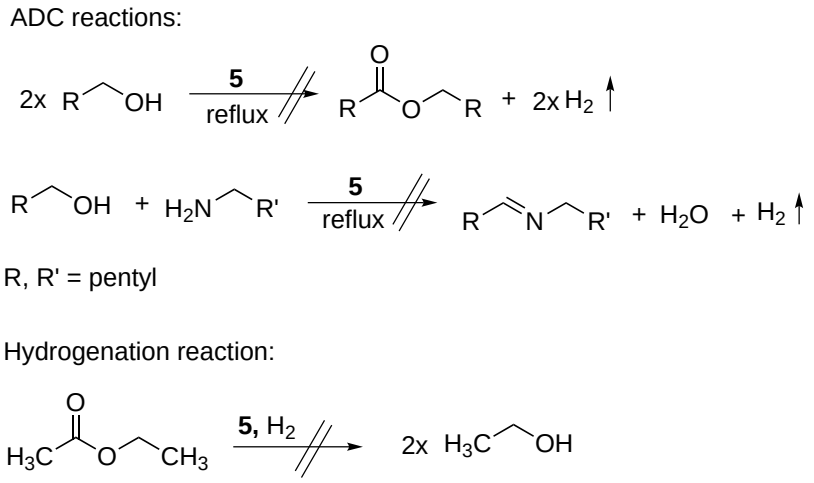

Scheme 3.23 – Catalytic test reactions employing complex **5** for ADC reactions and for hydrogenation reaction.

Summary and Outlook

With complex **5**, a new pyrrole based PNP ruthenium carbonyl complex has been presented. The key-step to isolate **5** was the microwave assisted decarbonylation reaction of the corresponding alcohol to stabilised the product-intermediate **11** with a CO ligand. It is assumable, that this approach opens up new synthetic pathways to obtain other transition metal carbonyl complexes with attached pyrrole PNP ligand **9**. In terms of ruthenium hydride complex **11**, no further attempts were performed to proper isolation and analysis; this remains as a great challenge for future work. In aspects of the catalytic application, it is planned to perform further test reactions towards other functional groups. Based on the first catalytic test reactions, complex **5** is not thought to be active for ADC nor hydrogenation reactions.

References

[1] M. Albrecht, G. van Koten, *Angew. Chem.-Int. Edit.* **2001**, *40*, 3750–3781.

[2] C. Gunanathan, Y. Ben-David, D. Milstein, *Science* **2007**, *317*, 790–792.

[3] D. Milstein, *Top. Catal.* **2010**, *53*, 915–923.

[4] C. Gunanathan, D. Milstein, *Science* **2013**, *341*, 10.1126/science.1229712.

[5] J. Choi, A. H. R. MacArthur, M. Brookhart, A. S. Goldman, *Chem. Rev.* **2011**, *111*, 1761–1779.

[6] B. Askevold, J. T. Nieto, S. Tussupbayev, M. Diefenbach, E. Herdtweck, M. C. Holthausen, S. Schneider, *Nat. Chem.* **2011**, *3*, 532–537.

[7] S. Kumar, G. Mani, S. Mondal, P. K. Chattaraj, *Inorg. Chem.* **2012**, *51*, 12527–12539.

[8] J. A. Kessler, V. M. Iluc, *Inor* **2014**, *53*, 12360–12371.

[9] G. T. Venkanna, S. Tammineni, H. D. Arman, Z. J. Tonzetich, *Organometallics* **2013**, *32*, 4656–4663.

[10] M. Kreye, M. Freytag, P. G. Jones, P. G. Williard, W. H. Bernskoetter, M. D. Walter, *Chem. Commun.* **2015**, *51*, 2946–2949.

[11] I. T. Kim, R. L. Elsenbaumer, *Macromolecules* **2000**, *33*, 6407–6411.

[12] J.-H. Choi, L. E. Heim, M. Ahrens, M. H. G. Prechtl, *Dalton Trans.* **2014**, *43*, 17248–17254.

4. Summary and Outlook

In response to the scientific aims in Chapter 2, this work connects the synthesis and characterisation of new ruthenium complexes with their application in catalysis. First, the synthesis and characterisation of new non-classical ruthenium hydride complexes based on aliphatic pincer ligands is reported. Strongly linked to the catalytic reactions of this work, the concrete testing of the obtained complexes towards functional groups, such as CO, R-OH, BH or R-CN, was successfully performed. With that, new complexes have been isolated and characterised, whereby some of the isolated complexes are considered as key intermediates in the performed catalytic reactions. For the first time, LIFDI-MS analysis was applied to ruthenium pincer complexes.

4.1. Synthesis and Characterisation of Ruthenium Hydride Complexes

Molecular Dihydrogen Pincer Complexes of Ruthenium

The one-pot direct hydrogenation of the ruthenium precursor in the presence of the corresponding pincer ligand has been reported as a reliable synthetic pathway to obtain non-classical ruthenium hydride pincer complexes.[1] New non-classical ruthenium hydride pincer complexes **1-3** were reported in this work with aliphatic PNP pincer ligands as stabilising agents (Figure 4.1). For complexes **1** and **2**, the synthesis resulted as a mixture of both (**1** and **2**) with 90% yield. Complex **1** is considered as the more stable hydride complex. In a hydrogen atmosphere, only the more labile complex **2** is exclusively present. In an argon atmosphere, both species are present as a mixture. Removing an equivalent of molecular hydrogen, by treating the mixture in a constant stream of argon and following in vacuo, complex **1** was isolated. T_1 measurement confirms that complex **1**, as a well balanced electronic summation is classified as a non-classical hydride with a H-H distance of 0.99 Å (triplet, -12.44 ppm, $^{2}J_{PH}$ = 10.6 Hz, $T_{1\mathrm{min}}$ = 48 ms at θ_{min} = 207 K in toluene-d_8 at 500 MHz). Complex **2** in

comparison, is assigned to an elongated hydride with d_{HH} of 1.17 Å (triplet, -8.26 ppm, $^2J_{PH} = 14.7$ Hz, T_{1min} of 132 ms, $\theta_{min} = 223$ K, in toluene-d_8, at 500 MHz). The IR spectroscopy exhibits a characteristic Ru-H_2 band at 1975 cm^{-1} for complex **1** and at 1726 cm^{-1} for complex **2**. Both complexes show Ru-H bands between 2034 and 2000 cm^{-1}. Interestingly, the LIFDI-MS spectrogram of [Ru(H_2)H(PNP)] **1** reveals, beside the isotope pattern of **1** overlapping multiple isotope patterns of co-existing [Ru(H_2)H_2(HPNP)], [Ru(H_2)(PNP)] and [RuH(PNP)]. These were formed under MS-conditions and shift the total m/z pattern towards lower mass ratio and alternate the intensities by overlapping isotope patterns. Analogously, the ruthenium pincer complex **3** with a methylated [(Me-N)PNP] ligand was synthesised and characterised (Figure 4.1). **3** was obtained with 67% yield and was assigned as non-classical hydride, with a characteristic T_{1min} of 54 ms and a θ_{min} of 224 K in toluene-d_8 at 500 MHz with a calculated d_{HH} of 1.01 Å (triplet, -8.68 ppm ($^2J_{PH} = 13.8$ Hz). The IR spectrum shows dihydrogen ligand vibration ν(M-H) between 1972 and 1923 cm^{-1} and the vibration of the hydrides ν(M–H_2) at 1776 cm^{-1}.

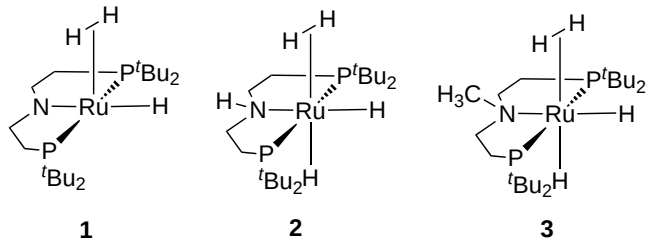

Figure 4.1. – Molecular Dihydrogen Complexes **1-3**.

Borylated Ruthenium Pincer Complexes

Complex **3** reacts with rapid hydrogen evolution, with B-H compounds such as pinacolborane, dimethylamineborane or THF borane complex to form defined complexes (Figure 4.2, **4-5**). In contrast, complexes **1** and **2** show high activity under the same conditions, but no defined complexes were obtained. Complex **4** was obtained in very good yields (87%) exhibiting broad singlets at -5.64 and -9.02 ppm, assigned to the two bridging hydrides and at -18.85 ppm assigned to Ru-H in the ^{1}H NMR. In the IR spectrum the ν(M–H) band appears at 2024 cm^{-1}. The bridging ν(M–H–B) hydride bands appear at 1973 and 1914 cm^{-1} and between 1744 and 1675 cm^{-1}. Complex **5** is formed as a "true" σ-B-H; in the ^{1}H NMR spectrum, broad singlet signals at -5.69 and -19.76 ppm appear, caused by the bridging hydrides. A characteristic triplet of doublets

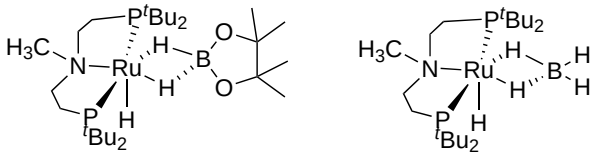

Figure 4.2. – [RuH_2(HBPin)(Me-PNP)] **4** and (σ-B-H) complex [$RuH_2(BH_3)$(Me-PNP)] **5**.

signal appears at -17.85 ppm ($^2J_{PH}$ = 19.22 Hz, $^2J_{BH}$ = 3.52 Hz, Ru-H) and was assigned to the hydride. The terminal B-H signals appear as a broad singlet signal at 5.42 ppm. At lower temperatures (≤278 K), the rapid hydride rotations are decreased and the broad signals shape into clear singlet signals. Furthermore, at lower temperatures, the Ru-H signal at -17.85 ppm transforms into a clean triplet signal. As mentioned above, the reaction of **3** with THF borane complex resulted with the formation of **5**, by the loss of the THF ligand. More interestingly, the analogue reaction with dimethylamine-borane caused the cleavage of the strong B-N bond forming the same complex. The NMR data as well as the IR data are congruent to each other. Characteristic vibration bands appear at 2394 and 2330 cm^{-1} assigned to the terminal B-H bonds, while the ν(M–H) band appears at 2020 cm^{-1}. No dimethylamine signals were found in the IR spectrum. Furthermore, a crystal structure of complex **5** was obtained, which supports the assumption of a "true" σ-B-H complex based on the calculated hydride distances.

CO-Functionalised Ruthenium Pincer Complexes

Introduced in the Section 1.7, ruthenium complexes are capable to decarbonylate alcohols, as well as aldehydes and ketones, to form a CO ligand.[2–6] In this work, the ADC reactions catalysed with **1** and **3** have demonstrated that non-classical hydride complexes are functionalised *in situ* with a CO ligand in the presence of primary alcohols. Complexes **6** and **8** are formed via decarbonylation of primary alcohols (Scheme 4.1). In both examples, the labile molecular hydrogen ligand is replaced by the CO ligand. With the subsequent *cis*/*trans* isomerisation, the *trans* species are exclusively present. The performed decarbonylation reactions were further confirmed by applying ^{13}C labelled ethanol. Furthermore, the online gas-phase MS was used for the detection of the generated H_2 gas along with the corresponding aliphatic compounds. Complex **6** was obtained in high yields (90%) and exhibits a triplet signal at -20.87 ppm ($^2J_{HP}$ = 16.3 Hz) in the ^{1}H NMR. Characteristic vibration bands were found at 1872 cm^{-1} for

ν(CO) and at 2052 cm^{-1} for ν(Ru-H). Analogously to the relations between **1** and **2**, in hydrogen atmosphere, **6** turns into **6a** with 79% conversion and shows two triplet signals at -5.86 ppm ($^{2}J_{PH}$ = 18.2 Hz) and at -6.13 ppm ($^{2}J_{PH}$ = 17.4 Hz). Dihydride complex **7** was obtained with 80% yield and characterised by the two triplet signals at -5.43 ppm ($^{2}J_{PH}$ = 16.1 Hz) and -5.54 ppm ($^{2}J_{PH}$ = 19.3 Hz) at higher frequencies (600 MHz). At lower frequencies (300 MHz), **7** shows overlapped signals of triplets around -5.5 ppm. Characterisation by IR spectroscopy shows the CO band at 1871 cm^{-1} and the Ru-H band at 1642 cm^{-1}. For the direct amination reactions of cyclohexanol with ammonia, complex **8** was synthesised with 70% yield. Characterisitic hydride signal in the ^{1}H NMR spectrum appears -16.10 ppm (t, 1H, $^{2}J_{PH}$ = 19.6 Hz). Vibration band ν(CO) appears at 1908 cm^{-1} in the IR spectrum. Moreover, as one of the first pyrrole based ruthenium PNP pincer complexes, compound **9** was presented in this work. Even though, its ruthenium hydride complex precursor was not successfully isolated, this species is an important intermediate for the formation of ruthenium carbonyl complex **9** via the microwave assisted decarbonylation reaction of ethanol. Complex **9** is characterised by a triplet signal at -25.57 ppm ($^{3}J_{PH}$ = 17.2 Hz in C_6D_6 at 300 MHz) in the ^{1}H NMR spectrum and by the vibration band of ν(CO) at 1889 cm^{-1} in the IR spectrum.

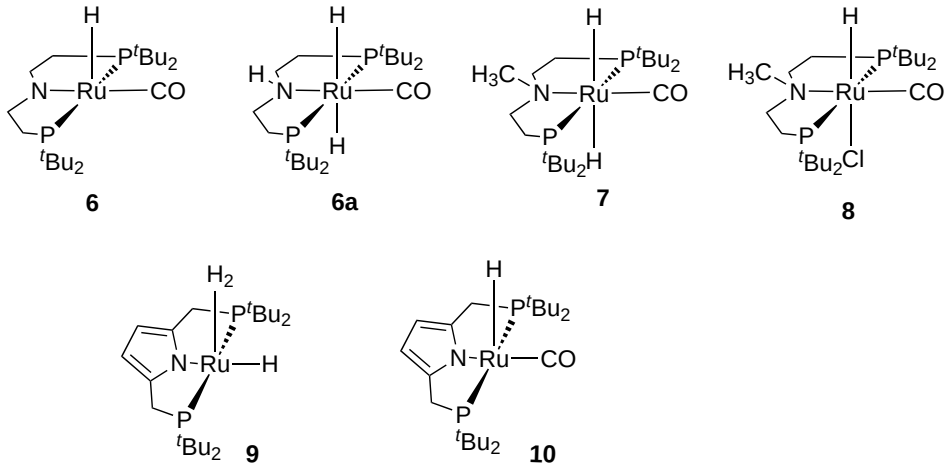

Scheme 4.1 – Formation of CO-functionalised complexes **6**-**8** and **9**.

4.2. Catalysis

For the catalytical aspects of this work, the following reactions were performed (Scheme 4.2):

1. Dehydrogenation reaction of alcohols into carboxylic acid salts.
2. Selective catalytic hydrogenation of nitriles into secondary imines or primary amines.
3. The direct amination of cyclohexanol into cyclohexylamine with ammonia.
4. The acceptorless dehydrogenative coupling reactions of alcohols with amines.

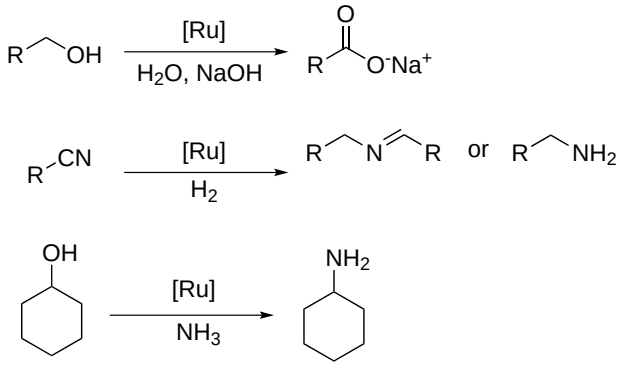

Scheme 4.2 – Overview of the performed catalytic reactions.

Dehydrogenation Reaction of Alcohols into Carboxylic Acid Salts

In this work, the dehydrogenation of primary alcohols was performed in the presence of basic aqueous medium catalysed by **1**, **3**, **6** and **7**. At mild reaction conditions (120 °C, 20 h, $NaOH/H_2O$) and low catalyst loadings (1 mol%), without the addition of further organic solvents and toxic additives, primary alcohols were transformed directly to carboxylic acid salts. With subsequent acidification and the extraction of the products, carboxylic acids were isolated with yields up to 92% with **7** (for hexanoic acid). With the decrease of the miscibility of the substrate in the aqueous medium, the obtained yields were decreased (32% for decanoic acid). In this reaction, the *in situ* decarbonylation of alcohols to form complexes **6** and **7** from **1** and **3** was confirmed with different experiments. Furthermore, the isolation of a stable carboxylated complex intermediate was accomplished, which was further analysed with the obtained spectroscopic, LIFDI-MS and single crystal analysis data.

Selective Catalytic Hydrogenation of Nitriles into Secondary Imines or Primary Amines

In the reduction of nitriles into secondary imines, complexes **1** and **6** can be applied very efficiently under mild reaction conditions. After the optimisation of the catalysis, **1**, operates most efficiently with 1 mol%, at 100 °C and 4 bar H_2 in toluene. Complex **6** is optimised with a catalyst loading of 0.5 mol%, 50 °C, 4 bar H_2 in toluene. Between 20-48 h, nitriles were converted into secondary imines with up to quantitative conversions and high selectivity. The reduction of nitriles were also performed in the presence of additional primary amines, giving cross-coupled secondary imine products with similar success. Highlighted in this work is the versatile use of **6**, which is, in contrast to **1**, also selective towards primary amine formation. Changing, in particular, two crucial reaction parameters, the increase of the temperature from 50 to 90 °C and replacing toluene as the solvent with the more polar and protic 2-propanol, only primary amine products were obtained. With an increased catalyst loading of 1 mol% and at 4 bar H_2, various nitriles were reduced into primary amines with mostly full conversions and excellent selectivity. Furthermore, a catalytic cycle was proposed, whereby a nitrile complex intermediate was isolated. Monitoring the hydrogenation of benzonitril into benzyl amine with **6** displayed the time resolved state of the catalytic equilibria. This experiment revealed that in the beginning of the reaction, the benzonitril is fully converted into the secondary imine, but over the course of time, the equilibria is shifted towards primary amine.

Direct Amination of Cyclohexanol with Ammonia

For the direct amination of alcohols, in particular secondary alcohols, the obtained complexes **1**, **3**, **6**, **7** and **8** were tested for this reaction using cyclohexanol as a model substrate. The catalyst-screening revealed that complexes based on secondary amine ligands able to form a *N*-Ru amide bond, such as **1** and **6** are not active. On the other hand, **3** and **7** with a tertiary amine PNP ligand are active for this reaction. Moreover, the results show that adding cyclohexanone to the catalytic process, as an additional substrate intermediate to accelerate the reaction, caused an opposite effect by deactivation of the complexes **3** and **7**. For detailed investigations, **3** was separately monitored via long-term NMR experiments in the presence of cyclohexanone. This experiment revealed that **3** forces the decarbonylation of cyclohexanone followed by a cyclometalisation, which deactivates the complex. The deactivated species was further

analysed via LIFDI-MS technique. With the results of the catalyst-screening reactions, complex **8** was designed. Activated by base, complex **8** showed, as predicted, very high activity for amination of cyclohexanol with catalyst loadings as low as 0.8 mol% (150 °C, 2.5 mL NH_3 (l)). Surprisingly, **8** is highly active for amination of primary alcohols (hexanol was used as model substrate), despite complexes **3** and **7** showing low activity towards primary alcohols.

ADC Reaction with Complexes 1 and 3

For ADC (acceptorless dehydrogenative coupling) reactions of primary alcohols with primary amines, complexes **1** and **3** were employed. In neat conditions (140 °C, 0.1-0.5 mol%), using hexanol, benzylalcohol, octanol, octylamine and benzylamine, high conversions were reached. Despite the high activity of the complexes, the selectivity was poor, yielding a mixture of mostly secondary imine and tertiary amine products, as well as products of esters and amides. An attempt to influence the selectivity was conducted by adding an excess of alcohol or amine without any satisfying results.

Outlook

For future work, it is desirable to test the reactivity of the presented ruthenium complexes towards CO_2. Not only for CO_2 hydrogenation reactions to formic acid or to methanol, which remains a great challenge in catalysis. The hydrogenation of carboxylic acids to the corresponding alcohols is also an interesting field of research to look forward. With the valuable insight obtained from the direct amination reactions of alcohols, new potential active catalysts can be designed. In general, it is very desirable to make catalytically highly efficient pincer complexes more applicable for industrial purposes. One approach could be the heterogenisation of pincer complexes, in which the catalyst recycling plays a major role.

References

[1] M. H. G. Prechtl, Y. Ben-David, D. Giunta, S. Busch, Y. Taniguchi, W. Wisniewski, H. Goerls, R. J. Mynott, N. Theyssen, D. Milstein, W. Leitner, *Chem.-Eur. J.* **2007**, *13*, 1539–1546.

[2] E. P. K. Olsen, R. Madsen, *Chem.-Eur. J.* **2012**, *18*, 16023–16029.

[3] R. Çelenligil-Çetin, L. A. Watson, C. Guo, B. M. Foxman, O. V. Ozerov, *Organometallics* **2005**, *24*, 186–189.

[4] R. Beck, U. Flörke, H.-F. Klein, *Inorg. Chem.* **2009**, *48*, 1416–1422.

[5] P. D. Bolton, M. Grellier, N. Vautravers, L. Vendier, S. Sabo-Etienne, *Organometallics* **2008**, *27*, 5088–5093.

[6] N. Sieffert, R. Réocreux, P. Lorusso, D. J. Cole-Hamilton, M. Bühl, *Chem. Eur. J.* **2014**, *20*, 4141–4155.

5. Appendix

5.1. Supporting Information - Synthesis and Characterisation of Ruthenium Dihydrogen Complexes and Their Reactivity Towards B-H Bonds

Jong-Hoo Choi,[a] Nils E. Schloerer[a] and Martin H. G. Prechtl*[a]
[a] Department of Chemistry, University of Cologne, Greinstr.6, 50939 Cologne

T1 Measurements of Complex 4-6

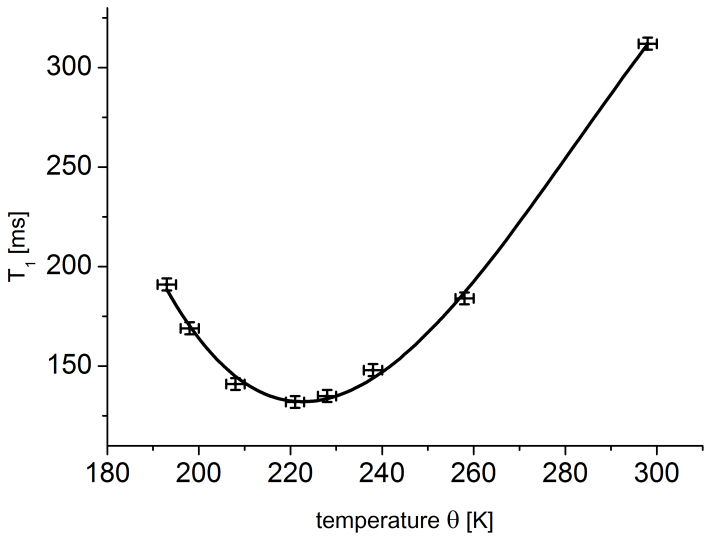

Figure S 5.1. – T_1 values of $[Ru(H_2)H_2(PNP)]$ **4** as a function of the temperature θ [K] at 500 MHz.

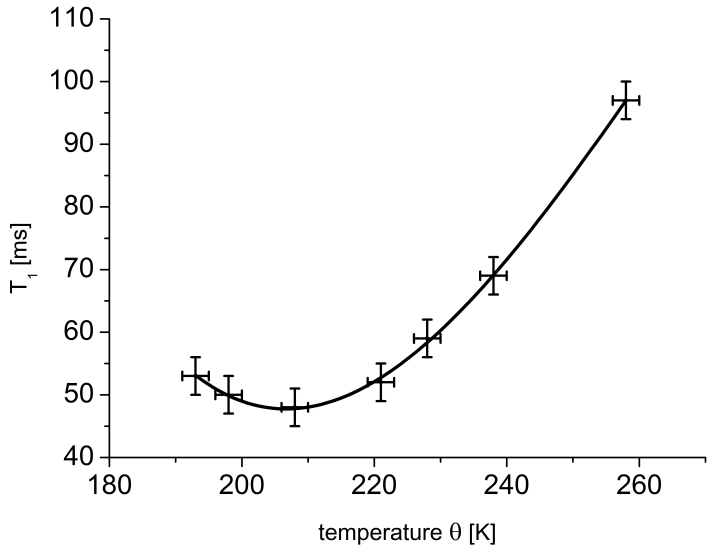

Figure S 5.2. – T_1 values of [Ru(H_2)H(PNP)] **5** as a function of the temperature θ [K] at 500 MHz.

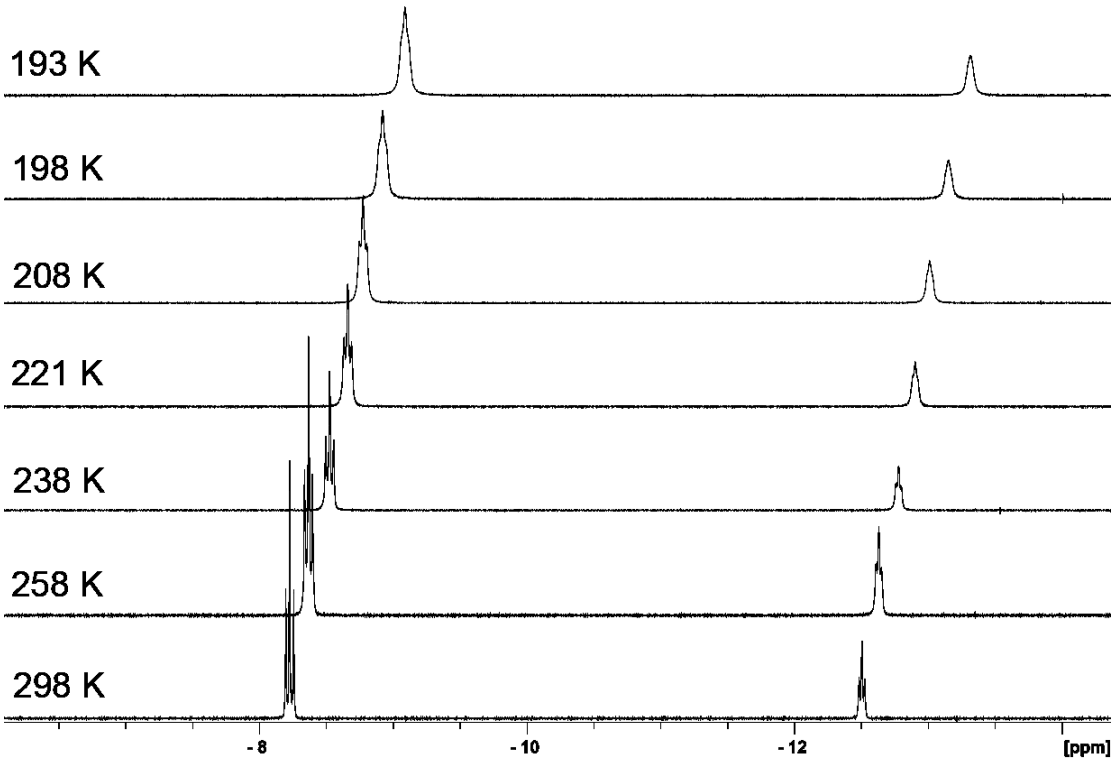

Figure S 5.3. – Hydride signals of complex **4** (-8.26 ppm) and 5 (-12.44 ppm) during T_1-measurements between 298 K – 193 K.

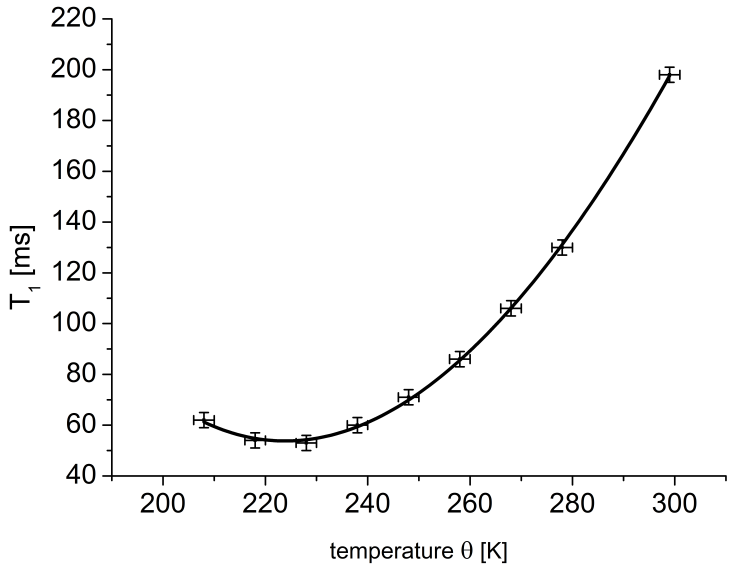

Figure S 5.4. – T_1 values of [Ru(H_2)H_2(MePNP)] **6** as a function of the temperature θ [K] at 500 MHz.

IR Data of Complexes 4-6, 10, 11

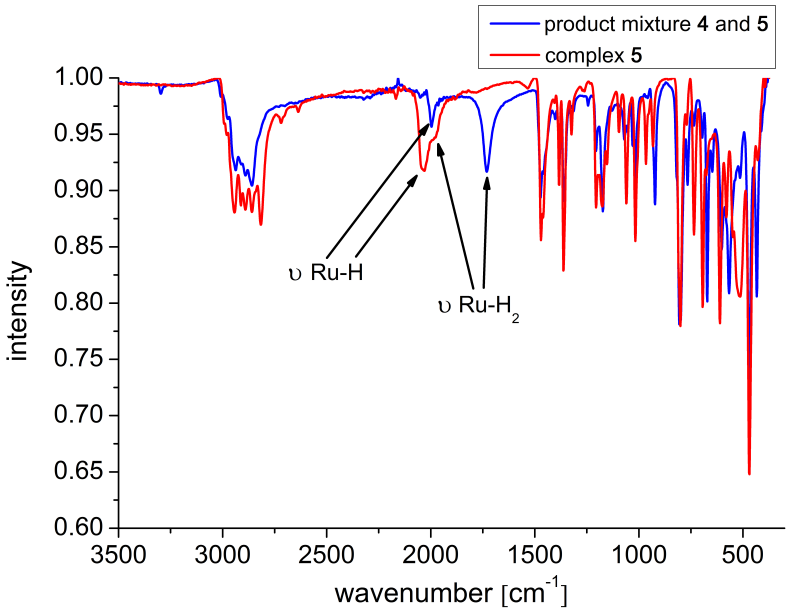

Figure S 5.5. – IR spectra of the product mixture **4** and **5** (blue) and [Ru(H_2)H(PNP)] **5** (red).

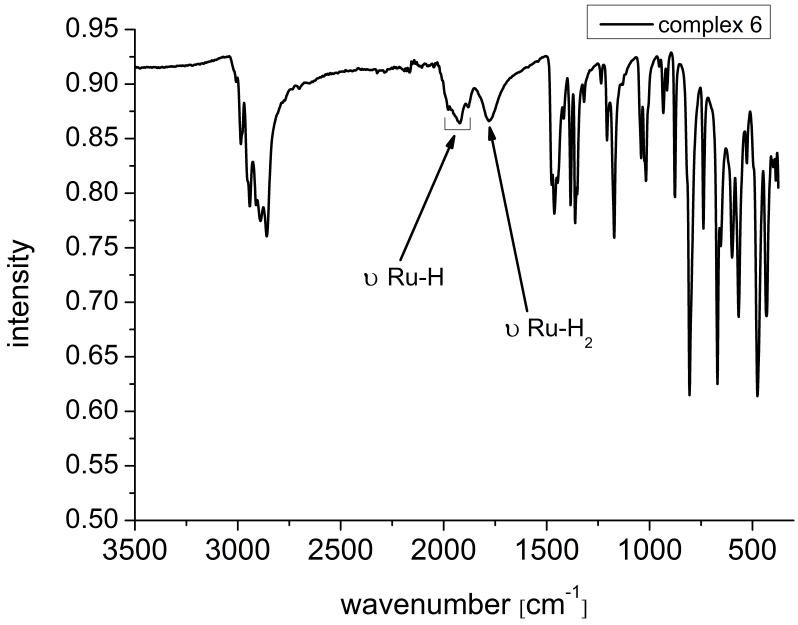

Figure S 5.6. – IR spectrum of [Ru(H_2)H_2(MePNP)] **6** (red).

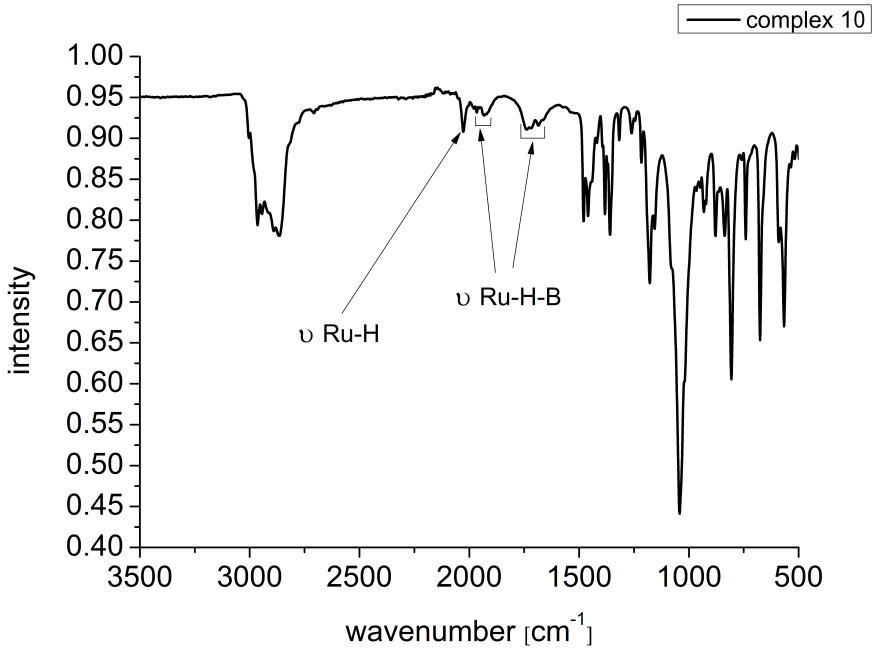

Figure S 5.7. – IR spectrum of [RuH_2(HBPin)(Me-PNP)] **10**.

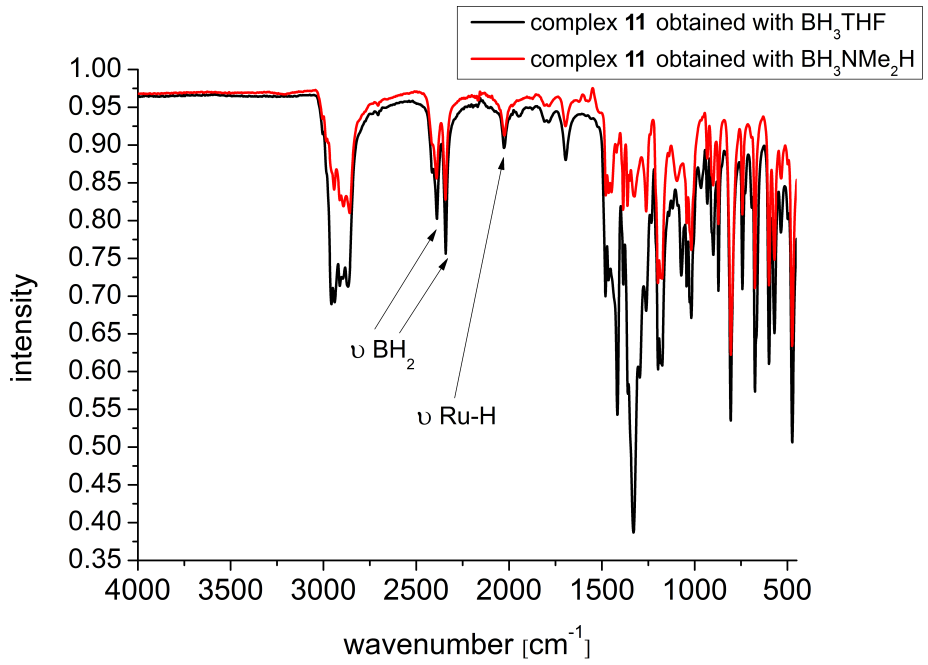

Figure S 5.8. – IR spectra of complex **11**. Vibrational bands are identical beside the THF traces independent from the different synthetic route with BH_3THF (black) or BH_3NMe_2H (red).

LIFDI-MS Data of Complexes 5, 6, 10, 11

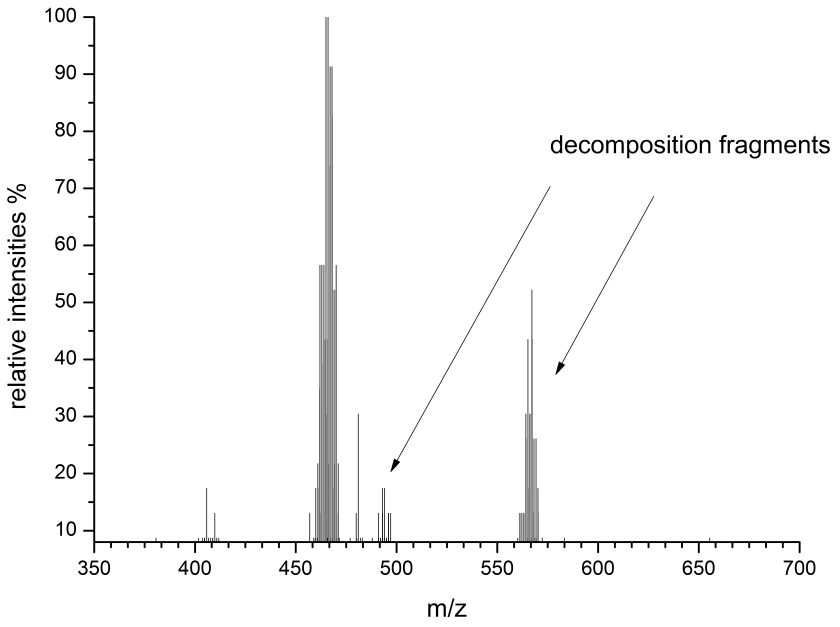

Figure S 5.9. – LIFDI-MS of [Ru(H_2)H(PNP)] **5** in toluene. Retention time (RT) at 3.14 min of 5.00 min. Decomposition of the analysed complexes begins when starting extensice heating of the filament during MS analysis.

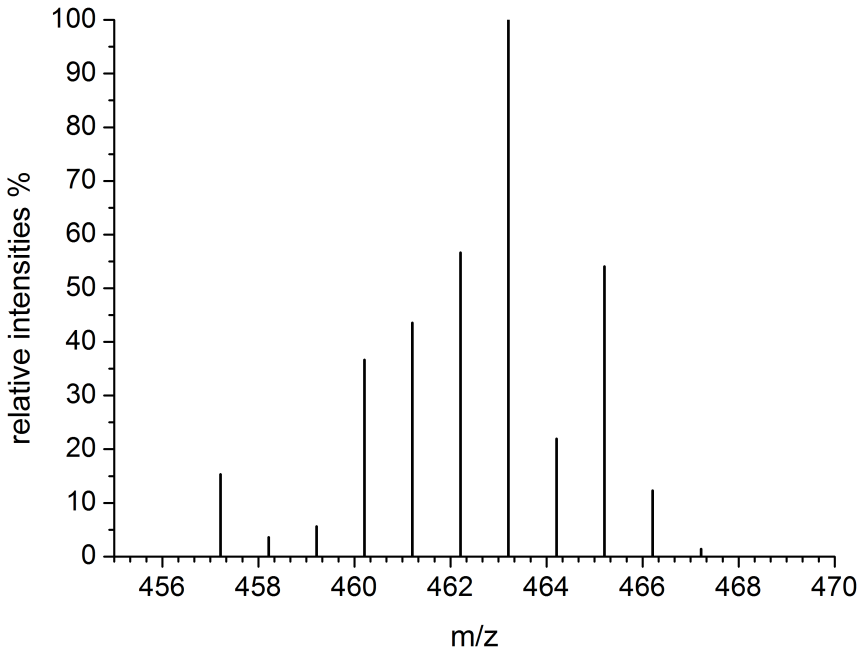

Figure S 5.10. – Simulated isotope pattern of [RuH(PNP)] 463.

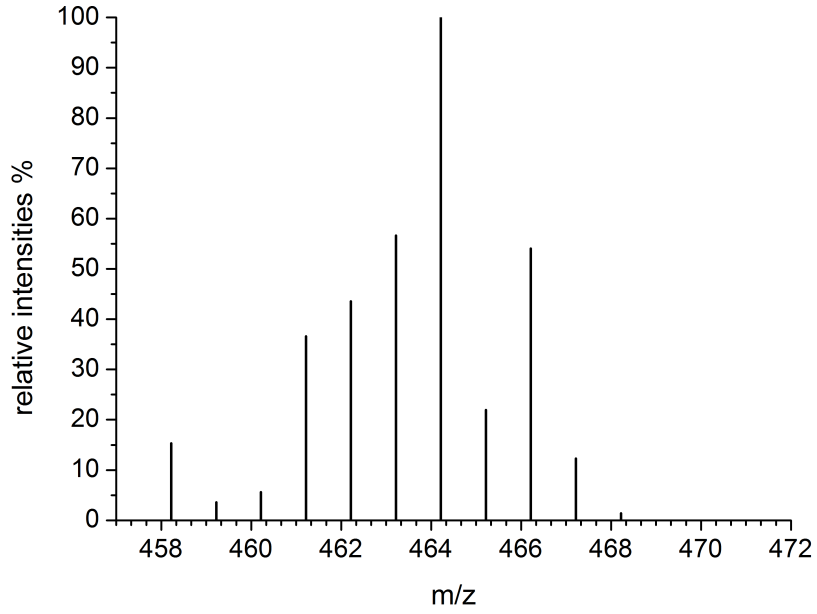

Figure S 5.11. – Simulated isotope pattern of [RuH_2(PNP)] 464.

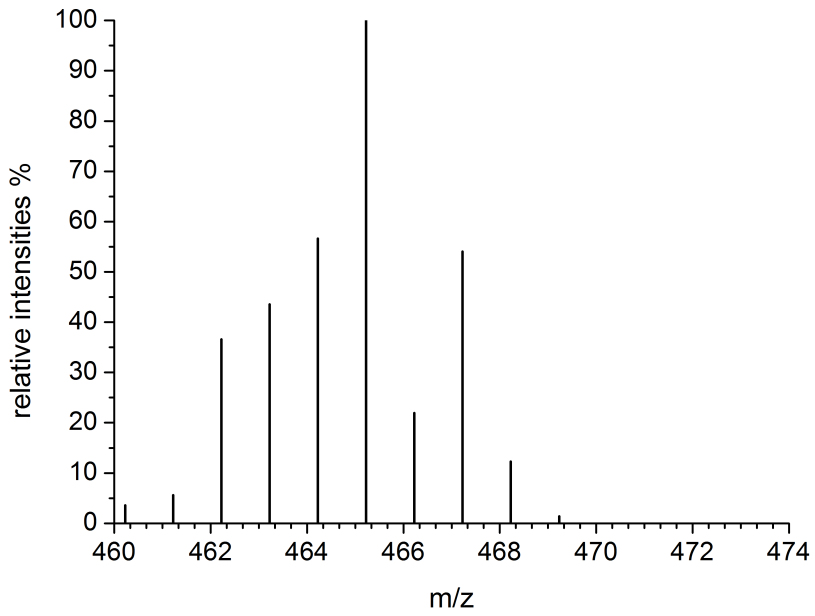

Figure S 5.12. – Simulated isotope pattern of [Ru(H_2)H(PNP)] 465.

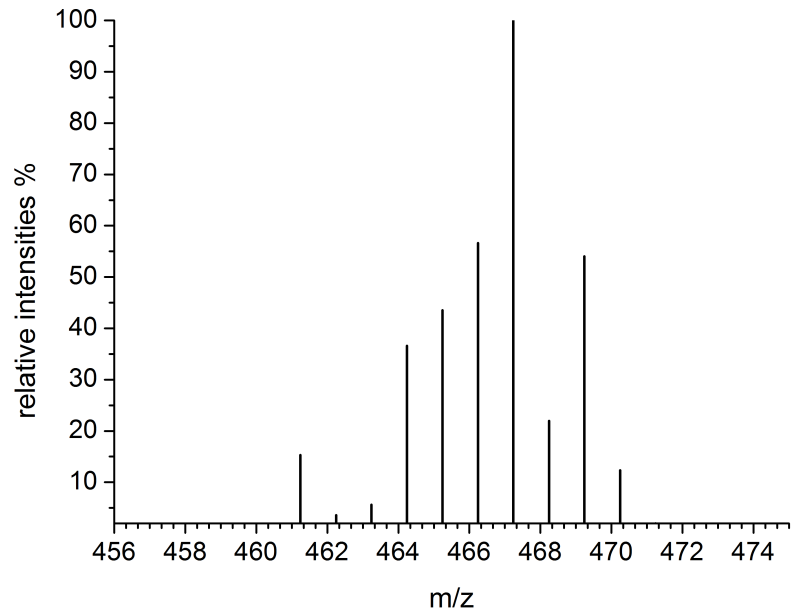

Figure S 5.13. – Simulated isotope pattern of [Ru(H_2)H_2(HPNP)] 467.

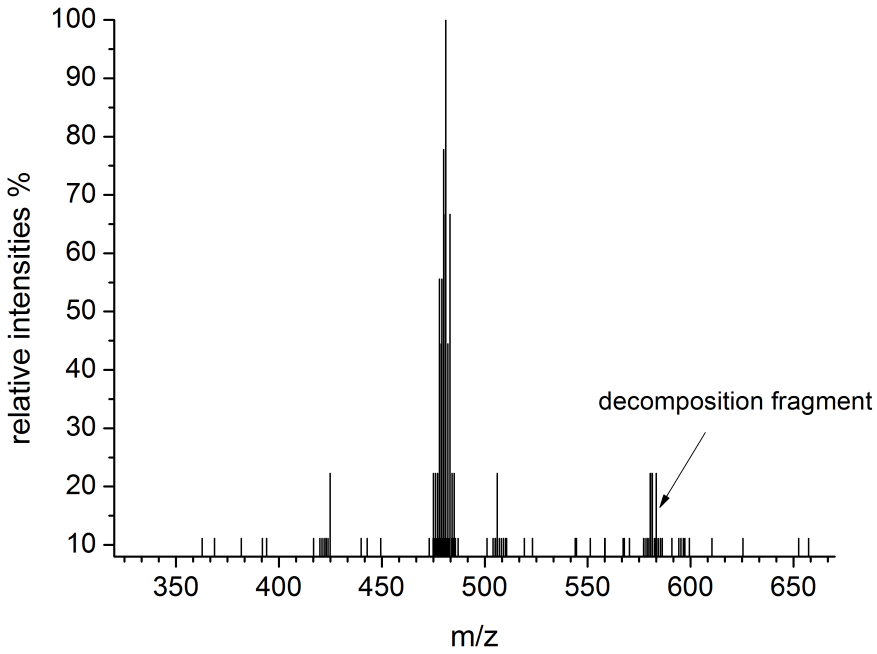

Figure S 5.14. – LIFDI-MS of [Ru(H_2)H_2(Me-PNP)] **6** in toluene. RT 2.16 min of 5.20 min.

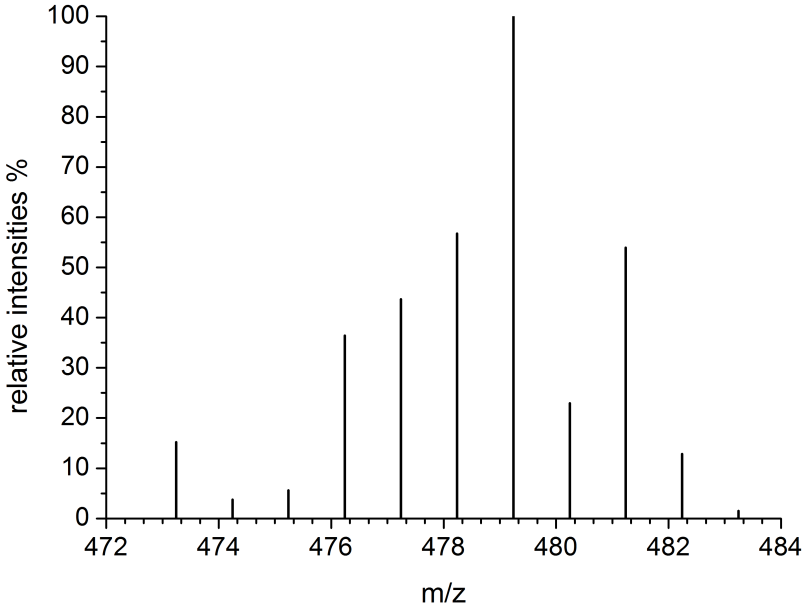

Figure S 5.15. – Simulated isotope pattern of [RuH_2(Me-PNP)] 479.

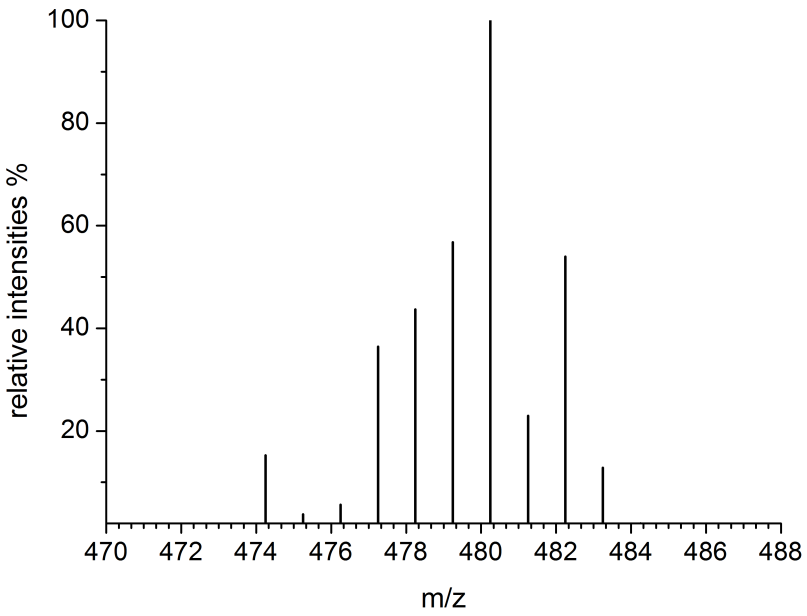

Figure S 5.16. – Simulated isotope pattern of [Ru(H_2)H(Me-PNP)] 480.

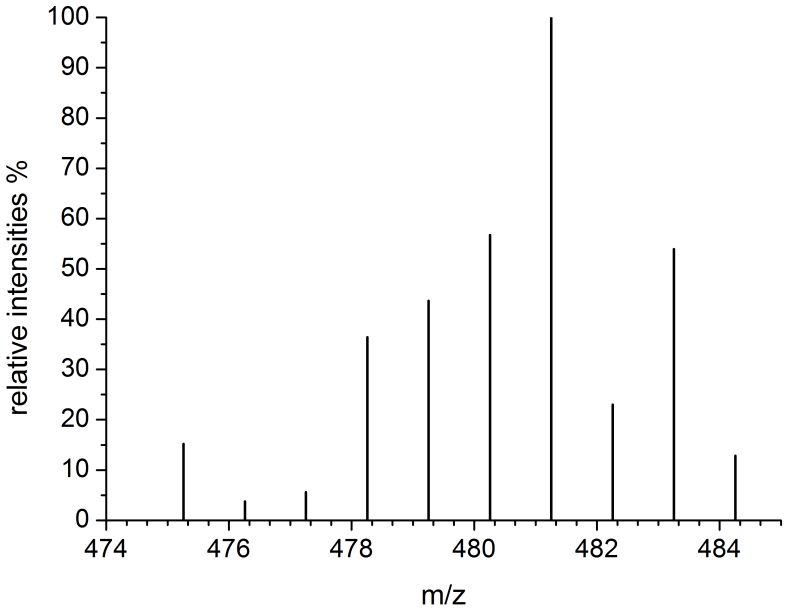

Figure S 5.17. – Simulated isotope pattern of [Ru(H_2)H_2(Me-PNP)] 481.

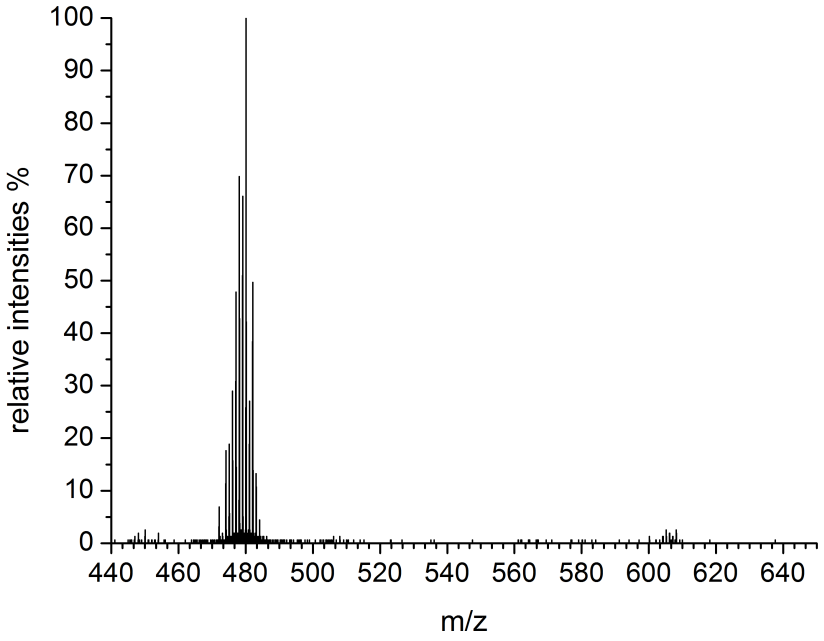

Figure S 5.18. – LIFDI-MS of [RuH_2(HBPin)(Me-PNP)] **10** in toluene. RT 2.04 min of 4.48 min.

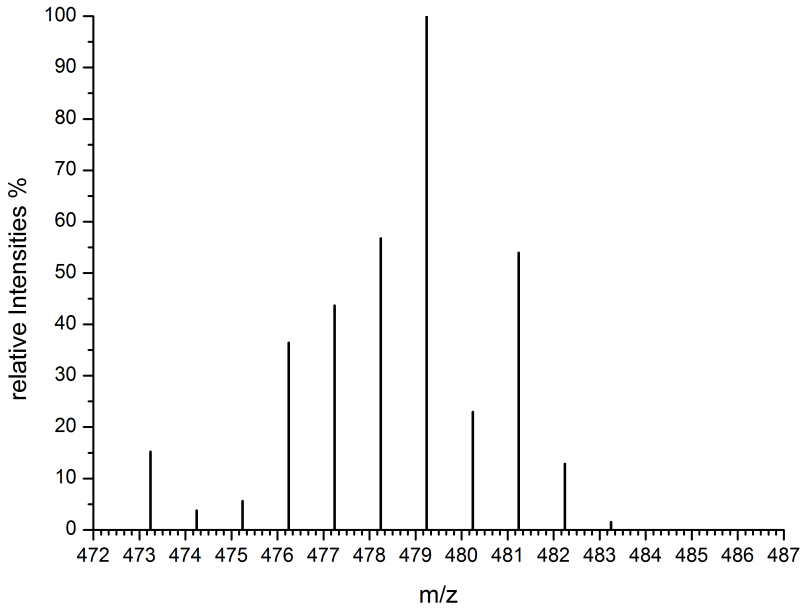

Figure S 5.19. – Simulated isotope pattern of fragment [RuH_2(Me-PNP)] 473 – 482.

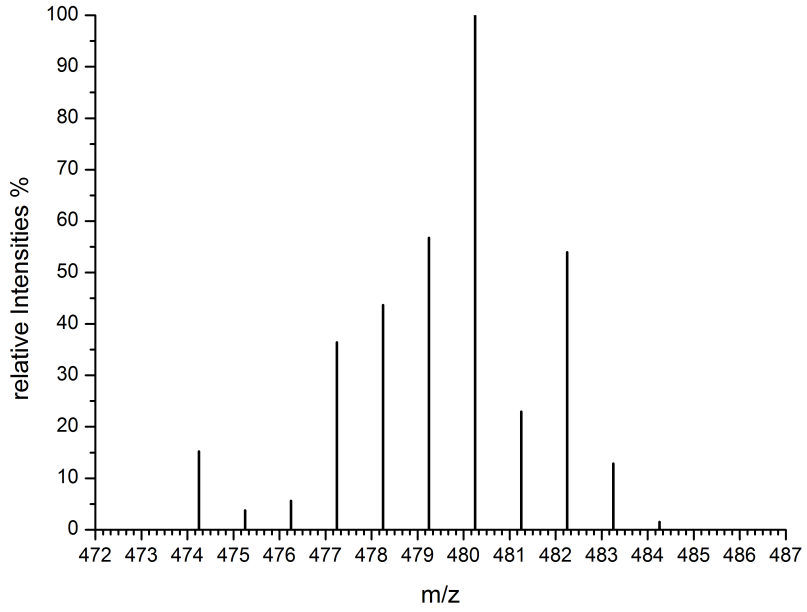

Figure S 5.20. – Simulated isotope pattern of fragment [RuH_3(Me-PNP)] 474 - 483.

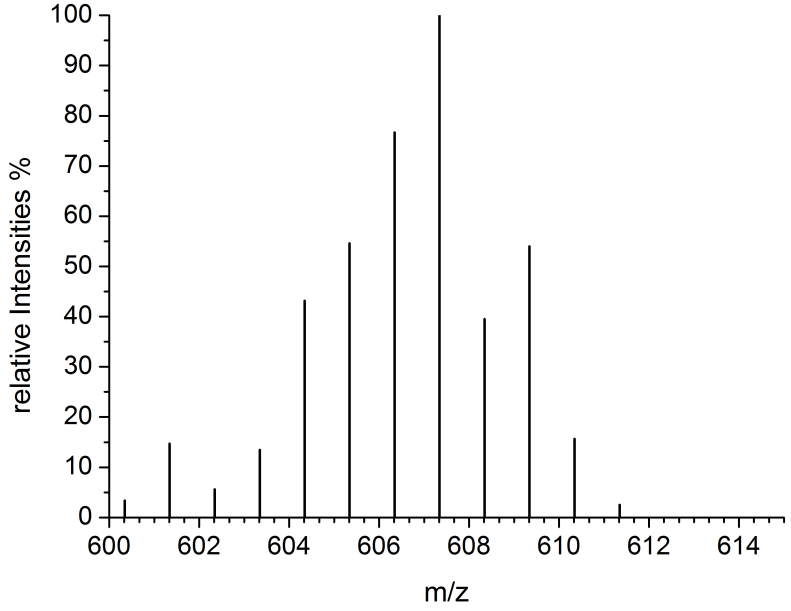

Figure S 5.21. – Simulated isotope pattern of [RuH_2(HBPin)(Me-PNP)] 607.

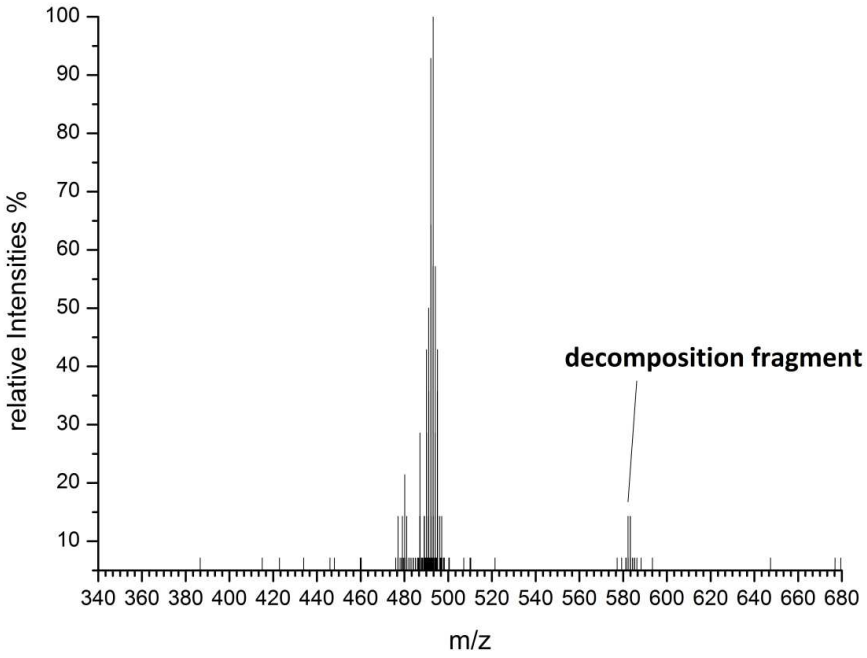

Figure S 5.22. – LIFDI-MS of $[RuH_2(BH_3)(Me\text{-}PNP)]$ **11** in toluene. RT 1.51 min of 5.20 min.

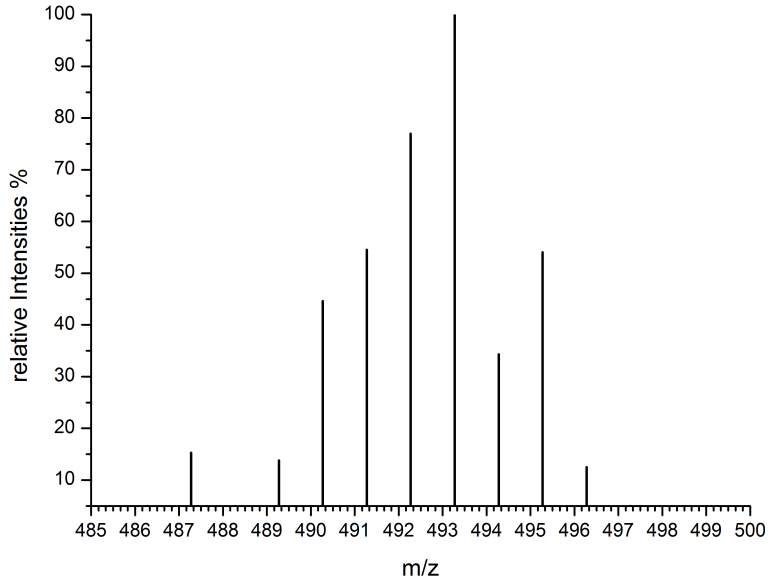

Figure S 5.23. – Simulated isotope pattern of $[RuH_2(BH_3)(Me\text{-}PNP)]$ 493.

Crystallographic Data

Table 5.1. – Crystallographic data of complex **11**

Compound	**11**
CCDC No.	952413
Formula	C21 H52 B N P2 Ru
M	492.46
Crystal System	Monoclinic
Space Group	C 2/c
T[K]	293
a[Å]	35.012(10)
b[Å]	8.148(5)
c[Å]	23.290(5)
α[deg]	90
β[deg]	125.001(14)
γ[deg]	90
V[Å^3]	5442(4)
Z	8
Density [gcm^{-3}]	1.202
μ(mm^{-1})	0.700
θ range[deg]	$0.983 \leq \theta \leq 27.35$
No. of reflections measured	31439
No. of independent reflections	6060
Reflns collected	2749
R_{int}	0.1306
Completeness	0.983
Final R_1 values [all data]	0.1476
wR_2 [all data]	0.1201
GoF	0.902

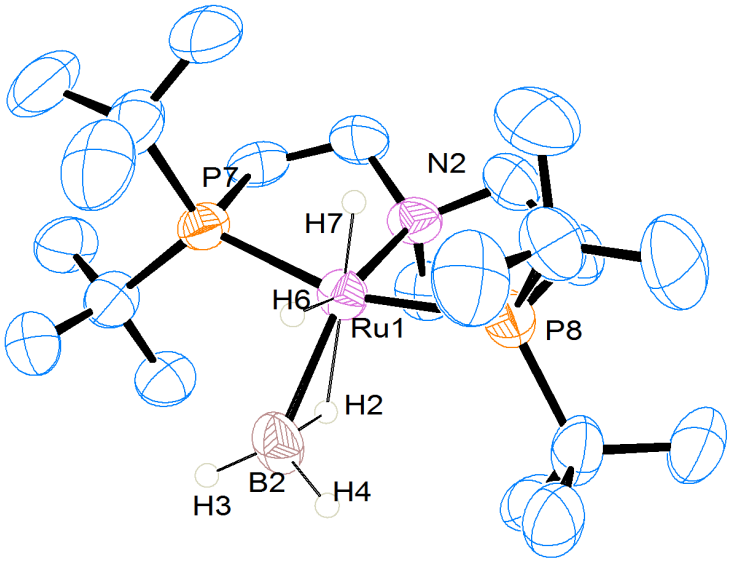

FigureS 5.24. – ORTEP diagram of the single crystal structure of complex **11**. Ellipsoids are illustrated at 50% possibility. All hydrogen atoms are faded out except for H7, H6, H4, H3 and H2 for clarity.

Table 5.2. – Selected bond distances [Å] and angles [deg].

Ru1–P7	2.32(7)	P7–Ru1–P8	163.06
Ru1–P8	2.33(3)	Ru1–H2–B2	92.76
Ru1–N2	2.18(9)	H7–Ru1–H2	170.78
Ru1–H7	1.36(6)	H7–Ru1–P7	63.28
Ru1–H6	1.48(8)	H7–Ru1–P8	65.96
Ru1–H2	1.69(2)	N2–Ru1–B2	143.08
Ru1–B1	2.19(2)	H3–B1–H4	108.16
B1–H2	1.31(6)		
B1–H6	1.84(2)		
B1–H3	1.04(6)		
B1–H4	1.15(7)		

Calculated with SXGRAPH SHELX Graphical Editor.

Addition and Corrections

Synthesis and Characterisation of Ruthenium Dihydrogen Complexes and Their Reactivity Towards B–H Bonds

Jong-Hoo Choi, Nils E. Schloerer, Josefine Berger and Martin H. G. Prechtl
Dalton Trans., **2014**, *43*, 290–299 (DOI: 10.1039/DOI: c3dt52037d). **Amendment published 11th March 2014**.

In the paper, the authors omitted the following information:
p. 290, right column, line 10 (additional references): In addition to the ref. 13 and 14 the following references *A1-4* should be added regarding general approaches with pincer complexes for catalytic amine borane dehydrogenation:
A1. A. Friedrich, M. Drees and S. Schneider, *Chem. Eur. J.*, **2009**, *15*, 10339-10342.
A2. M. Kass, A. Friedrich, M. Drees and S. Schneider, *Angew. Chem. Int. Ed.*, **2009**, *48*, 905-907.
A3. A. Staubitz, M. E. Sloan, A. P. M. Robertson, A. Friedrich, S. Schneider, P. J. Gates, J. S. A. D. Gunne and I. Manners, *J. Am. Chem. Soc.*, **2010**, *132*, 13332-13345.
A4. B. Askevold, H. W. Roesky and S. Schneider, *Chemcatchem*, **2012**, *4*, 307-320.
20 p. 290, right column, line 15-18; the sentence should be read as: "Besides complex **3**, *Schneider et al.* reported formation of ruthenium hydride complexes (**4** and **5**) during ruthenium nitride hydrogenolysis to ammonia.[19]"
p. 291, left column, line 1-7; the sentences should be read as: "The spectroscopic evidence was provided by NMR relaxation time measurements and DFT calculations. The authors found for complex **4** respectively for complex **5** H-H distances of 1.57 Å and 1.31 Å."
p. 291, left column, penultimate line (add ref. 19): The ref. 19 should be cited regarding the NMR data of complexes **4** and **5**.
p. 291, right column, line 2-3 (change to): "[Ru(H_2)H_2(HPNP)] **4**"
p. 291, right column, line 5 (change to): "[Ru(H_2)H(PNP)] **5**"
p. 291, right column, line 11 (additional explanations and references to be inserted as footnote): "Footnote: In this work, for the reported H-H bond length calculations rapid ligand spinning has been considered and not slow motion.[A5] On the NMR time scale we observed in the whole temperature range no decoalescence of the single hydride/dihydrogen signal which is characteristic for *cis* hydrido dihydrogen complexes.[A6] Moreover, in case of slow motion decoalescence of the signal should occur due to "magnetic or chemical inequivalence of the two nuclei" in the dihydrogen ligand.[A5] This has not been

observed. Additionally, rapid spinning occurs when the H_2-ligand is situated *trans* to a classical hydride ligand, like in the equatorial plane of complex **4** or **5**.[A5] However, a *trans* situation of H_2 to the N-ligand in a [Ru(H_2)H_2(PNP)] is not possible (see ref. 3). Therefore, the calculation considers rapid rotation of the H_2 ligand which is related to a low energy barrier for rotation.[A5] Moreover, due to the dynamic exchange with the classical hydrides, and higher $T_{1(min)}$ values for classical hydrides, the reported overall $T_{1(min)}$ values for the H_2 ligand can be assigned only as upper limit for the distance in the coordinated H_2 moiety (see ref. 18). Consequently we calculated the H-H distance considering rapid spinning and not slow motion of the ligand."

A5. R. H. Morris, *Coord. Chem. Rev.*, **2008**, *252*, 2381-2394.

A6. S. Sabo-Etienne and B. Chaudret, *Coord. Chem. Rev.*, **1998**, *178*, 381-407.

p. 292, left column, line 17-18; the sentence should be read as follows including new citations: "The lability of tetrahydride **4** in equilibrium with **5** can be explained by the cooperative properties of the H-PNP pincer backbone, according to the observations by other groups with similar systems.[A2, A4, A7-9]"

A7. A. Friedrich, M. Drees, M. Kass, E. Herdtweck and S. Schneider, *Inorg. Chem.*, **2010**, *49*, 5482-5494.

A8. S. Schneider, J. Meiners and B. Askevold, *Eur. J. Inorg. Chem.*, **2012**, 412-429.

A9. T. C. Wambach, J. M. Ahn, B. O. Patrick and M. D. Fryzuk, *Organometallics*, **2013**, *32*, 4431-4439.

p. 292, right column, line 5; additional reference: *A8*

p. 294, left column, last paragraph, first sentence should be read as: "The structure of complex 11 (Fig. 8, Table 1) was tentatively determined also by X-ray analysis, however we are aware of the limitations of this technique regarding metal hydrides and related compounds."

p. 295, right column, line 3 (delete): "rigid"

p. 295, right column, line 6-10; compare to original citations: *4, 13, 15, 24*

p. 296, left column, line 28 (change to): "Synthesis of [Ru(H_2)H_2(H-PNP)] **4** and [Ru(H_2)H(PNP)] **5**"

p. 296, left column, line 29-31 (change to): "[...]H-PNP ligand **8**[...]."

The Royal Society of Chemistry apologises for these errors and any consequent inconvenience to authors and readers.

5.2. Supporting Information - Selective Conversion of Alcohols in Water to Carboxylic Acids by in situ generated Ruthenium Trans Dihydrido Carbonyl PNP Complexes

Jong-Hoo Choi,[a] Leo E. Heim,[a] Mike Ahrens,[b] and Martin H. G. Prechtl[a*]
[a] Department of Chemistry, University of Cologne, Greinstr.6, 50939 Cologne, Germany. Fax: +49 221 470 1788; Tel: +49 221 470 1981; E-mail: martin.prechtl@uni-koeln.de Web: www.catalysislab.de [b] Institute of Chemistry, Humboldt University at Berlin, Brook-Taylor-Straße 2, D-12489 Berlin, Germany.

Online Gas-Phase Mass Spectrometry of the Alcohol Decarbonylation by Complex 3

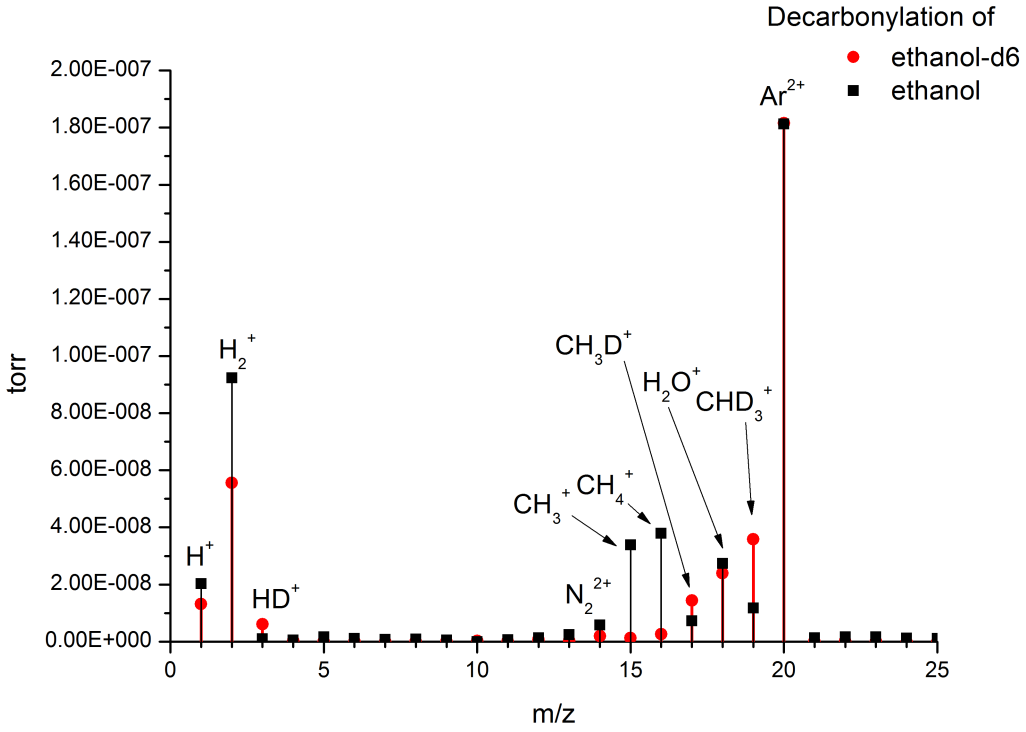

Fig. S 5.25. – MS-monitoring of the decarbonylation reaction of ethanol (black) and ethanol-d_6 (red) by 0.2 mmol complex **2**. Diagram shows the detected averaged distribution of evolved hydrocarbons.

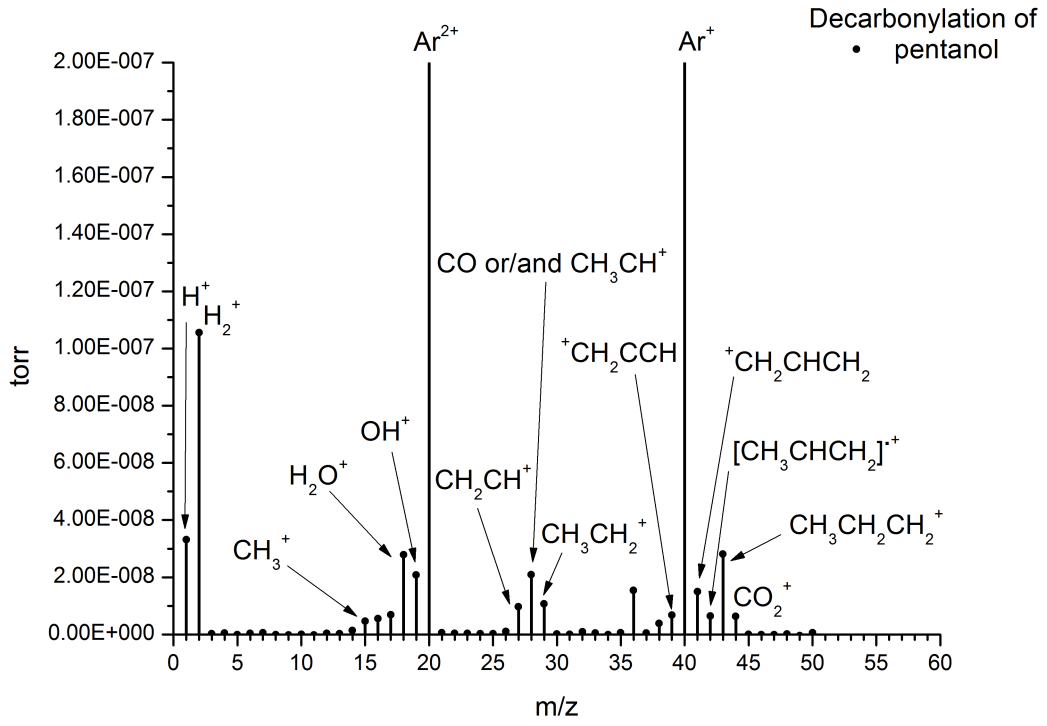

Fig. S 5.26. – MS-monitoring of the decarbonylation reaction of pentanol by 0.2 mmol complex 2. Diagram shows the detected averaged distribution of evolved hydrocarbons.

LIFDI-MS Analysis of Complexes 3, 4a, 4b and 6

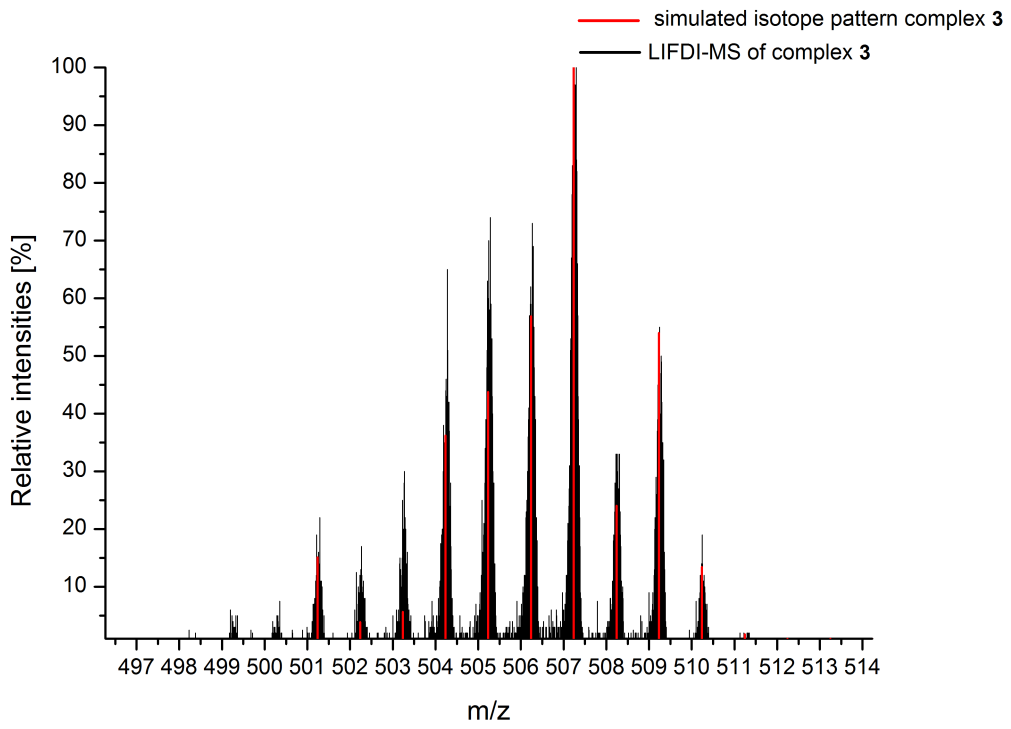

Fig. S 5.27. – LIFDI-MS (Argon collided) of $[RuH_2(CO)(Me\text{-}PNP)]$ **3** (black, 501 – 511) in toluene compared to simulated isotope pattern of $[RuH_2(CO)(Me\text{-}PNP)]$ 507 (red, 501 – 511). Retention time (RT) 2.14 min of 7.00 min.

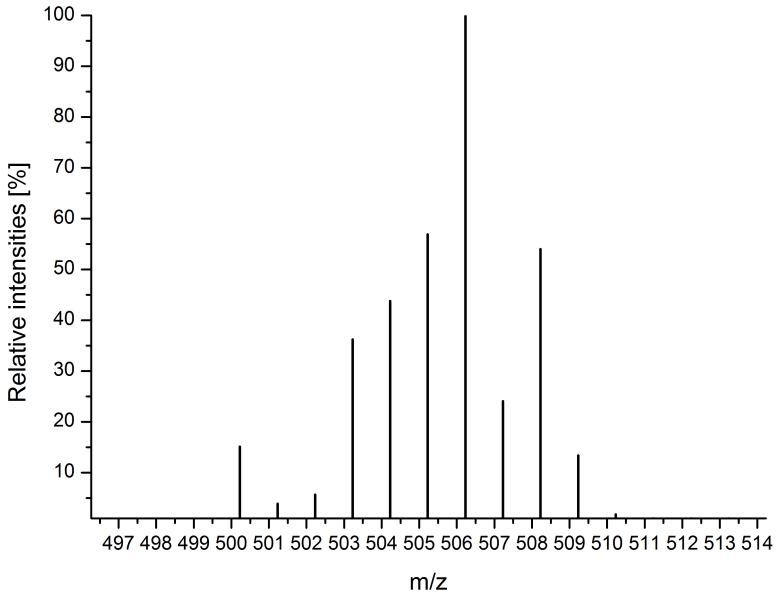

Fig. S 5.28. – Simulated istope pattern of fragment [RuH(CO)(Me-PNP)] 500 – 509.

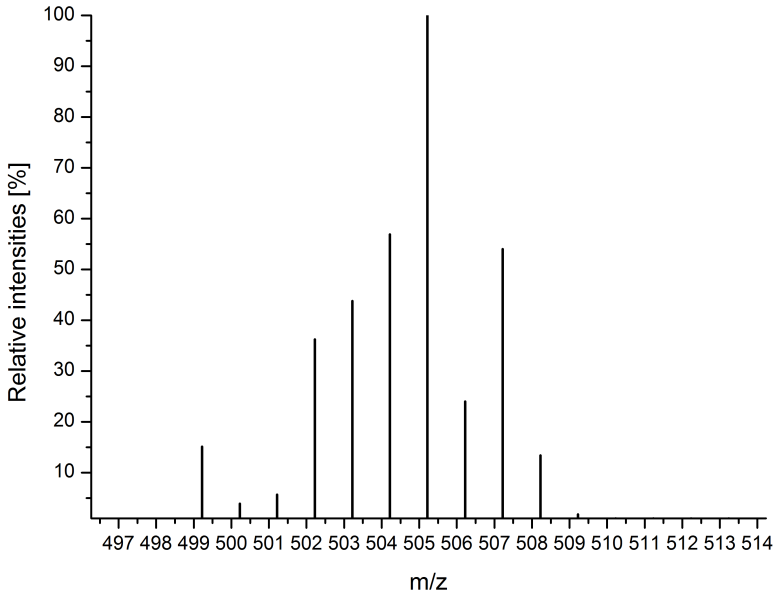

Fig. S 5.29. – Simulated istope pattern of fragment [Ru(CO)(Me-PNP)] 499 – 508.

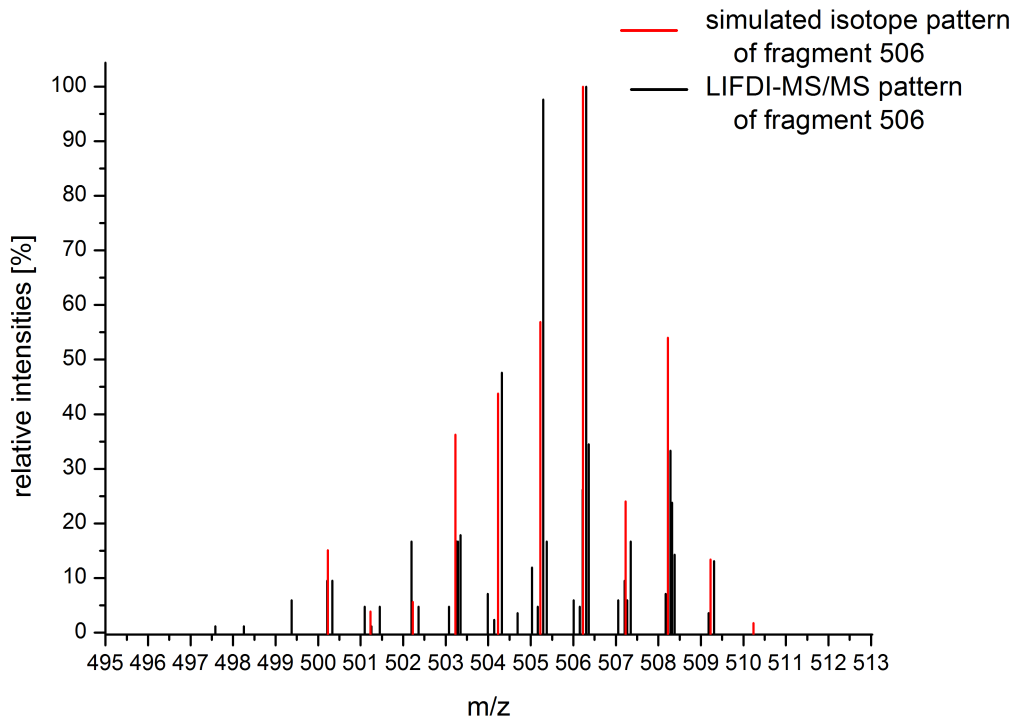

Fig. S 5.30. – LIFDI-MS/MS of [RuH(CO)(Me-PNP)] 506 (black, 501 – 509) in toluene decomposed from complex **4a** under MS conditions compared to simulated isotope pattern of [RuH(CO (Me-PNP)] 506 (red, 501 – 509). RT 5.23 min of 7.00 min. Compared to the simulated isotope pattern of [RuH(CO(Me-PNP)] 506 m/z in red, the detected fragment differs slightly towards lower mass value, which can be explained by the detection of a fragmentation mixture of the species [Ru(CO)(Me-PNP)] 505 (see simulated isotope pattern in Fig. S5.29) and [RuH(CO)(Me-PNP)] 506.

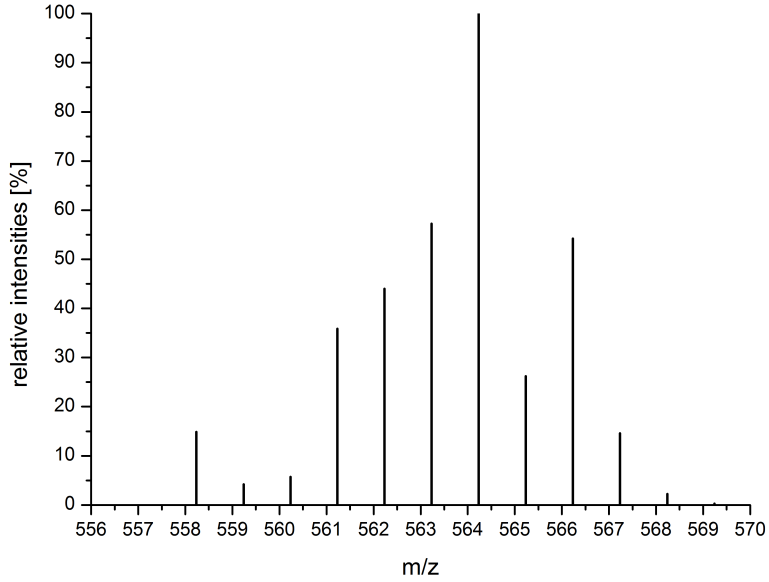

Fig. S 5.31. – Simulated istope pattern of fragment [Ru(CO)($OOCCH_3$)(Me-PNP)] 558 – 569.

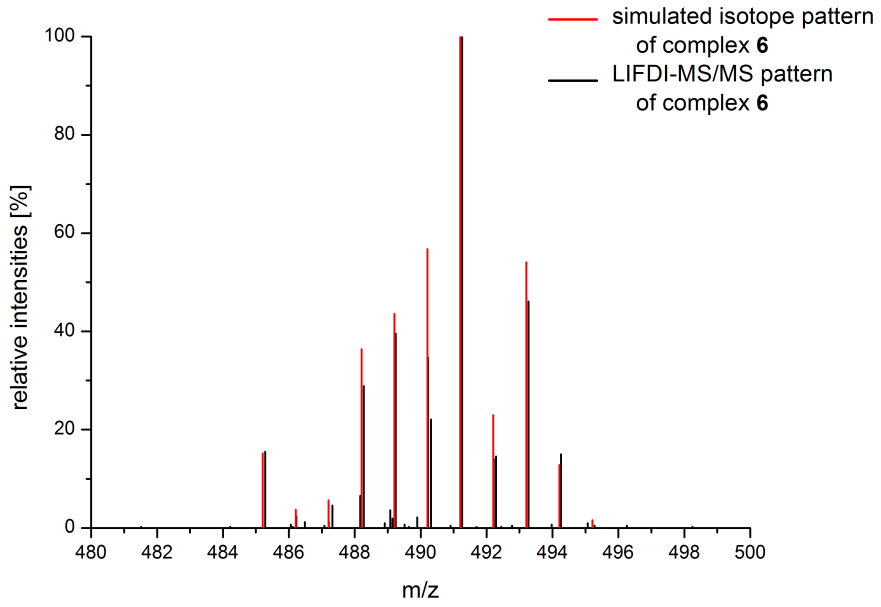

Fig. S 5.32. – LIFDI-MS/MS of [RuH(CO)(PNP)] **6** (black, 485 – 495) in toluene compared to simulated isotope pattern of [RuH(CO)(PNP)] 491 (red, 485 – 495). Retention time (RT) 2.61 min of 7.00 min.

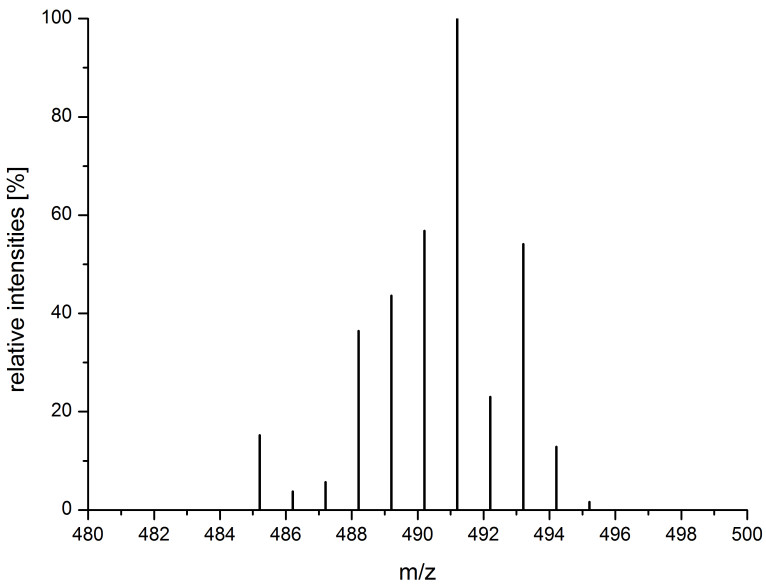

Fig. S 5.33. – Simulated istope pattern of fragment [Ru(CO)(PNP)] 484 – 494.

IR Spectra of Complexes 3, 4a, 4b and 6

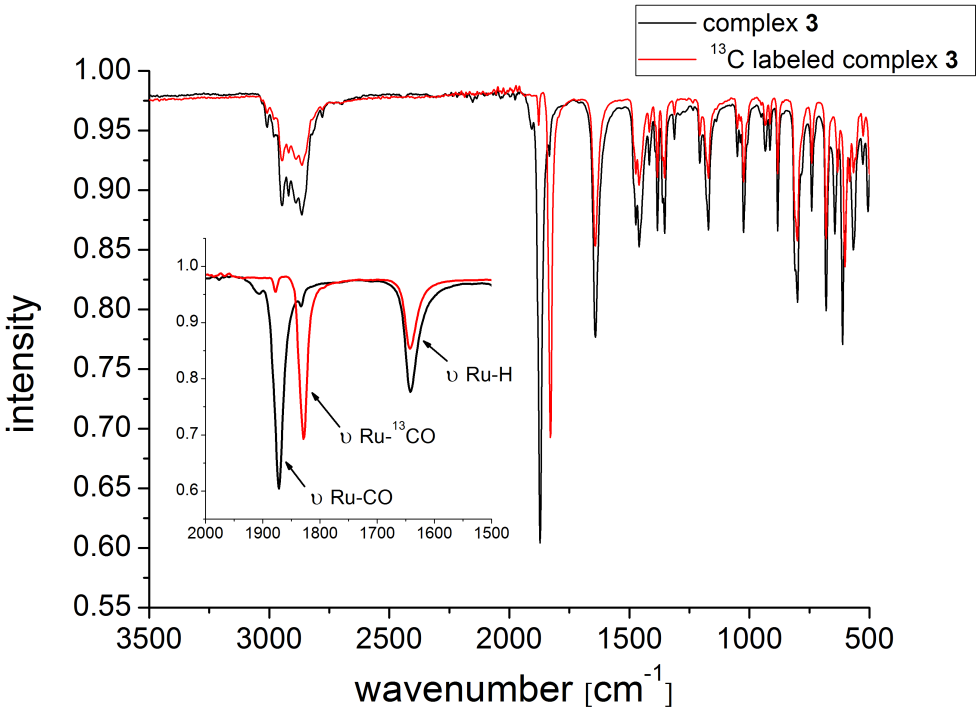

Fig. S 5.34. – IR spectra of [RuH_2(CO)(Me-PNP)] **3** (black) and [RuH_2(^{13}CO)(Me-PNP)] **3** (red).

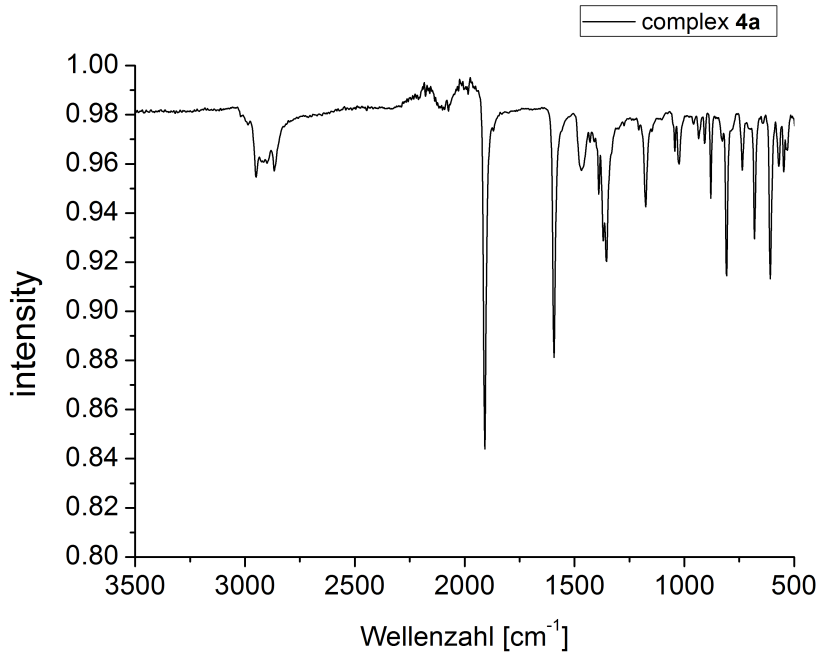

Fig. S 5.35. – IR spectrum of [RuH(CO)(hexanolate)(Me-PNP)] **4a**.

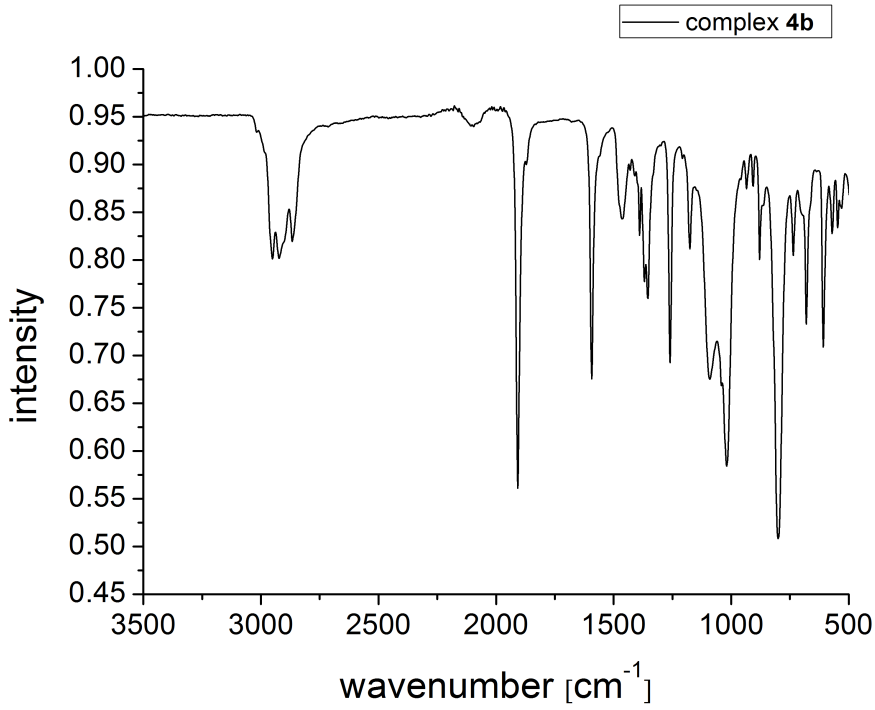

Fig. S 5.36. – IR spectrum of [RuH(CO)($OOCCH_3$)(Me-PNP)] **4b**.

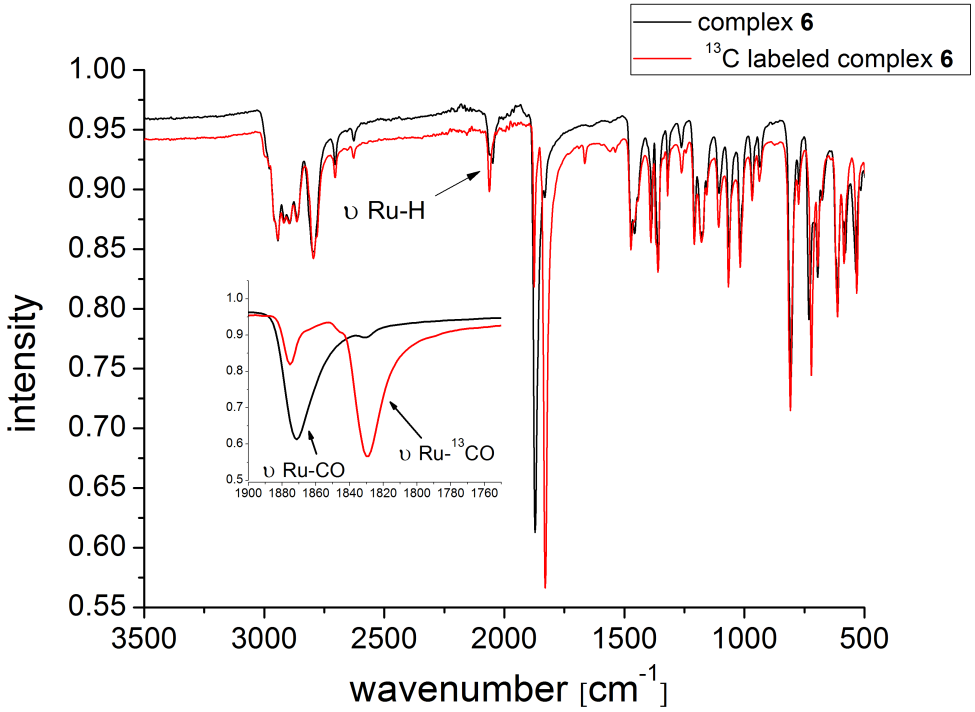

Fig. S 5.37. – IR spectra of [RuH(CO)(PNP)] **6** (black) and [RuH(^{13}CO)(PNP)] **6** (red).

NMR Spectra of Complexes 3, 4a, 4b and 6

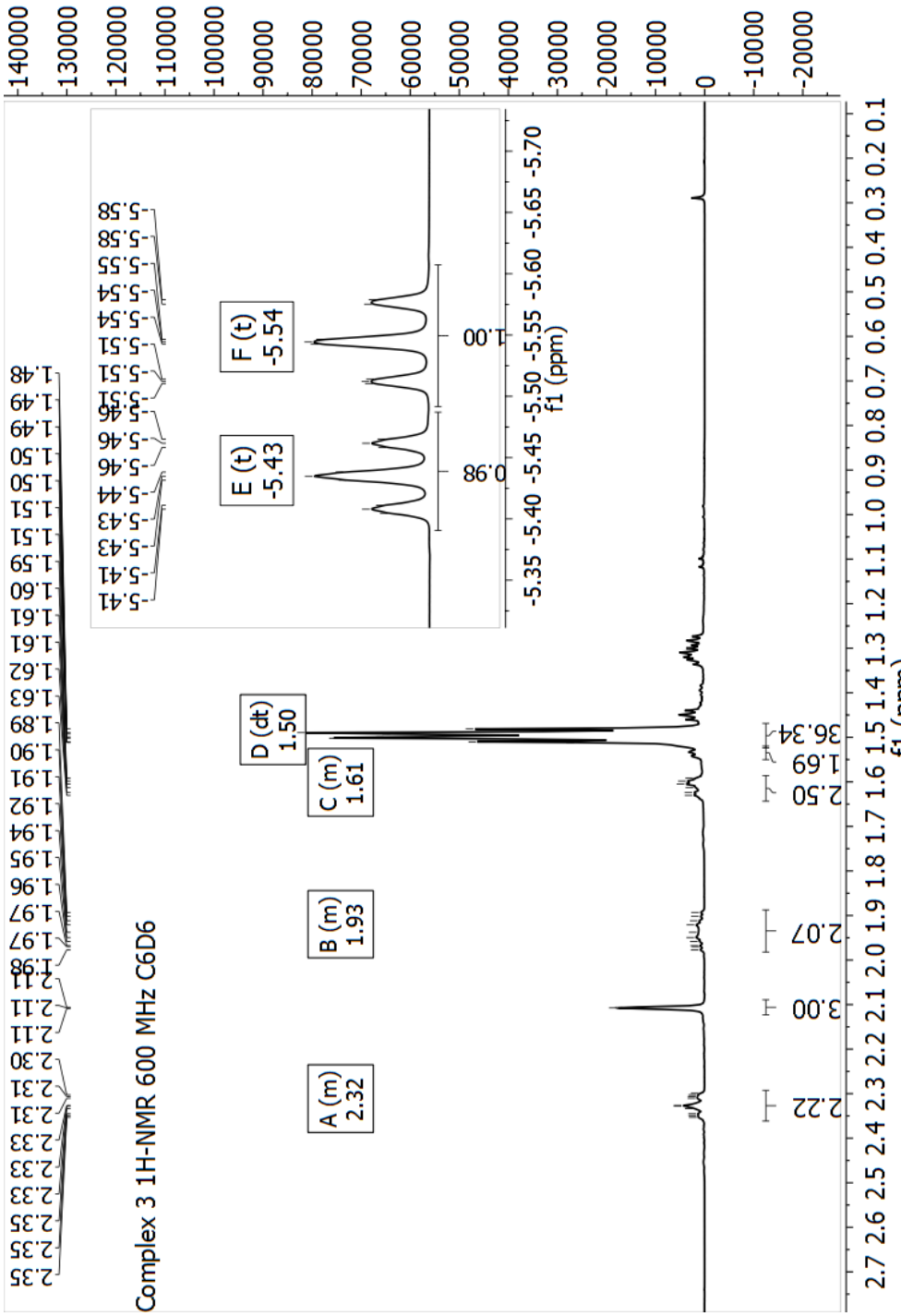

Fig. S 5.38. – ^{1}H NMR of [RuH_2(CO)(Me-PNP)] **3** in C_6D_6 at 600 MHz.

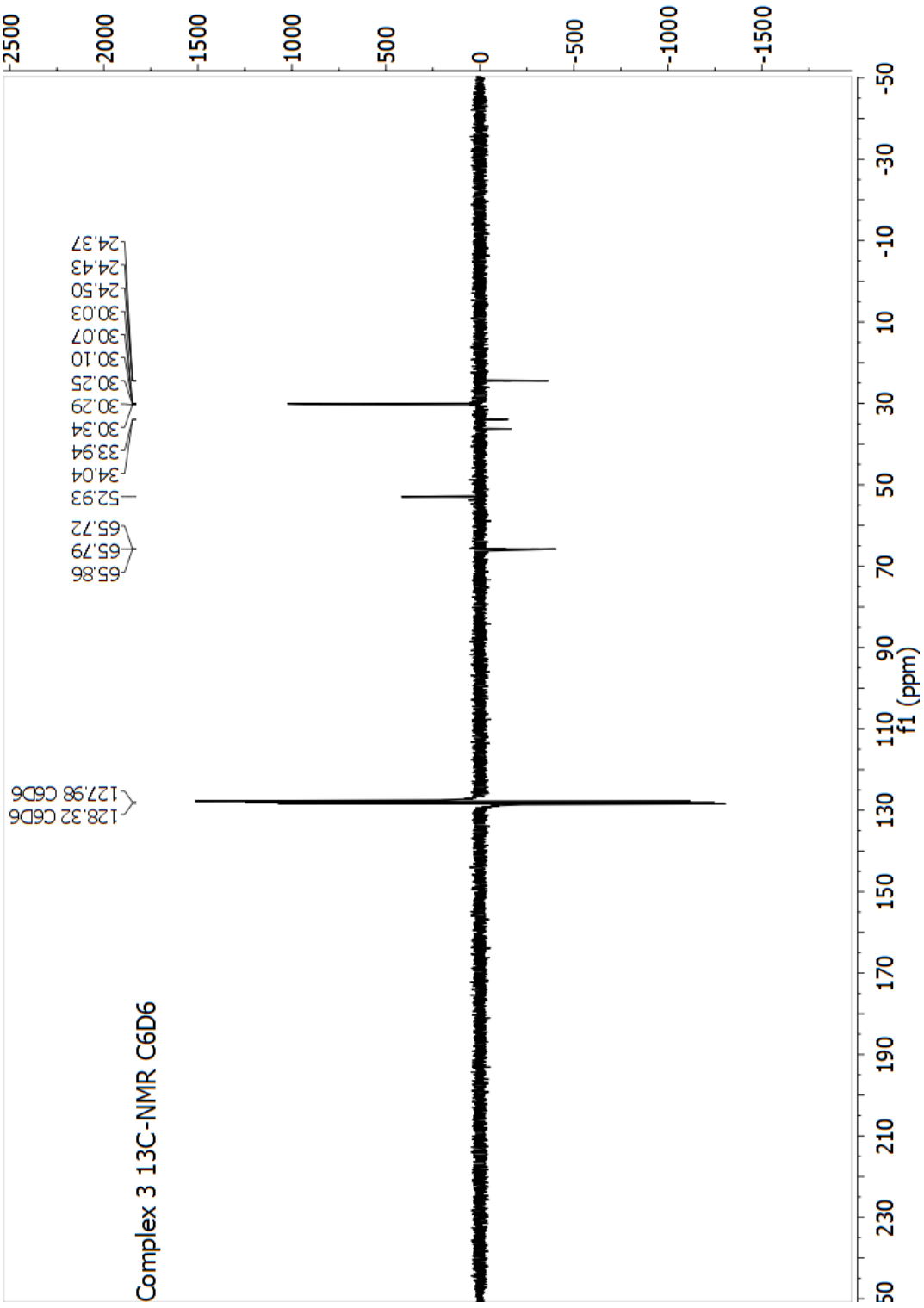

Fig. S 5.39. – $^{13}C_{APT}$ NMR of **3** in C_6D_6 at 75 MHz.

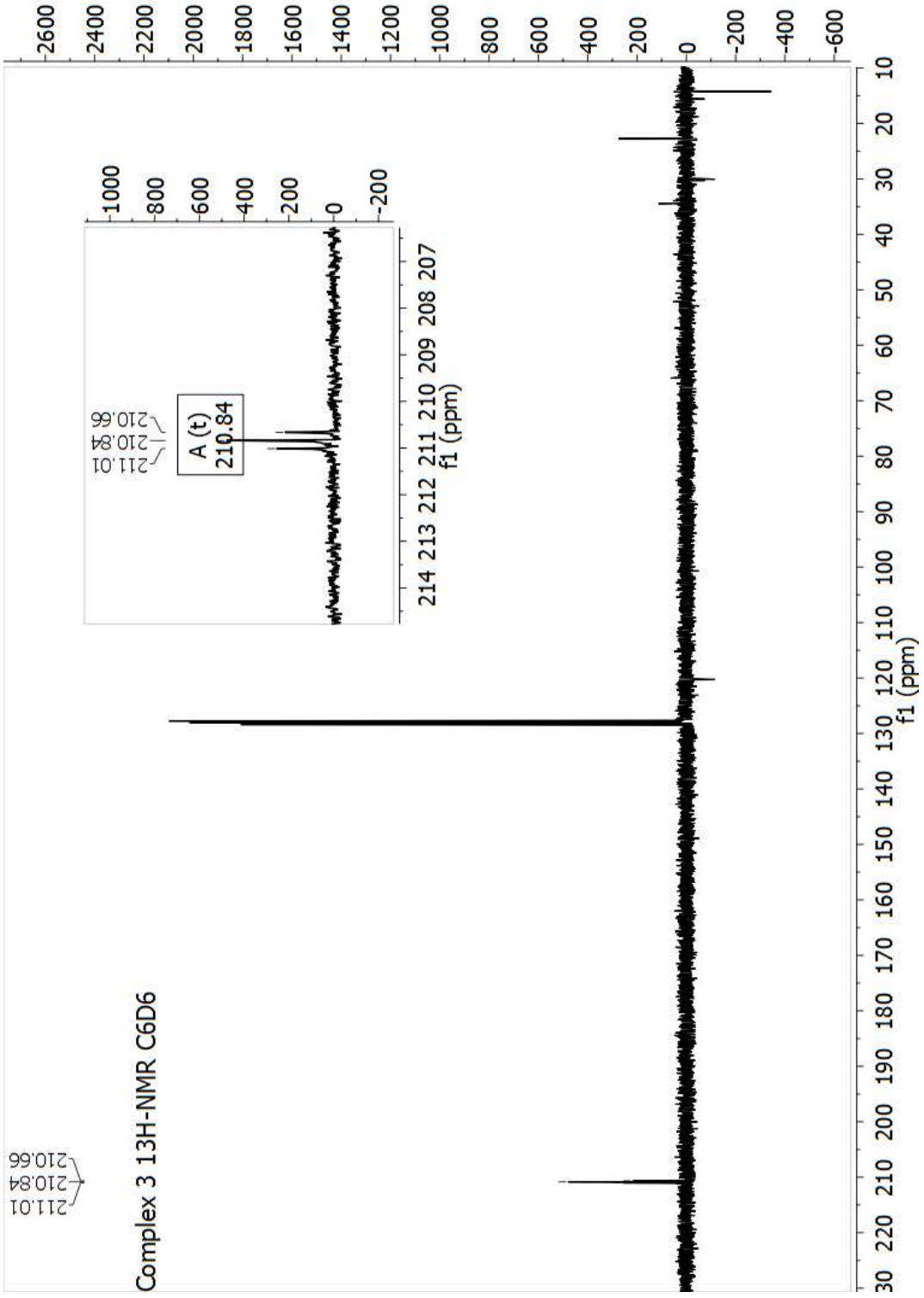

Fig. S 5.40. – $^{13}C_{APT}$ NMR of [RuH_2(^{13}CO)(Me-PNP)] **3** at 75 MHz.

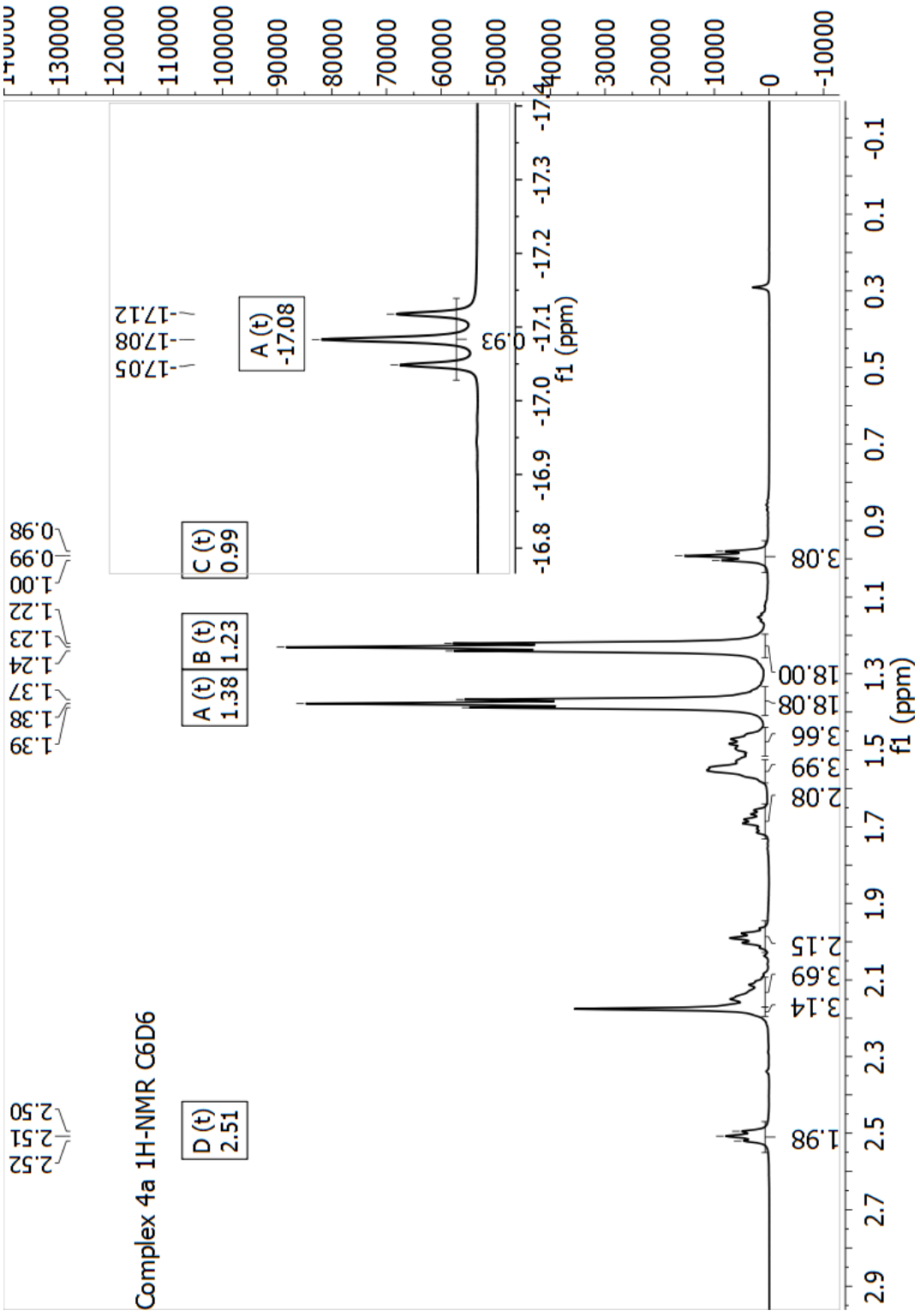

Fig. S 5.41. – ^{1}H NMR of [RuH(CO)(hexanolate)(Me-PNP)] **4a** in C_6D_6 at 600 MHz.

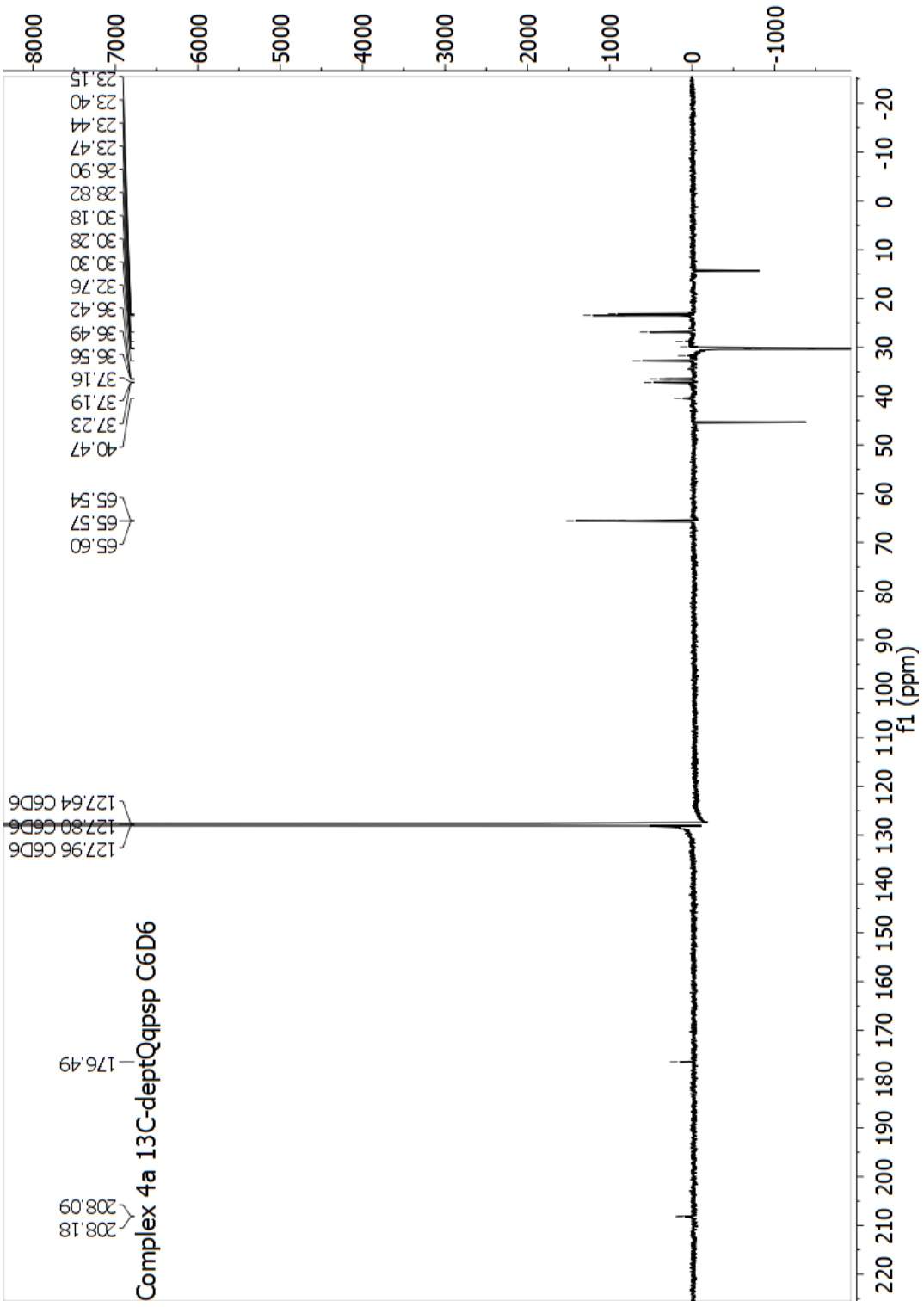

Fig. S 5.42. – $^{13}C_{APT}$ NMR of **3** in C_6D_6 at 75 MHz.

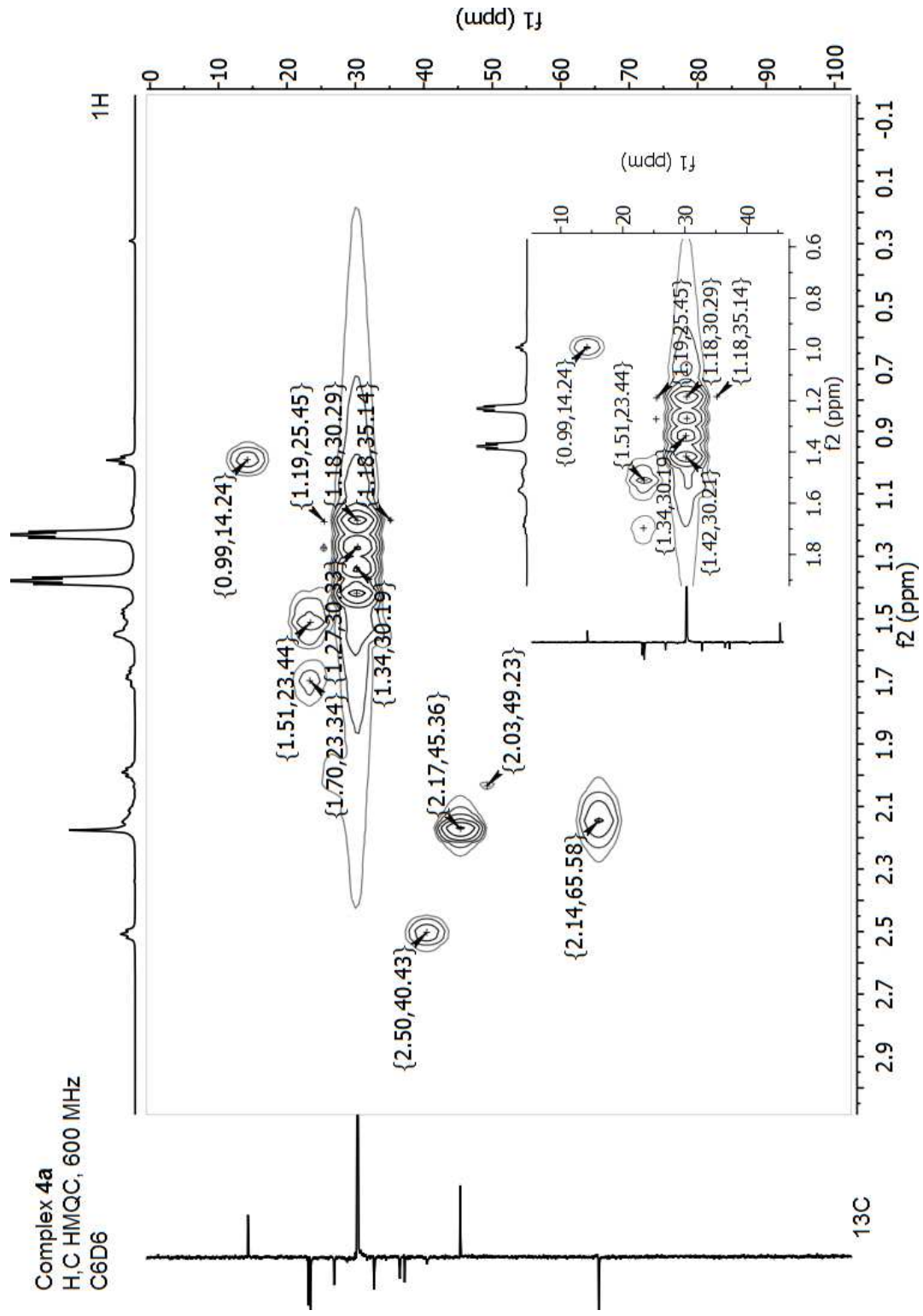

Fig. S 5.43. – H,C HMQC of [RuH(CO)(hexanolate)(Me-PNP)] **4a** in C_6D_6 at 600 MHz (^{1}H) 150 MHz (^{13}C).

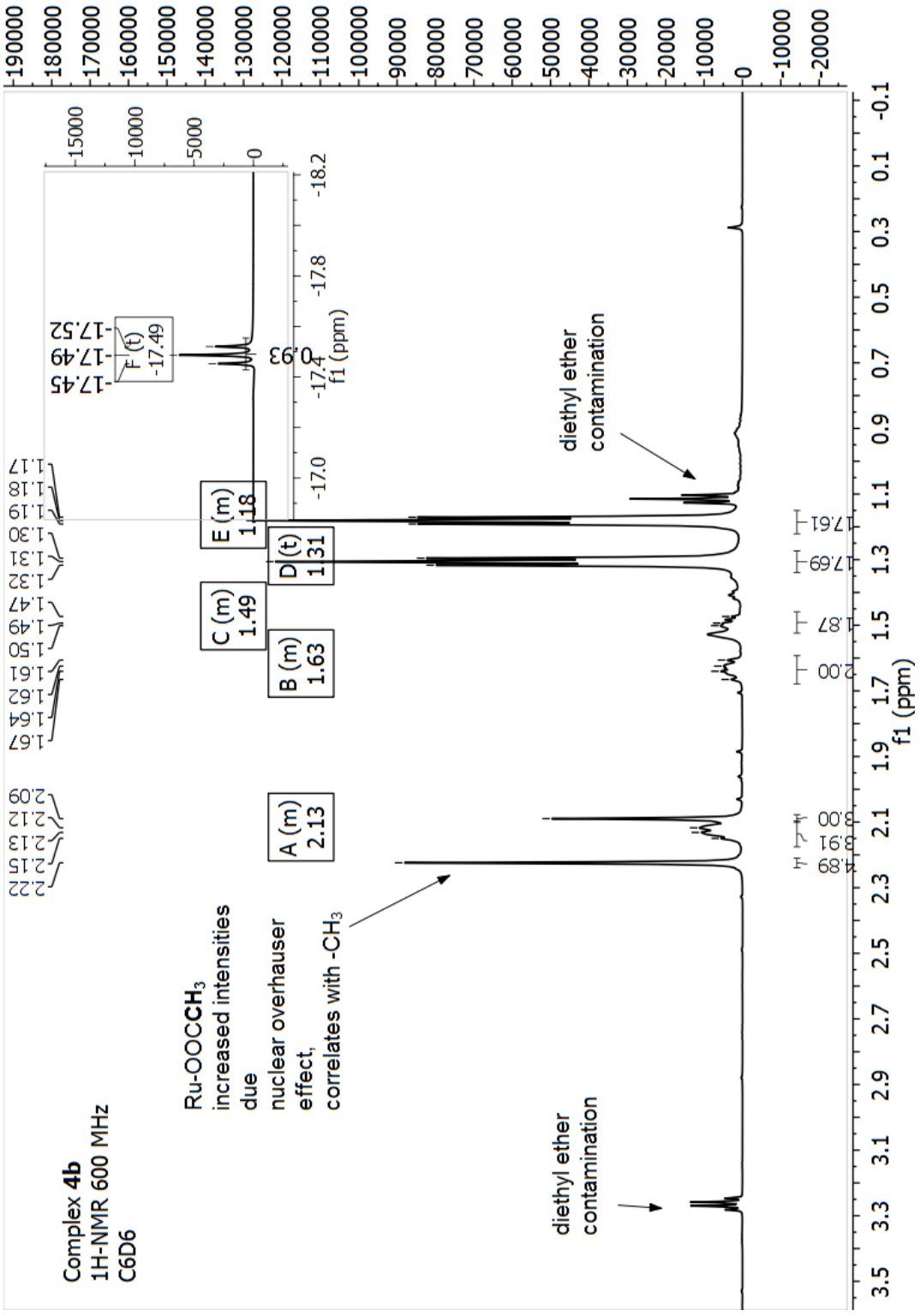

Fig. S 5.44. – ^{1}H NMR of [RuH(CO)(OOCCH$_3$)(Me-PNP)] **4b** in C_6D_6 at 600 MHz.

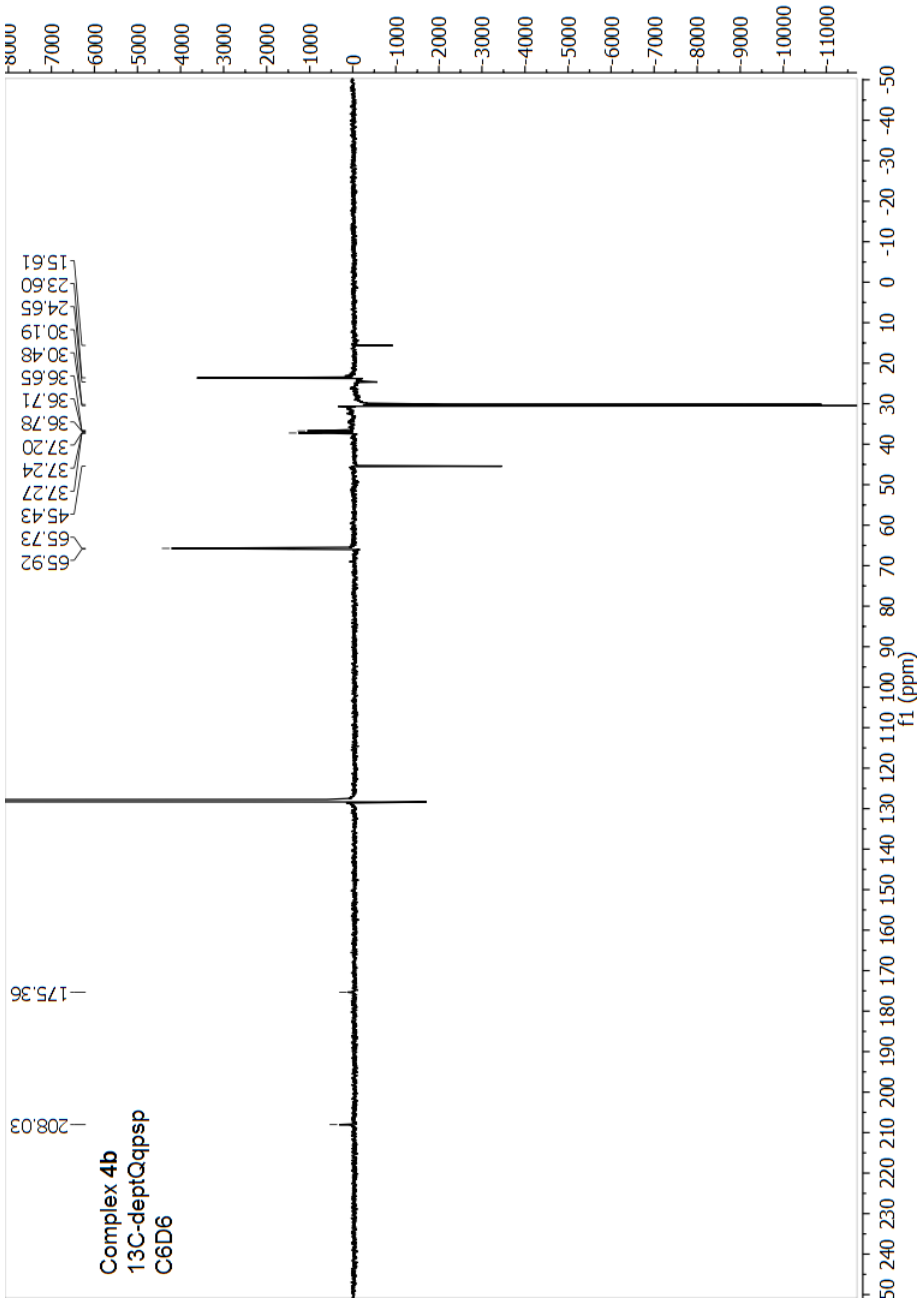

Fig. S 5.45. – ^{13}C-deptQ NMR of [RuH(CO)(OOCCH$_3$)(Me-PNP)] **4b** in C_6D_6 at 150 MHz.

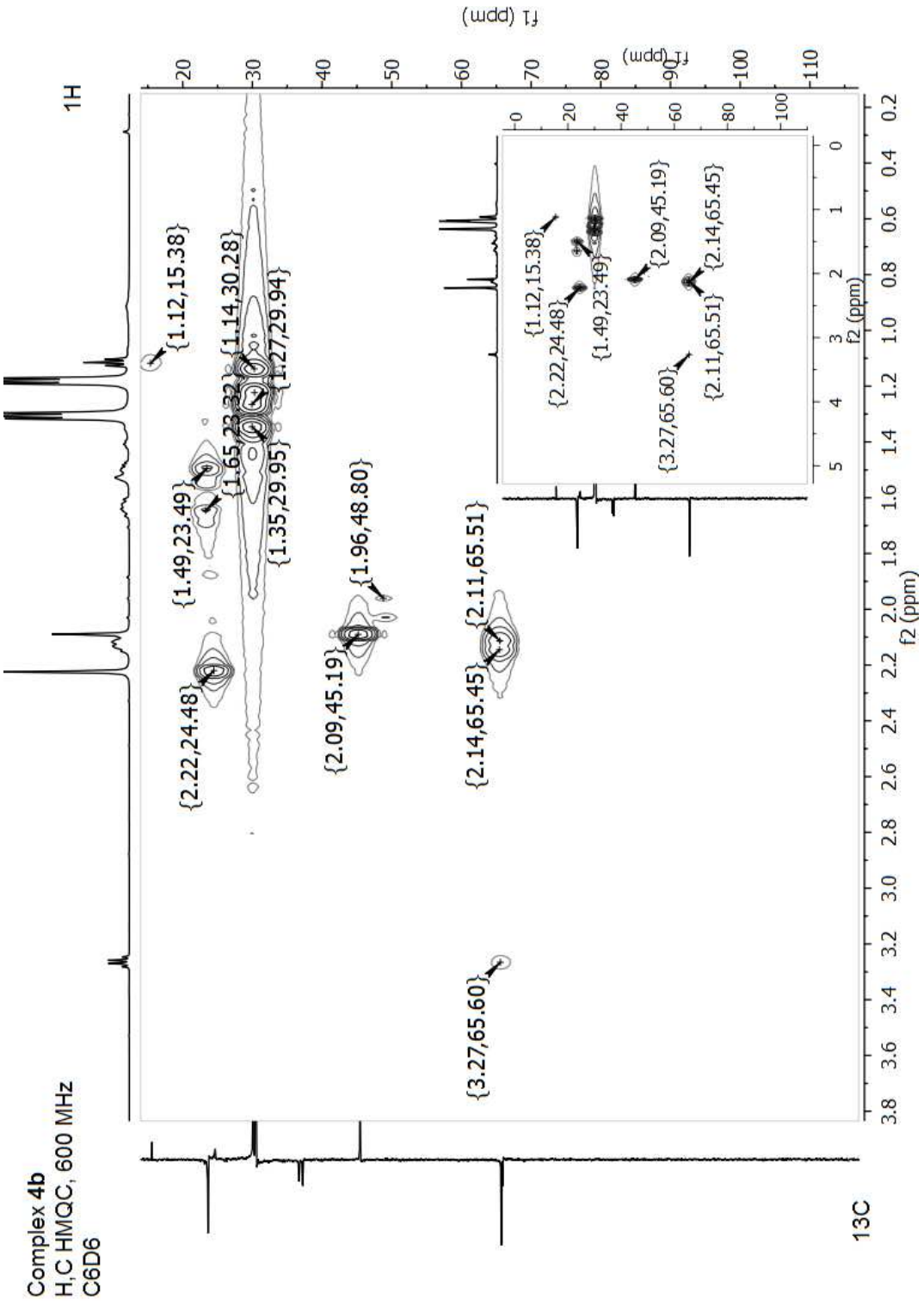

Fig. S 5.46. – H,C HMQC of [RuH(CO)(OOCCH$_3$)(Me-PNP)] **4b** in C_6D_6 at 600 MHz (1H)/ 150 MHz (13C).

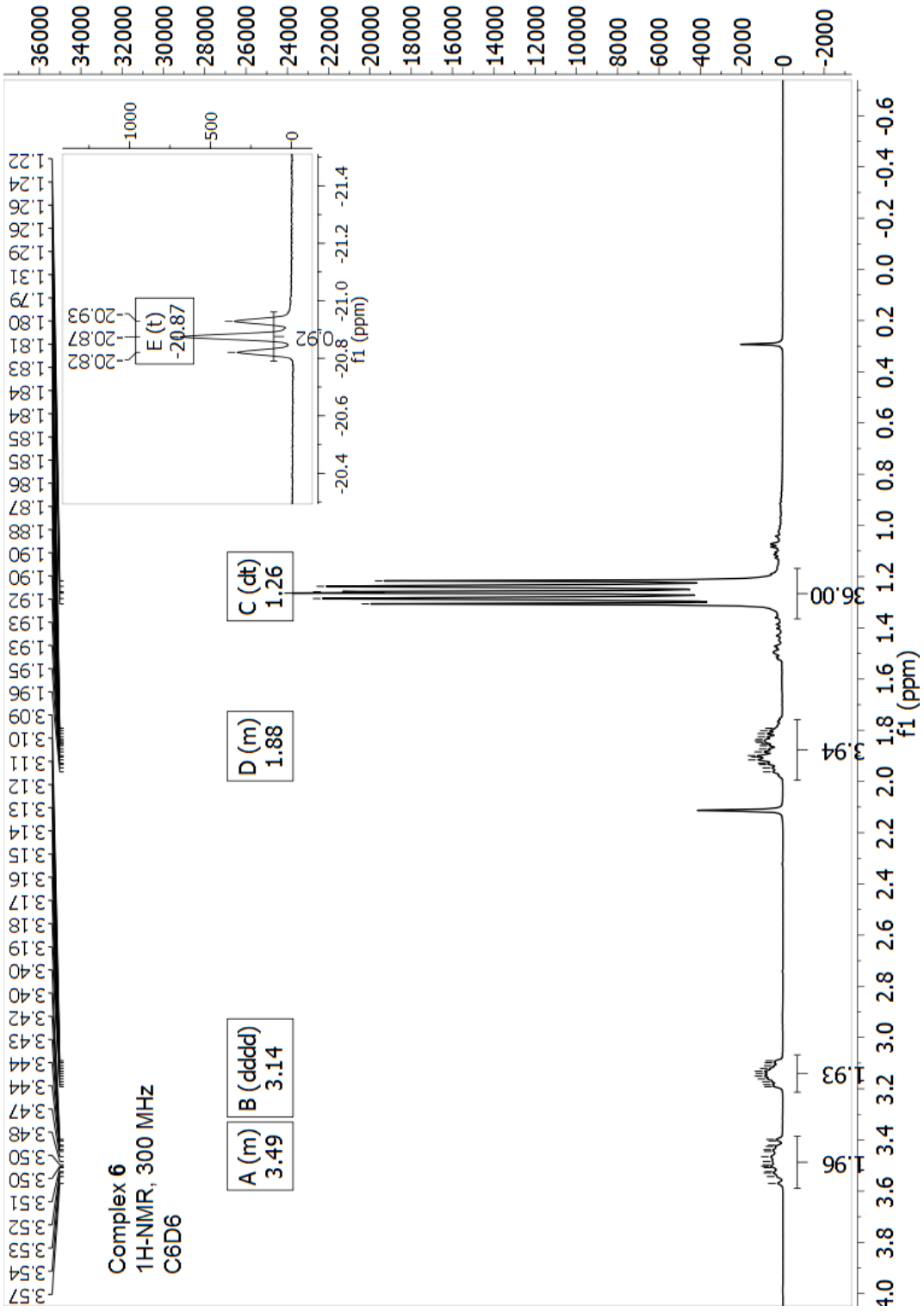

Fig. S 5.47. – ^{1}H NMR of [RuH(CO)(PNP)] **6** in C_6D_6 at 300 MHz.

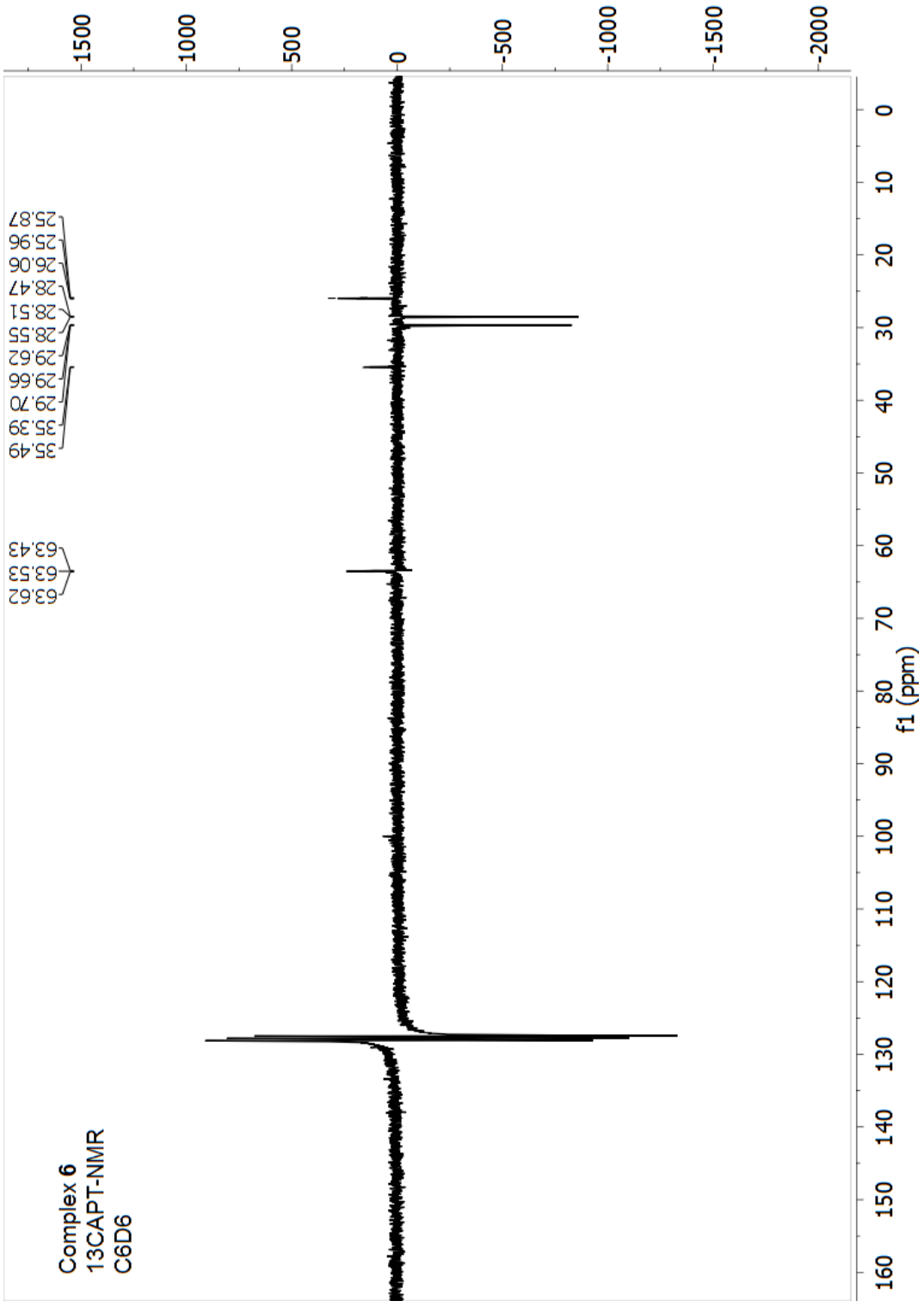

Fig. S 5.48. – $^{13}C_{APT}$ NMR of [RuH(CO)(PNP)] **6** in C_6D_6 at 75 MHz.

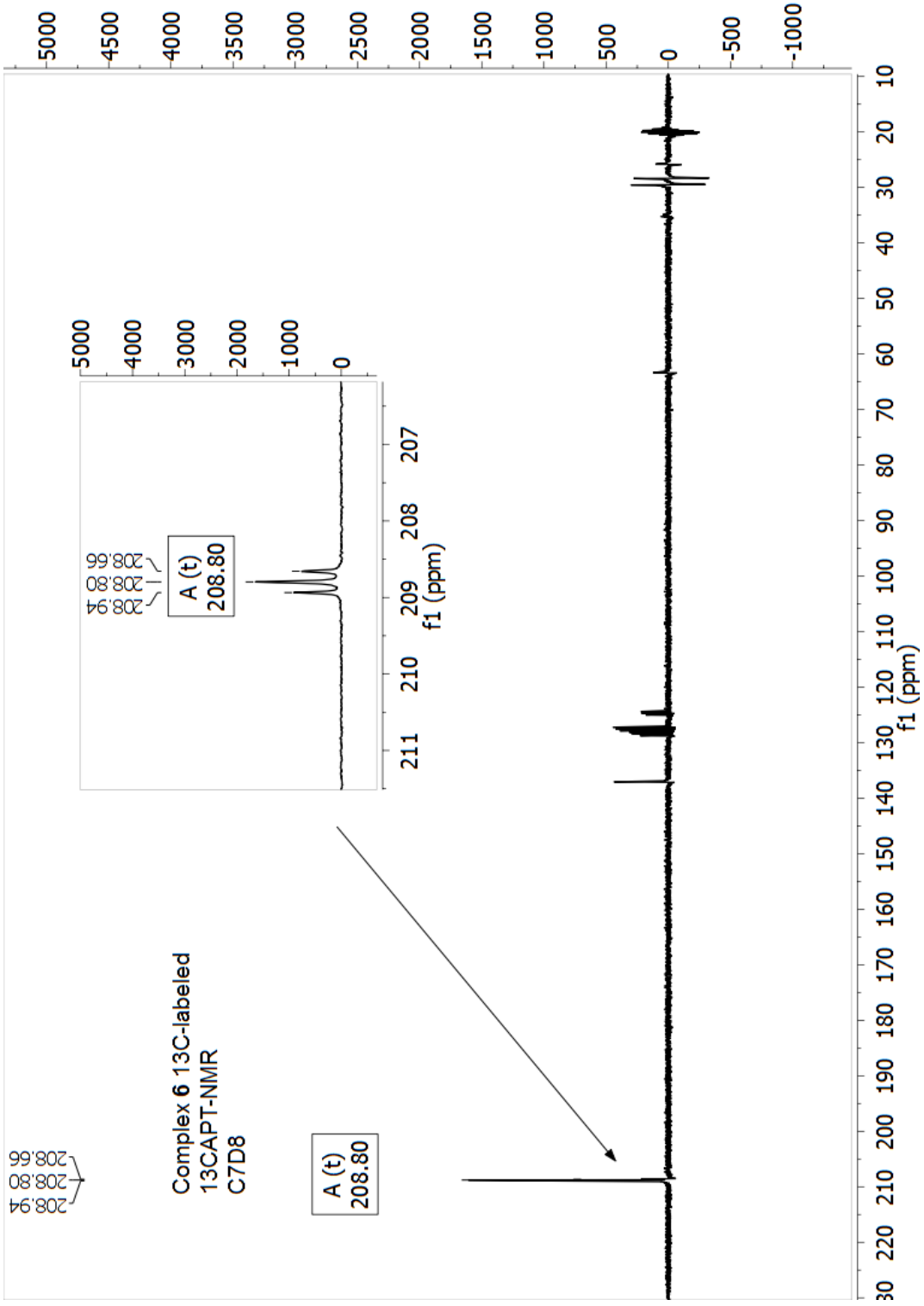

Fig. S 5.49. – $^{13}C_{APT}$ NMR of [RuH(^{13}CO)(PNP)] **6** in C_8D_8 at 75 MHz.

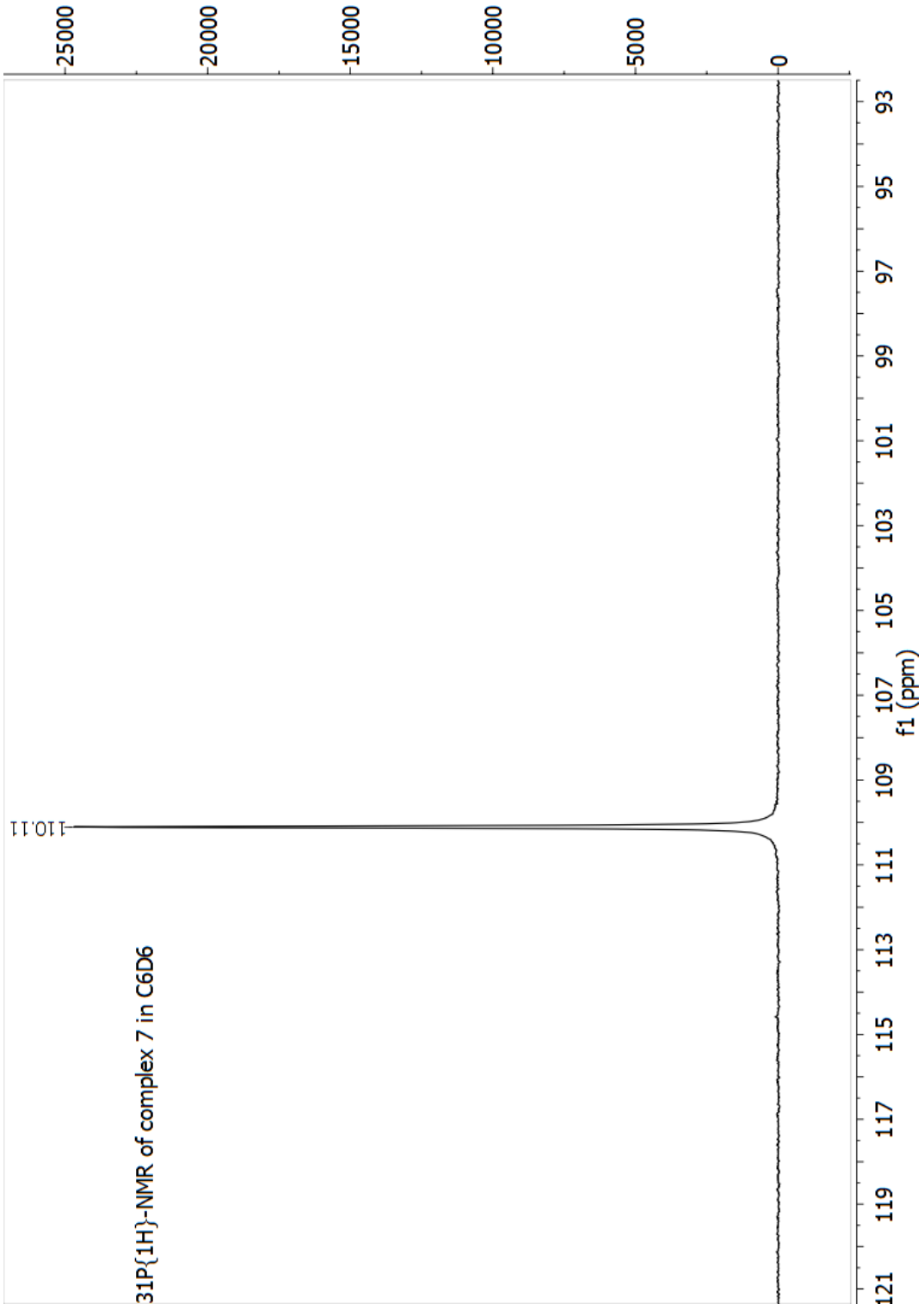

Fig. S 5.50. – $^{31}P^{1}H$ NMR of [RuH(CO)(PNP)] **6** in C_6D_6 at 121 MHz.

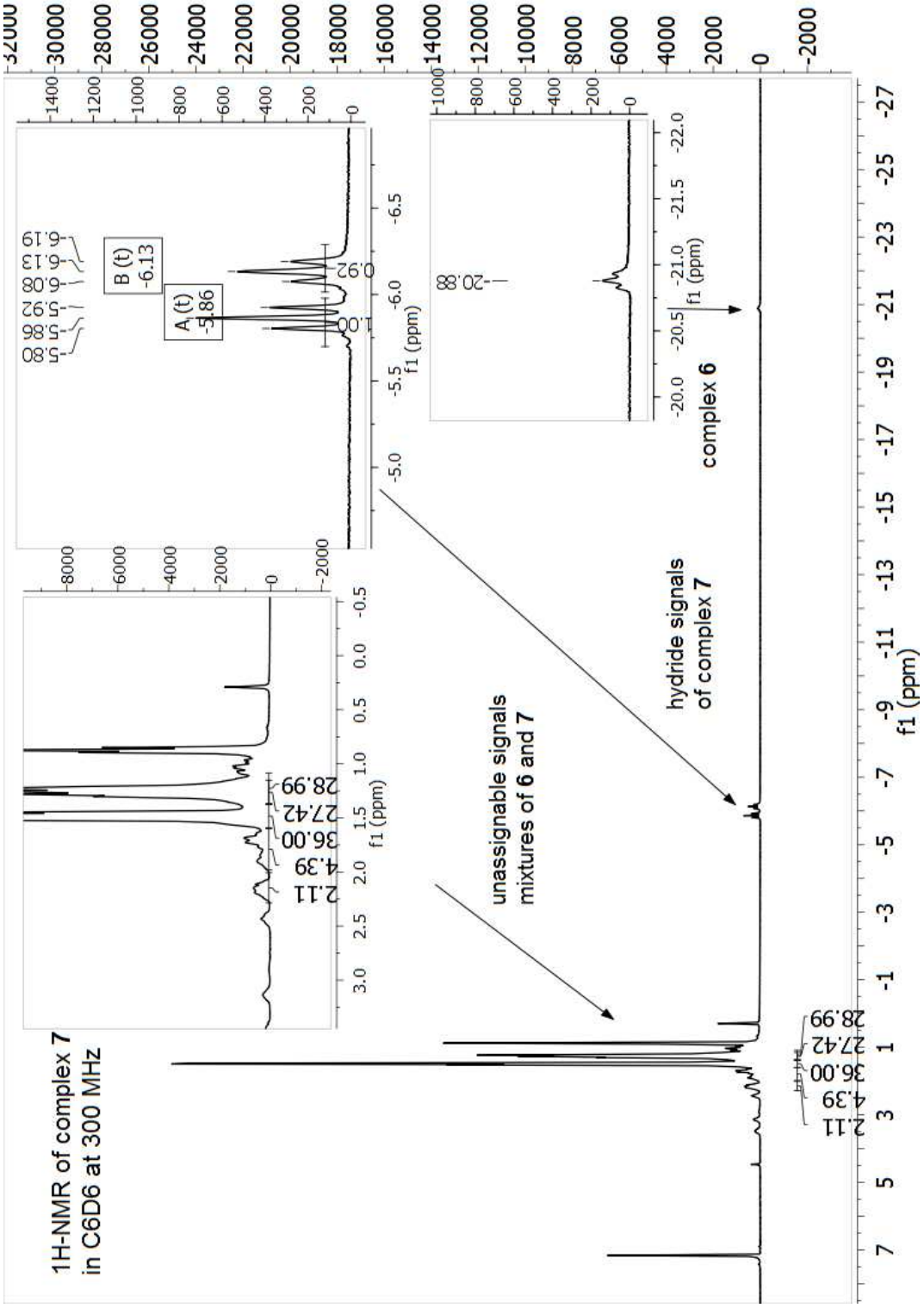

Fig. S 5.51. – ^{1}H NMR of complex **7** in C_6D_6 at 300 MHz. Hydrogenation of complex **6** to complex **7** with 1.5 bar H_2.

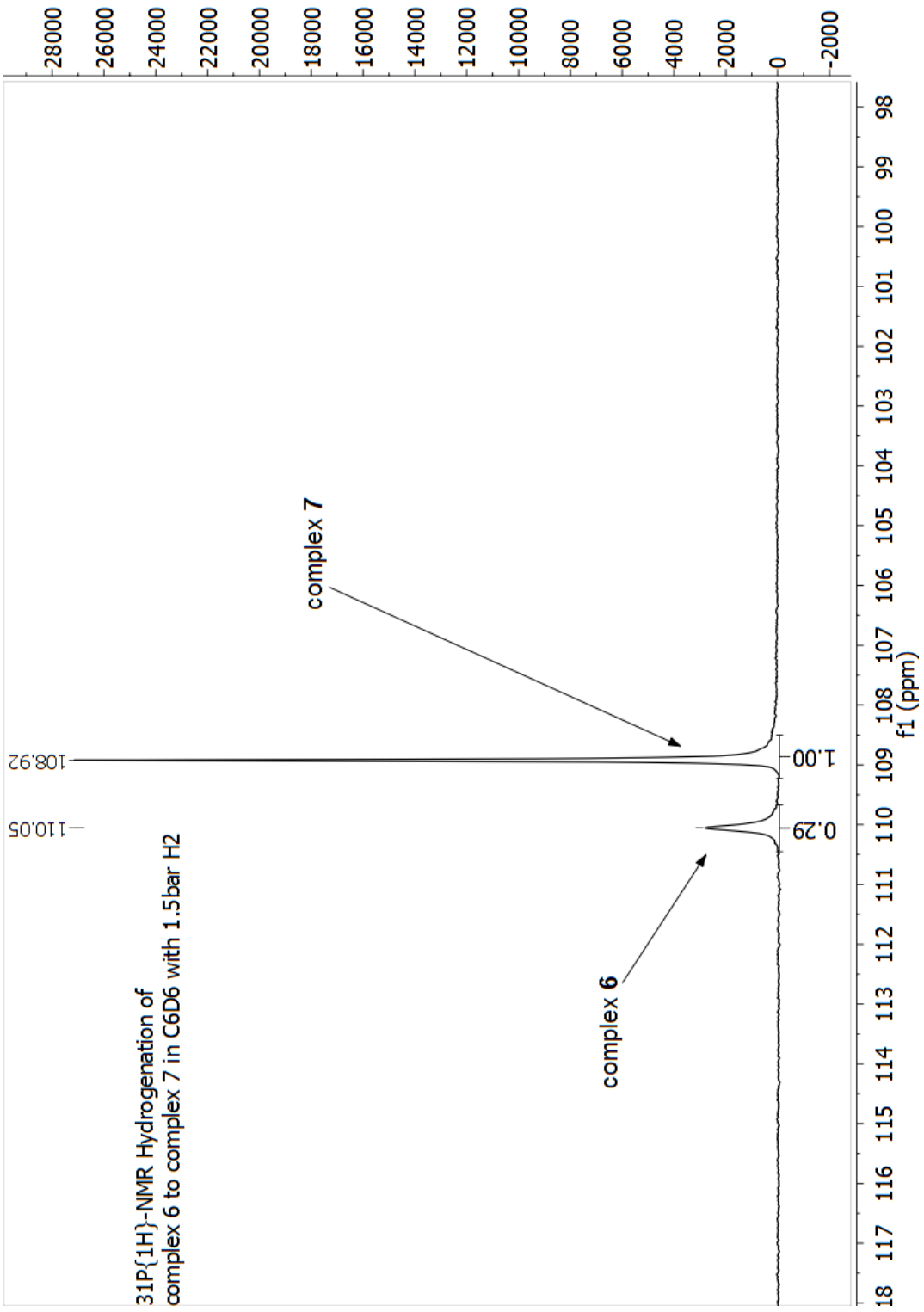

Fig. S 5.52. – $^{31}P\{^{1}H\}$ NMR of complex **7** in C_6D_6 at 121 MHz. Hydrogenation of complex **6** to complex **7** with 1.5 bar H_2, 79% conversion.

Single Crystal Structure of Complex 4b

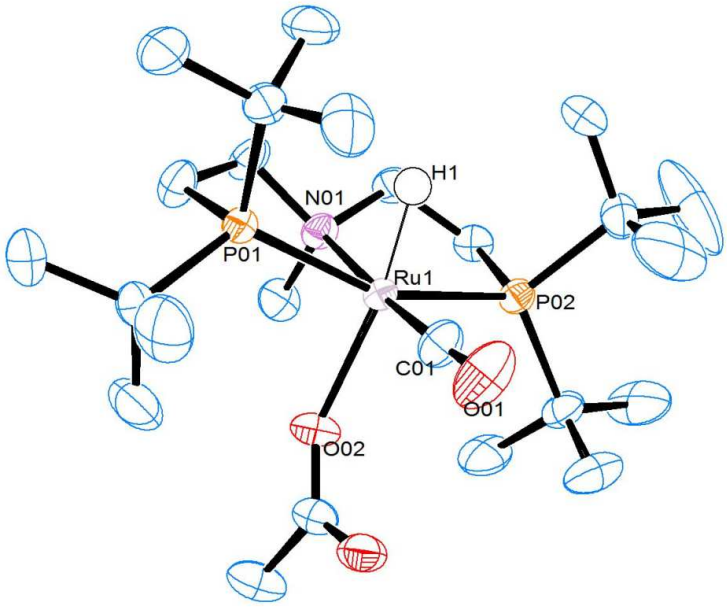

Fig. S 5.53. – ORTEP diagram of the single crystal structure of complex **4b**. Ellipsoids are illustrated at 50% possibility. All hydrogen atoms not depicted here except for H1 for clarity.

Table 5.3. – Crystal data and structure refinement for shelx.

Identification code	shelx
Empirical formula	C26 H55 N O5 P2 Ru
Formula weight	624.72
Temperature	293(2) K
Wavelength	0.71073 Å
Crystal system	Monoclinic
Space group	P 21/n
Unit cell dimensions	a = 11.6024(4) Å, α = 90°
	b = 20.5977(6) Å, β = 113.029(2)°
	c = 14.1642(4) Å, γ = 90°
Volume	3115.24(17) $Å^3$
Z	4
Density (calculated)	1.332 Mg/m^3
Absorption coefficient	0.639 mm^{-1}
F(000)	1328
Crystal size	? x ? x ? mm3
Theta range for data collection	1.849 to 26.789°.
Index ranges	-14<=h<=14, -25<=k<=26, -17<=l<=17
Reflections collected	31157
Independent reflections	6585 [R(int) = 0.0394]
Completeness to theta = 25.242°	100.0%
Refinement method	Full-matrix least-squares on F^2
Data / restraints / parameters	6585 / 0 / 316
Goodness-of-fit on F^2	1.027
Final R indices [I>2sigma(I)]	R1 = 0.0308, wR2 = 0.0780
R indices (all data)	R1 = 0.0376, wR2 = 0.0823
Extinction coefficient	n/a
Largest diff. peak and hole	0.701 and -0.620 $e.Å^{-3}$

Table 5.4. – Atomic coordinates (x 104) and equivalent isotropic displacement parameters (Å^2 x 103) for shelx. U(eq) is defined as one third of the trace of the orthogonalized U^{ij} tensor.

x	y	z	U(eq)	
Ru(1)	2715(1)	1478(1)	7506(1)	23(1)
P(02)	1067(1)	1667(1)	8038(1)	26(1)
P(01)	4037(1)	874(1)	6936(1)	26(1)
O(03)	3880(2)	3090(1)	7651(1)	41(1)
O(02)	2581(2)	2371(1)	6594(1)	36(1)
O(01)	4724(2)	1916(1)	9466(2)	58(1)
N(01)	1177(2)	1077(1)	6100(1)	28(1)
C(02)	3108(2)	2915(1)	6786(2)	34(1)
C(17)	595(2)	2531(1)	8155(2)	37(1)
C(07)	5311(2)	1257(1)	6601(2)	37(1)
C(21)	1115(2)	1175(1)	9194(2)	37(1)
C(04)	665(2)	1567(1)	5269(2)	39(1)
C(05)	1617(2)	502(1)	5687(2)	39(1)
C(01)	3947(2)	1755(1)	8691(2)	37(1)
C(11)	4689(3)	112(1)	7703(2)	40(1)
C(15)	133(2)	837(1)	6378(2)	32(1)
C(16)	-296(2)	1332(1)	6960(2)	32(1)
C(13)	5374(3)	290(2)	8833(2)	57(1)
C(19)	273(3)	2851(2)	7110(2)	54(1)
C(06)	2916(2)	593(1)	5682(2)	40(1)

x	y	z	U(eq)	
C(22)	1313(4)	466(2)	9042(3)	66(1)
C(12)	5554(3)	-282(2)	7327(3)	51(1)
C(08)	4850(4)	1922(2)	6171(3)	66(1)
C(03)	2777(3)	3382(2)	5893(2)	50(1)
C(09)	5676(3)	883(2)	5830(3)	56(1)
C(14)	3605(3)	-345(1)	7622(3)	59(1)
C(10)	6494(3)	1354(2)	7585(3)	63(1)
C(20)	1724(3)	2883(2)	8931(3)	57(1)
C(18)	-538(4)	2622(2)	8429(4)	79(1)
C(24)	-66(5)	1211(3)	9394(4)	133(3)
C(23)	2220(5)	1391(2)	10138(3)	98(2)
O(201)	-192(2)	796(1)	2858(2)	39(1)
O(200)	1496(2)	253(1)	3002(2)	56(1)
C(101)	948(2)	764(1)	2880(2)	37(1)
C(100)	1527(3)	1392(2)	2756(3)	53(1)

5.3. Supporting Information - Tuneable Hydrogenation of Nitriles into Imines or Amines with a Ruthenium Pincer Complex Under Mild Conditions

Jong-Hoo Choi,[a] and Martin H. G. Prechtl[a*]

[a] Department of Chemistry, University of Cologne, Greinstr.6,50939 Cologne, Germany. Fax: +49 221 470 1788; Tel: +49 221 470 1981; E-mail: martin.prechtl@uni-koeln.de Web: www.catalysislab.de

General Remarks

Sovents and substrates were purchased from *Acros*, *Alfa Asaer*, *Sigma Aldrich*, *Strem Chemicals* or were charged from the institute stock and were used as received if denoted as dry and oxygen-free. If necessary, solvents and substrates were degassed at least three times via "pump-freeze-thaw" method. Used complexes **1**, **2**, **3** and **4** were synthesised following our protocol.[1,2] All reactions were prepared in argon atmosphere, using a *MBraun Labmaster 200* glovebox and a 25 mL *Büchi tinylclave* glas autoclave. For higher pressures (10 bar, Figure 4, entry 1), the reaction content was charged in a 25 mL glas vial, which was placed in a *Büchi* steel autoclave.

Analytical Methods

^{1}H, ^{13}C, ^{31}P NMR spectra were recorded at 300 MHz (^{1}H), 75 MHz (^{13}C) and 121 MHz (^{31}P) on a *Bruker Avance II 300* and on a *Bruker Avance II+ 600* spectrometer at 600 MHz (^{1}H), 150 MHz (^{13}C) and 242 MHz (^{31}P) at room temperature. ^{1}H shifts were reported in ppm (δH) downfield from TMS and were determined by reference to the residual solvent peaks (C_6D_6: 7.16 ppm, C_7D_8: 7.09 ppm, C_4D_8O: 1.73 ppm). Chemical shifts were reported as singlet (s), doublet (d), triplet (t), quartet (q) and multiplet (m). Coupling constants J were reported in Hz. Infrared spectra (IR) were measured at room temperature with a *Bruker Alpha* spectrometer equipped with a Diamond-ATR IR unit. Data are reported as follows: absorption $\tilde{\nu}$[cm^{-1}], weak (w), medium (m), strong (s). LIFDI-MS[3] (Liquid Injection Field Desorption/Ionisation-Mass Spectrometry) was performed using a *Waters micromass Q-ToF-2^{TM}* mass spectrometer equipped with a *LIFDI 700* ion source (*Linden CMS*).

Preparation of Complexes

Preparation of Complex 1a/b

In an argon flushed *Büchi* glass autoclave, 320 mg (1.0 mmol, 1.0 eq.) [Ru(COD)(2-methylallyl)$_2$] were added to 400 mg (1.1 mmol, 1.1 eq.) of PNP ligand in 5 ml pentane. After the autoclave was filled with H_2 gas to 5 bar at room temperature, the content was stirred for 48 h at 55 °C. With the increase in temperature to 55 °C, a H_2 pressure of 7 bar was reached. After the reaction mixture was cooled to room temperature, the autoclave was depressurised and flushed twice with argon. After separating the orange mother liquor with a cannula from the yellow solid (mixture **1a** and **1b**), the product mixture was washed twice with pentane. The pentane was removed via cannula and the product mixture was dried under argon and stored at -34 °C. Yield: 397.0 mg (product mixture), 0.85 mmol, 85%.[1]
Spectral data of complex **1a**:
^{1}H NMR (500 MHz, toluene-d$_8$): δH [ppm] = 3.46 – 3.44 (m, 4H, NCH$_2$), 1.91 – 1.85 (m, 4H, PCH$_2$), 1.30 (t, 36H, $^3J_{PH}$ = 12.1 Hz, PC(CH$_3$)$_3$), -12.44 (t, $^2J_{PH}$ = 10.6 Hz). ^{13}C NMR (75 MHz, benzene-d$_6$): δC [ppm] = 65.6 (-*C*H$_2$-), 34.7 (P*C*(CH$_3$)$_3$), 29.6 (PC(*CH$_3$*)$_3$), 26.1 (-*C*H$_2$-). ^{31}P NMR (121 MHz, toluene-d$_8$): δP [ppm] = 114.3 (s). T_1 (500 MHz, toluene-d$_8$) = 298 K (138 ms), 258 K (97 ms), 238 K (69 ms), 228 K (59 ms), 221 K (52 ms), 208 K (48 ms), 198 K (50 ms), 193 K (53 ms); ($T_{1\mathrm{min}}$ = 48 ms, 207 K). IR (**1a** and **1b**): $\tilde{\nu}$[cm^{-1}] = 3291 (w), 2852 – 2947 (m), 2034 - 1995 (m), 1726 (m), 1470 (m), 1383 (m), 1359 (m), 1202 (w), 1174 (m), 1053 (w), 1016 (m), 923 (m), 798 (s), 764 (w), 672 (m), 644 (w), 600 (m), 565 (m), 471 (s), 432 (m).
Spectral data of complex **1b**:
^{1}H NMR (500 MHz, toluene-d$_8$): δH [ppm] = 4.55 (weak s, 1H, (H/D-exchange)), 2.91 – 2.86 (m, 2H, NCH$_2$), 2.54 – 2.44 (m, 2H, NCH$_2$), 2.14 – 2.12 (m, 2H, PCH$_2$), 1.67 – 1.63 (m, 2H, PCH$_2$), 1,41 (t, 18H, $^3J_{PH}$ = 6.1 Hz, PC(CH$_3$)$_3$), 1.36 (t, 18H, $^3J_{\mathrm{PH}}$ = 6.0 Hz, PC(CH$_3$)$_3$), -8.26 (t, 4H, $^2J_{PH}$ = 14.7 Hz, Ru-H). ^{13}C NMR (75 MHz, benzene-d$_6$): δC [ppm] = 55.7 (-*C*H$_2$-), 34.7 – 32.1 (P*C*(CH$_3$)$_3$), 30.8 – 30.5 (PC(*CH$_3$*)$_3$), 27.4 (-*C*H$_2$-). ^{31}P NMR (121 MHz, toluene-d$_8$): δp [ppm] = 111.9 (s). T_1 (500 MHz, toluene-d$_8$) = 298 K (312 ms), 258 K (184 ms), 238 K (148 ms), 228 K (135 ms), 221 K (132 ms), 208 K (141 ms), 198 K (169 ms), 193 K (191 ms); ($T_{1\mathrm{min}}$ = 132 ms, 223 K).

Preparation of Complex 2

In an argon flushed *Büchi* glass autoclave 100 mg (0.215 mmol) of [Ru(H$_2$)H(PNP)] **1a** were dissolved in 6 mL toluene. After the addition of 3.5 eq. (0.753 mmol) of a primary alcohol (e.g. ethyl, pentyl, hexyl alcohol), the content was heated at 80 °C for 48 h. After the appropriate time, the solvent was removed in vacuo and the residue was washed twice with pentane. The

orange powder was stored at -34 °C. Yield: 90%.[2]

LIFDI-MS/MS: m/z 495.1 (1.0), 494.3 (15.9), 493.3 (46.1), 492.3 (14.6), 491.3 (100), 490.2 (34.7), 489.2 (39.6), 488.3 (28.9), 487.3 (4.6), 486.2 (2.4), 485.3 (15.5).

^{1}H NMR (300 MHz, benzene-d_6): δH [ppm] = 3.49 (m, 2H, CH_2), 3.14 (m, 2H, CH_2), 1.88 (m, 4H, PCH_2), 1.26 (dt, 36H, $^{2}J_{PH}$ = 14.3 Hz, $PC(CH_3)_3$), -20.87 (t, 1H, $^{2}J_{PH}$ = 16.3 Hz, Ru-H). $^{13}C_{APT}$ NMR (75 MHz, benzene-d_6): δC [ppm] = 208.8 ppm (t, *C*O, $^{2}J_{CP}$ = 10.5 Hz, data extracted from ^{13}CO labled probe in toluene-d_8), 63.5 (t, $^{2}J_{CP}$ = 7.1 Hz, -N*C*H$_2$-), 35.4 (t, $^{1}J_{CP}$ = 7.7 Hz, P*C*$(CH_3)_3$), 33.9 (t, $^{1}J_{CP}$ = 7.4 Hz, P*C*$(CH_3)_3$), 29.7 (t, $^{2}J_{CP}$ = 3.0 Hz, PC(*CH*$_3)_3$), 28.5 (t, $^{2}J_{CP}$ = 3.2 Hz, PC(*CH*$_3)_3$), 26.0 (t, $^{1}J_{CP}$ = 6.9 Hz, -P*C*H$_2$-). $^{31}P\{^{1}H\}$ NMR (121 MHz, benzene-d_6): δP [ppm] = 110.1 (s).

IR: $\tilde{\nu}$[cm^{-1}] = 2943 - 2800 (m), 2706 (w), 2628 (w), 2068 - 2048 (m), 1869 (s), 1469 (m), 1454 (m), 1385 (m), 1358 (m), 1318 (w), 1262 (m), 1206 (m), 1178 (m), 1157 (w), 1106 (w), 1063 (m), 1017 (m), 967 (m), 936 (w), 806 (s), 773 (w), 729 (s), 695 (m), 674 (w), 611 (m), 579 (m), 536 (m), 471 (s).

Catalysis

General Preparation of the Hydrogenation of Nitriles, exemplary with Complex 2

Into a 25 mL *Büchi tinyclave* glass autoclave, 0.01 mmol of complex **2** was solvated in 3 mL toluene. After the addition of 2 mmol of the nitrile to the content, the autoclave was charged with 4 bar H_2 at room temperature and heated to 50 °C for 20 h.

General Preparation of the Hydrogenation of Nitriles in the Presence of Primary Amines, exemplary with Complex 2

Into a 25 mL *Büchi tinyclave* glass autoclave, 0.01 mmol of complex **2** was added and solvated with 3 mL toluene. After the addition of 2 mmol of the nitrile and 2 mmol of the primary amine to the content, the autoclave was charged with 4 bar H_2 at room temperature and heated to 50 °C for 20 h.

Investigation of Complex Intermediates

Isolation of 2a

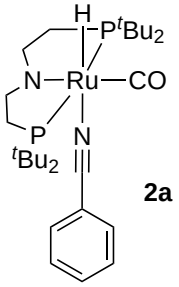

2a

In an argon flushed *schlenk* flask, 40 mg (0.08 mmol) of complex **2** was solvated in 4 mL toluene. After the addition of 30 eq. (2.4 mmol) of benzonitrile, the *schlenk* flask was sealed and the mixture was stirred at 50 °C under argon atmosphere for 24 h. The solvent was removed under reduced pressure and the residue was washed with pre-cooled pentane twice and was dried under reduced pressure. Yield: 20 mg, dark-red residue (0.03 mmol, 41%).

LIFDI-MS: m/z 494.3 (34.6), 493.2 (50.0), 492.2 (19.2), 491.2 (100), 490.3 (96.2), 489.2 (65.4), 488.3 (34.6), 487.2 (19.2), 486.2 (7.7), 485.2 (7.7).

^{1}H NMR (600 MHz, THF-d$_8$): δH [ppm] = 7.63 (d, 2H, Ar-H) 7.18 (m, 3H, Ar-H), 2.30 (m, 2H, -CH$_2$-), 2.23 (m, 2H, -CH$_2$-), 2.11 (m, 2H, -CH$_2$-), 1.38 (t, 18H, $^2J_{PH}$ = 6.2, PC(CH$_3$)$_3$), 1.32 (t, 18H, $^2J_{PH}$ = 6.3, PC(CH$_3$)$_3$), 1.12 (overlapped m, assigned via C-H$_{\mathrm{hmQc}}$, 2H, PCH$_2$-) -14.45 (t, 1H, ^{2}J$_{\mathrm{PH}}$ = 21.4, Ru-H). ^{13}C$_{\mathrm{deptQgpsp}}$ NMR (150 MHz, THF-d$_8$): δC [ppm] = 207.9 (*C*O), 177.2 (*C*N), 142.6 (*C*-CN), 128.3 (*Ph*), 123.0 (*Ph*), 127.0 (*Ph*), 53.8 (N-*C*H$_2$-), 38.5 (P*C*(CH$_3$)$_3$), 37.5 (P*C*(CH$_3$)$_3$), 32.9 (N*C*H$_2$-), 30.8 (PC(*CH$_3$*)$_3$), 30.7 (PC(*CH$_3$*)$_3$), 27.8 (P*C*H$_2$-), 23.6 (P*C*H$_2$-). ^{31}P{^{1}H} NMR (242 MHz, THF-d$_8$): δP [ppm] = 88.4 (s).

IR: $\tilde{\nu}$[cm^{-1}] = 3012 - 2721 (m), 2093 (w), 1898 (s), 1857 (w), 11685 (w), 1586 (m), 1555 (m), 1466 (m), 1426 (m), 1388 (w), 1365 (m), 1257 (w), 1218 (m), 1176 (m), 1127 (w), 1073 (m), 1022 (m), 983 (w), 932 (w), 917 (w), 844 (m), 804 (s), 777 (m), 734 (m), 699 (s), 681 (s), 621 (m), 582 (m), 572 (m), 536 (m), 478 (s), 436 (m).

Reaction of Complex 2 with Acetonitrile to Complex 5

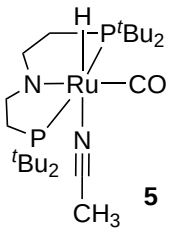

5

In an argon flushed *schlenk* flask, 20 mg (0.04 mmol) of complex **2** was solvated in 4 mL toluene. After the addition of 50 eq. (2 mmol) of acetonitrile, the schlenk flask was sealed and the mixture was stirred at 50 °C under argon atmosphere for 24 h. The solvent was removed under reduced pressure and the residue was solvated in 0.5 mL deuterated toluene for NMR measurement. A partial conversion to **5** (70%) was determined via ^{31}P NMR spectrum.

^{1}H NMR (300 MHz, toluene-d$_8$): δH [ppm] = -14.41 (t, 1H, $^{2}J_{PH}$ = 21.4, Ru-H, complex **5**), -20.91 (t, 1H, $^{2}J_{PH}$ = 16.4, Ru-H, complex **2**). ^{31}P{^{1}H} (121 MHz, toluene-d$_8$): δP [ppm] = 110.1 (s, complex **2**). 88.3 (s, complex **5**).

NMR-Spectra

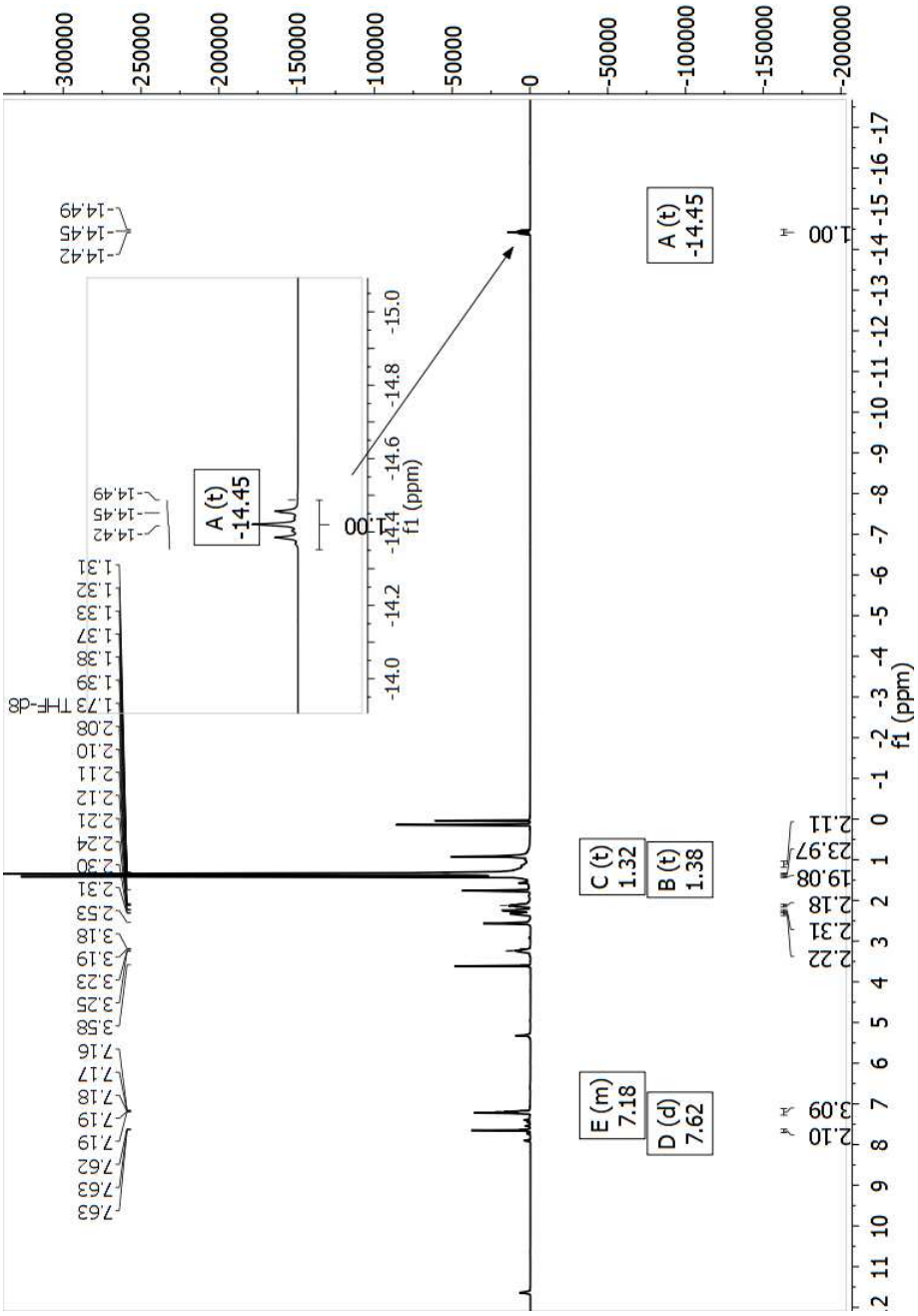

Fig. S 5.54. – ^{1}H NMR spectrum of complex **2a** in THF-d_8 at 600 MHz.

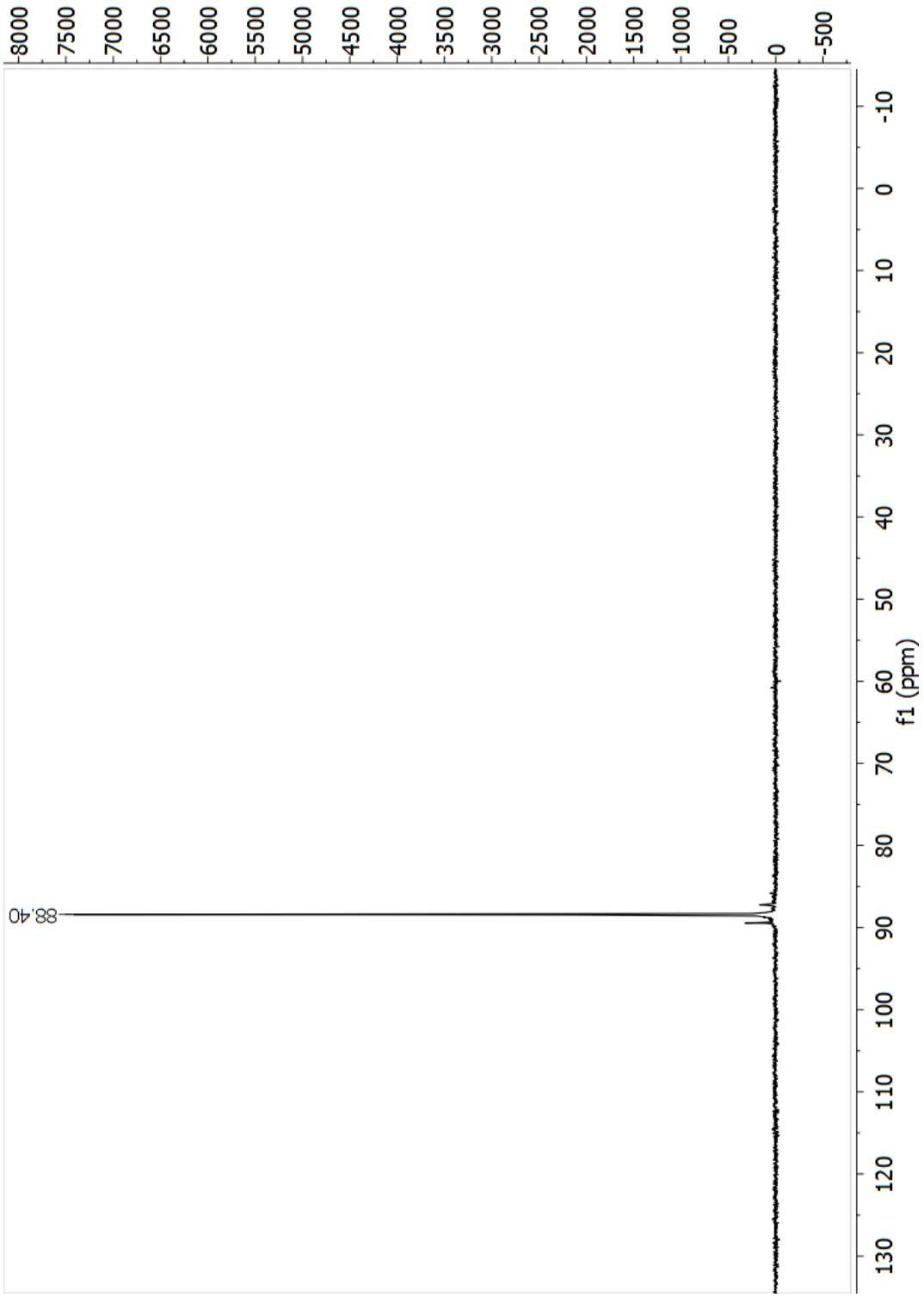

Fig. S 5.55. – $^{31}P\{^{1}H\}$ NMR spectrum of complex **2a** in THF-d_8 at 240 MHz.

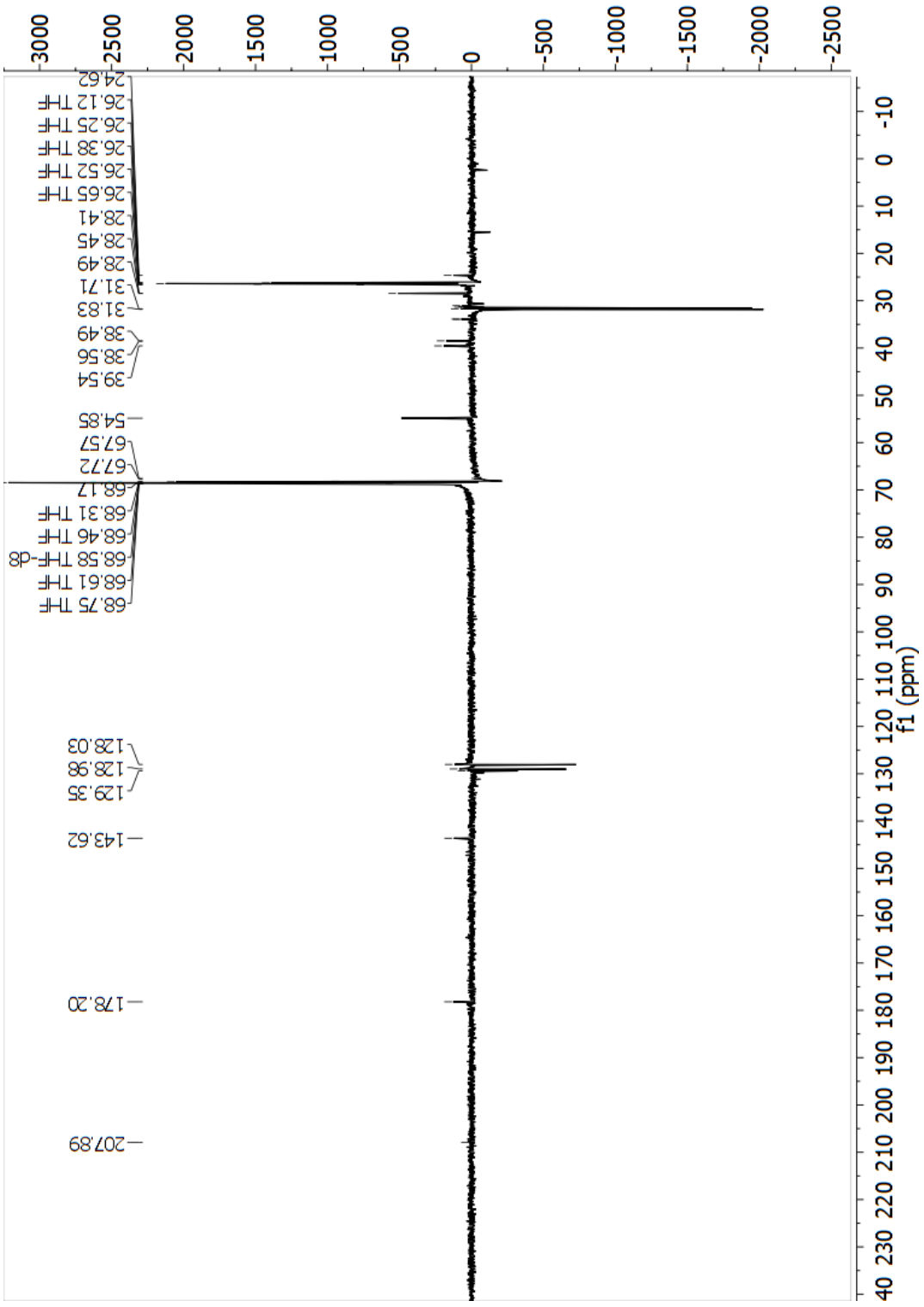

Fig. S 5.56. – $^{13}C_{deptQgpsp}$ NMR spectrum of complex **2a** in THF-d_8 at 150 MHz.

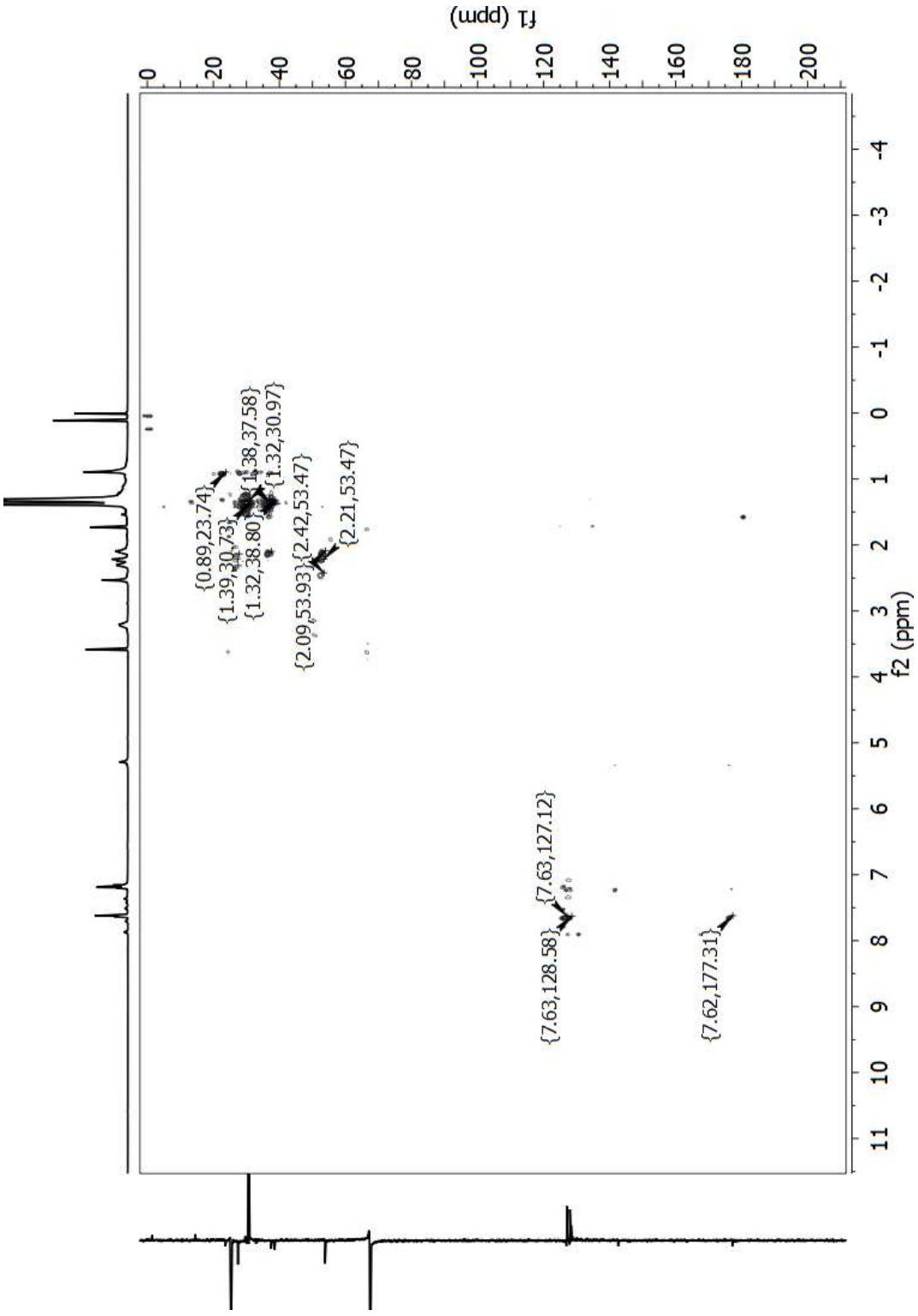

Fig. S 5.57. – CH_{HMQC} NMR spectrum of complex **2a** in THF-d_8 at 600 MHz/150 MHz.

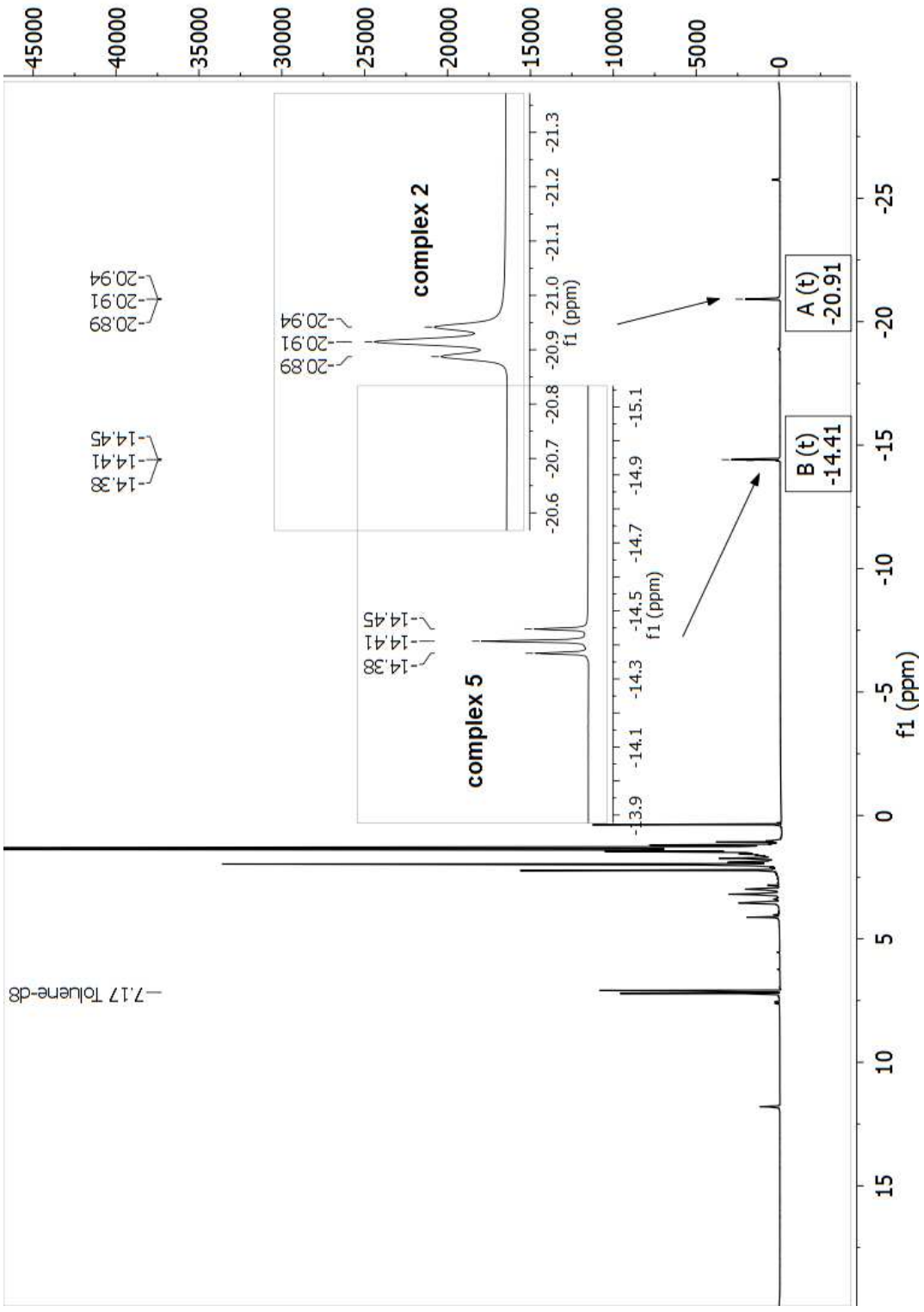

Fig. S 5.58. – ^{1}H NMR spectrum of complex **2** after the addition of acetonitrile in toluene-d_8 at 300 MHz.

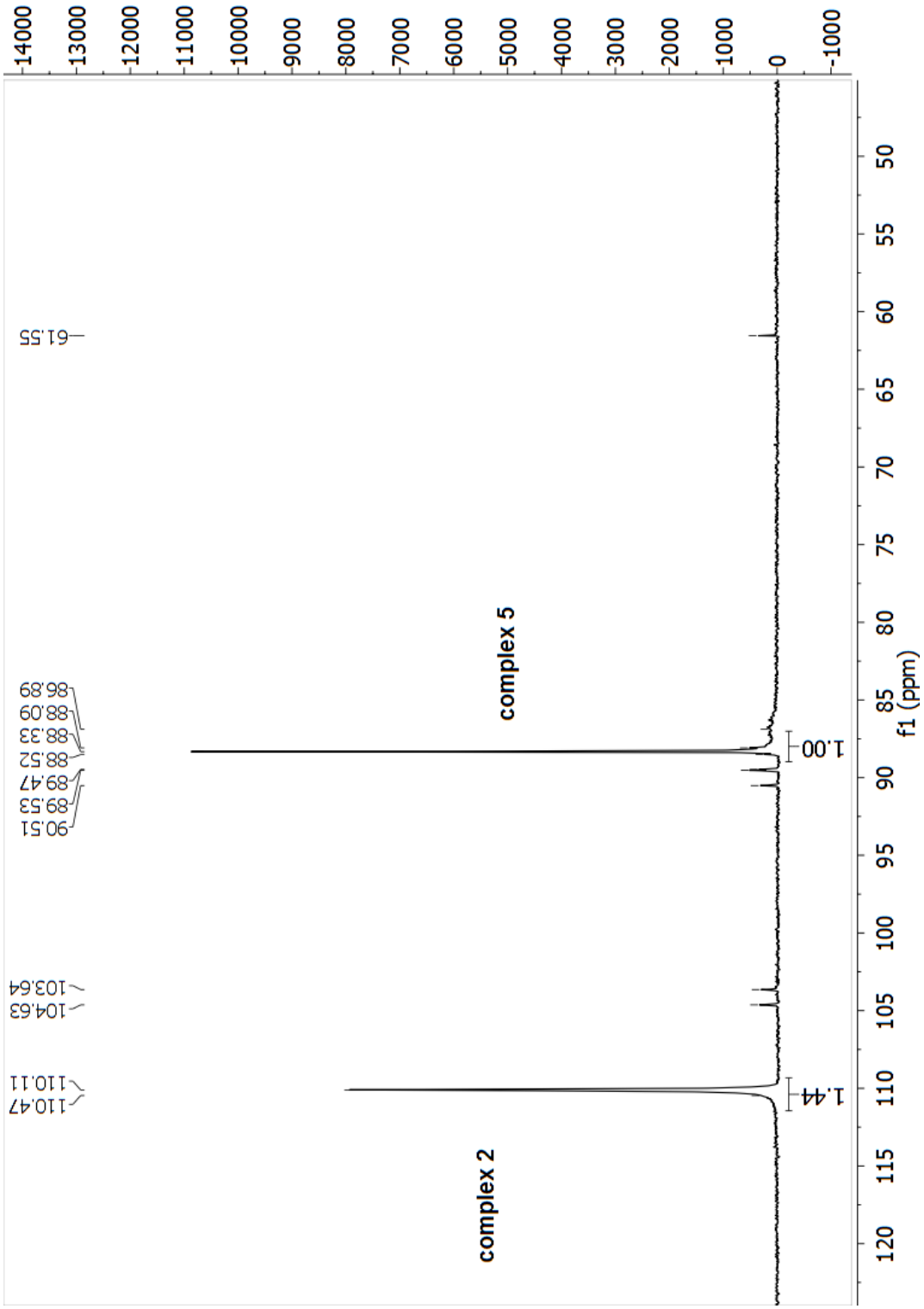

Fig. S 5.59. – $^{31}P\{^{1}H\}$ NMR spectrum of complex **2** after the addition of acetonitrile in toluene-d_8 at 121 MHz.

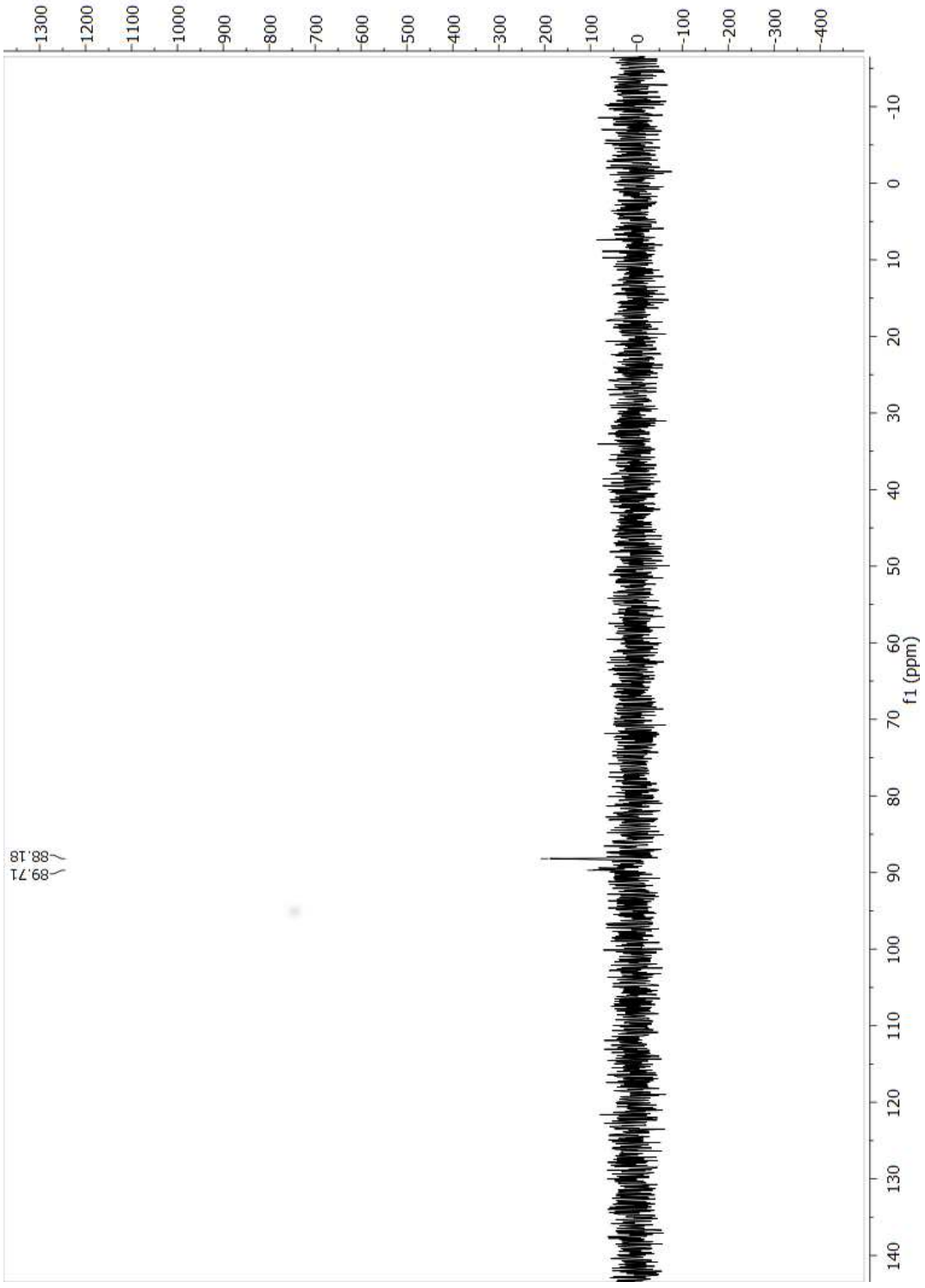

Fig. S 5.60. – $^{31}P\{^{1}H\}$ NMR spectrum of complex **2** in benzene-d_6 at 121 MHz after a 20 h catalytic hydrogenation of benzonitrile into N-benzylidene-benzylamine.

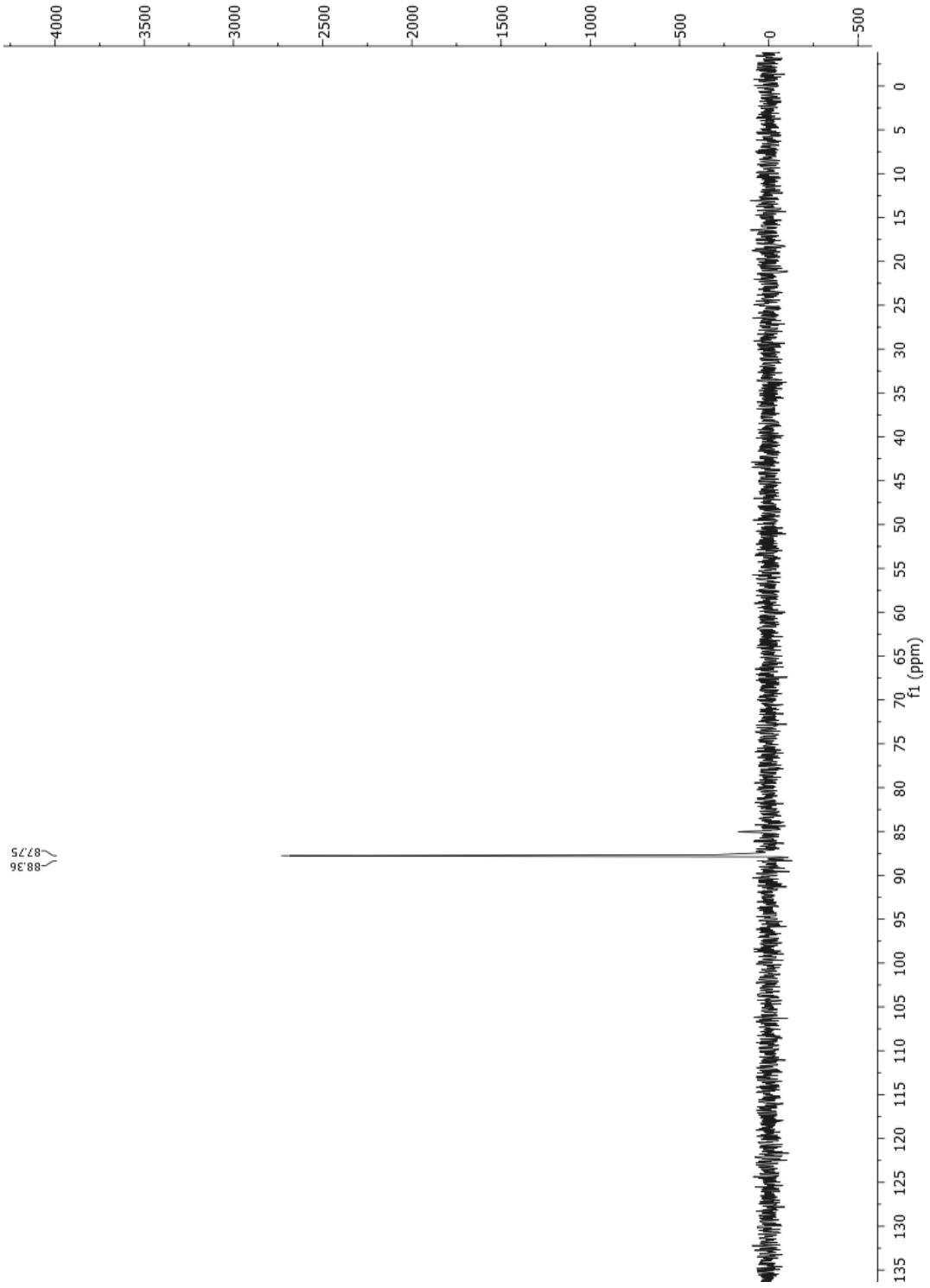

Fig. S 5.61. – $^{31}P\{^{1}H\}$ NMR spectrum of complex **2** in benzene-d_6 at 121 MHz after a 20 h catalytic hydrogenation of benzonitrile into benzylamine.

IR Spectra of Complexes 2 and 2a

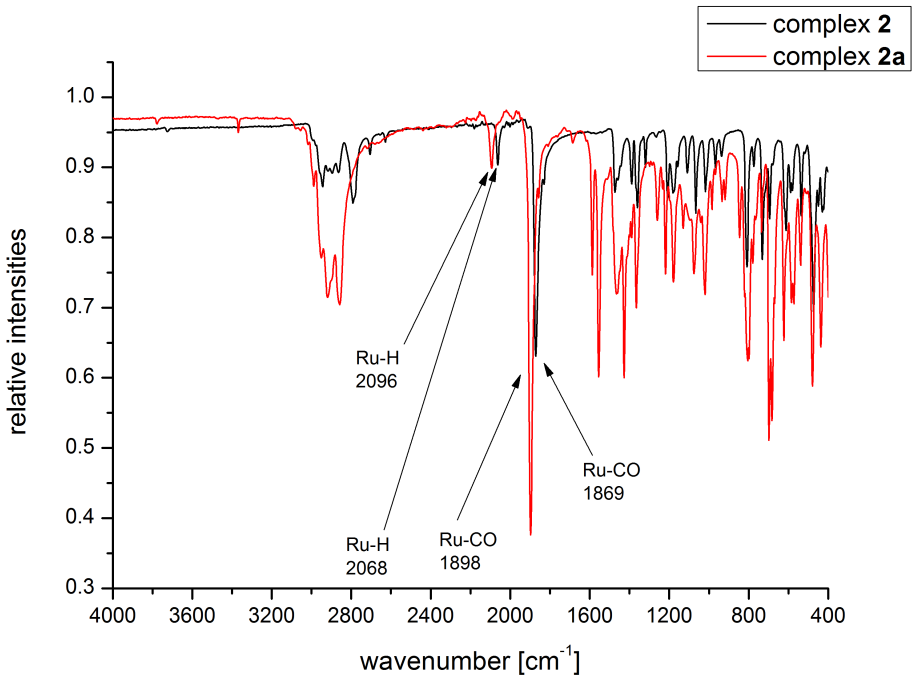

Fig. S 5.62. – IR spectra of **2** and **2a** (for more references see other report).[2]

LIFDI-MS of Complex 2a, Fragment 491

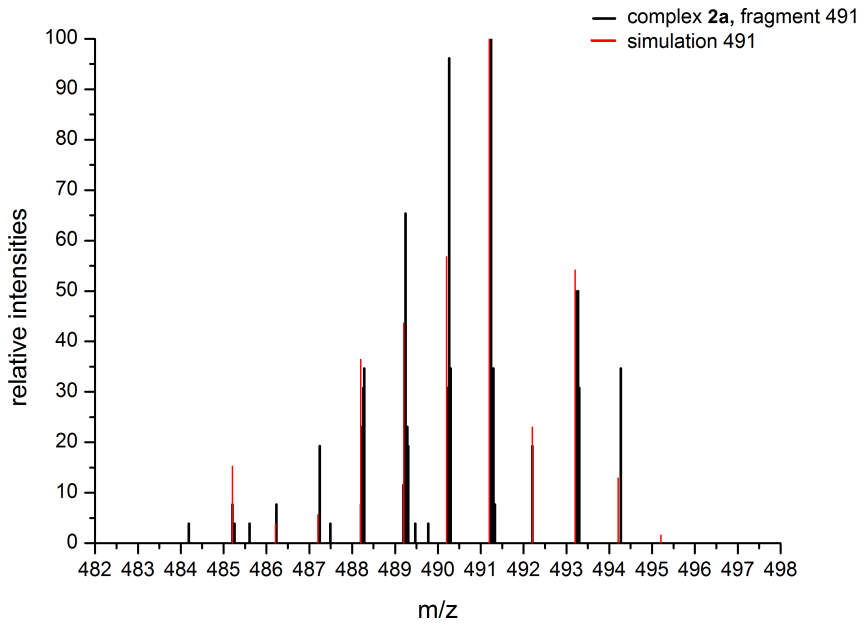

Fig. S 5.63. – LIFDI-MS of complex **2a**, fragment [RuH(CO)(PNP)] 491 (black) in toluene at retention time of 4.72 min vs simulated MS-pattern of fragment [RuH(CO)(PNP)] 491 (red).

Monitoring of the Conversion and Selectivity of the Hydrogenation of Benzonitrile into Benzylamine by Complex 2

Monitoring the Selectivity During Reaction

Into a 50 mL *Büchi miniclave* glas autoclave, 0.06 mmol of complex **2** was added and solvated with 9 mL 2-propanol. After the addition of 6 mmol of the benzonitrile content, the autoclave was charged with 4 bar H_2 at room temperature and heated to 90 °C for 24 h. The autoclave was constantly connected to a hydrogen reservoir. After each defined time t [h], a sample for GC(FID) was taken out via Hamilton syringe under pressure (PRECAUTION, syringe stamp needs to be hold tight and the cannula should have a small perimeter).

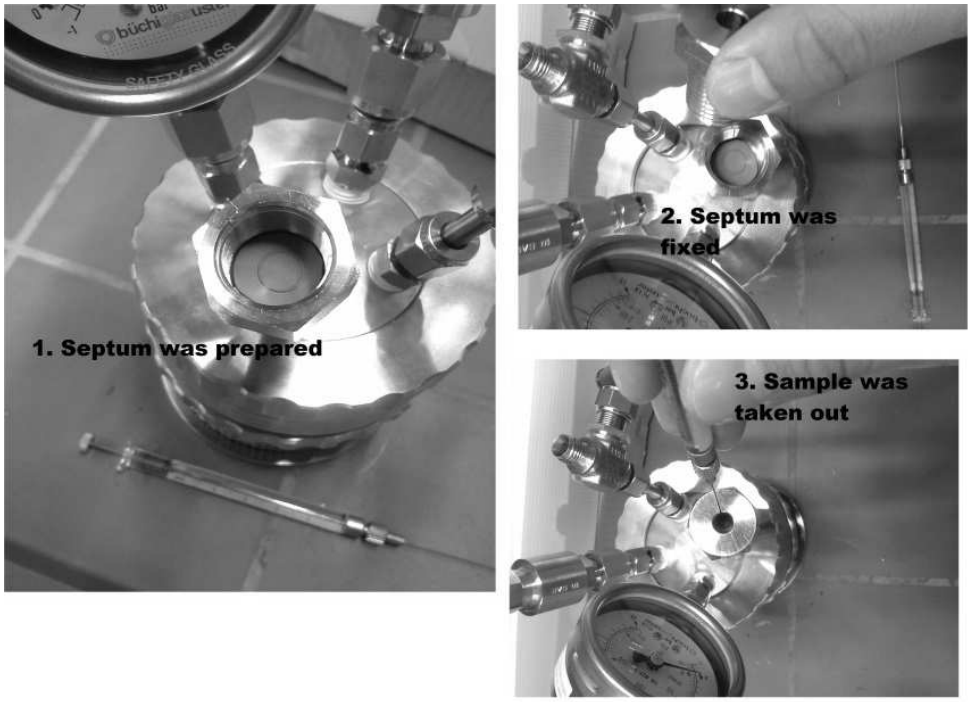

Fig. S 5.64. – a blank 50 mL *Büchi miniclave* glas autoclave. 1. The Septa was cutted and fitted into the opening. 2. Fixation of the septum. 3. Sample was taken out via *Hamilton* syringe.

Monitoring the Conversion via Hydrogen Consumption

Into a 25 mL *Büchi tinyclave* glas autoclave, 0.02 mmol of complex **2** was solvated in 3 mL 2-propanol. After the addition of 2 mmol of the benzonitrile to the content, the autoclave was charged with 4 bar H_2 at room temperature and heated to 90 °C for 18 h. The autoclave was constantly connected to a hydrogen reservoir whereby the hydrogen consumption was monitored using a pressure-interface. Due to full conversion at the end of the reaction, the hydrogen consumption was normalised as conversion as a function over time.

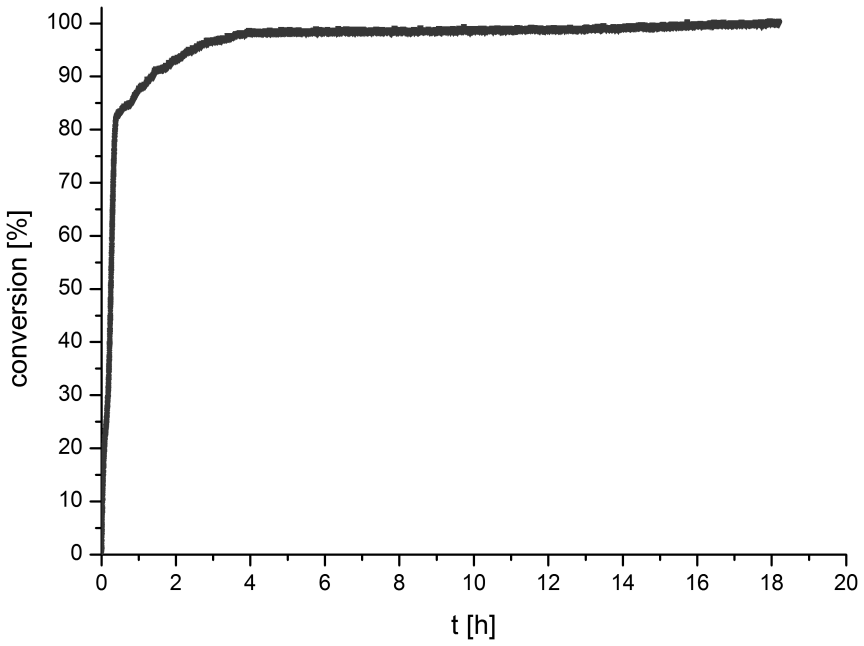

Fig. S 5.65. – Hydrogenation of benzonitrile into benzylamine in 2-propanol at 90 °C by 1mol% complex **2**. Normalised conversion as a function of time.

References

[1] J.-H. Choi, N. E. Schloerer, J. Berger, M. H. G. Prechtl, *Dalton Trans.* **2014**, *43*, 290–299.

[2] J.-H. Choi, L. E. Heim, M. Ahrens, M. H. G. Prechtl, *Dalton Trans.* **2014**, *43*, 17248–17254.

[3] J. H. Gross, *J. Am. Soc. Mass Spectrom.* **2007**, *18*, 2254 –2262.

5.4. Supporting Information - Amide vs. Amine Paradigm in the Direct Amination of Alcohols with Ru-PNP Complexes

Dennis Pingen[b], Jong-Hoo Choi[c], Martin H. G. Prechtl[c] and Dieter Vogt[a]*,
[a] Dr. D. Vogt, School of Chemistry, King's Building, Joseph Black Building, The University of Edinburgh, EH9 3JJ, Scotland, UK, E-mail: d.vogt@ed.ac.uk; [b] Dr. D. L. L. Pingen, Chemical Materials Science, Department of Chemistry, University of Konstanz, Universitätsstrasse 10, Konstanz, Germany. E-mail: dennis.pingen@uni-konstanz.de [c] Department of Chemistry, University of Cologne, Greinstr. 6, 50939 Cologne, Germany. E-mail: martin.prechtl@uni-koeln.de

General Remarks

Reactions were generally prepared under an argon atmosphere using *Schlenk* techniques, flame-dried glassware and a *Labmaster 200* glove-box from *MBraun*. High-pressure amination reactions were performed in a homemade 75 mL stainless steel autoclave equipped with a manometer and a sampling unit for 50 L samples. Liquid ammonia was purchased from *Linde Gas Benelux* and used as received. The NH_3 (l) was dosed using a *Bronkhorst Liqui-Flow* mass flow meter/controller. Samples were subjected directly to GC without further workup. All solvents and reagents were purchased from *Acros, Merck, Sigma-Aldrich, Fluka*, or *Strem* or were acquired from the institute stock. Commercial anhydrous solvents and argon as-packed reagents were used as received and stored in the glove-box under argon. Non-anhydrous solvents were dried and distilled (under vacuum or argon) prior to use, applying standard procedures. Complexes are synthesised following the protocol of our previous reports.[1,2] For shortened reaction time to synthesise the complexes **4** and **5**, microwave reactions were carried out in a *Monowave 300 microwave* from *Anton Paar* with a maximum power of 850 W at 2.45 MHz at 150 °C, 15 min.

Analytical Methods

^{1}H, ^{13}C, ^{31}P NMR spectra were recorded at 300 MHz (^{1}H), 75 MHz (^{13}C) and 121 MHz (^{31}P) on a *Bruker Avance II 300* and on a *Bruker Avance II+ 600* spectrometer at 600 MHz (^{1}H), 150 MHz (^{13}C) and 242 MHz (^{31}P) using deuterated benzene and toluene at room temperature. ^{1}H shifts were reported in ppm (δH) downfield from TMS and were determined by reference to the residual solvent peaks (C_6D_6: 7.16 ppm, C_7D_8: 7.09 ppm.). Chemical shifts were reported as singlet (s), doublet (d), triplet (t), quartet (q) and multiplet (m). Coupling

constants J were reported in Hz. For monitoring experiments, *Young-Teflon* capped NMR tubes from *Wilmad* were used. Infrared spectra (IR) were measured at room temperature with a *Bruker Alpha* spectrometer equipped with a Diamond-ATR IR unit. LIFDI-MS (Liquid Injection Field Desorption/Ionization-Mass Spectrometry) was performed using a *Waters micromass Q-ToF-2*^{TM} mass spectrometer equipped with a *LIFDI 700 ion source (Linden CMS)*.

Preparation of Complexes

For synthesis of complexes **2**, **3**, **4** and **5** see references.[1,2]

Synthesis of [RuHCl(CO)(Me-PNP)] 8

In an argon flushed, flame-dried *Schlenk* tube, 280 mg (0.3 mmol) of [$RuHCl(CO)(PPh_3)_3$] was added into a solution of 180 mg (0.31 mmol, note: purification grade of the Me-PNP ligand was 55-60%) bis[2-(di-*tert*-butylphosphino)ethyl]methyl-amine solvated in 6 mL toluene. The *Schlenk* tube was equipped with a condenser and the reaction mixture was refluxed under a stream of argon at 120 °C for 5 h. After the reaction time, the solvent was removed in vacuo and washed twice with each 3 mL pentane. Yield: 113 mg, 0.2 mmol, 70%.

^{1}H NMR (300 MHz, $CDCl_3$): δH [ppm] = 2.72-2.56 (m, 4H, CH_2), 2.22-2.04 (m, 2H, CH_2), 1.48 (t, 18H, $^{3}J_{PH}$ = 13.2 Hz, $PC(CH_3)_3$), 1.31 (t, 18H, $^{3}J_{PH}$ = 12.4 Hz, $PC(CH_3)_3$), -16.10 (t, 1H, $^{2}J_{PH}$ = 19.6 Hz, Ru-H).$^{13}C_{APT}$ NMR (75 MHz, $CDCl_3$): δC [ppm] = 207.8 ppm (s, *C*O), 66.1 (d, $^{2}J_{CP}$ = 4.5 Hz, -N*C*H_2-), 47.8 (s, -N*C*H_3), 38.7 (t, textit$^{1}J_{CP}$ = 5.5 Hz, P*C*$(CH_3)_3$), 36.7 (t, $^{1}J_{CP}$ = 10.3 Hz, P*C*$(CH_3)_3$), 31.3 (t, $^{1}J_{CP}$ = 2.7 Hz, $PC(CH_3)_3$), 31.0 (t, $^{1}J_{CP}$ = 2.1 Hz, $PC(CH_3)_3$), 23.5 (t, $^{1}J_{CP}$ = 5.7 Hz, -*C*H_2-). $^{31}P\{^{1}H\}$ NMR (121 MHz, $CDCl_3$): δP [ppm] = 83.3 (s).

IR: $\tilde{\nu}$[cm^{-1}] = 2994-2858 (m), 2222-2086 (w), 2052-1970 (w), 1908 (s), 1477 (m), 1385 (w), 1359 (m), 1317 (w), 1211 (w), 1174 (m), 1048 (w), 1033 (m), 936 (w), 912 (w), 882 (m), 820-790 (m), 739 (m), 684 (m), 604 (m), 568 (s), 541 (m), 480 (s), 433 (m).

^{1}H NMR Spectrum of Complex 8

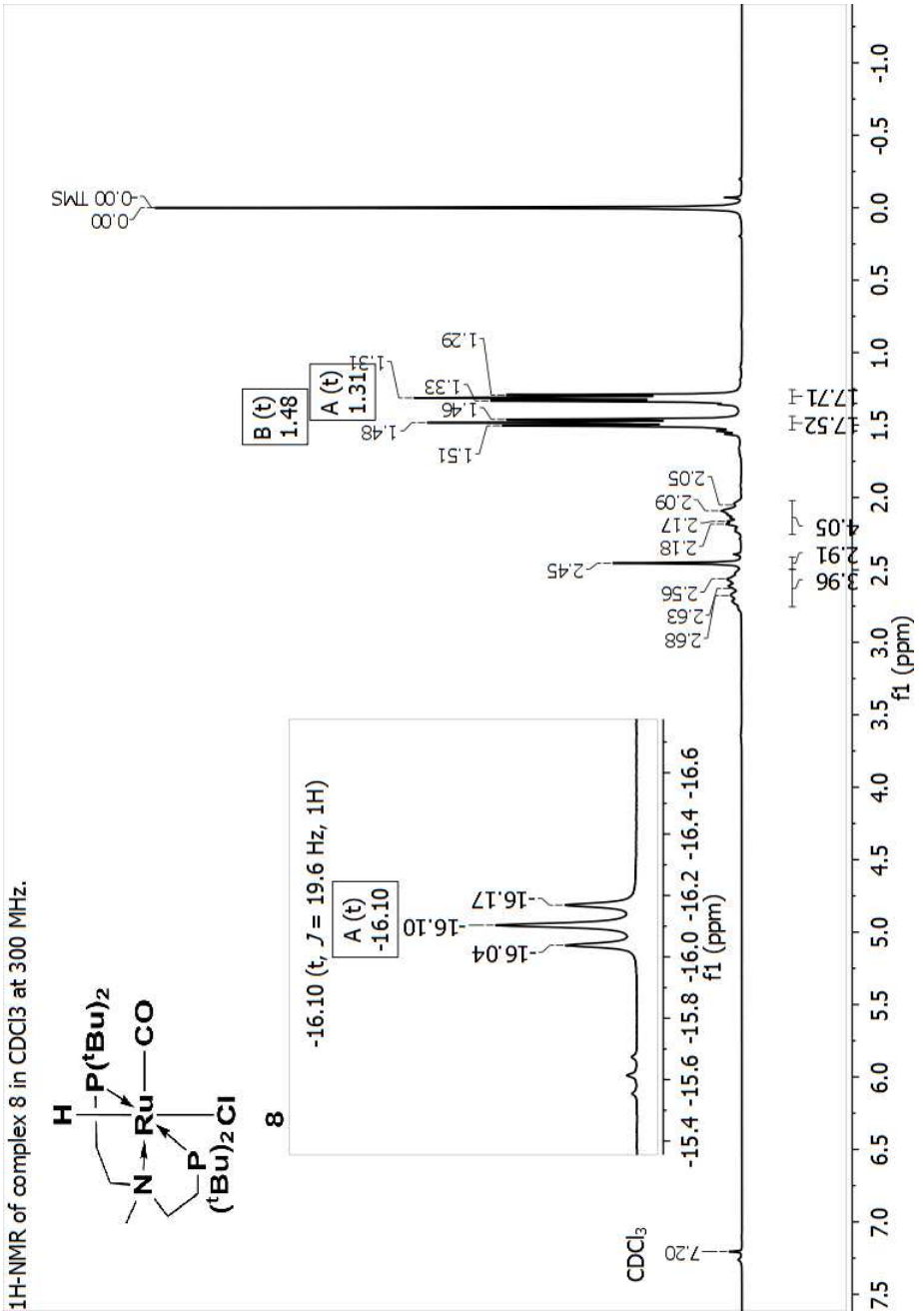

Fig. S 5.66. – ^{1}H NMR spectrum of complex **8** in $CDCl_3$ at 300 MHz.

$^{13}C_{APT}$ NMR Spectrum of Complex 8

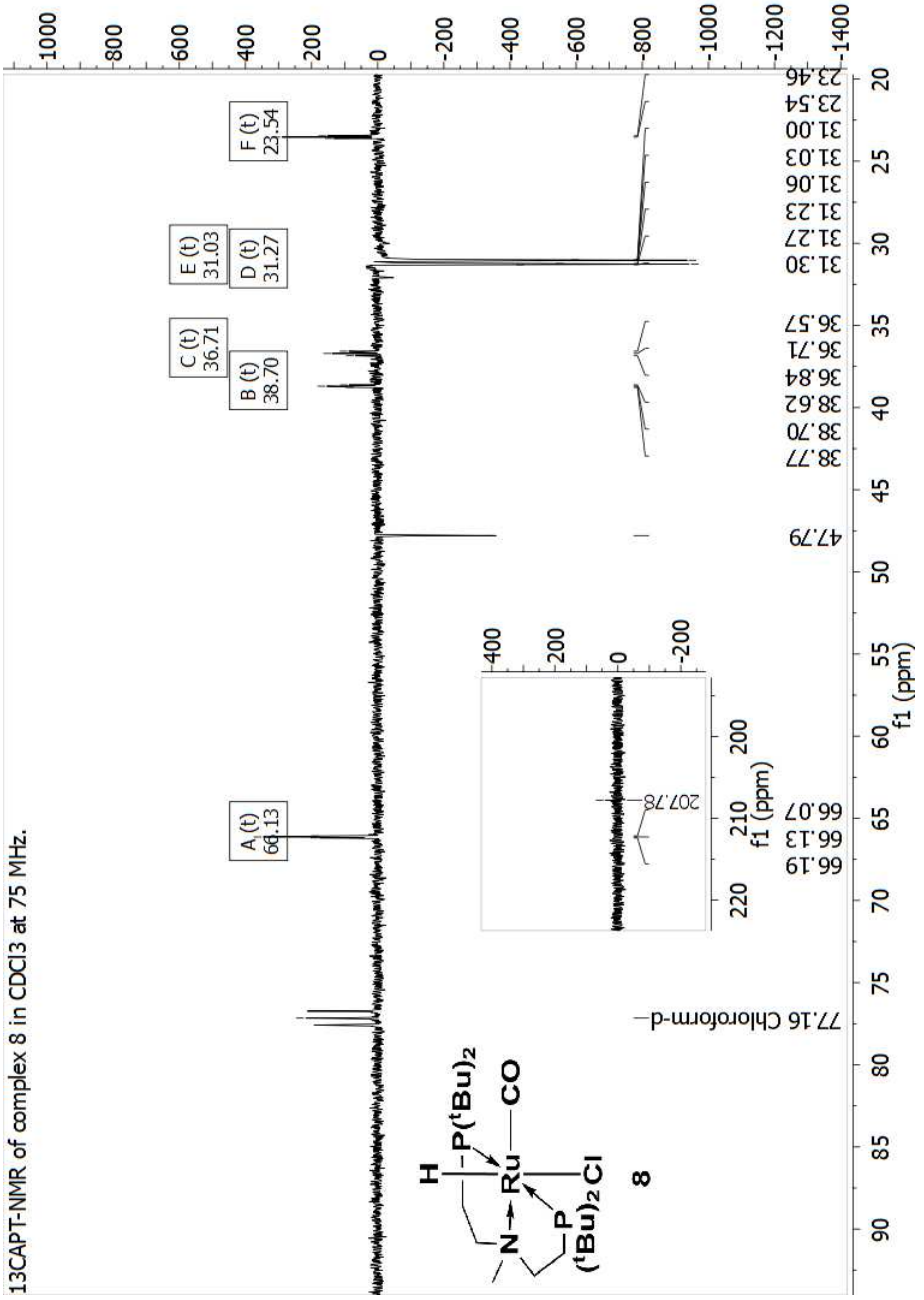

Fig. S 5.67. – $^{13}C_{APT}$ NMR spectrum of complex **8** in $CDCl_3$ at 75 MHz.

$^{31}P\{^{1}H\}$ NMR Spectrum of Complex 8

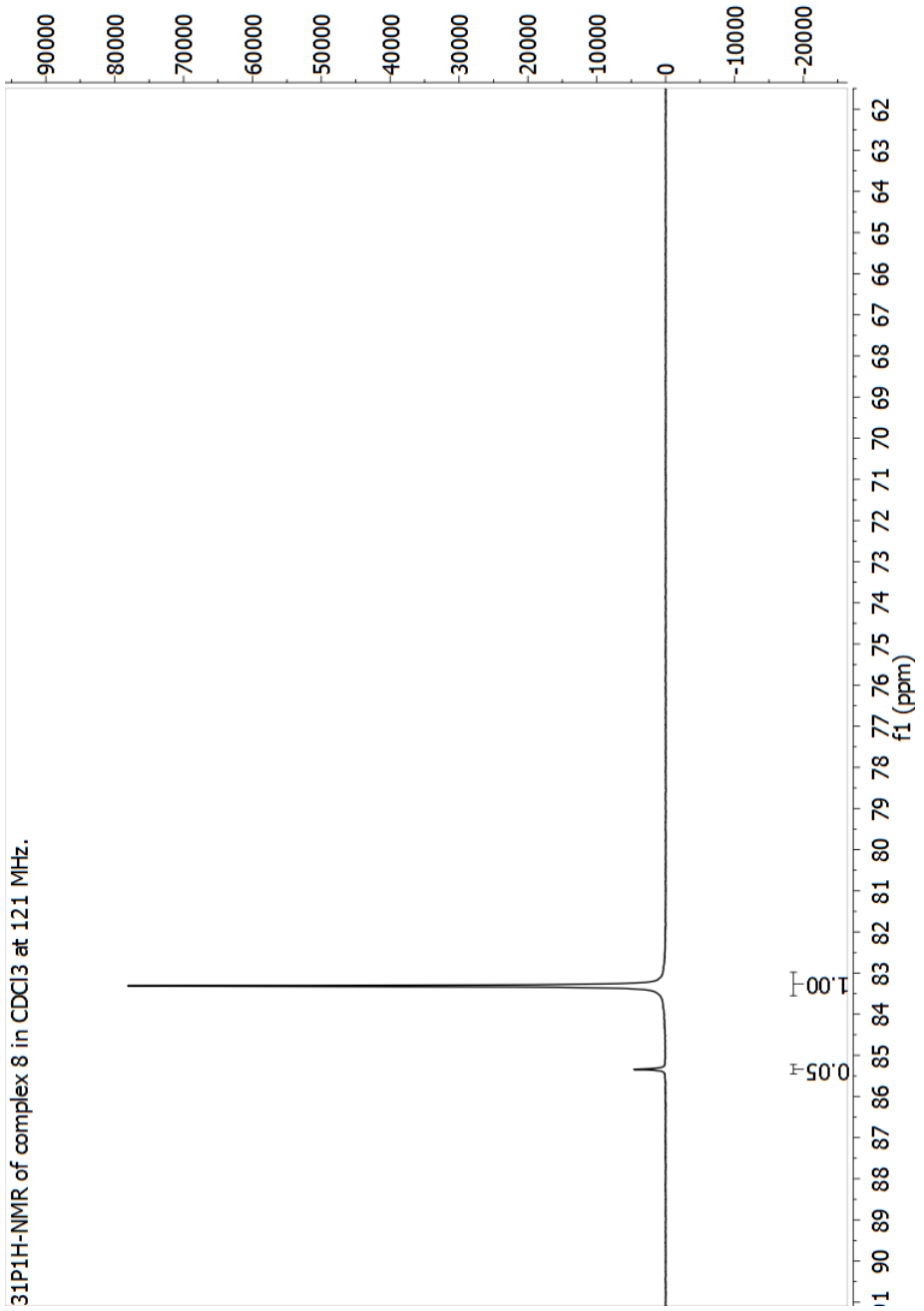

Fig. S 5.68. – $^{31}P\{^{1}H\}$ NMR spectrum of complex **8** in $CDCl_3$ at 121 MHz.

IR Spectrum of Complex 8

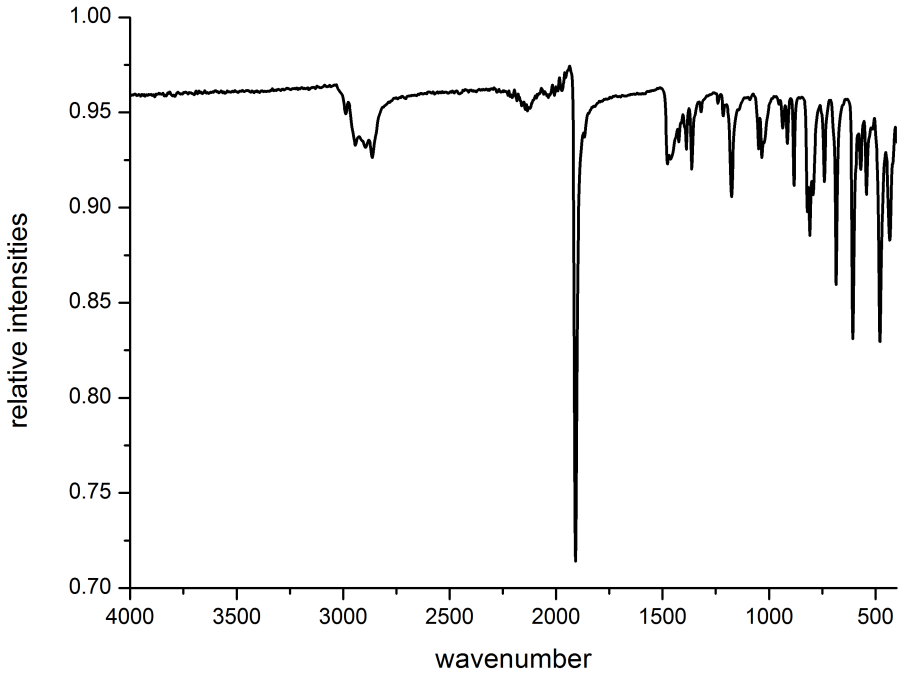

Fig. S 5.69. – IR spectrum of complex **8**.

Catalysis

General Description of the Direct Amination of Alcohols

In a *Schlenk* tube, 0.04 mmol of the complex were solvated in 15 mL *t*-amylalcohol and added into the argon-flushed 75 mL stainless steel autoclave. After the addition of 5 mmol cyclohexanol, the autoclave was charged with 2.5 mL liquid NH_3 and heated to 150 °C.

Addition of Substrates

When substrates (such as benzylaldehyde, cyclohexanone or KO^tBu) were added during the catalysis, the autoclave was cooled down to ambient temperature and depressurised to release the gaseous ammonia. The substrates were added trough a counter-stream of argon and the autoclave was recharged with 2.5 mL liquid NH_3 and heated to 150 °C.

GC Measurements

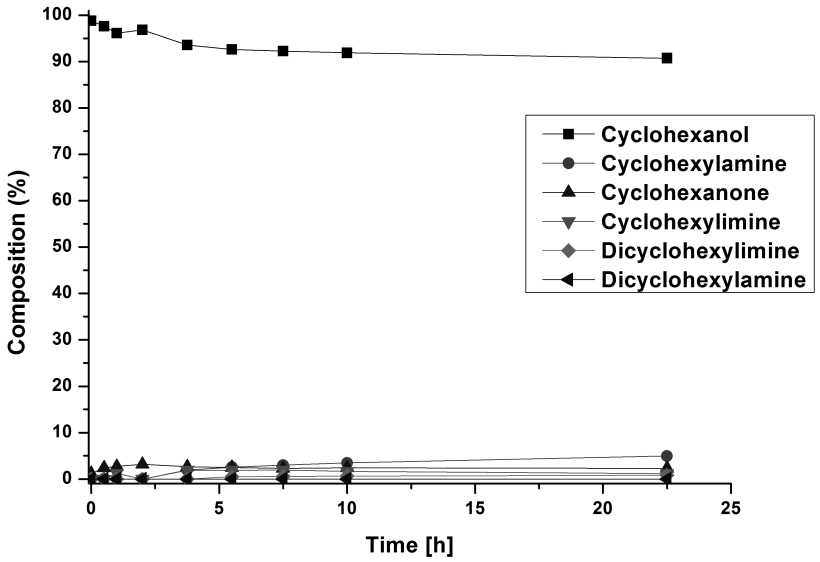

Fig. S 5.70. – Amination of cyclohexanol with complex **3**. Conditions: 0.04 mmol **3**, 5 mmol cyclohexanol, 15 mL *t*-amylalcohol, 2.5 mL NH_3, 150 °C, 52 h.

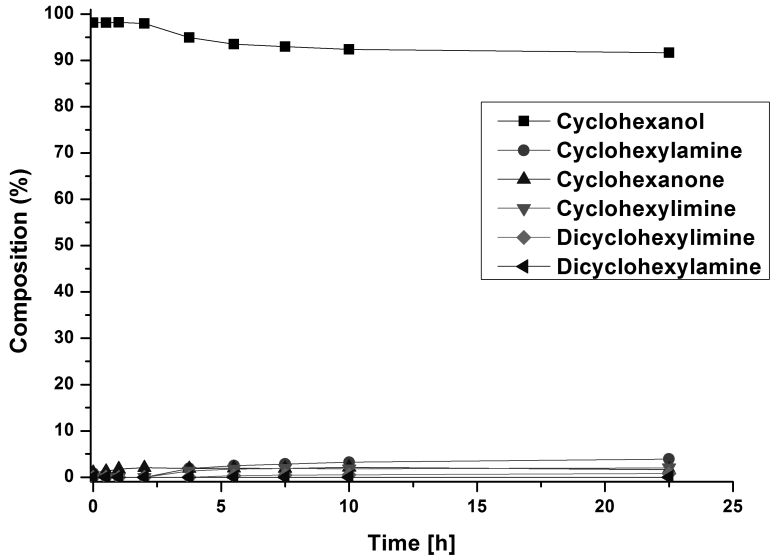

Fig. S 5.71. – Amination of cyclohexanol with complex **5**. Conditions: 0.04 mmol **5**, 5 mmol cyclohexanol, 15 mL *t*-amylalcohol, 2.5 mL NH_3, 150 °C, 52 h.

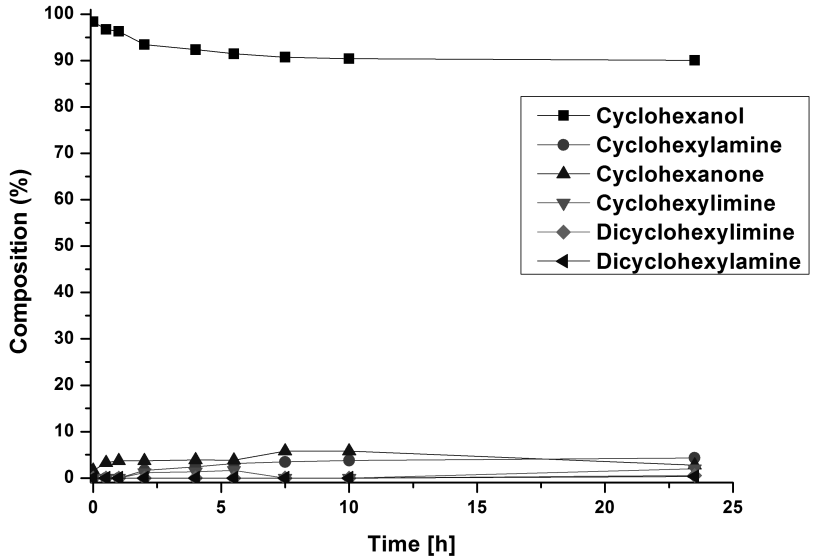

Fig. S 5.72. – Amination of cyclohexanol with complex **3** with additional 1 mol% of KO^tBu. Conditions: 0.04 mmol **3**, 5 mmol cyclohexanol, 0.04 mmol KO^tBu, 15 mL *t*-amylalcohol, 2.5 mL NH_3, 150 °C, 52 h.

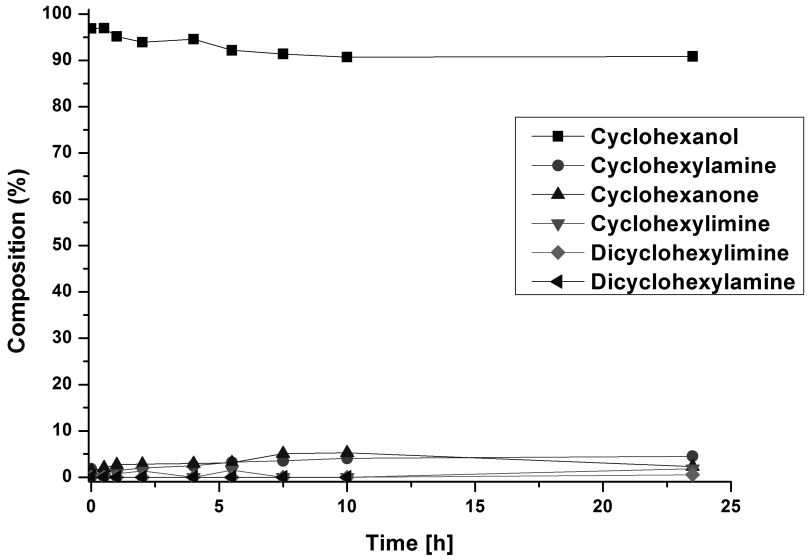

Fig. S 5.73. – Amination of cyclohexanol with complex **5** with additional 1 mol% of KO^tBu. Conditions: 0.04 mmol **5**, 5 mmol cyclohexanol, 0.04 mmol KO^tBu, 15 mL *t*-amylalcohol, 2.5 mL NH_3, 150 °C, 52 h.

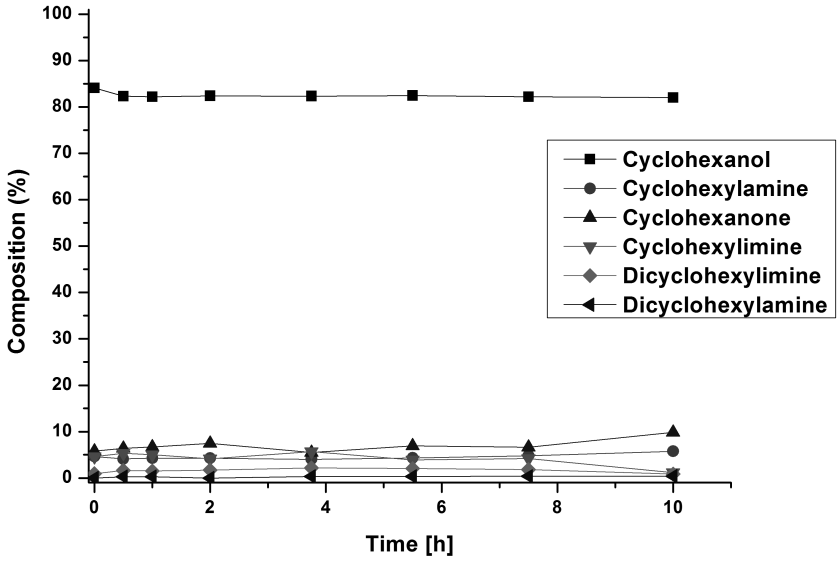

Fig. S 5.74. – Amination of cyclohexanol with complex **3** with additional 10 mol% cyclohexanone. Conditions: 0.04 mmol **3**, 5 mmol cyclohexanol, 0.5 mmol cyclohexanone, 15 mL *t*-amylalcohol, 2.5 mL NH_3, 150 °C, 52 h.

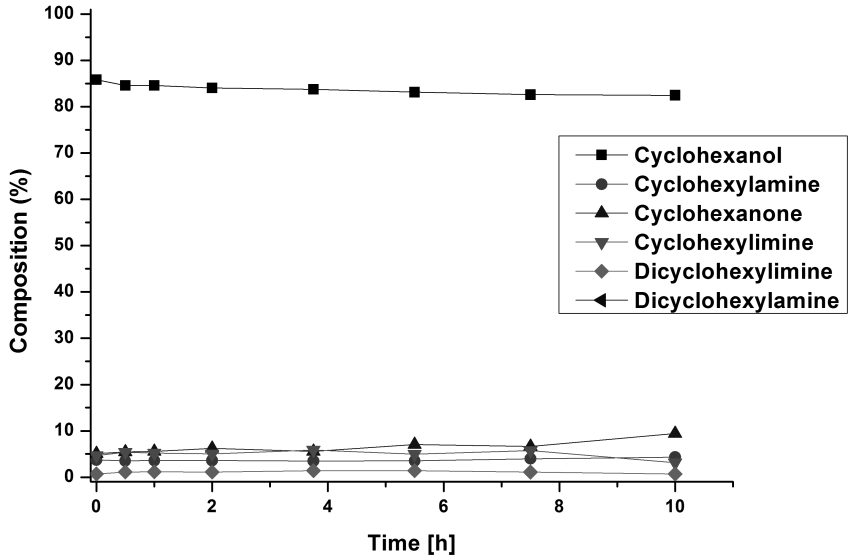

Fig. S 5.75. – Amination of cyclohexanol with complex **5** with additional 10 mol% cyclohexanone. Conditions: 0.04 mmol **5**, 5 mmol cyclohexanol, 0.5 mmol cyclohexanone, 15 mL *t*-amylalcohol, 2.5 mL NH_3, 150 °C, 52 h.

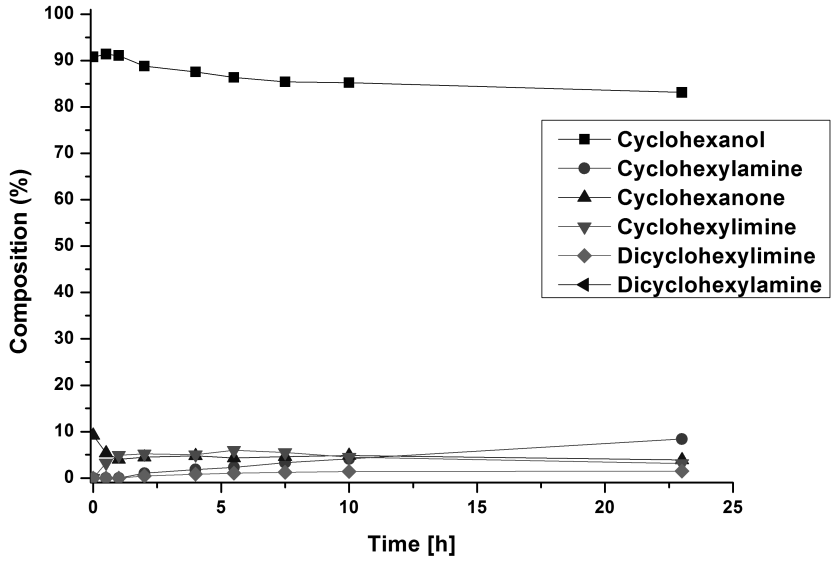

Fig. S 5.76. – Amination of cyclohexanol with complex **2** with additional 10 mol% cyclohexanone. Conditions: 0.04 mmol **2**, 5 mmol cyclohexanol, 0.5 mmol cyclohexanone, 15 mL *t*-amylalcohol, 2.5 mL NH_3, 150 °C, 52 h.

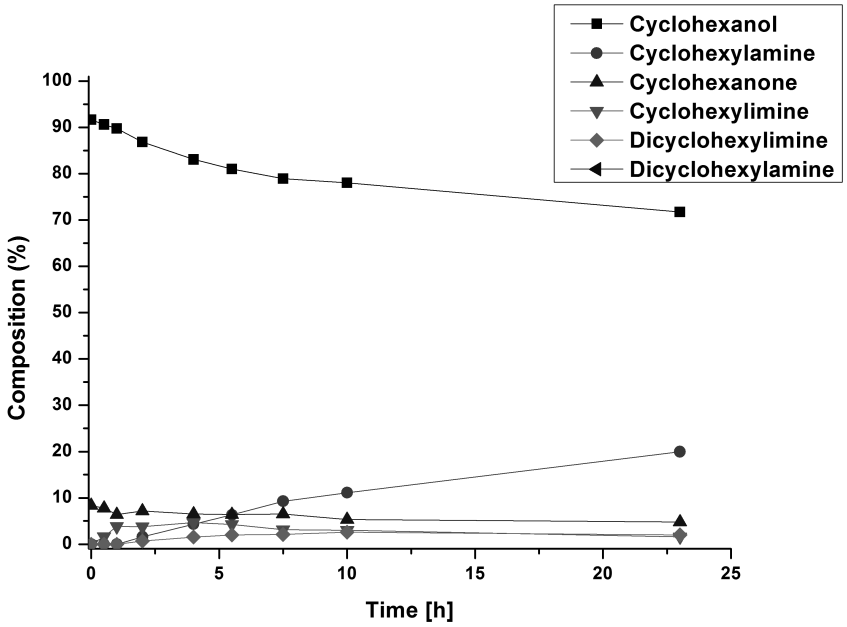

Fig. S 5.77. – Amination of cyclohexanol with complex **4** with additional 10 mol% cyclohexanone. Conditions: 0.04 mmol **4**, 5 mmol cyclohexanol, 0.5 mmol cyclohexanone, 15 mL *t*-amylalcohol, 2.5 mL NH_3, 150 °C, 52 h.

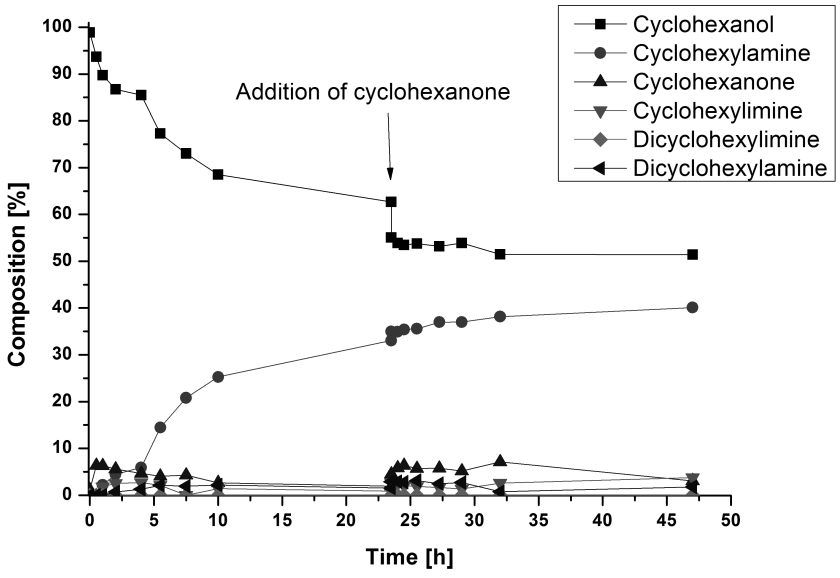

Fig. S 5.78. – Amination of cyclohexanol with complex **4**. 10 mol% cyclohexanone were added after 23.5 h. Conditions: 0.04 mmol **4**, 5 mmol cyclohexanol, 0.5 mmol cyclohexanone, 15 mL *t*-amylalcohol, 2.5 mL NH_3, 150 °C, 52 h.

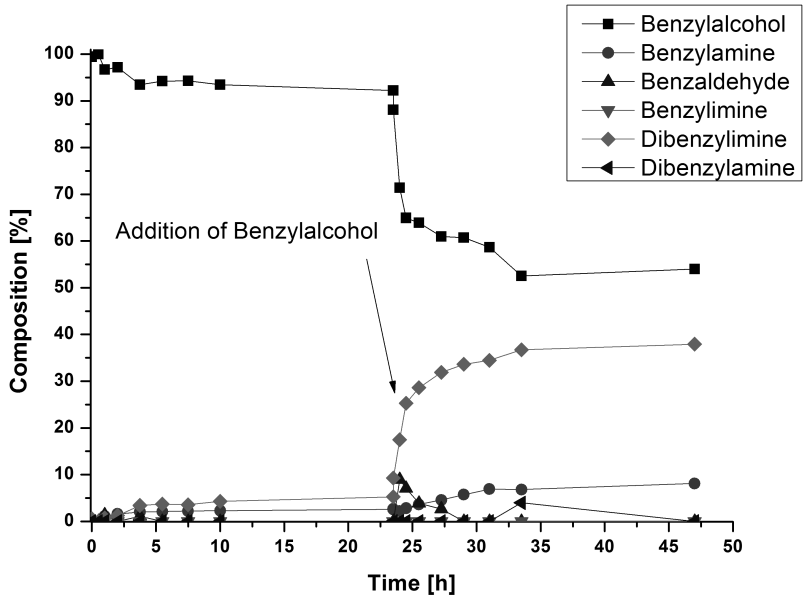

Fig. S 5.79. – Amination of benzylalcohol with complex **2**. 10 mol% benzylaldehyde were added after 23.5 h. Conditions: 0.04 mmol **2**, 5 mmol benzylalcohol, 15 mL *t*-amylalcohol, 2.5 mL NH_3, 150 °C, 52 h.

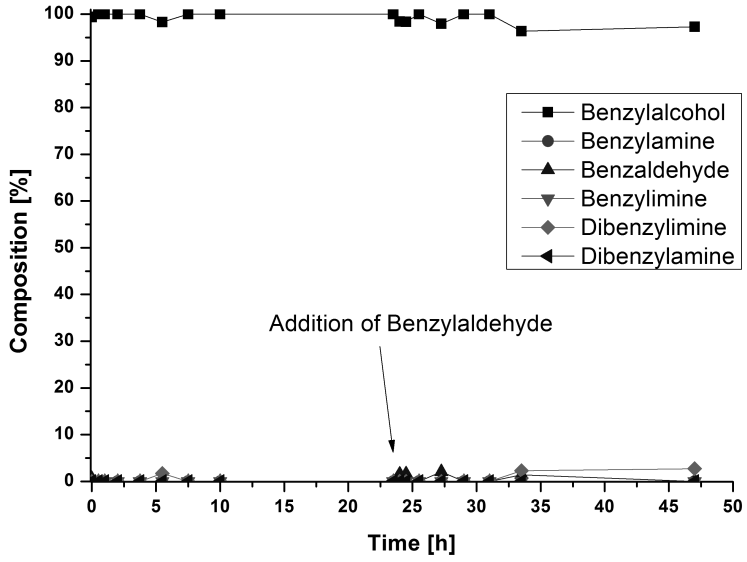

Fig. S 5.80. – Amination of benzylalcohol with complex **4**. 10 mol% benzylaldehyde were added after 23.5 h. Conditions: 0.04 mmol **4**, 5 mmol benzylalcohol, 15 mL *t*-amylalcohol, 2.5 mL NH_3, 150 °C, 52 h.

Analyses

GC-method details

Injection Mode/ ratio:	Split/100
Temperature:	270 °C
Carrier Gas:	He
Flow Control Mode:	Pressure
Pressure:	121.0 kPa
Total Flow:	144.0 mL/min
Column Flow:	0.70 mL/min
Liner Velocity:	25.8 cm/sec
Pressure program:	121.0 → 164.0 @ 1.8 kPa/min 164.0 hold 15 min
Temperature program:	80 °C → 270 °C @ 8 °C/min 270 hold 15 min
Column type:	Ultra-2 serial nr.: US8649351H
Column length:	25 m, 0.33 m film thickness, 0.20 mm inner diameter
Column Max. Temp.:	310 ^{o}C

Investigation of Deactivated Complex Intermediate 6

Isolation of Deactivated Complex Intermediate 6

In a teflon capped *Young* NMR tube (*Wilmad 300 MHz*) complex **2** (20 mg, 0.04 mmol) and cyclohexanone (33.2 µL, 0.32 mmol) were placed. These were then dissolved in toluene-d_8 (0.5 mL). The mixture was heated to 80 °C and measured periodically after t = 0, 2, 4 and 20 h. After 20 h, the solvent was removed from the reaction mixture. The mixture was isolated as a black muddy solid and was further analysed via LIFDI-MS/MS technique. Note: with increasing reaction time, H/D exchange reactions occur with toluene-d_8 and **2**, which consequently lowers the intensities, while the signal intensities of toluene increases.

Selective signals after heating to 80 °C for t = 20 h in the presence of 4 eq. cyclohexanone in toluene-d_8. ^{1}H NMR (300 MHz in toluene-d_8): δH [ppm] = 7.1 (s, toluene), 7.05 (s, toluene), 7.01 (s, toluene), 3.40-3.33 (m, CH_2, Me-PNP), 2.94-2.81 (m, CH_2, Me-PNP), 2.38 (toluene, -CH_3), 1.96 (t, $J = 6.6$ Hz), 1.44-1.26 ($PC(CH_3)_3$, overlap with cyclohexanone), -7.6–8.4 (bs), -8.71 (t, 1H, $^2J_{PH} = 13.7$ Hz, Ru-H, complex **2**). ^{31}P{^{1}H} NMR (After heating to 80 °C for t = 20 h in the presence of 4 eq. cyclohexanone in toluene-d_8), (121 MHz, toluene-d_8): δP [ppm] = 108.4 (s), 107.7 (s), 98.2 (s), 76.1 (s), 75.1 (s), 73.9 (s), 67.4 (s).

IR: $\tilde{\nu}$[cm^{-1}] (After heating to 80 °C for t = 20 h in the presence of 4 eq. cyclohexanone in toluene-d_8) = 2913-2900 (s), 2858 (s), 2205-2189 (w), 2153 (w), 2077 (w), 1925 (w), 1879 (m), 1711 (m), 1606 (w), 1551 (w), 1449 (s), 1364 (m), 1280 (m), 1236 (w), 1206 (w), 1162-1111 (m), 1079 (m), 1017 (m), 976 (w), 876 (w), 843 (m), 804 (s), 764 (w), 737 (s), 674 (s), 613-541 (m), 461 (s), 420 (s).

LIFDI-MS/MS (After heating to 80 °C for t = 20 h in the presence of 4 eq. cyclohexanone in toluene-d_8. Retention time 4.25 min): *m/z* 575.3 (M^+, 100), 579.3 (14.3), 578.3 (28.6), 577.4 (57.1), 576.3 (42.9), 575.3 (100), 574.3 (42.9), 571.3 (14.3), 570.3 (14.3), 569.3 (14.0).

LIFDI-MS/MS Spectrogram

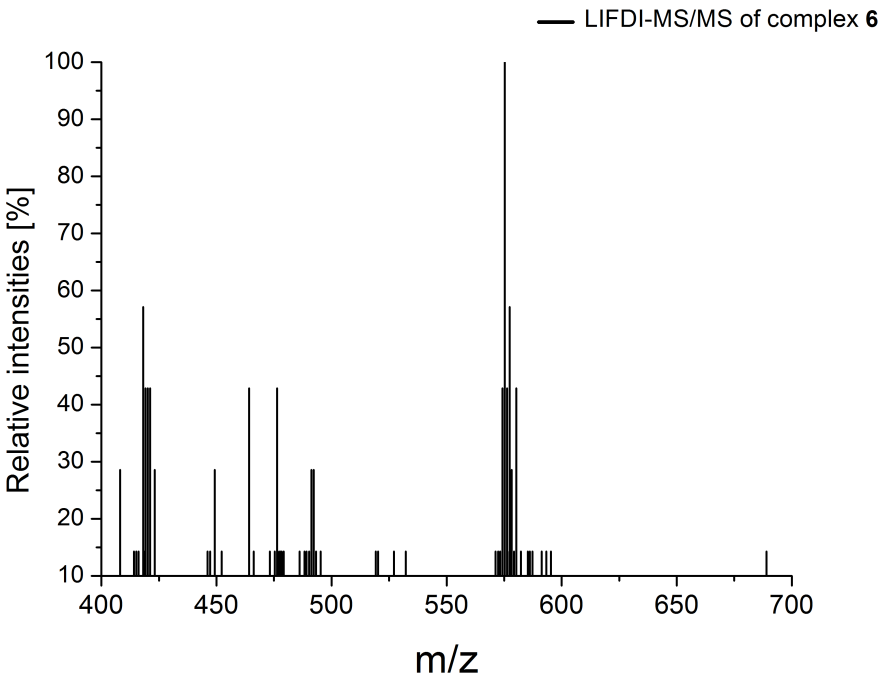

Fig. S 5.81. – LIFDI-MS/MS of complex **6** in toluene at retention time 2.90 min.

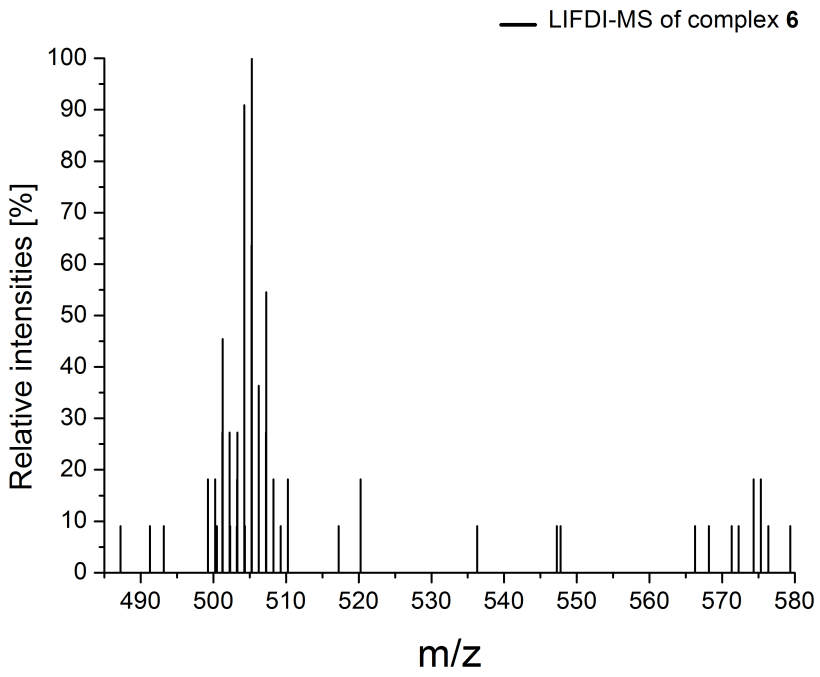

Fig. S 5.82. – LIFDI-MS/MS of complex **6** in toluene at retention time 4.25 min.

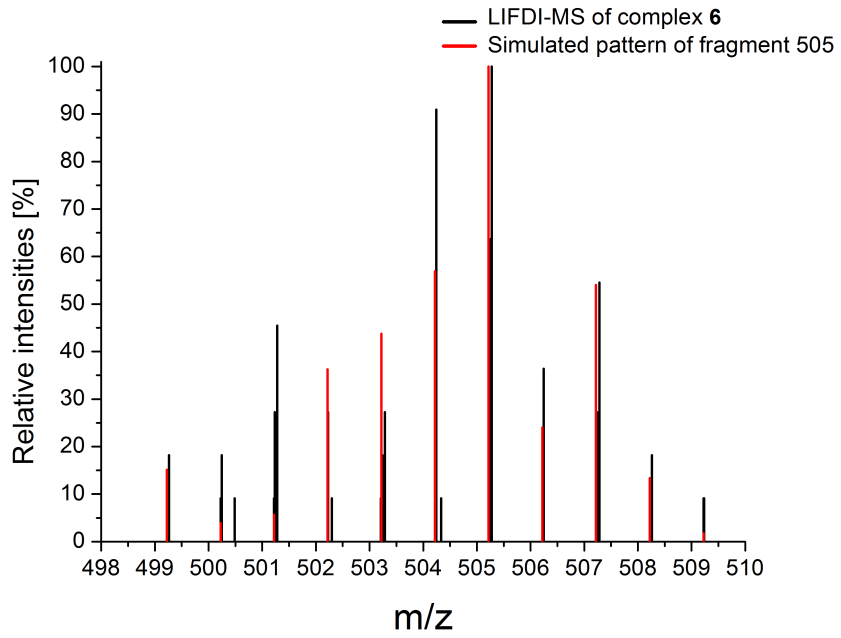

Fig. S 5.83. – LIFDI-MS/MS of fragment [Ru(Me-PNP)CO] 499-509 vs simulated pattern of fragment [Ru(Me-PNP)CO] 505 at retention time 4.25 min.

IR Spectrum of 2 in the Presence of 8 eq. Cyclohexanone

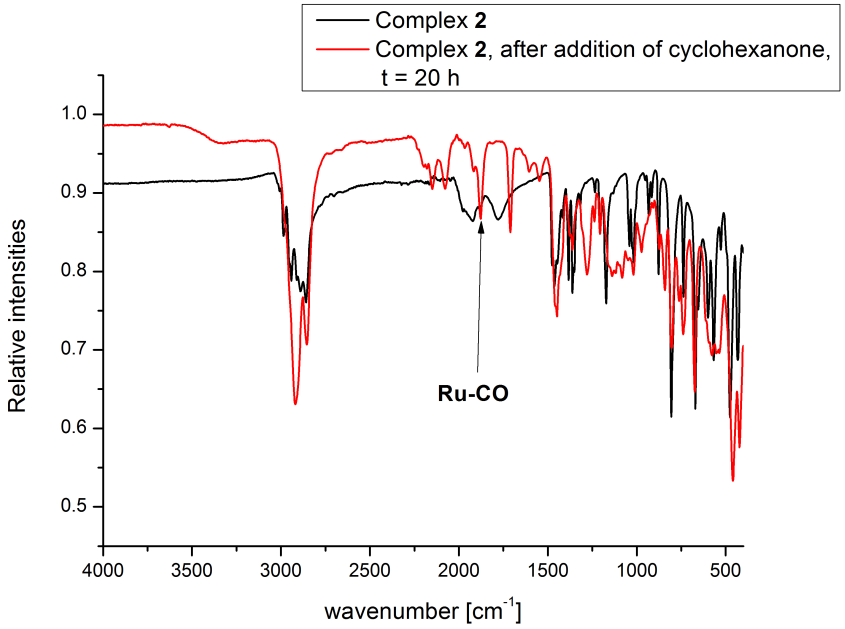

Fig. S 5.84. – IR spectrum of **2** in the presence of 8 eq. cyclohexanone after heated to 80 °C for 20 h vs IR spectrum of **2**.

NMR Spectra of 2 in the Presence of 8 eq. Cyclohexanone

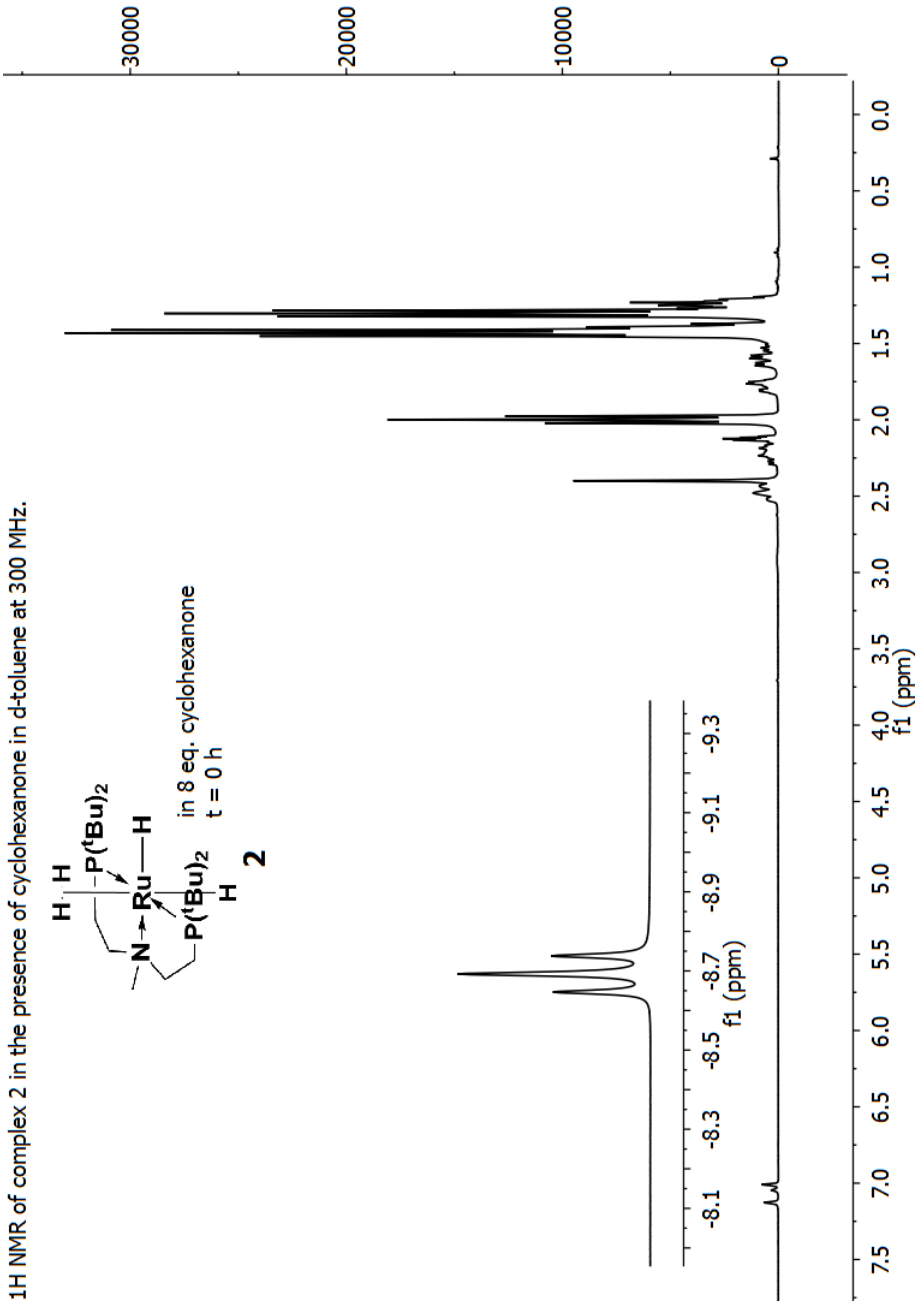

Fig. S 5.85. – ^{1}H NMR spectrum of **2** in the presence of 8 eq. cyclohexanone t = 0 h in toluene-d_8 at 300 MHz.

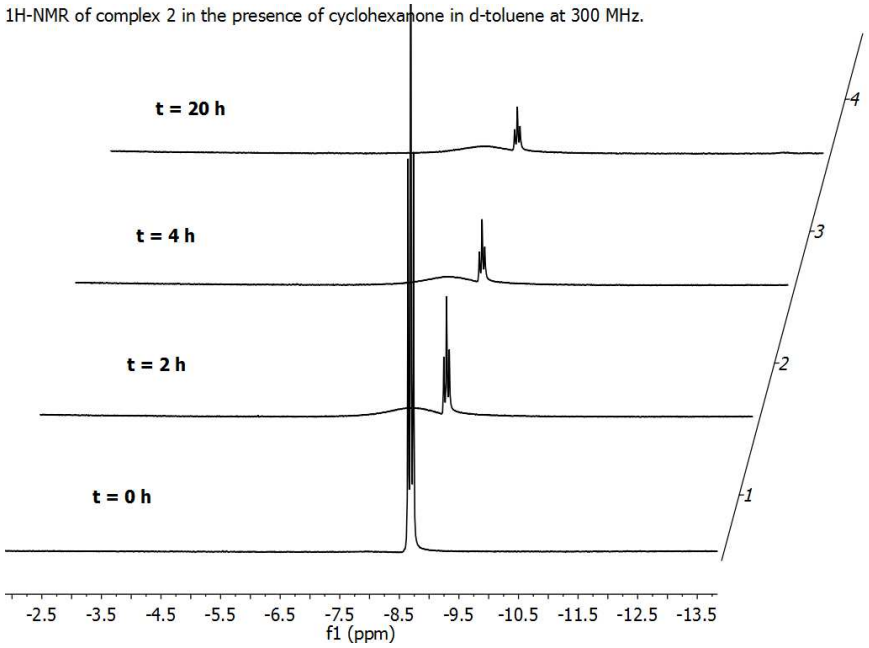

Fig. S 5.86. – Stacked ^{1}H NMR spectra of the hydride area of **2** in the presence of 8 eq. cyclohexanone after heating to 80 °C. Spectra were recorded after t = 0, 2, 4 and 20 h in toluene-d_8 at 300 MHz.

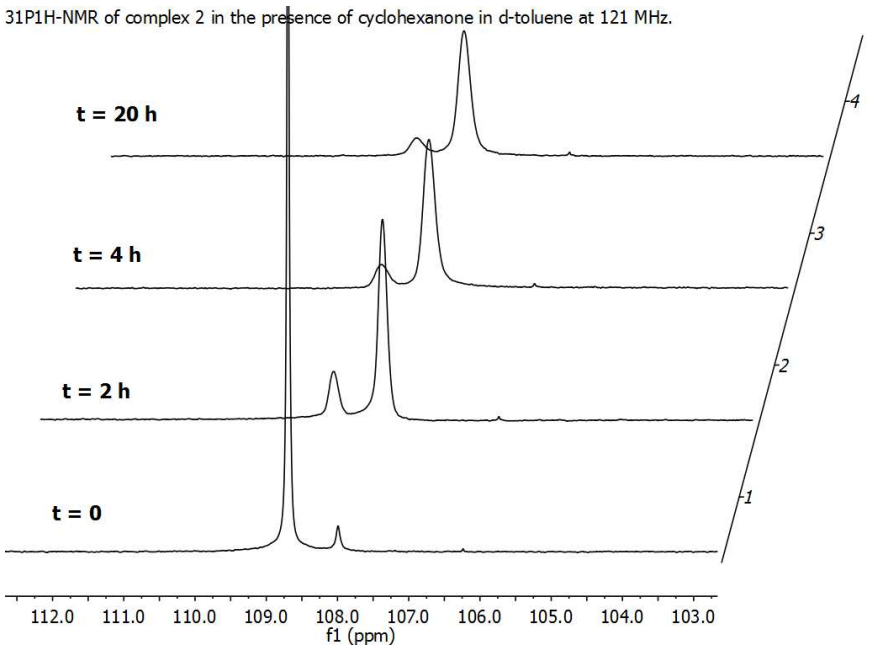

Fig. S 5.87. – Stacked ^{31}P{^{1}H} NMR spectra of **2** in the presence of 8 eq. cyclohexanone after heating to 80 °C. Spectra were recorded after t = 0, 2, 4 and 20 h in toluene-d_8 at 121 MHz.

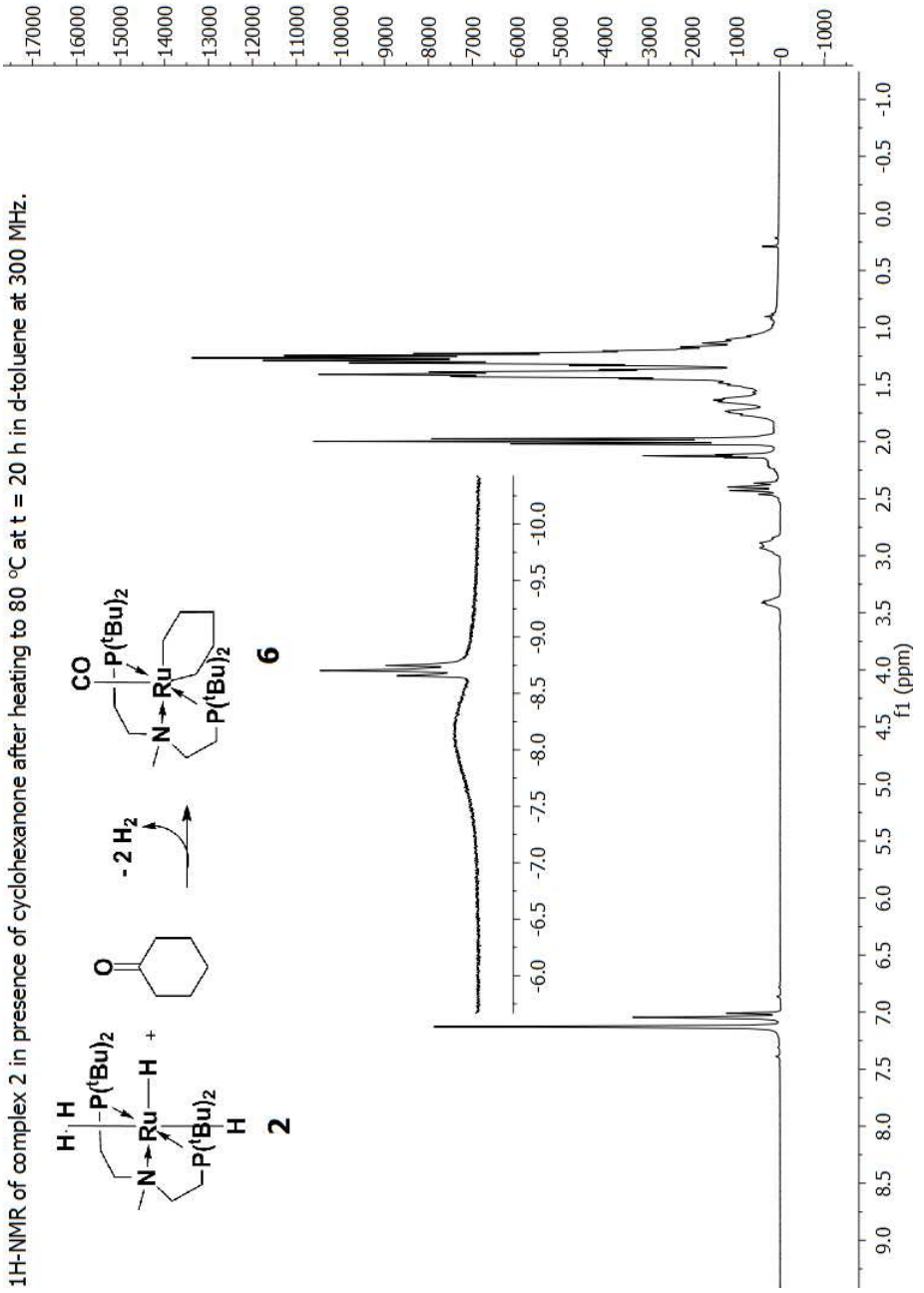

Fig. S 5.88. – ^{1}H NMR spectra of **2** in the presence of 8 eq. cyclohexanone after heating to 80 °C. Spectra were recorded after t = 20 h in toluene-d_8 at 300 MHz.

Long time NMR Monitoring Experiments of 2 in the Presence of 4 eq. Cyclohexanone

In a teflon capped *Young* NMR tube (*Wilmad 300 MHz*) complex **2** (20 mg, 0.04 mmol) and cyclohexanone (16.6 µL, 0.16 mmol) were placed. These were then dissolved in toluene-d_8

(0.5 mL). The mixture was heated to 80 °C and measured periodically after t = 0, 1, 2, 4, 7, 10, 20, 24, 30, 40, 50, 60, 70 h. Note: these NMR experiments were measured within 10 days, due to the limited accessibility to our spectrometer (e.g. waiting loops of the auto sampler. Note: with increasing reaction time, H/D exchange reactions occur with toluene-d_8 and **2**, which consequently lowers the intensities, while the signal intensities of toluene increases.

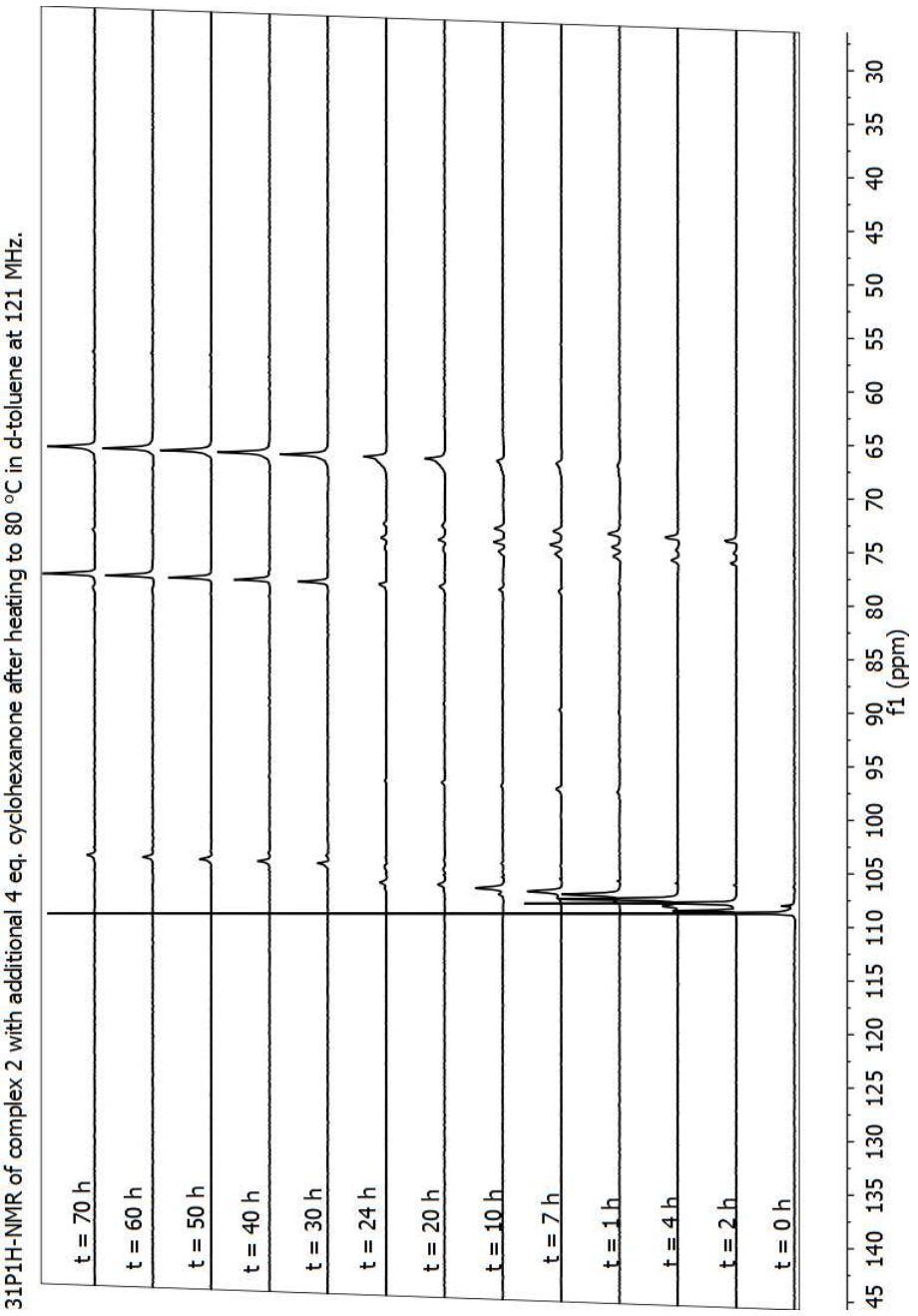

Fig. S 5.89. – Stacked $^{31}P\{^1H\}$ NMR spectra of the deactivation process of **2** after t = 0, 1, 2, 4, 7, 10, 20, 24, 30, 40, 50, 60, 70 h in toluene-d_8 at 121 MHz.

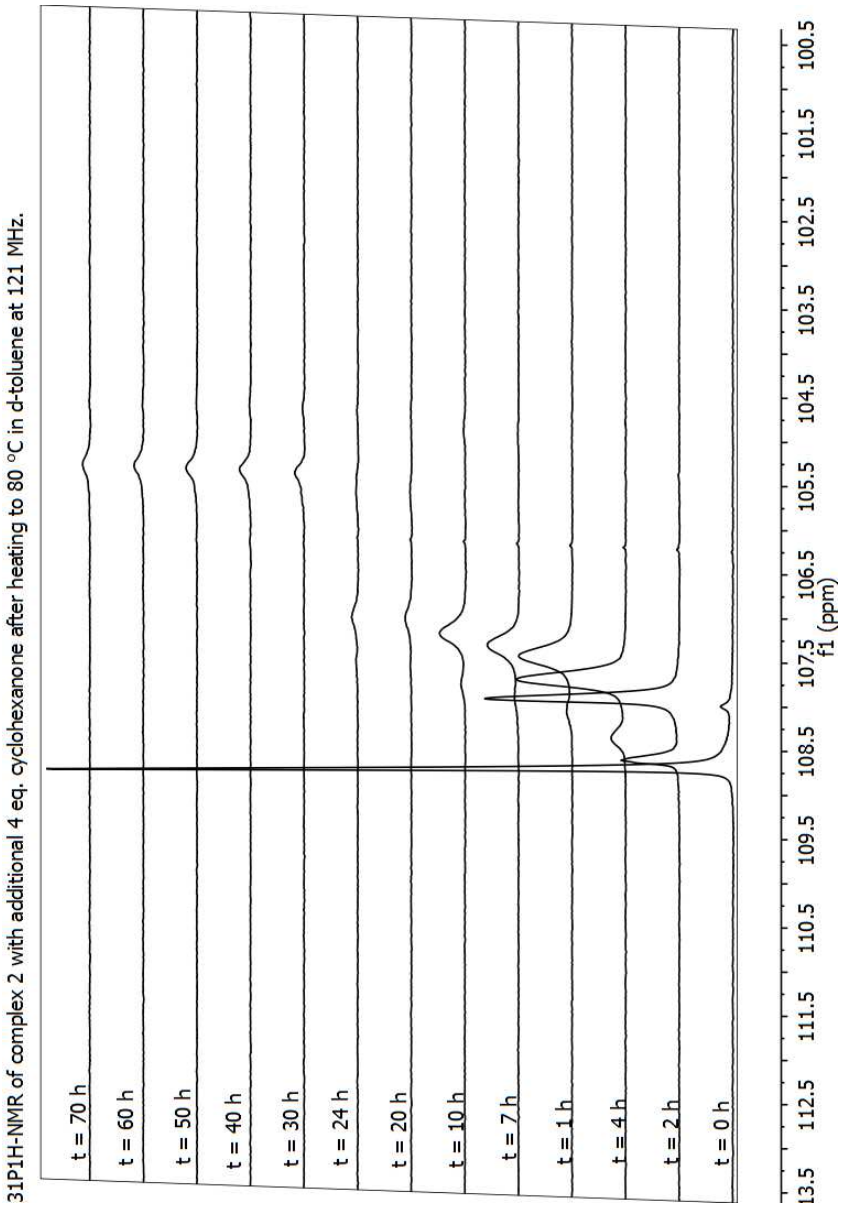

Fig. S 5.90. – Close-up, stacked $^{31}P\{^{1}H\}$ NMR spectra of the deactivation process of **2** after t = 0, 1, 2, 4, 7, 10, 20, 24, 30, 40, 50, 60, 70 h in toluene-d_8 at 120 MHz.

From every recorded ^{31}P NMR spectra, complex **6** seems most present at t = 2 h (107.9 ppm). Therefore, in the ^{13}C spectrum of t = 2 h, a small signal at 207.7 ppm is detectable (note: cyclohexanone CO = 211.6 ppm), which could be the Ru-CO carbonyl peak of the species (Figure S. 5.91). This observation needs to be interpreted carefully, since the same signal appears in t = 0 and t = 2. Simultaneously decomposed complexes appear around 79 – 67 ppm. After 20 – 24 hours (t = 20, 24 h), the signal of deactivated species **6** is only

present as minor peak. Interestingly, at t = 30 h, the signal of complex **6** disappeared while a new signal rises at 105.5 ppm and only two decomposed complexes are visible at 79.2 and 67.3 ppm (ca. 4:6 ratio). In the following NMR spectra of t = 40, 50, 60 and 70 h, the three signals remain with the ratio of (ca. 1:5:5, Figure S. 5.92 after t = 50 h).

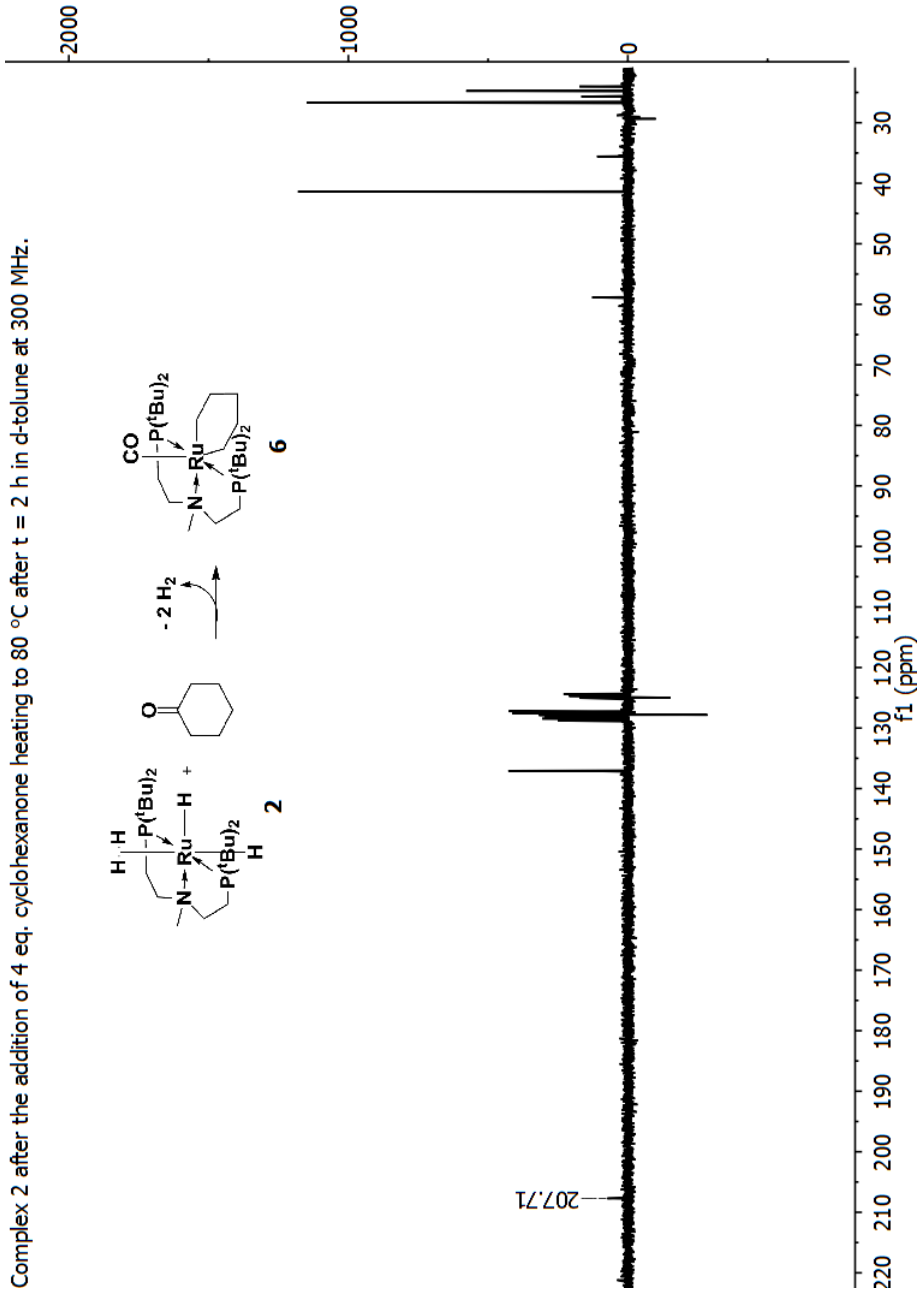

Fig. S 5.91. – $^{13}C_{APT}$ NMR spectrum of complex **6** in the presence of cyclohexanone in toluene-d_8 after t = 2h heating to 80 °C. at 75 MHz.

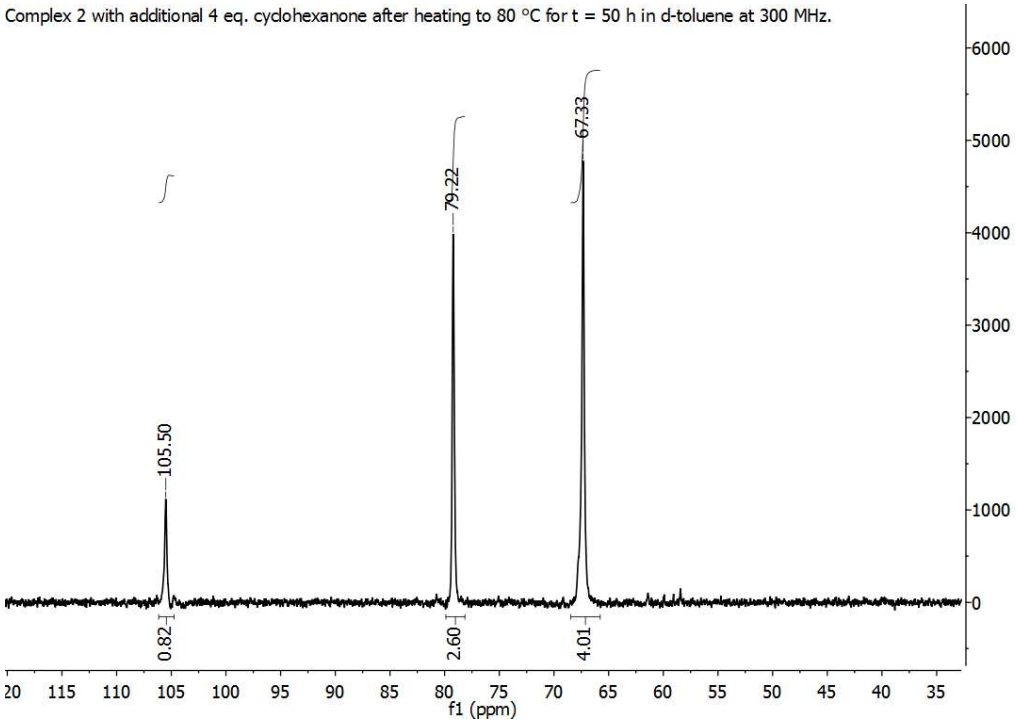

Fig. S 5.92. – $^{31}P\{^{1}H\}$ NMR of complex **6** in the presence of cyclohexanone in toluene-d_8 after t = 50 h heating to 80 °C at 121 MHz.

The new signal at 105.5 ppm might indicate that an insignificant amount of the deactivated species **6** remained stable by the loss of the bidentate C5 alkyl ligand due to two reasons: first, the signal around 105.5 ppm is similar to complex **4** which appears around 106.3 and second, in the ^{1}H NMR, traces of hydride signals as multiplets appear around -5.40 to -5.70 ppm (Figure S. 5.93), which is also familiar to complex **4** (ca. -5.50 ppm as multiplets at 300 MHz and as triplets at -5.43, -5.54 ppm at 600 MHz).

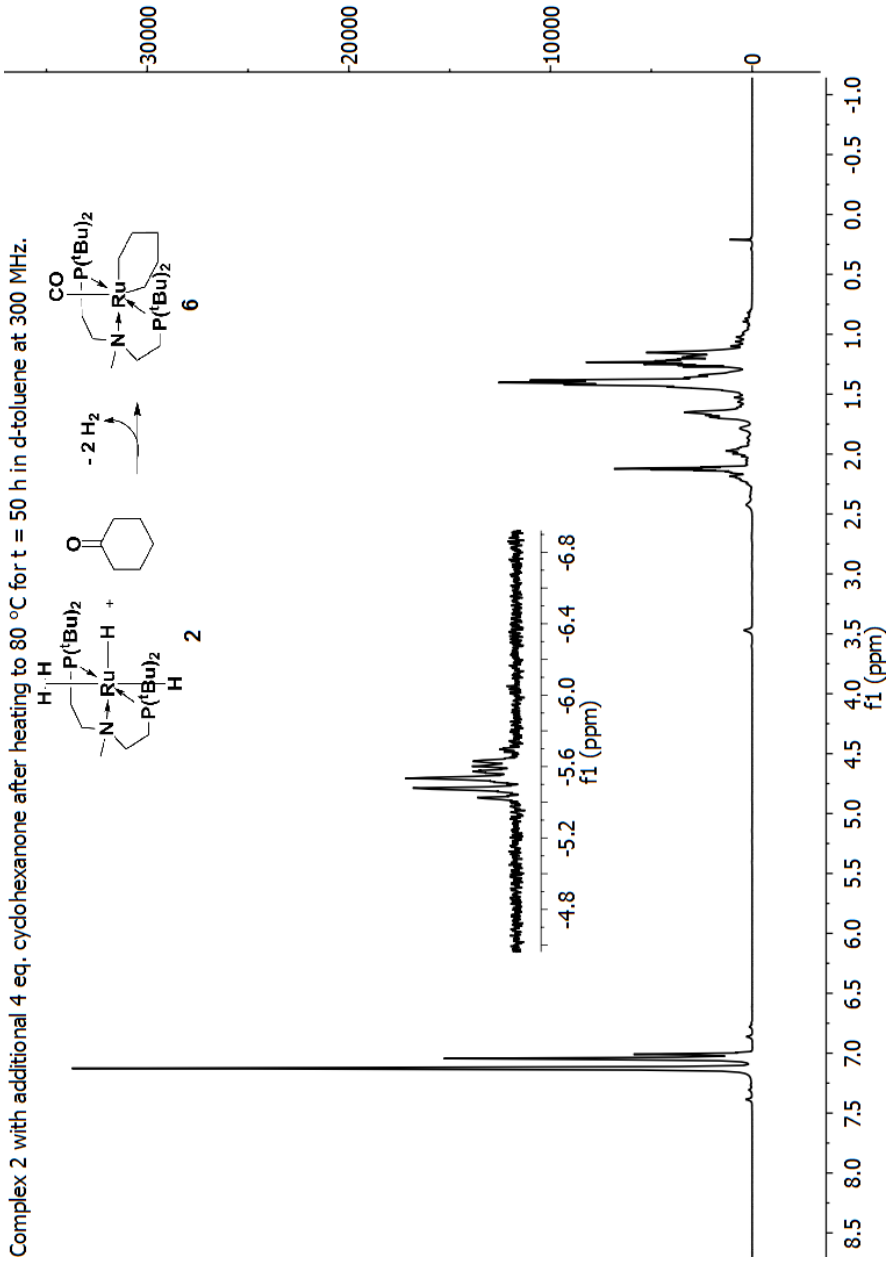

Fig. S 5.93. – ^{1}H NMR of complex **2** in the presence of cyclohexanone forming to **6** in toluene-d_8 after t = 50 h heating to 80 °C at 300 MHz.

A further look in the hydride area (Figure S. 5.94) shows that the observation of the ^{31}P NMR is congruent with the ^{1}H NMR. The broad signal around -8.14 ppm appears with the ^{31}P signal at 107.9 ppm, which is assumable the signal of the cycloalkylated complex **6**. Starting from t = 7 h, the broad signal disappears as well as the signal at 107.9 ppm in the phosphorus NMR spectrum. From t = 30 h on, hydride signals around -5.40 to -5.70 ppm appear.

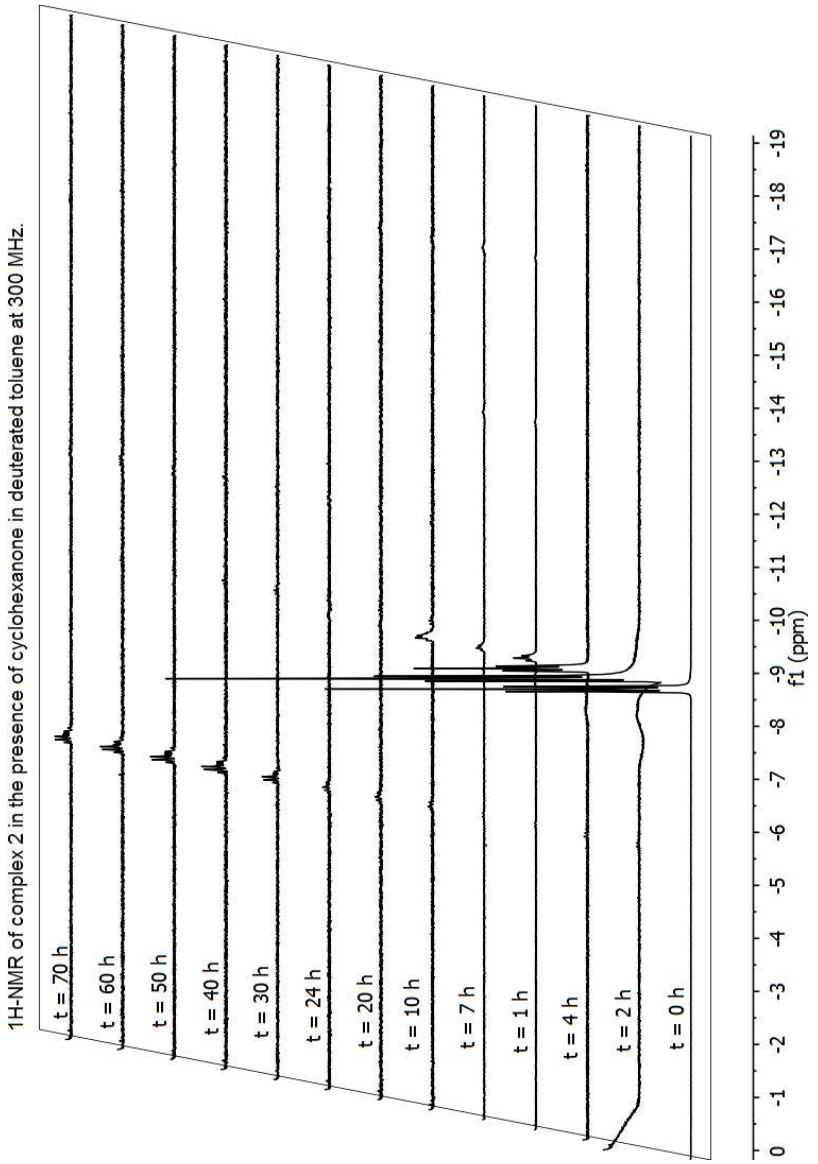

Fig. S 5.94. – Stacked ^{1}H NMR of the hydride area of complex **2** in the presence of 4 eq. cyclohexanone in toluene-d_8 after heating to 80 °C. NMR were recorded after t = 0, 1, 2, 4, 7, 10, 20, 24, 30, 40, 50, 60, 70 h at 300 MHz.

References

[1] J.-H. Choi, N. E. Schloerer, J. Berger, M. H. G. Prechtl, *Dalton Trans.* **2014**, *43*, 290–299.

[2] J.-H. Choi, L. E. Heim, M. Ahrens, M. H. G. Prechtl, *Dalton Trans.* **2014**, *43*, 17248–17254.

5.5. Supporting Information - Miscellaneous Results Part I and II

Jong-Hoo Choi and Martin H. G. Prechtl
Department of Chemistry, University of Cologne, Greinstr. 6, 50939 Cologne, Germany.

Part I

General Remarks

Reactions were generally prepared under an argon atmosphere using *Schlenk* techniques, flame-dried glassware and a *Labmaster 200* glove-box from *MBraun*. All solvents and reagents were purchased from *Acros, Merck, Sigma-Aldrich, Fluka*, or *Strem* or were acquired from the institute stock. Commercial anhydrous solvents and argon as-packed reagents were used as received and stored in the glove-box under argon. Non-anhydrous solvents were dried and distilled (under vacuum or argon) prior to use, applying standard procedures. Complexes are synthesised following the protocol of our previous reports.[1,2] For shortened reaction time to synthesise the complexes, microwave reactions were carried out in a *Monowave 300 microwave* from *Anton Paar* with a maximum power of 850 W at 2.45 MHz.

Analytical Methods

^{1}H, ^{13}C, ^{31}P NMR spectra were recorded at 300 MHz (^{1}H), 75 MHz (^{13}C) and 121 MHz (^{31}P) on a *Bruker Avance II 300*. ^{1}H shifts were reported in ppm (δH) downfield from TMS and were determined by reference to the residual solvent peaks (C_6D_6: 7.16 ppm, C_7D_8: 7.09 ppm.). Chemical shifts were reported as singlet (s), doublet (d), triplet (t), quartet (q) and multiplet (m). Coupling constants J were reported in Hz.

General Description of the Alkylation of Alcohols via ADC

In a *Schlenk* tube, 0.04 mmol of the complex were added. After the addition of 5 mmol hexanol and 5 mmol benzylamine, the *Schlenk* tube was equipped with a condenser and placed in an oil bath. The content was heated to 140 °C for 20 h. Routine ^{1}H NMR and GC-MS (FID) samples were withdrawn after the reaction.

In situ Formation of Catalysts via Microwave Radiation - A General Description for Complex 2

In a 10 mL glass vessel (G10), 20 mg (0.02 mmol) of complex **2** were solvated in 3 mL benzene. After the addition of 21 µL (9.6 eq., 0.4 mmol) of benzylamine and 20.5 µL (10 eq., 0.04 mmol) of hexanol, the vessel was placed in the microwave reactor. After the reaction mixture was heated to 140 °C for 15 min, the solvent was removed in vacuo. The residue was solvated in benzene-d_6 and measured via NMR.

NMR Spectra

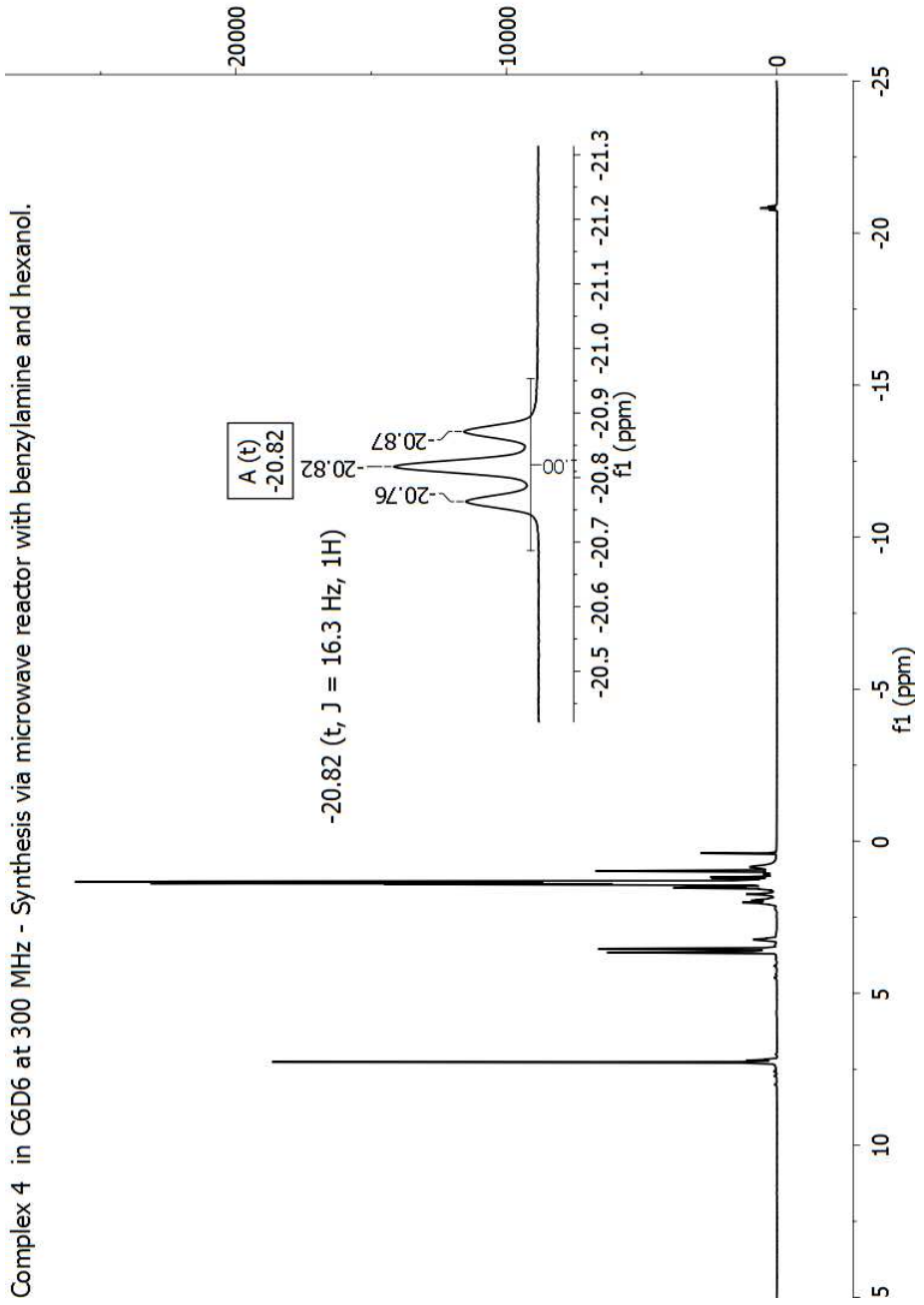

Fig. S 5.95. – ^{1}H NMR spectrum of complex **4** (synthesised in the presence of hexanol and hexylamine) in C_6D_6 at 300 MHz.

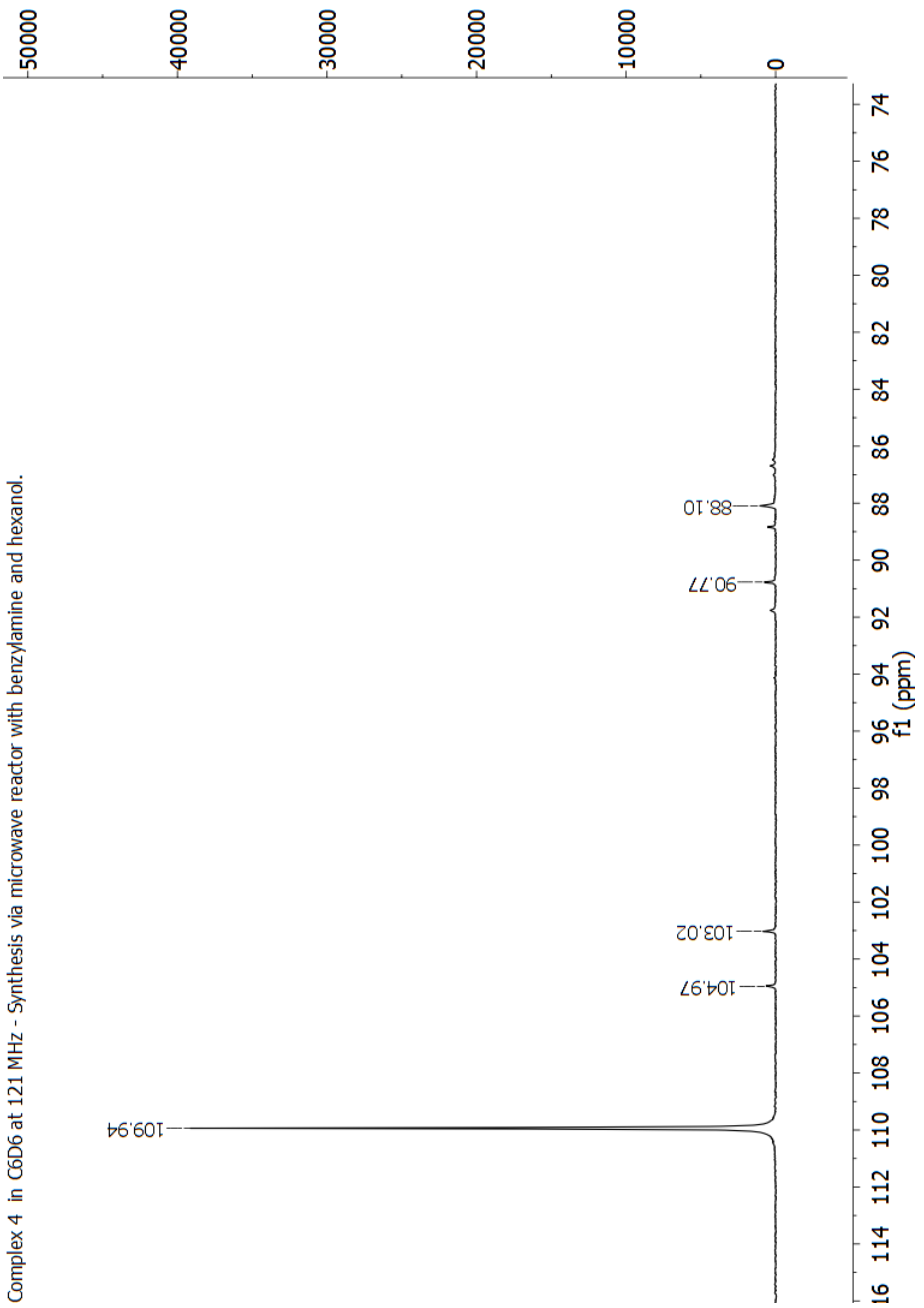

Fig. S 5.96. – $^{31}P\{^{1}H\}$ NMR spectrum of complex **4** (synthesised in the presence of hexanol and hexylamine) in C_6D_6 at 121 MHz.

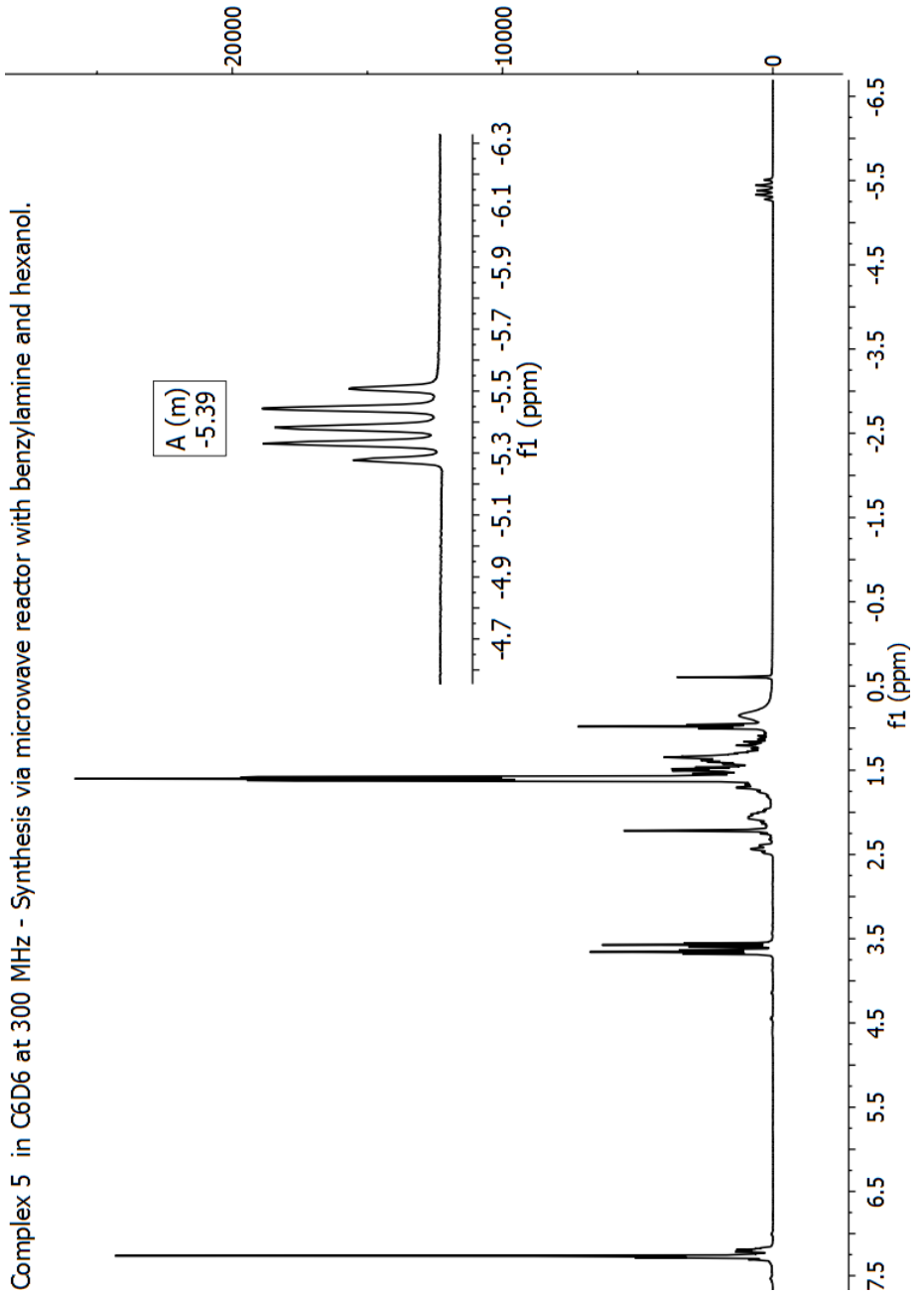

Fig. S 5.97. – ^{1}H NMR spectrum of complex **5** (synthesised in the presence of hexanol and hexylamine) in C_6D_6 at 300 MHz.

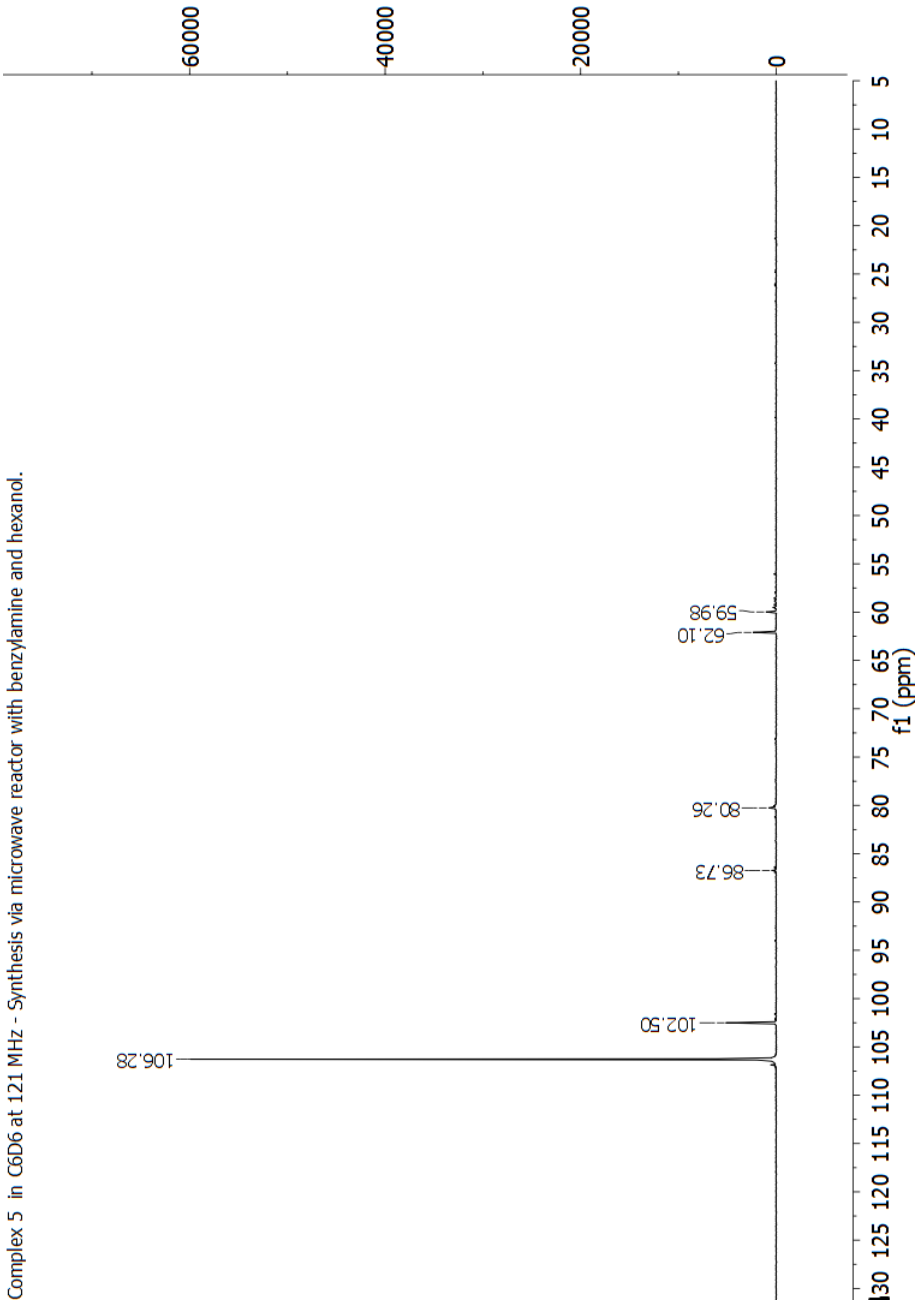

Fig. S 5.98. – $^{31}P\{^{1}H\}$ NMR spectrum of complex **5** (synthesised in the presence of hexanol and hexylamine) in C_6D_6 at 121 MHz.

INSTRUMENT CONTROL PARAMETERS

==========

6890 GC METHOD

==========

OVEN

Initial temp: 50 'C (On) Maximum temp: 340 'C

Initial time: 2.00 min Equilibration time: 0.50 min

Ramps:

#	Rate	Final temp	Final time
1	25.00	300	5.00
2	0.0(Off)		

Post temp: 320 'C

Post time: 5.00 min

Run time: 17.00 min

FRONT INLET (SPLIT/SPLITLESS) BACK INLET (UNKNOWN)

Mode: Split

Initial temp: 300 'C (On)

Pressure: 0.769 bar (On)

Split ratio: 5:1

Split flow: 10.0 mL/min

Total flow: 19.9 mL/min

Gas saver: On

Saver flow: 20.0 mL/min

Saver time: 2.00 min

Gas type: Hydrogen

COLUMN 1 COLUMN 2

Capillary Column (not installed)

Model Number: MN 725820.30

optima 5 accent

Max temperature: 335 'C

Nominal length: 30.0 m

Nominal diameter: 250.00 um

Nominal film thickness: 0.25 um

Mode: constant flow

Initial flow: 2.0 mL/min

Nominal init pressure: 0.769 bar

Average velocity: 52 cm/sec

Inlet: Front Inlet

Outlet: MSD

Outlet pressure: ambient

FRONT DETECTOR (FID) BACK DETECTOR (NO DET)

Temperature: 250 'C (On)

Hydrogen flow: 40.0 mL/min (On)

Air flow: 450.0 mL/min (On)

Mode: Constant makeup flow

Makeup flow: 45.0 mL/min (On)

Makeup Gas Type: Nitrogen

Flame: On

Electrometer: On

Lit offset: 2.0

SIGNAL 1

Data rate: 20 Hz

Type: front detector

Save Data: On

Zero: 0.0 (Off)

Range: 0

Fast Peaks: Off

Attenuation: 0

SIGNAL 2

Data rate: 20 Hz

Type: test plot

Save Data: Off

Zero: 0.0 (Off)

Range: 0

Fast Peaks: Off

Attenuation: 0

COLUMN COMP 1

Derive from front detector

COLUMN COMP 2

Derive from front detector

THERMAL AUX 2

Use: MSD Transfer Line Heater

Description:

Initial temp: 300 'C (On)

Initial time: 0.00 min

#	Rate	Final temp	Final time
1	0.0(Off)		

POST RUN

Post Time: 5.00 min

Oven Temperature: 320 'C

Column 1 Flow: 3.0 mL/min

TIME TABLE

Time	Specifier	Parameter & Setpoint

Miscellaneous Results Part II

General Remarks

Reactions were generally prepared under argon atmosphere using *Schlenk* techniques, flame-dried glassware and a *Labmaster 200* glove-box from *MBraun*. High-pressure amination reactions were performed in a homemade 20 mL stainless steel autoclave. All solvents and reagents were purchased from *Acros, Merck, Sigma-Aldrich, Fluka*, or *Strem* or were acquired from the institute stock. Commercial anhydrous solvents and argon as-packed reagents were used as received and stored in the glove-box under argon. Non-anhydrous solvents were dried and distilled (under vacuum or argon) prior to use, applying standard procedures. For shortening the reaction time to synthesise complex **5**, microwave reactions were carried out in a *Monowave 300 microwave* from *Anton Paar* with a maximum power of 850 W at 2.45 MHz. LIFDI-MS (Liquid Injection Field Desorption/Ionization-Mass Spectrometry) was performed using a *Waters micromass Q-ToF-2*^{TM} mass spectrometer equipped with a *LIFDI 700 ion source (Linden CMS)*.

Analytical Methods

^{1}H, ^{13}C, ^{31}P NMR spectra were recorded at 300 MHz (^{1}H), 75 MHz (^{13}C) and 121 MHz (^{31}P) on a *Bruker Avance II 300*. ^{1}H shifts were reported in ppm (δH) downfield from TMS and were determined by reference to the residual solvent peaks (C_6D_6: 7.16 ppm, C_7D_8: 7.09 ppm). Chemical shifts were reported as singlet (s), doublet (d), triplet (t), quartet (q) and multiplet (m). Coupling constants J were reported in Hz. Infrared spectra (IR) were measured at room temperature with a *Bruker Alpha* spectrometer equipped with a Diamond-ATR IR unit.

Synthesis of Pyrrole PNP Ligand 9

Synthesis of ligand precursor 8: In to a 500 mL *Schlenk* flask, 9.09 g (110.4 mmol) of dimethylamine hydrochloride were placed. Water was added until solvation of the content. After cooling to 0 °C in an ice bath, 8.9 mL (110.4 mmol) 37% aqueous formaldehyde solution was added drop-wise into the content. After the reaction mixture was stirred for 15 min in the ice bath, 3.85 mL (55.7 mmol) of pyrrole **8** were added drope-wise. The reaction mixture was stirred in the ice bath for another 1 h. At ambient temperature (23 °C), the content was stirred over night. Approximately 20 mL of a 15% NaOH solution were added to the mixture until a pH value of 12 was reached. After water was added to the content to solvate the crystallised sodium chloride salt, the reaction mixture was extracted three times each with 30 mL diethylether. The organic phase was combined and the amount of the diethylether was removed under reduced pressure until 30 mL of the total volume was left. The organic

phase was dried over magnesium sulfate and filtrated. After the diethylether was removed in vacuo, a yellow oil was obtained, which was subsequently purified under vacuum distillation (105 °C, oil bath at $7*10^{-3}$ mbar. The product was isolated as a yellow oil with 54% yield. Yield: 5.41 g, 29.8 mmol, 54%. ^{1}H NMR (300 MHz, benzene-d_6): δH [ppm] = 5.82-5.80 (d, 2H, pyrrole), 3.24 (s, 4H, -CH_2-), 2.08 (s, N(CH_3)$_2$).

Synthesis of pyrrole PNP ligand 9: In an argon flushed, flame-dried *Schlenk* tube, 1.08 g (6 mmol) of **8** were placed. 2.3 mL (12.3 mmol) di-*tert*-butyl phosphine were added drop-wise to the content and heated in neat condition at 140 °C for 20 h. Ligand **9** was obtained as a dark-red oil and was used without any further purification. Yield: 2.3 g, 6 mmol, 100% (purification grade: 86% according to ^{31}P{^{1}H} NMR). ^{1}H NMR (300 MHz, benzene-d_6): δH [ppm] = 6.06-6.05 (d, 2H, pyrrole), 2.72 (s, 4H, -CH_2-), 1.06-1.02 (d, PC(CH_3)$_2$). ^{31}P{^{1}H} NMR (121 MHz, benzene-d_6): δP [ppm] = 22.5 (s).

Synthesis of Complex 5

Synthesis of complex-intermediate 11: In a argon flushed *Büchi tiny clave* glass autoclave 150 mg (0.4 mmol) of ligand **9** were solvated in 3 mL pentane. After the addition of 115.5 mg (0.36 mmol) of [Ru(COD)(2-methylallyl)$_2$] **12**, the autoclave was pressurised to 6 bar with H_2 gas and heated to 60 °C for 18 h. After the appropriate reaction time, the autoclave was depressurised to atmospheric pressure. In a flame-dried *Schlenk* tube, the solvent was removed in vacuo until a dark-red oil was obtained. Routine NMR analysis were performed for further confirmation. Significant signals are listed below:
^{1}H NMR (300 MHz, benzene-d_6): δH [ppm] = 1.17 (m, 36H, PC(CH_3)$_2$), -15.39 (m, Ru-H).
^{31}P{^{1}H} NMR (121 MHz, benzene-d_6): δP [ppm] = 105.0 (s).

Synthesis of complex 5: In a 10 mL microwave glass vessel (G10), the product **11** (0.36 mmol) was solvated in 3 mL toluene. After the addition of 70 µL (1.2 mmol) ethanol, the content was heated under microwave radiation at 150 °C for 15 min (850 W at 2.45 MHz). After the content was placed in a flame-dried 100 mL *Schlenk* flask, the solvent was removed in vacuo and replaced with 20 mL of diethylether. The *Schlenk* flask was put into dry ice to force the crystallisation of complex **5** as a orange solid. The mother-liquor was removed via cannula and the solid was dried in vacuo. Yield: 54.8 mg, 0.1 mmol, 25%.
LIFDI-MS/MS: m/z 507.3 (17.2), 510.2 (6.9), 510.3 (13.8), 511.3 (27.6), 512.3 (62.1), 512.3 (20.7), 513.3 (100.0), 513.3 (31.0), 514.2 (10.3), 515.2 (6.9), 515.3 (44.8), 515.3 (13.8), 516.4 (6.9).

^{1}H NMR (300 MHz, benzene-d_6): δH [ppm] = 6.53 (s, 2H, pyrrole), 3.13 (t, 4H, $^{2}J_{PH}$ = 7.8 Hz, CH_2), 1.11 (m, 36H, PC(CH_3)$_3$), -25.57 (t, 1H, $^{3}J_{PH}$ = 17.2 Hz, Ru-H). ^{13}C$_{APT}$ NMR

(75 MHz, benzene-d_6): δC [ppm] = 140.2 (s, pyrrole, *C*H), 105.51 (t, $^{3}J_{CP}$, pyrrole, C_q), 37.1 (s, -*C*H_2-), 30.4 (t, $^{2}J_{CP}$ = 3.0 Hz, PC(*CH*$_3$)$_3$), 29.7 (t, $^{2}J_{CP}$ = 3.0 Hz, PC(*CH*$_3$)$_3$), 26.8 (t, $^{1}J_{CP}$ = 9.1 Hz, P*C*$(CH_3)_3$). $^{31}P\{^{1}H\}$ NMR (121 MHz, benzene-d_6): δP [ppm] = 101.5 (s).

IR: [cm^1] = 2957-2862 (m), 2168 (w), 2109 (w), 1889 (s), 1559-1536 (w), 1467 (m), 1389 (m), 1365 (w), 1252 (m), 1178 (m), 1123 (m), 1066 (m), 1018 (m), 936 (w), 821 (m), 756 (m), 722 (m), 667 (m), 590 (m), 531 (w), 477 (m), 456 (s), 426 (m).

Catalysis

ADC reaction with hexanol to yield hexyl hexanoate: In a flame-dried *Schlenk* tube, 10 mg (0.02 mmol) of **5** were solvated in 3 mL toluene. After the addition of 2.5 mL (2 mmol) hexanol, the *Schlenk* tube was equipped with a condenser. Under a constant stream of argon, the content was heated to 120 °C and refluxed for 20 h. No conversion was detected in the ^{1}H NMR spectrum. An analogous reaction was performed with additional 1 mol% KO^{t}Bu under the same reaction conditions; no conversion was detected.

ADC reaction with hexanol in the presence of hexyl amine: In a flame-dried *Schlenk* tube 10 mg (0.02 mmol) of **5** were solvated in 3 mL toluene. After the addition of 2.5 mL (2 mmol) hexanol and 2.6 mL (2 mmol) hexylamine , the *Schlenk* tube was equipped with a condenser. Under a constant stream of argon, the content was heated to 120 °C and refluxed for 20 h. No conversion was detected in the ^{1}H NMR spectrum.

Hydrogenation of ethyl acetate: In a 20 mL headspace vial, 10 mg (0.02 mmol) of **5** were solvated in 4 mL THF. After the addition of 0.2 mL (2 mmol) ethyl acetate, the headspace vial was placed in a homemade stainless steel 20 mL autoclave and the autoclave was charged with 50 bar H_2 gas. After 20 h, no conversion was detected in the ^{1}H NMR spectrum.

^{1}H NMR Spectrum of Complex 8

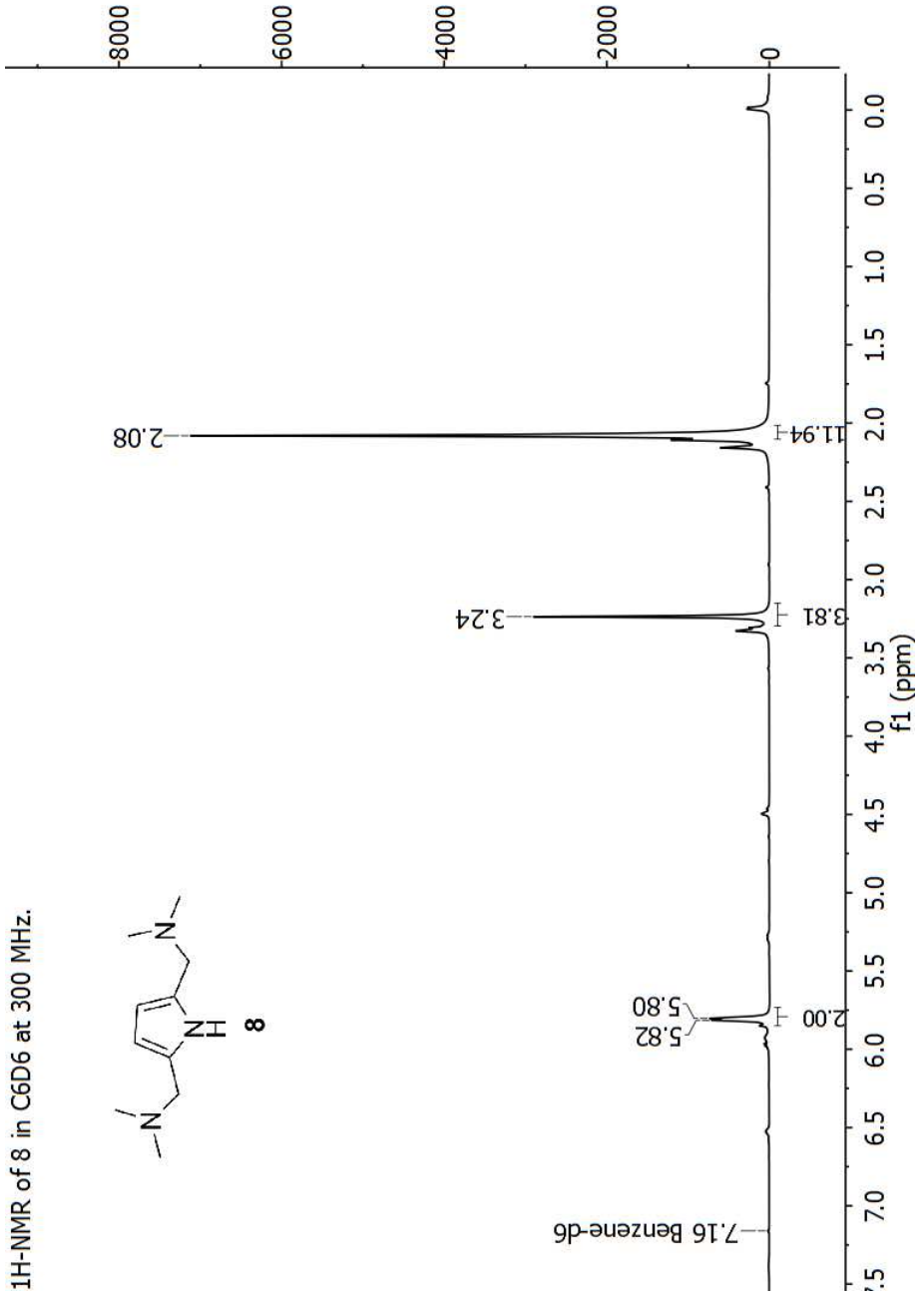

Fig. S 5.99. – ^{1}H NMR spectrum of complex **8** in C_6D_6 at 300 MHz.

^{1}H NMR Spectrum of Ligand 9

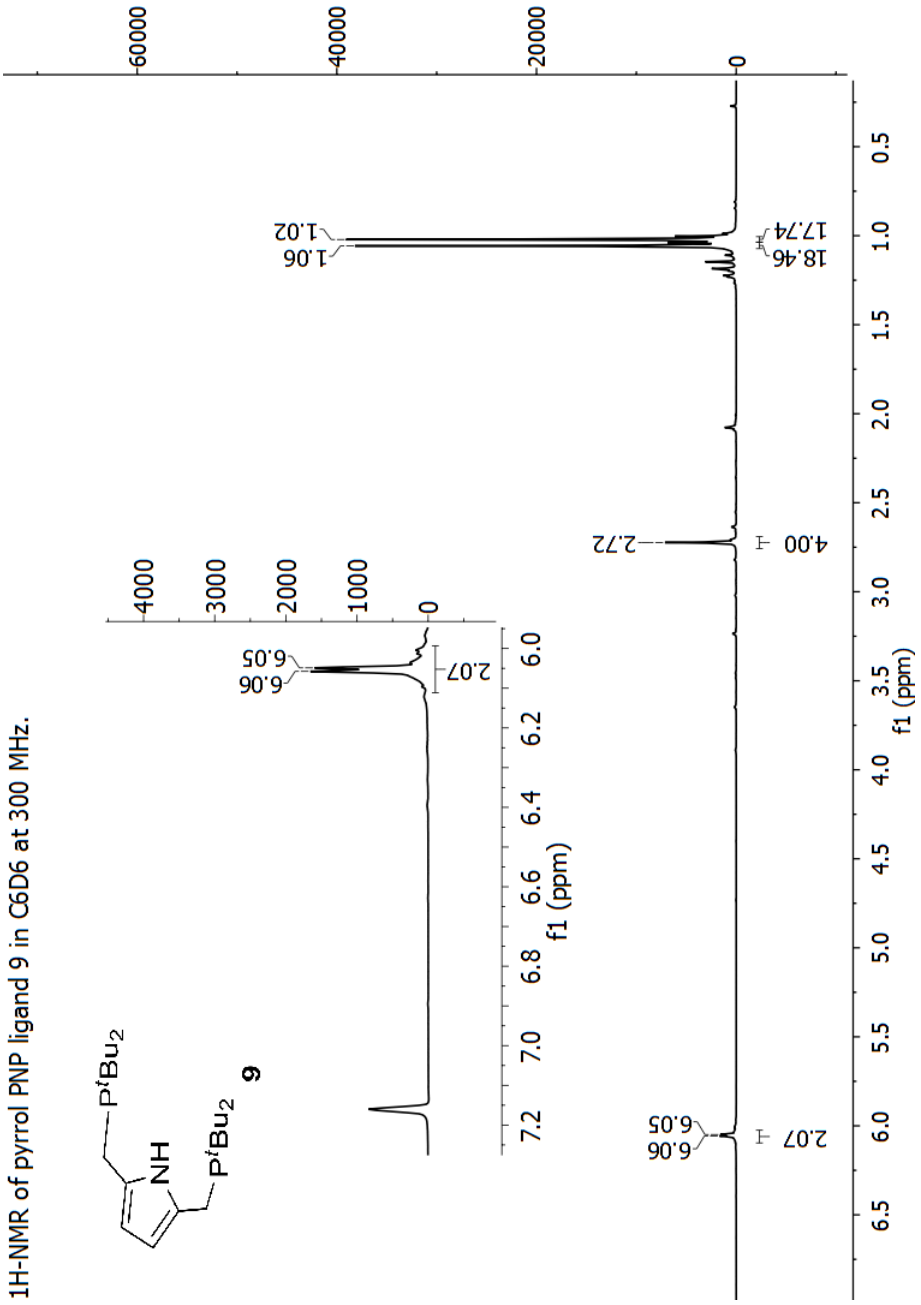

Fig. S 5.100. – ^{1}H NMR spectrum of ligand **9** in C_6D_6 at 300 MHz.

$^{31}P\{^{1}H\}$ NMR Spectrum of Ligand 9

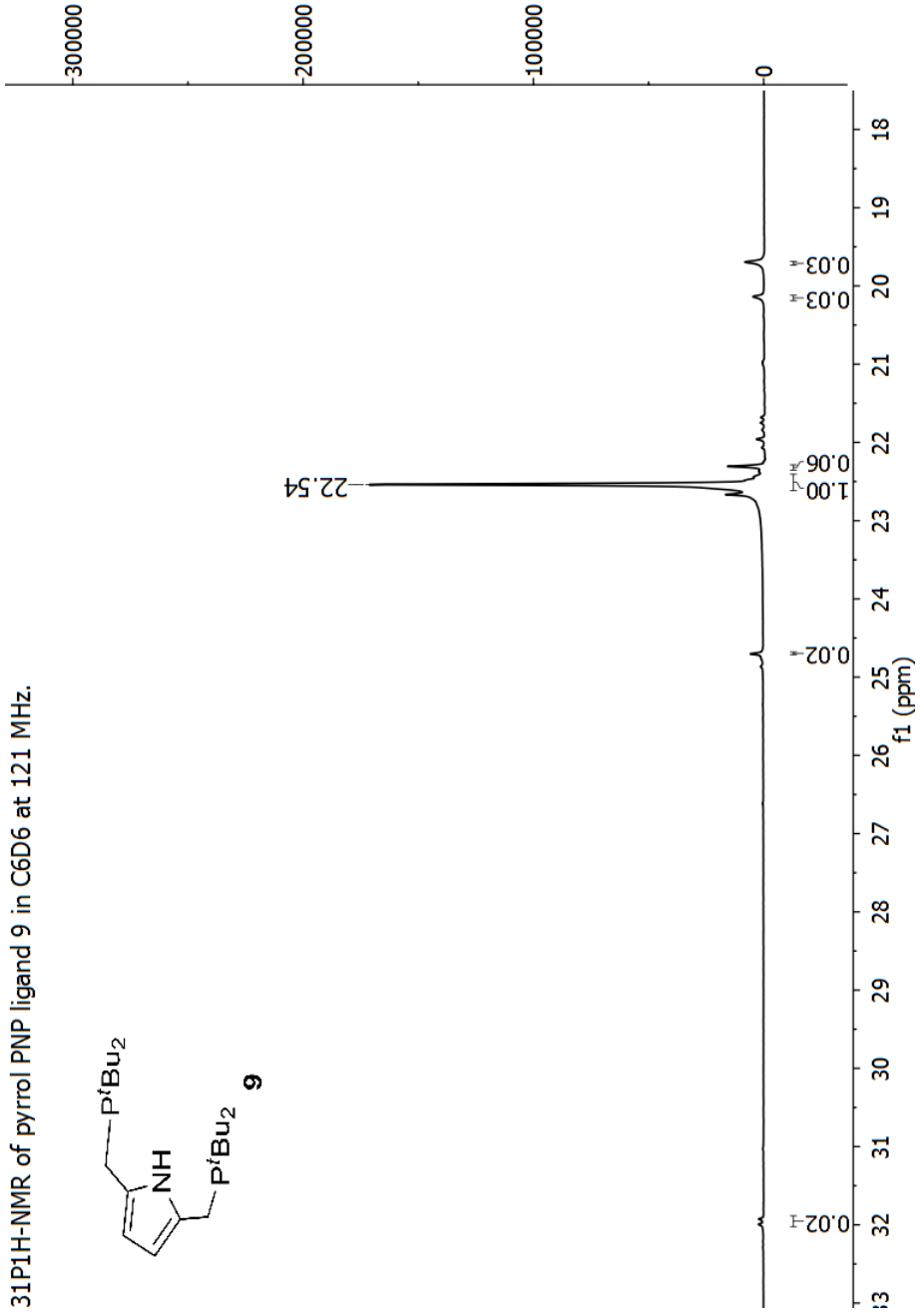

Fig. S 5.101. – $^{31}P\{^{1}H\}$ NMR spectrum of ligand **9** in C_6D_6 at 121 MHz.

^{1}H NMR Spectrum of Complex 11

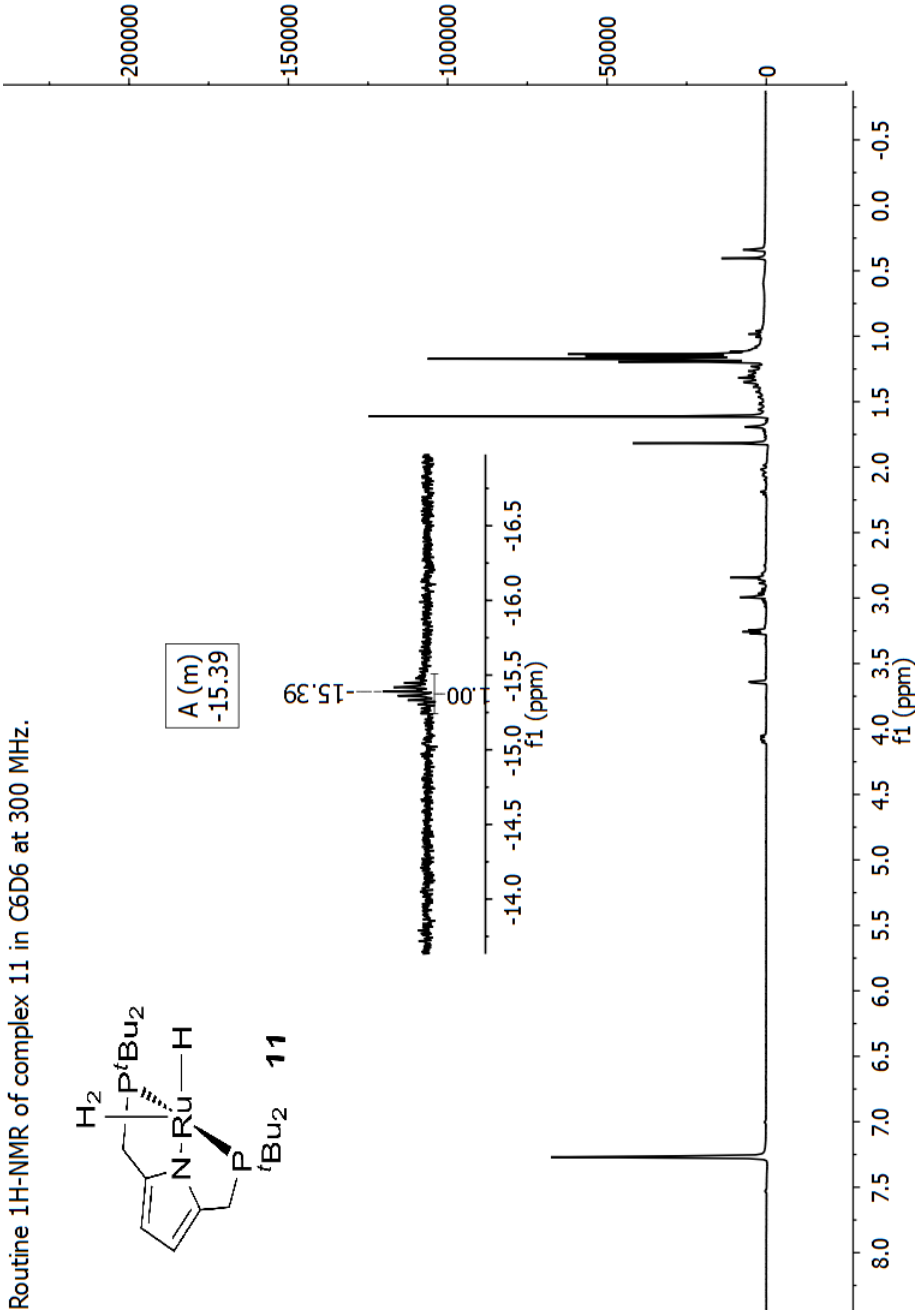

Fig. S 5.102. – ^{1}H NMR spectrum of complex **11** in C_6D_6 at 300 MHz.

$^{31}P\{^{1}H\}$ NMR Spectrum of Complex 11

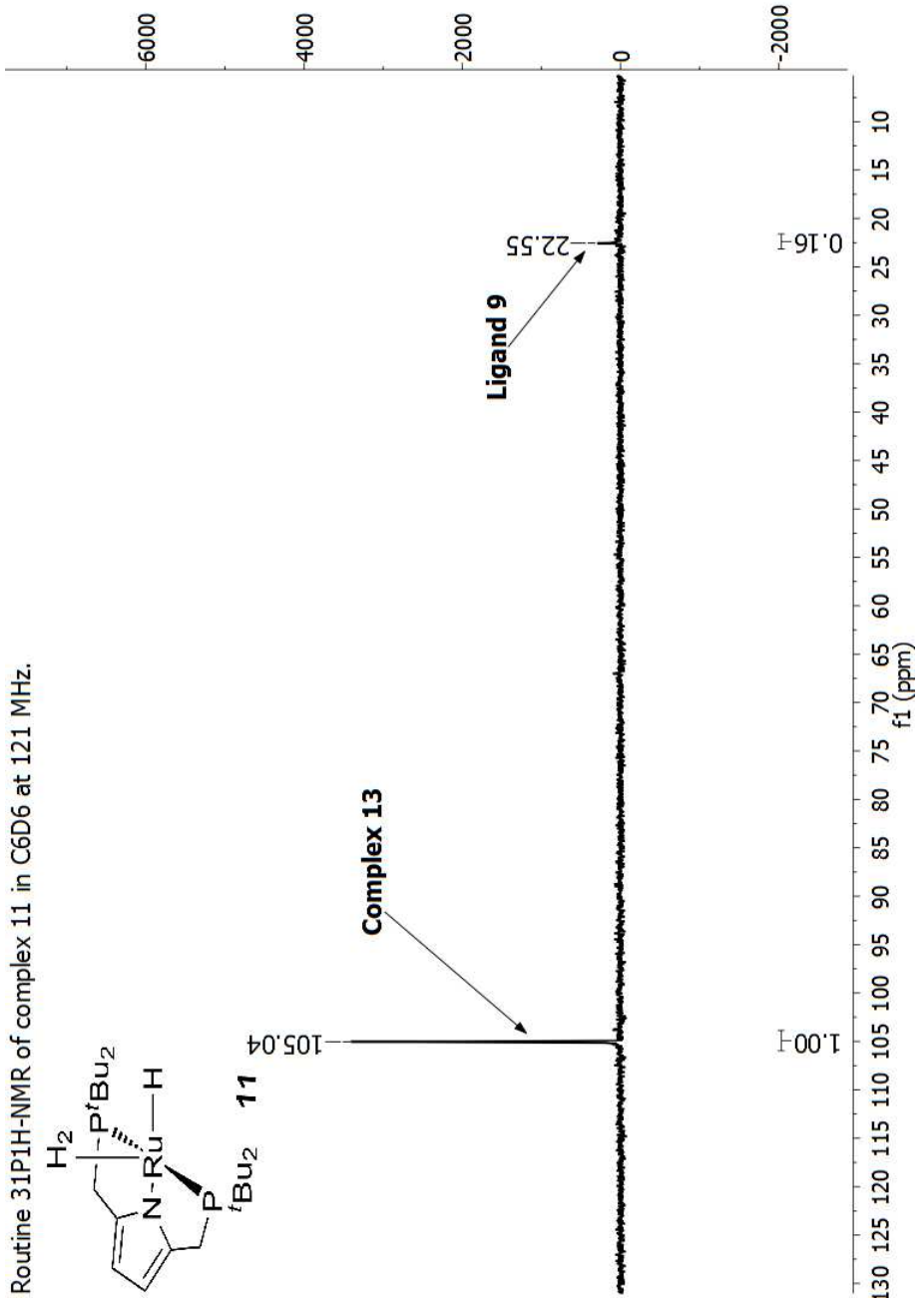

Fig. S 5.103. – $^{31}P\{^{1}H\}$ NMR spectrum of complex **11** in C_6D_6 at 121 MHz.

^{1}H NMR Spectrum of Complex 5

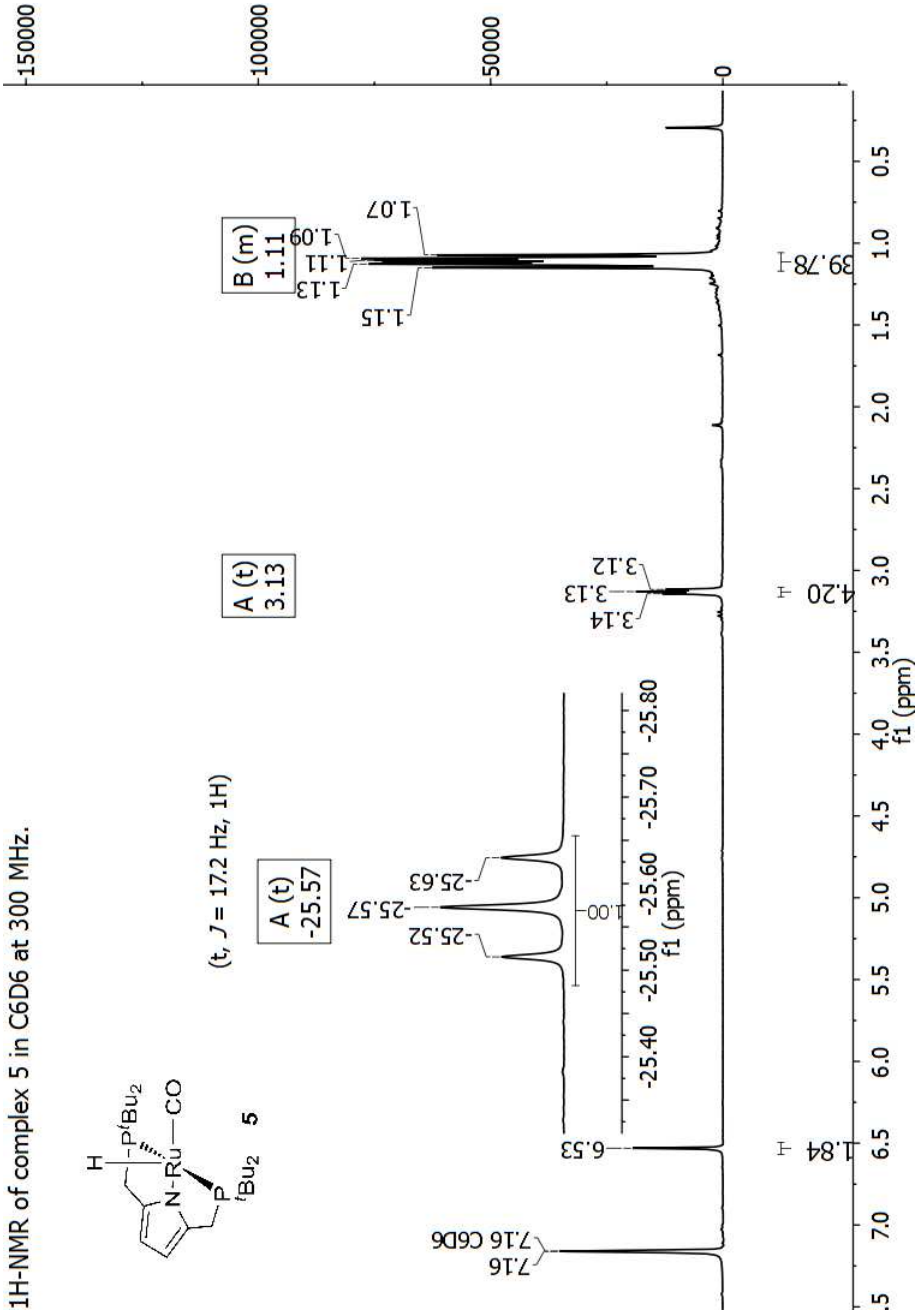

Fig. S 5.104. – ^{1}H NMR Spectrum of complex **5** in C_6D_6 at 300 MHz.

$^{31}P\{^{1}H\}$ NMR Spectrum of Complex 5

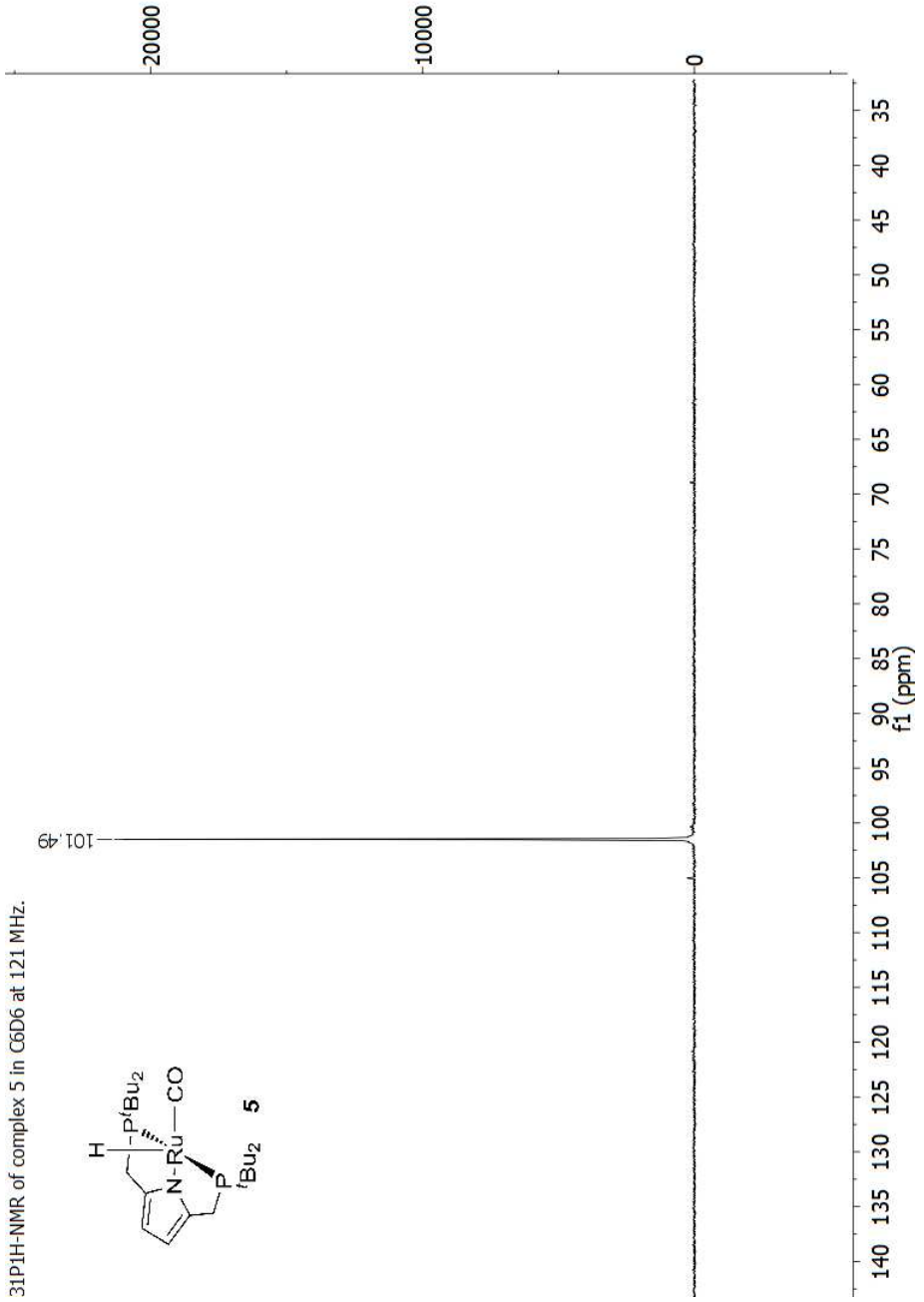

Fig. S 5.105. – $^{31}P\{^{1}H\}$ NMR spectrum of complex **5** in C_6D_6 at 121 MHz.

$^{13}C_{APT}$ NMR Spectrum of Complex 5

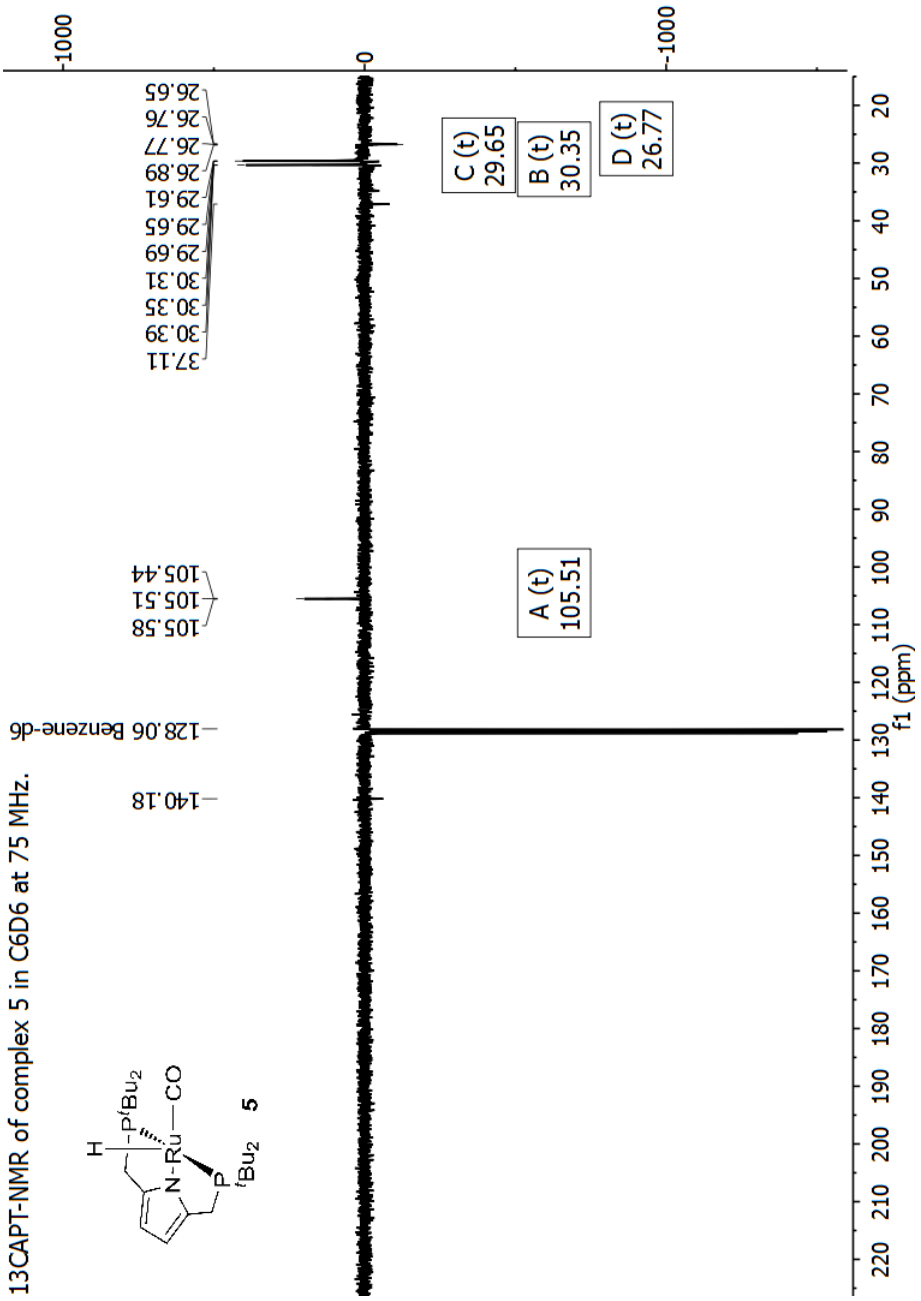

Fig. S 5.106. – $^{13}C_{APT}$ NMR spectrum of complex **5** C_6D_6 at 75 MHz.

IR Spectrum of Complex 5

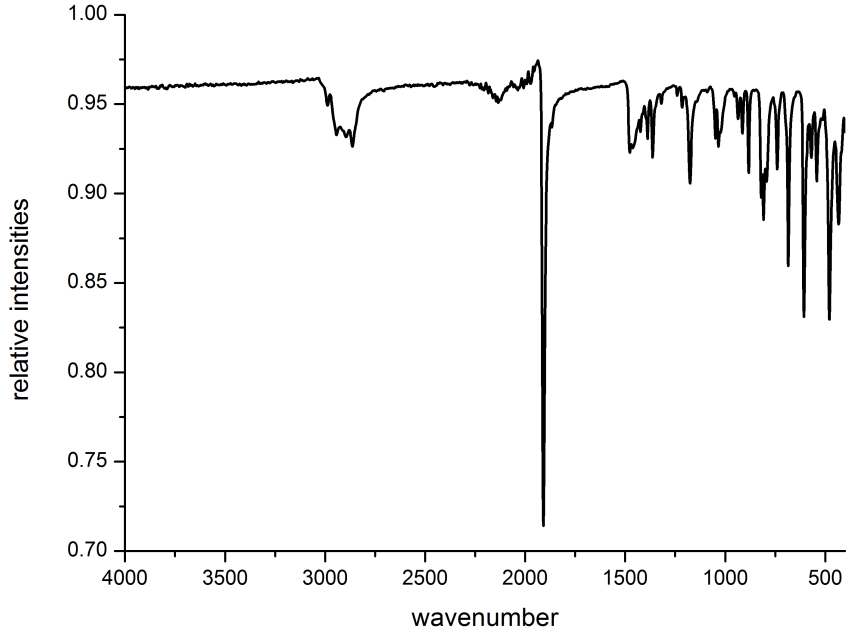

Fig. S 5.107. – IR spectrum of complex **5**.

LIFDI MS/MS of Complex 5

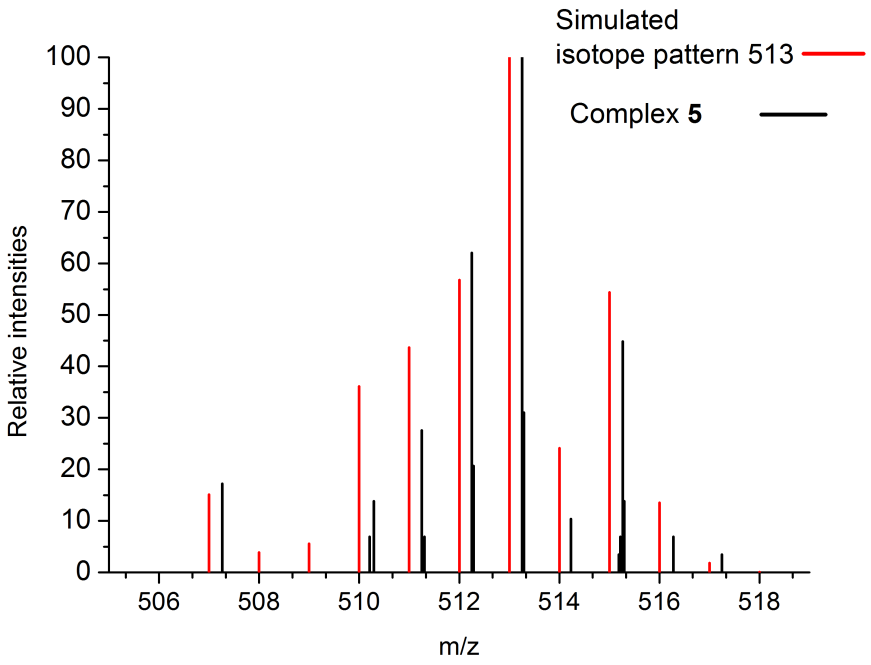

Fig. S 5.108. – LIFDI MS/MS spectrogram of complex **5** (black) and the simulated isotope pattern 513 (red) in toluene, r.t. 1.94 min, 507-518.

List of Schemes

List of Figures

List of Tables

5.6. Reprint Permissions and Copyrights

Permissions from Wiley-VCH (Weinheim) and the Royal Society of Chemistry (London) for the included publications in this manuscripts. All corresponding (co-)authors are aware of the actions of including this manuscript into the author's (Jong-Hoo Choi) doctoral thesis.

1. Jong-Hoo Choi, Nils E. Schloerer, Josefine Berger and Martin H. G. Prechtl*, Synthesis and characterisation of ruthenium dihydrogen complexes and their reactivity towards B–H bonds, *Dalton Transactions*, **2014**, *43*, 290-299 (Full-Paper).[1]

2. Jong-Hoo Choi, Leo E. Heim, Mike Ahrens, Martin H. G. Prechtl*, Selective conversion of alcohols in water to carboxylic acids by *in situ* generated ruthenium trans dihydrido carbonyl PNP complexes, *Dalton Transactions*, **2014**, *43*, 17248-17254 (Full-Paper).

3. Jong-Hoo Choi, Martin H. G. Prechtl*, Tuneable Hydrogenation of Nitriles into Imines or Amines with a Ruthenium Pincer Complex under Mild Conditions, *ChemCatChem*, **2015**, *7*, 1023–1028 (Full-Paper).

All corresponding (co-)authors are aware of the action of including this manuscript into the author's (Jong-Hoo Choi) doctoral thesis:

1. Dennis Pingen, Jong-Hoo Choi, Martin H. G. Prechtl*, Dieter Vogt*, Amide vs. Amine Paradigm in the Direct Amination of Alcohols with Ru-PNP Complexes, *ACS Catalysis*, **2015**, (Full-Paper, manuscript in preparation).

[1] In this publication complex system **4/5** was discussed in the diploma thesis by the author Jong-Hoo Choi in 2012. An "Additions and Corrections" manuscript was submitted and published (), see Appendix.

RSC | Advancing the Chemical Sciences

Royal Society of Chemistry
Thomas Graham House
Science Park
Milton Road
Cambridge
CB4 0WF

Tel: +44 (0)1223 420 066
Fax: +44 (0)1223 423 623
Email: contracts-copyright@rsc.org

www.rsc.org

Acknowledgements to be used by RSC authors

Authors of RSC books and journal articles can reproduce material (for example a figure) from the RSC publication in a non-RSC publication, including theses, without formally requesting permission providing that the correct acknowledgement is given to the RSC publication. This permission extends to reproduction of large portions of text or the whole article or book chapter when being reproduced in a thesis.

The acknowledgement to be used depends on the RSC publication in which the material was published and the form of the acknowledgements is as follows:

- For material being reproduced from an article in *New Journal of Chemistry* the acknowledgement should be in the form:
  - [Original citation] - Reproduced by permission of The Royal Society of Chemistry (RSC) on behalf of the Centre National de la Recherche Scientifique (CNRS) and the RSC
- For material being reproduced from an article *Photochemical & Photobiological Sciences* the acknowledgement should be in the form:
  - [Original citation] - Reproduced by permission of The Royal Society of Chemistry (RSC) on behalf of the European Society for Photobiology, the European Photochemistry Association, and RSC
- For material being reproduced from an article in *Physical Chemistry Chemical Physics* the acknowledgement should be in the form:
  - [Original citation] - Reproduced by permission of the PCCP Owner Societies
- For material reproduced from books and any other journal the acknowledgement should be in the form:
  - [Original citation] - Reproduced by permission of The Royal Society of Chemistry

The acknowledgement should also include a hyperlink to the article on the RSC website.

The form of the acknowledgement is also specified in the RSC agreement/licence signed by the corresponding author.

Except in cases of republication in a thesis, this express permission does not cover the reproduction of large portions of text from the RSC publication or reproduction of the whole article or book chapter.

A publisher of a non-RSC publication can use this document as proof that permission is granted to use the material in the non-RSC publication.

Datum: 19.05.2015 [15:07:47 CEST]
Von: "CONTRACTS-COPYRIGHT (shared)" <Contracts-Copyright@rsc.org>
An: "'jong-hoo.choi@uni-koeln.de'" <jong-hoo.choi@uni-koeln.de>
Betreff: RE: permission requests for my thesis

Dear Jong-Hoo Choi

The Royal Society of Chemistry (RSC) hereby grants permission for the use of your paper(s) specified below in the printed and microfilm version of your thesis. You may also make available the PDF version of your paper(s) that the RSC sent to the corresponding author(s) of your paper(s) upon publication of the paper(s) in the following ways: in your thesis via any website that your university may have for the deposition of theses, via your university's Intranet or via your own personal website. We are however unable to grant you permission to include the PDF version of the paper(s) on its own in your institutional repository. The Royal Society of Chemistry is a signatory to the STM Guidelines on Permissions (available on request).

Please note that if the material specified below or any part of it appears with credit or acknowledgement to a third party then you must also secure permission from that third party before reproducing that material.

Please ensure that the thesis states the following:

Reproduced by permission of The Royal Society of Chemistry

and include a link to the paper on the Royal Society of Chemistry's website.

Please ensure that your co-authors are aware that you are including the paper in your thesis.

This permission extends to the cover designed by your group.

Regards

Gill Cockhead
Publishing Contracts & Copyright Executive

Gill Cockhead
Publishing Contracts & Copyright Executive
Royal Society of Chemistry,
Thomas Graham House,
Science Park, Milton Road,
Cambridge, CB4 0WF, UK
Tel +44 (0) 1223 432134

Follow the Royal Society of Chemistry:
www.rsc.org/follow

Winner of The Queen's Award for Enterprise, International Trade 2013

-----Original Message-----
From: jong-hoo.choi@uni-koeln.de [mailto:jong-hoo.choi@uni-koeln.de]
Sent: 15 May 2015 10:36
To: CONTRACTS-COPYRIGHT (shared)
Subject: permission requests for my thesis

Dear RSC editors,

for my purpose to write a cumulative phD thesis (non-commercial use), it is my intention to integrate my two articles into my thesis. Both articles are published in Dalton Transactions.

Dalton Trans., 2014, 43, 290-299
DOI: 10.1039/C3DT52037D
Dalton Trans., 2014, 43, 17248-17254
DOI: 10.1039/C4DT01634C

For this purpose, I want to ask you for an official permission form to re-print both publications incl. figures, schemes, tables, text-contents, "addition and correction" and the supporting information manuscripts in my thesis.
For my second publication in Dalton Trans., 2014, 43, 17248-17254, I also want to re-print the Journal-Cover-Letter (December, 2014, no 46), which is designed by our group.

Many thanks in advance and I am looking for your reply.
Sincerly yours,
Jong-Hoo Choi

DISCLAIMER:

This communication (including any attachments) is intended for the use of the addressee only and may contain confidential, privileged or copyright material. It may not be relied upon or disclosed to any other person without the consent of the Royal Society of Chemistry. If you have received it in error, please contact us immediately. Any advice given by the Royal Society of Chemistry has been carefully formulated but is necessarily based on the information available, and the Royal Society of Chemistry cannot be held responsible for accuracy or completeness. In this respect, the Royal Society of Chemistry owes no duty of care and shall not be liable for any resulting damage or loss. The Royal Society of Chemistry acknowledges that a disclaimer cannot restrict liability at law for personal injury or death arising through a finding of negligence. The Royal Society of Chemistry does not warrant that its emails or attachments are Virus-free: Please rely on your own screening. The Royal Society of Chemistry is a charity, registered in England and Wales, number 207890 - Registered office: Thomas Graham House, Science Park, Milton Road, Cambridge CB4 0WF

JOHN WILEY AND SONS LICENSE
TERMS AND CONDITIONS

Jul 29, 2015

This Agreement between Jong ("You") and John Wiley and Sons ("John Wiley and Sons") consists of your license details and the terms and conditions provided by John Wiley and Sons and Copyright Clearance Center.

License Number	3678081475796
License date	Jul 29, 2015
Licensed Content Publisher	John Wiley and Sons
Licensed Content Publication	ChemCatChem
Licensed Content Title	Tuneable Hydrogenation of Nitriles into Imines or Amines with a Ruthenium Pincer Complex under Mild Conditions
Licensed Content Author	Jong-Hoo Choi,Martin H. G. Prechtl
Licensed Content Date	Mar 2, 2015
Pages	6
Type of use	Dissertation/Thesis
Requestor type	Author of this Wiley article
Format	Print and electronic
Portion	Full article
Will you be translating?	No
Title of your thesis / dissertation	Catalytic Activation of Small Molecules - Development and Characterisation of Ruthenium Complexes for Application in Catalysis
Expected completion date	Dec 2015
Expected size (number of pages)	260
Requestor Location	Jong-Hoo Choi Greinstr.6 Cologne, Germany 50939 Attn: Jong-Hoo Choi
Billing Type	Invoice
Billing Address	Jong-Hoo Choi Greinstr.6 Cologne, Germany 50939 Attn: Jong-Hoo Choi
Total	0.00 EUR
Terms and Conditions	

5.7. List of Publications and The Author's Contributions to each Publication

Articles

- D. Pingen, J.-H. Choi, M. H. G. Prechtl, D. Vogt, *ACS Catalysis* **2015**, manuscript in preparation, "Amide vs. Amine Paradigm in the Direct Amination of Alcohols with Ru-PNP Complexes".

- J.-H. Choi, M. H. G. Prechtl, *ChemCatChem* **2015**, *7*, 1023-1028, doi:10.1002/cctc.201403047, "Tuneable hydrogenation of nitriles into imines or amines with a ruthenium pincer complex".

- J.-H. Choi, L. E. Heim, M. Ahrens, M. H. G. Prechtl, *Dalton Transactions* **2014**, *43*, 17248-17254, *Cover-Art Letter*, doi:10.1039/c4dt01634c, "Selective conversion of alcohols in water to carboxylic acids by in situ generated ruthenium trans dihydrido carbonyl PNP complexes".

- L. E. Heim, N. Schloerer, J.-H. Choi, M. H. G. Prechtl, *Nature Communications* **2014**, Article number: 3621, doi:10.1038/ncomms4621, "Selective and mild hydrogen production using water and formaldehyde".

- J.-H. Choi, N. Schloerer, J. Berger, M. H. G. Prechtl, *Dalton Transactions* **2014**, *43*, 290-299, doi:10.1039/c3dt52037d, "Synthesis and characterisation of ruthenium dihydrogen complexes and their reactivity towards B–H bonds".

Conference Presentations

- 2015, 48. Jahrestreffen Deutscher Katalytiker, annual meeting of german catalysts, Weimar, Germany. Poster presentation, J.-H. Choi, M. H. G. Prechtl, "Tuneable hydrogenation of nitriles into imines or amines with a ruthenium pincer complex".
- 2015, 48. Jahrestreffen Deutscher Katalytiker, annual meeting of german catalysts, Weimar, Germany. Poster presentation, D. Pingen, J.-H. Choi, M. H. G. Prechtl, D. Vogt, "New insights in the importance of ligand binding mode in the direct amination of alcohols using ammonia."
- 2014, 7th Green Solvents Conference, Dresden, Germany. Poster presentation, L. E. Heim, N. E. Schloerer, J.-H. Choi, M. H. G. Prechtl, "Catalytic Hydrogen Production using Water and Formaldehyde as Hydrogen Source".
- 2014, 7th Green Solvents Conference, Dresden, Germany. Poster presentation, J.-H. Choi, M. H. G. Prechtl, "Mechanistic insight into the catalytic dehydrogenation of alcohols and the effect of water".
- 2014, 7th Green Solvents Conference, Dresden, Germany. Oral presentation, L. E. Heim, N. E. Schloerer, J.-H. Choi, M. H. G. Prechtl, "Catalytic Hydrogen Production using Water and Formaldehyde as Hydrogen Source".
- 2014, Vortragstagung für Anorganische Chemie der Wöhler-Vereinigung 2014, Saarbruecken, Germany. Oral presentation, L. E. Heim, N. E. Schloerer, J.-H. Choi, M. H. G. Prechtl, "Catalytic Hydrogen Production using Water and Formaldehyde as Hydrogen Source".
- 2014, XXVI ICOMC, 26. International Conference on Organometallic Chemistry, Sapporo, Japan. Oral presentation, L. E. Heim, N. E. Schloerer, J.-H. Choi, M. H. G. Prechtl, "Catalytic Hydrogen Production using Water and Formaldehyde as Hydrogen Source".
- 2014, 19th ISHC, International Symposium on Homogeneous Catalysis (ISHC-XIX), Ottawa, ON, Canada. Oral presentation, L. E. Heim, N. E. Schloerer, J.-H. Choi, M. H. G. Prechtl, "Catalytic Hydrogen Production using Water and Formaldehyde as Hydrogen Source".
- 2014, EKC 2014, EU-Korea Conference on Science and Technology, Vienna, Austria. Oral and poster presentation, poster price award winner, J.-H. Choi, M. H. G. Prechtl, "Direct conversion of alcohols in water to carboxylic acids – a "green" approach towards sustainable chemistry".

- 2014, 19th ISHC, International Symposium on Homogeneous Catalysis (ISHC-XIX), Ottawa, ON, Canada. J.-H. Choi, L. E. Heim, M. H. G. Prechtl, "Mechanistic insight into the catalytic dehydrogenation of alcohols and the effect of water".

- 2014, 47. Jahrestreffen Deutscher Katalytiker, annual meeting of german catalysts, Weimar, Germany. Poster presentation, J.-H. Choi, L. E. Heim, M. H. G. Prechtl, "Mechanistic insight into the catalytic dehydrogenation of alcohols and the effect of water".

- 2013, 20th EuCheMS Conference on Organometallic Chemistry (EuCOMC XX), St. Adrews, UK. J.-H. Choi, N. Schloerer, M. H. G. Prechtl, "Synthesis Characterisation of [Ru-H_2] Complexes and their Reactivity towards E-H Bonds (E-H = O-H, N-H, C-H, B-H)".

- 2013, OMCOS 17, 17. International IUPAC Conference on Organometallic Chemistry Directed Towards Organic Synthesis, Fort Collins, CO, USA. Poster presentation, J.-H. Choi, N. Schloerer, M. H. G. Prechtl, "Synthesis and Characterisation of Ruthenium Dihydrogen Complexes and their Reactivity towards Functional Groups."

- 2013, 46. Jahrestreffen Deutscher Katalytiker, annual meeting of german catalysts, Weimar, Germany. Poster presentation, J.-H. Choi, N. Schloerer, M. H. G. Prechtl, "Development of Dehydrogenation Catalysts: Synthesis, Characterisation and Evaluation for Reactions with Hydrogen Evolution".

- 2012, XXV ICOMC, 25. International Conference on Organometallic Chemistry, Lisbon, Portugal. Oral and poster presentation, J.-H. Choi, N. Schloerer, M. H. G. Prechtl, "Development of Dehydrogenation Catalysts: Synthesis, Characterisation and Evaluation for Reactions with Hydrogen Evolution".

Table 5.5. – Author's Contributions to Publications.

Title	Article type	Planning	Experiments	Analytics	Manuscript	**Sum**
J.-H. Choi, N. E. Schloerer, J. Berger, M. H. G. Prechtl*, *Dalton Trans.* **2014**, *43* , 290-299.	Scientific article	80%	95%	75%	85%	84%
J.-H. Choi, L. E. Heim, M. Ahrens, M. H. G. Prechtl*, *Dalton Trans.* **2014**, *43*, 17248-17254.	Scientific article	90%	95%	85%	85%	89%
J.-H. Choi, M. H. G. Prechtl*, *ChemCatChem* **2015**, *7*, 1023-1028.	Scientific article	90%	95%	95%	85%	91%
	Overall sum	**87%**	**95%**	**85%**	**85%**	**88%**

5.8. Erklärung

Ich versichere, dass ich die von mir vorgelegte Dissertation selbständig angefertigt, die benutzten Quellen und Hilfsmittel vollständig angegeben und die Stellen der Arbeit -einschließlich Tabellen, Karten und Abbildungen-, die anderen Werken im Wortlaut oder dem Sinn nach entnommen sind, in jedem Einzelfall als Entlehnung kenntlich gemacht habe; dass diese Dissertation noch keiner anderen Fakultät oder Universität zur Prüfung vorgelegen hat; dass sie - abgesehen von unten angegebenen Teilpublikationen - noch nicht veröffentlicht worden ist sowie, dass ich eine solche Veröffentlichung vor Abschluss des Promotionsverfahrens nicht vornehmen werde. Die Bestimmungen der Promotionsordnung sind mir bekannt. Die von mir vorgelegte Dissertation ist von Priv.-Doz. Dr. Martin H. G. Prechtl betreut worden.

Ort (Location), Datum (Date) *Jong-Hoo Choi*

5.9. Akademischer Lebenslauf

Name	Jong-Hoo Choi
Geboren am	7. März 1986
Geburtsort	Seoul, Republik Korea
Nationalität	Deutsch/Republik Korea
08/2012 - 10/2015	Promotionsstudium zur Erlangung des Doktorgrades (Dr. rer. nat.) im Institut für Anorganische Chemie, Universität zu Köln. Arbeiten zum Thema: "Catalytic Activation of Small Molecules - Development and Characterisation of Ruthenium Complexes for Application in Catalysis". Betreuung: Priv.-Doz. Dr. Martin H. G. Prechtl. Gutachter: Priv.-Doz. Dr. Martin H. G. Prechtl, Prof. Dr. Axel Klein, Reader Dr. George Britovsek.
12/2011 - 05/2012	Abschluss als Diplom-Chemiker Diplomarbeit im Institut für Anorganische Chemie, Universität zu Köln. Arbeiten zum Thema: "Katalytische Aktivierung von Alkoholen". Betreuung: Dr. Martin H. G. Prechtl. Gutachter: Prof. Dr. Axel Klein, Prof. Dr. Sanjay Mathur.
10/2005 - 05/2012	Chemiestudium, Universität zu Köln.
08/1996 - 06/2005	Allgemeine Hochschulreife, Städt. Apostelgymnasium, Köln.
08/1992 - 06/1996	Grundschule, Celéstin-Freinet Schule, Köln.